THE EXPANDED VERY LARGE ARRAY

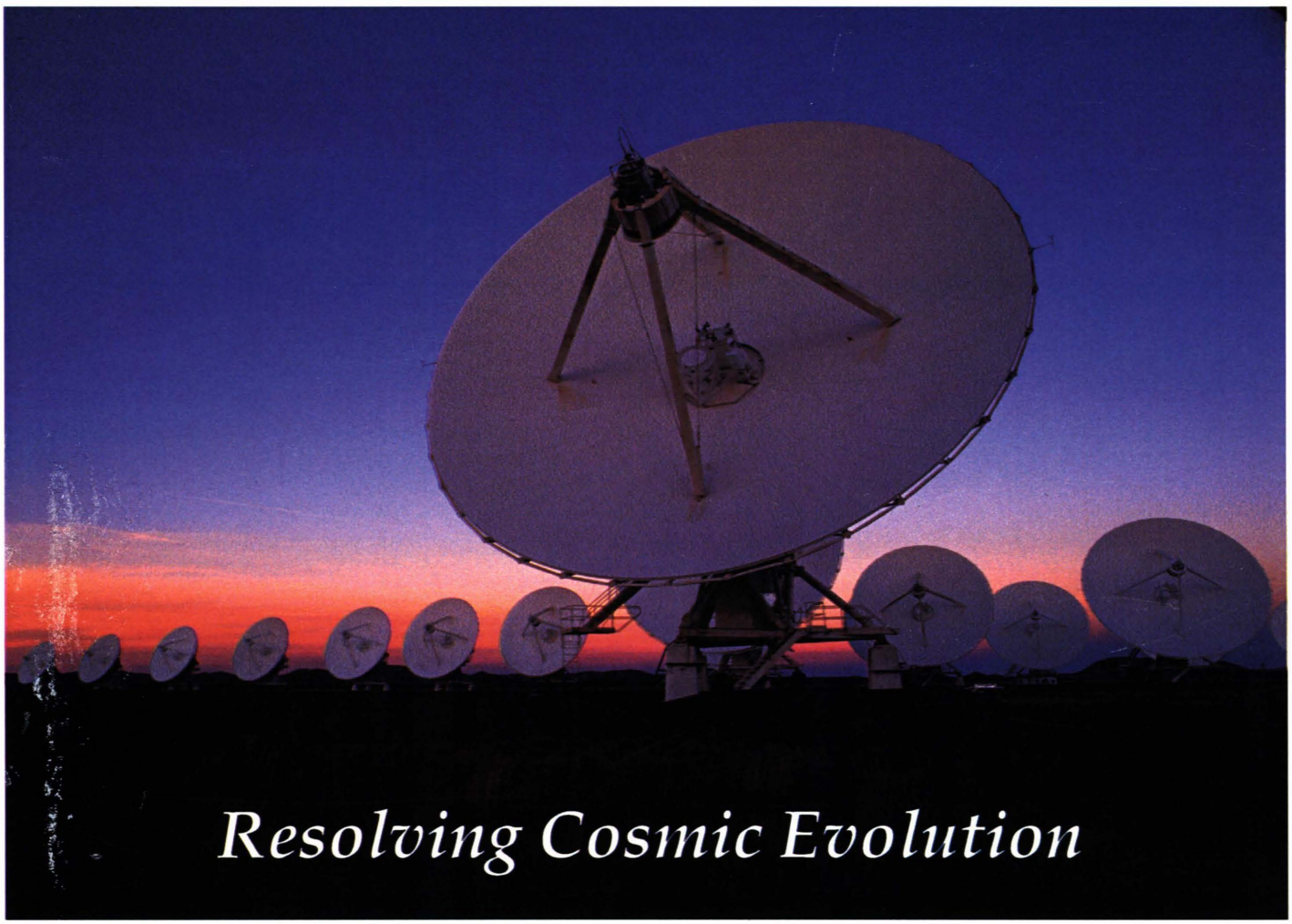

Phase II

Expanded Very Large Array

NRAO

Associated Universities, Inc.

NATIONAL RADIO ASTRONOMY OBSERVATORY

Expanded Very Large Array Project Phase II

The National Radio Astronomy Observatory is a facility of the
National Science Foundation operated by Associated Universities, Inc.

Contents

List of Figures

List of Tables

Chapter 1

Project Description: Summary

1.1 The Expanded Very Large Array: A Radio Telescope to Resolve Cosmic Evolution

Astronomy is the science of the Universe – its constitution, its history, and its destiny. The past decade has seen an explosion in our knowledge of the large-scale properties of the Universe, as studies of distant supernovae, and observations of the large angular scale structure of the cosmic microwave background, have shown that we live in a Universe whose geometry is flat, and whose expansion is accelerating. These breakthroughs now emphasize the need to understand the formation and evolution of the constituents of the Universe – its galaxies and galaxy clusters, its stars and the dusty nebulae out of which stars are born – over the maximum possible range of distance and time.

Understanding the structure, formation, and evolution of the components of the Universe will require detection and resolution of the electromagnetic emission from galaxies and their constituents throughout cosmic time. To achieve this, new telescopes of unprecedented sensitivity, resolution and imaging capability are needed. The luminosities and physical scales of the processes of galaxy and star formation dictate the primary instrumental requirements: The ability to image with tens of milliarcseconds resolution over angular scales of hundreds of arcseconds with a surface brightness sensitivity (expressed in temperature units) of tens of Kelvin. A telescope with these capabilities will be able to image galactic star-forming complexes with 1 AU resolution, track supernova remnant expansion and image compact H II region structure with 1 pc resolution at the distance of the Virgo cluster, and resolve the components of galaxies with tens of parsecs resolution anywhere in the Universe.

The NRAO is now building two complementary telescopes with these capabilities. One of these the Atacama Large Millimeter Array (ALMA) will eventually cover the frequency range between 30 and 950 GHz, where thermal emission processes are dominant. The other – the Expanded Very Large Array (EVLA) – will cover the frequencies between 1 and 50 GHz, where the emissions from both thermal and non-thermal emission processes are found. The two telescopes will measure different physical processes due to their different frequency ranges, and so will provide complementary information vital for understanding the formation and evolution of the constituents of the Universe.

This document describes the capabilities of the completed EVLA, plus the cost and means of completing the EVLA Project. The Project has been organized into two, overlapping phases. The first phase started in 2001, and will provide major improvements in the sensitivity, frequency coverage, bandwidth and spectroscopic capability of the VLA. The second phase would complete the EVLA by providing an order-of-magnitude improvement in spatial resolution. Upon completion in 2013, the EVLA will be a new telescope which will enable unique studies into the evolution of the components of the Universe, as well as gain new science over the full range of astronomy. The completed EVLA will:

- give the highest resolution images of any waveband of the earliest galaxies – even as far back as $z \sim 30$, should such galaxies exist.
- resolve the central regions of galaxies and quasars, to understand the environment of relativistic jets at all cosmic epochs.

- measure density structures in clusters of galaxies on scales of 50 kpc at any redshift through observations of the Sunyaev-Zel'dovich effect, to understand cluster structure formation throughout the Universe;
- resolve the dusty cores of galaxies, to distinguish star formation from black hole accretion, and provide an unbiased census of both processes over most of the age of the Universe;
- resolve the expansion of all galactic novae from one week after explosion, to provide detailed three-dimensional estimates of mass, temperature and density throughout the expansion phase;
- provide AU-scale images of massive star formation, to probe the intimate connections between accretion and outflow;

These examples of original science are chosen to illustrate the capability of the EVLA to resolve the evolution of cosmic structures throughout space and time. However, the EVLA will be much more than a cosmic resolver – its sensitivity, resolution, field of view, wide frequency coverage, and powerful correlator will make the EVLA the telescope of choice for studies of the physics of radio-emitting bodies throughout astronomy, from the solar system to the furthest edges of the Universe.

1.1.1 Strengths of Radio Astronomy

Radio astronomy is uniquely capable of addressing many of the key problems of modern astronomy because of the characteristics of emission and transmission processes at radio wavelengths. These include the following.

- Synchrotron emission, Zeeman splitting, and Faraday rotation are all manifest at radio wavelengths, are all directly dependent upon the strength and orientation of magnetic fields, and hence can be used to determine the role of magnetic fields in cosmic evolution.
- Synchrotron emission from the relativistic particles associated with superluminal jets, their terminal hotspots, and the strong shocks associated with jets and supernova remnants, is found most prominently at meter and centimeter wavelengths. Observations in this waveband are thus critical for understanding these ubiquitous and violent processes.
- Long wavelength radiation penetrates dust, allowing detection and resolution of objects such as galactic nuclei and star-forming regions whose emissions are obscured at other wavebands.
- Emission from warm bodies, including the dust and gas within star-forming regions, is most prominent in the radio, millimeter, and infrared bands. The sensitivity of radio telescopes makes observations at radio and millimeter wavelengths critical for understanding these objects.
- Emission from ionized gas surrounding hot stars is optically thin in the radio and millimeter bands, permitting investigation of the internal structures of these sources from observations made within these bands.

Radio astronomy has available the technologies to design, build, and operate the large arrays needed to detect and resolve low surface-brightness emission on milliarcsecond scales. The VLA and VLBA routinely demonstrate radio astronomy's capability to collect, transport, and correlate signals on baselines up to thousands of kilometers. Furthermore, the discipline currently has available the self-calibration techniques developed over the past 20 years which are needed to remove the corrupting influences of the atmosphere. The NRAO, and many other groups, are now developing the techniques for atmospheric phase correction at high frequencies ($\nu \geq 10$ GHz) where the strong sources needed to ensure the success of self-calibration are not always available. With these technologies and techniques, radio astronomy is ready to provide true diffraction-limited imaging with milliarcsecond resolution, and thus take maximum advantage of the unique information available within the radio window.

The uniqueness of the EVLA and ALMA in their resolution and imaging capabilities is illustrated in Figure 1.1, which shows the astronomical 'Discovery Space' coverage of these and other current and planned telescopes over the full breadth of the electromagnetic spectrum. The ~10 milliarcsecond imaging capability needed to resolve the evolution of cosmic structures can only be attained by interferometry within the radio, IR, and optical windows. However, the brightness temperature sensitivity of the optical and infrared

interferometers are typically ~1000K, and can not match the tens of Kelvin brightness temperature sensitivity provided by radio interferometry. Finally, only radio interferometry can provide both this resolution and sensitivity over the fields of view of thousands of resolution elements needed to image entire star-forming regions and distant galaxies.

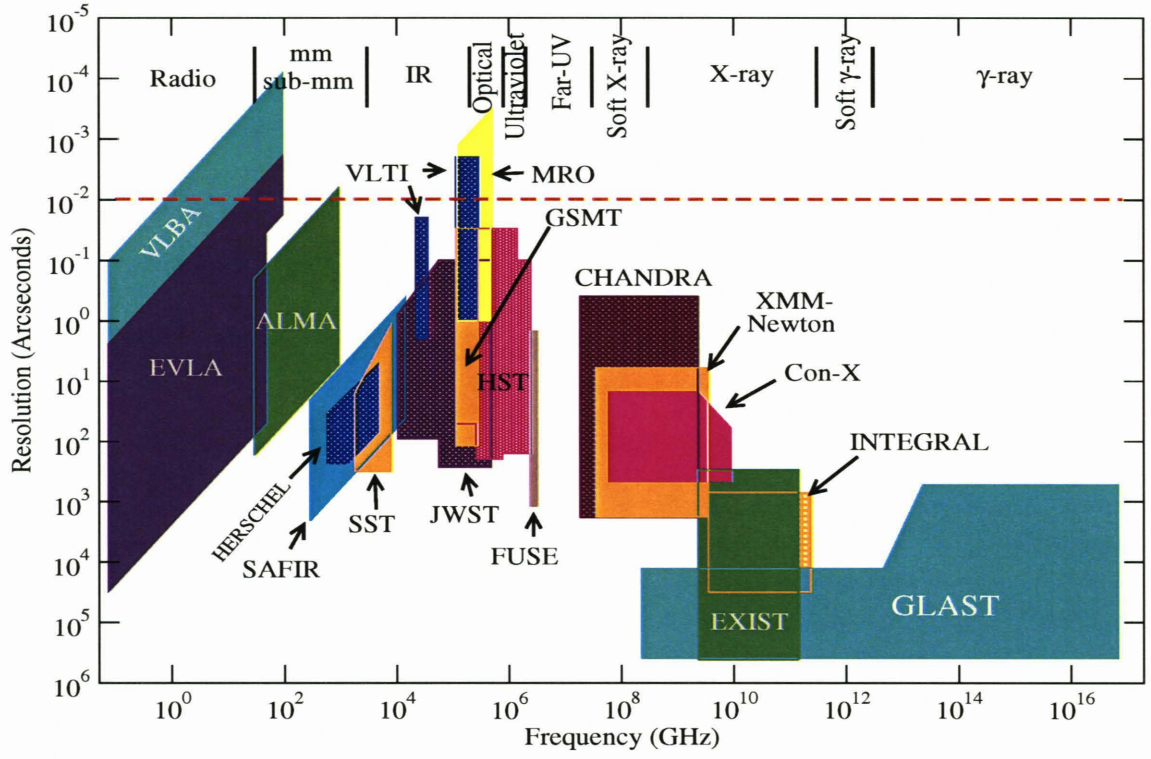

Figure 1.1: The resolution and field of view as a function of frequency for selected current and future astronomical imaging telescopes. Many proposed and current instruments have been omitted due to lack of space. The high resolution limit for each instrument is determined either by the diffraction limit or the detector pixel size. The low resolution limit is the field of view, set either by the element beamwidth, or the size of the pixel array. Nearly all instruments utilize mosaicing modes to enable coverage of much larger angles, which will generally extend each instrument's angular coverage by one to two orders of magnitude downwards. These extensions are not depicted here. The boundaries shown are approximate, and for most instruments, the coverage within each box is not continuous. The red horizontal dashed line marks the 10 milliarcsecond resolution capability needed for resolving cosmic evolution.

1.1.2 Costs and Timing of the Expanded VLA Project

The EVLA Project comprises two, overlapping phases. The first phase addresses all observational requirements except that of spatial resolution, which is the goal of the second phase. The decision to split the project in this way was made in the late 1990s because the technical issues addressing implementation of higher spatial resolution needed more study, while those concerning frequency coverage, sensitivity, and correlator capability were adequately understood at that time to allow an initial proposal for funding to be submitted in 2000.

Funding by the National Science Foundation for this initial phase (Phase I) began in 2001, and will continue through to scheduled completion at a cost to the NSF of $55M in FY2003 dollars. With funding from both Canada and Mexico, and with a contributed effort from the NRAO, the total cost of Phase I is $86M. Phase I progress is good, and we expect its completion, as planned, by 2012 on time and budget.

To complete the EVLA, the NRAO would requre $117M in FY2003 dollars for the second, and final phase (Phase II) of the project. Presuming a start in 2006, Phase II will be completed in 2013, shortly after completion of Phase I. Completing both phases together has significant benefits in enabling the key science

expeditiously, and in reducing the total cost of the project, as most of the electronics required is common to both phases.

Why complete the EVLA now? The instrumental capabilities are unique, so that the science questions that the completed EVLA can address are exciting and timely, while the technologies needed to achieve the required instrumental capabilities are available now. Furthermore, the planned timescale for completion and operation matches those for other major new instruments, such as ALMA, the JWST and the GSMT, which will operate in other frequency bands. Such complementarity is crucial for a comprehensive view, and understanding, of the physics of the Universe. Finally, rapid development of the EVLA will encourage continued development of the calibration and imaging techniques necessary for the next generation radio telescope – the Square Kilometer Array.

These points are expanded upon in the following sections, and are discussed in detail within this document.

1.2 Goals of the Expanded VLA Project

The overall goal of the Expanded VLA Project is to build the most cost-effective state-of-the-art radio telescope for astronomical research in the meter-to-millimeter wavelength band. Because the 27 existing VLA telescopes are fully operational, and operate efficiently in this wavelength band, we have adopted the approach of applying modern technologies to this sound infrastructure to produce a new telescope, the EVLA, with ten or more times the instrumental capability of the VLA. This 'leveraged' approach will result in a cost reduction by approximately a factor of two over that of a new facility, as well as a significant time savings, as the array infrastructure is already in place.

As described earlier, the project has been divided for practical reasons into two, overlapping phases. The major goals for each phase are described below.

1.2.1 Phase I

Phase I builds on the existing infrastructure to improve all aspects of the VLA *except* its angular resolution. The major goals for this phase of the project are as follows:

- **Sensitivity:** The continuum sensitivity will be improved by factors ranging from a few at lower frequencies to more than 20 at the high-frequency end of the useful frequency range of the EVLA.

- **Frequency Accessibility:** The EVLA will be able to observe at any frequency between 1.0 and 50 GHz. Two pairs of signals, each comprising opposite polarizations of up to 4 GHz bandwidth, will be independently tunable to any frequency within any given band.

- **Spectral Capabilities:** A new correlator will provide many more frequency channels (a minimum of 16,384, with many times more for certain correlator modes), process wider bandwidths (up to 8 GHz in each polarization), give higher frequency/velocity resolution (better than 1 Hz), and offer many more operational modes than are now available.

- **Operational Changes:** The EVLA will be dynamically operated, with observing blocks scheduled on the basis of weather, array configuration, and science considerations. The EVLA will also routinely and automatically produce images for all observing programs. These 'default' images will be archived and made available to users through an improved user interface. Users will have the capability to monitor the progress of, and modify the course of, their observations.

Following National Science Board approval, this phase began in 2001 with funding from the Division of Astronomical Sciences, National Science Foundation, at a planned rate of $5.3M/year (in FY2003 dollars), with completion currently scheduled by 2012. Following completion of Phase I, the 27-antenna subset of the EVLA, when operating as a single subarray, will be denoted the EVLA27.

1.2.2 Phase II

Phase II will improve the imaging range of the array by improving the resolution by an order of magnitude while retaining the full field of view and imaging fidelity provided by Phase I, and by improving the low resolution, wide-field imaging capability. These will be accomplished by the following:

1. **Resolution Enhancement:** The angular resolution will be improved by an order of magnitude by constructing eight new 25-meter antennas located up to 250 km from the array center, and by upgrading and incorporating two existing VLBA antennas. The planned locations of the eight new antennas are shown in Figure 1.2. These sites have been chosen after careful consideration of the imaging quality, road and optical fiber access, land availability, and expected radio interference environment. The two VLBA antennas which will be incorporated are at Pie Town and Los Alamos. As Los Alamos National Laboratory has requested that the NRAO vacate our Los Alamos site, we have designed the new array presuming the Los Alamos VLBA antenna will be moved to a site near Vaughn, NM.

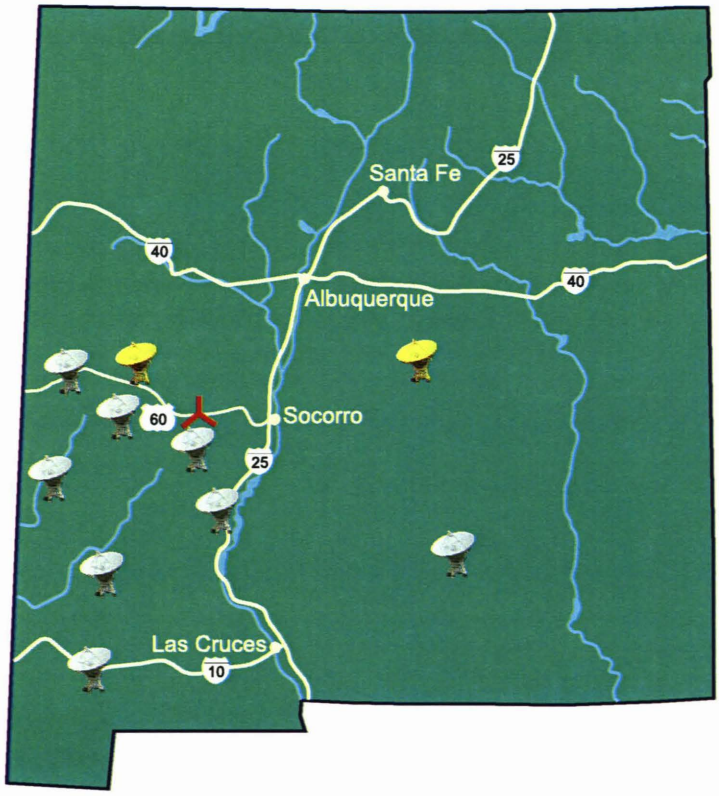

Figure 1.2: A map of New Mexico showing the approximate locations of the ten New Mexico Array antennas. Eight of these will be new, while two (colored yellow) are existing VLBA antennas which will be upgraded to EVLA capabilities. The Los Alamos VLBA antenna, currently located to the northwest of Santa Fe, will be moved to a location near Vaughn – the northeasternmost antenna shown in the figure. All antennas will be connected to the new correlator by optical fiber, permitting real-time operation with 16 GHz total bandwidth.

These ten antennas will be outfitted to cover the same frequency range as the EVLA27 antennas. They will be connected to the new correlator by fiber optic lines, thus permitting real-time correlation of a 37-antenna array which will provide an unprecedented combination of resolution, frequency coverage, angular imaging range, and sensitivity. The ten antennas will define a new array – the New Mexico Array (NMArray) – which when not combined with the EVLA can be operated as an independent, real-time subarray offering superb resolution and sensitivity, or can be combined with the VLBA to greatly improve its sensitivity and imaging capabilities. As part of this project, eight new NMArray antennas would be equipped with 2 Gb/sec Mark 5 recording systems to match the anticipated record-

ing capability of the VLBA in 2013. Funding to outfit the ten VLBA antennas with this recording capability and to upgrade their electronic capabilities would not be included as part of the project.

2. **Wide-field, Low-Surface-Brightness Imaging:** A new, short-spacing configuration, called the E-configuration, will be constructed to enable fast, high fidelity imaging of emission whose angular scale is comparable to, or larger than, that of the primary beam of the component antennas. Data taken by this configuration, when combined with single-dish data from the GBT, will provide high-fidelity μKelvin brightness temperature sensitivity imaging on angular scales ten times larger than those currently available with the VLA, at a resolution three times better than that provided by the GBT alone.

The frequency coverage and bandwidth of Phase I will be retained in Phase II. To provide sufficient correlation capacity for the completed EVLA, the 32-station correlator currently under construction for Phase I will be expanded to 40 stations.

1.2.3 Incorporation of the VLBA

The expansion of the correlator to 40 inputs, combined with its designed capability to simultaneously process both real-time and recorded data, will permit correlation of all VLBA data with much greater bandwidth and flexibility than that provided by the existing VLBA correlator. At the completion of the project, a single correlator, located at the central EVLA site, will process the data from 45 antennas (the 27 EVLA27 antennas, eight new NMArray antennas, 10 VLBA antennas), in real time (for the EVLA and NMArray antennas) or from disk-recorded media (for the VLBA and NMArray antennas), with very flexible combinations of subarrays and observing modes. Both the VLA and VLBA correlators will be decommissioned after the new correlator comes on line, providing significant long-term operational savings.

The operational integration of the VLBA with the EVLA, and the utilization of a single correlator for both arrays, will allow improved operational efficiency and will result in a great improvement in science capability. This plan will also enable planning for a more distant goal – connection of the VLBA with wide-band fiber so as to allow complete integration of the VLBA with the EVLA as a fully real-time single telescope.

1.3 Capabilities of the Expanded Very Large Array

The major instrumental capabilities of the EVLA after Phase I (denoted EVLA27), the New Mexico Array, and the completed EVLA are summarized in Table 1.1. This shows the significant increases in sensitivity, frequency coverage, and spectroscopic capabilities provided by Phase I, the factor of ten improvement in resolution provided by Phase II, and the impressive stand-alone capabilities of the New Mexico Array.

Compared to the existing VLA, the completed EVLA will increase:

- the maximum bandwidth by a factor of 80,
- the maximum number of spectral channels by a factor of 8192,
- the maximum spectral resolution by a factor of 3000,
- the logarithmic frequency coverage by a factor of four, and
- the maximum spatial resolution by a factor of 10.

In addition, most known sources of systematic errors which are responsible for limiting the current imaging fidelity will be eliminated or greatly reduced. Overall, the VLA will be transformed into a new telescope with unique and powerful scientific capabilities.

The continuum brightness temperature sensitivities of both ALMA and the EVLA as a function of frequency and resolution are shown in Figure 1.3. The coverage provided by the EVLA is shown in green, that by ALMA is in maroon. The upper and lower boundaries for each are set by the maximum and minimum baselines contained within each array's configurations. The array resolutions are shown with the approximately diagonal red lines.

Table 1.1: **Major Capabilities of the Current and the Expanded VLA.**

Parameter	VLA[a]	EVLA27[b]	NMArray[c]	EVLA[d]
Point Source Sensitivity[e]	10μJy	0.8μJy	2.2μJy	0.6μJy
No. of baseband pairs	2	4	4	4
Maximum bandwidth in each polarization	0.1 GHz	8 GHz	8 GHz	8 GHz
No. of frequency channels at maximum bandwidth	16	16,384	16,384	16,384
Maximum number of frequency channels	512	4,194,304	4,194,304	4,194,304
Highest frequency resolution	381 Hz	0.12 Hz	0.12 Hz	0.12 Hz
(Log) Frequency coverage, 1–50 GHz	22%	100%	100%	100%
Number of baselines	351	351	45	666
Spatial Resolution (5 GHz)	0.4 arcsec	0.4 arcsec	0.04 arcsec	0.04 arcsec
Spatial frequency coverage:[f]				
-Single configuration	35	35	7	350[g]
-All configurations	1000	1000	-	10000

[a]The current Very Large Array
[b]The 27-antenna array at the central site, after completion of Phase I of the project
[c]The New Mexico Array, comprising the two modified VLBA and eight new antennas
[d]The full 37-antenna array comprising the EVLA27 and the New Mexico Array
[e]1-σ in 12 hr for Stokes I. 1μJy = 10^{-32} Watt m^{-2} Hz^{-1}
[f]The ratio of maximum to minimum baseline. Does not include foreshortening.
[g]Assumes the EVLA27 is in its A-configuration.

The capabilities of the VLBA will also be considerably enhanced by Phase II. The NMArray antennas will often be combined with those of the VLBA, nearly doubling its collecting area. The additional eight antennas will greatly improve the *u,v* coverage, resulting in dramatic improvement in the VLBA's imaging capabilities. The New Mexico Array antennas will be outfitted by the EVLA Project with disk-based systems for recording at 2 Gb/sec providing 16 times the sustainable bandwidth of the currently-outfitted VLBA in anticipation of the VLBA's recording capability in 2013. With this, the sensitivity obtained by combining the VLBA with the NMArray will be at least a factor of six higher than the current VLBA. The resulting surface brightness sensitivity will also be improved in proportion. Although not shown in Figure 1.3, the VLBA's brightness sensitivity (when combined with the New Mexico Array) will extend the green area upwards, from a few hundred Kelvin (when heavily tapered) to to approximately 10^5K at full resolution. The expanded correlator will have the capacity to process data from the New Mexico Array plus the VLBA at this bandwidth, in addition to real-time correlation of all data from EVLA27.

1.4 Costs and Timescale for Phase II of the Expanded VLA Project

The total cost of Phase II of the Expanded VLA Project is estimated to be $117M in FY2003 dollars. The cost breakdown by component is shown in Table 1.2. This total does not include the $5M cost of moving the Los Alamos VLBA antenna, since this is driven by requirements of the Los Alamos National Laboratory that are independent of the EVLA requirements.

We have developed an aggressive but feasible implementation plan which minimizes cost while at the same time completes Phase II in 2013, shortly after the completion of Phase I. Implementation of Phase II has been planned as shown in Table 1.3.

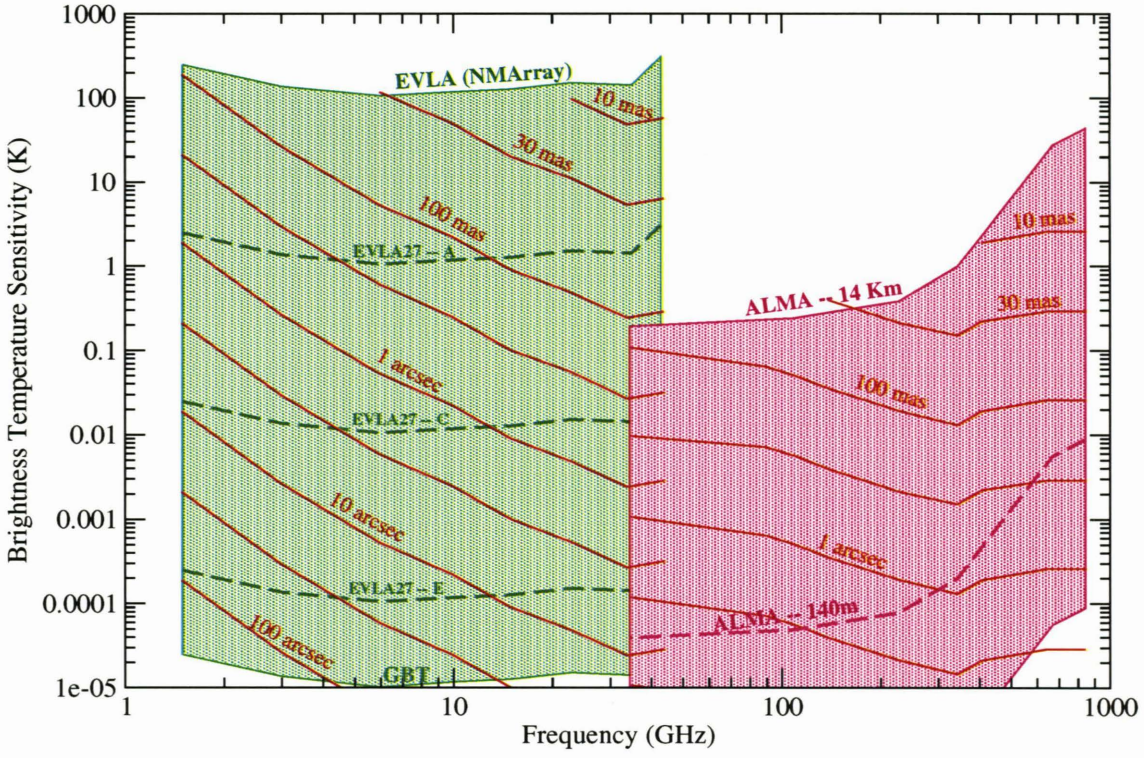

Figure 1.3: The $1-\sigma$ continuum brightness temperature sensitivity of the EVLA and ALMA, with one hour integration. The green shaded area shows the brightness coverage for the EVLA, with the upper boundary set by the full-resolution full EVLA, and the lower boundary set by the GBT. For ALMA, the boundaries are set by its equivalent full-resolution aperture of 14 km and the component antenna diameter of 12 m. The dashed line marked 'ALMA – 140 m' delineates the effective diameter of the smallest ALMA standard configuration. The area below this will be convered by the Japanese compact array. The diagonal red lines give the array resolution at which the specified brightness temperature sensitivity is obtained. The horizontal dashed green lines mark the EVLA27's A, C, and E configuration resolution limits. The VLBA's coverage, when combined with the NMArray, will extend the green area upwards by a factor of 1000.

1.5 Incremental Operations Costs for the EVLA

An analysis of the expected basic operating costs for the EVLA and VLBA shows an increment of $2.3M per year over the combined current operating costs of the VLA and VLBA. All of this increase is due to the addition of the eight new antennas. Additional operating costs for the EVLA27 are expected to be negligible since aging and difficult-to-replace components will be replaced with modern, more reliable equipment. However, concatenation of the EVLA and VLBA operational structures, and the replacement of the VLA and VLBA correlators with the new EVLA correlator will result in a savings of about $360K per year. Thus, the net increment in basic operational costs is only $2.1M per year – about 10% of the current total operational costs of the VLA and VLBA. That the VLA's capabilities can be enhanced by one or more orders of magnitude with so small an increment in operations costs is a clear illustration of the advantages of leveraging the EVLA project on the existing infrastructure of the VLA.

1.6 User Support and Instrumental Development

The estimated operational budget increment of $2.1M described above is for minimal basic support – sufficient to operate the telescope at its initial level in a manner similar to that achieved by current operations. However, this level of support will not be sufficient to provide for ongoing technical development, or to

Table 1.2: **Component Budget Summary in FY2003$k**

WBS	Description	NMArray	E-Config	Total
6.01	Project Management	8167	167	**8334**
6.02	System Integration	1570	0	**1570**
6.03	Civil Construction	6441	5254	**11695**
6.04	Antennas	36326	0	**36326**
6.05	Front End Systems	6860	0	**6860**
6.06	LO System	3504	0	**3504**
6.07	Fiber Optics	4521	20	**4541**
6.08	IF System	844	0	**844**
6.09	Correlator	6436	0	**6436**
6.10	Monitor & Control	1109	0	**1109**
6.11	DM &Computing	1176	0	**1176**
	M&S	**76953**	**5441**	**82394**
	Wages&Benefits	16481	153	**16634**
	Sub-Total	**93434**	**5594**	**99028**
	Contingency	17650	559	**18210**
	Project Total	**111085**	**6153**	**117238**

Table 1.3: **Implementation Schedule for Phase II of the EVLA Project**

Milestone	Date	Milestone	Date
Relevant Phase I Milestones		**New Mexico Array**	
Start retrofitting VLA ant. @ 4/yr	Sep 2004	First planning money available	Jan 2006
First science with correlator subset	Dec 2007	Start site EIS process	Jan 2006
32-station correlator operational	Jan 2009	Funding for correlator expansion	Aug 2006
Retrofit last VLA antenna	Oct 2010	Fiber network test to Pie Town	Jan 2007
Last EVLA receiver installed	Apr 2012	Final decision on antenna elements	Jan 2007
		Go to bid on antennas	Jun 2007
E-Configuration		Start design of new VLBA feeds	Jun 2007
Decide final concept	Jan 2006	Fiber network test to first site	Dec 2007
Go to bid for rail and foundation	Jun 2006	Place antenna contract	Jan 2008
Place rail and foundation contract	Oct 2006	Move Los Alamos antenna	Jan 2008
Complete rail and foundation work	Apr 2008	Complete EIS process	Jun 2008
Start installation of fiber and electrical	Apr 2008	Acquire first sites	Jun 2008
Finish installation of fiber and electrical	Oct 2008	Start civil works on first site	Jun 2008
Completed	Oct 2008	First new ant. available for outfitting	Jun 2009
		40 station correlator fully operational	Jan 2011
		Last antenna outfitted	Dec 2012

provide adequate user support. The NRAO will request an increment in operations funding of $5.5M/year, to be phased in over three years following completion of the project, to permit ongoing technical development in such areas as data transmission, data archiving, imaging research, and post processing. The NRAO will also encourage the National Science Foundation to establish a vigorous program for support of user access for its major facilities, at a suggested level of $5.5M/year for the EVLA.

The 2000 AASC has recommended funding for instrumental development and user support at a level of 3% of the capital cost of new major facilities. The levels we are proposing are in good agreement with the AASC recommendations.

1.7 Broader Impact of the EVLA

1.7.1 Establishing Infrastructure for Other Projects

Phase II of the EVLA project will develop a wide-bandwidth, real-time fiber-optic network to ten remote sites within the state of New Mexico, using already available commercial fiber. The establishment of this network will attract other projects which need real-time access to data taken over a wide geographical area, and will encourage such projects to locate within New Mexico. Examples include:

- The Long-Wavelength Array, a low-frequency radio astronomy telescope, being promoted by a consortium led by the University of New Mexico, and including the University of Colorado, the University of Texas, LANL, and NMIMT.
- The Square Kilometer Array (SKA), a 'next-generation' radio telescope which seeks one square kilometer of collecting area (approximately 50 times the VLA), with baselines extending to a few hundred kilometers.
- EarthScope, a $200M interdisciplinary Earth Observatory which will include deployment of 2000 seismograph sites with real-time data delivery.

1.7.2 Technological Development

The EVLA will be a major developer and user of networked information systems. The 37 antennas will each be sending to the central correlator approximately 100 Gb/second via a partially owned and partially leased fiber optic network. The aggregate of 3.7 Tb/sec will be conveyed over fiber that is already in place – dark rural fiber for the NMArray antennas, and fiber laid by Phase I of the project for the EVLA27 antennas. The technical development for this phase-stable, wide-bandwidth, long-distance capability will be directly applicable to future arrays such as the Square Kilometer Array, as described in the preceding section.

The theoretical maximum correlator output will be about 30 GB/sec. Although the EVLA will rarely operate at such an output rate (the currently planned maximum rate is 1.6 GB/sec, and the initial rate is a relatively modest 25 MB/sec), the archiving and processing requirements for the normal observing modes will be extremely challenging. Part of the requested budget is for development of the archiving and processing systems which will be needed to handle the anticipated data flow. The archive will contain the calibrated data and automatically-generated default images which will be available to all users through interfaces established by the National Virtual Observatory. The solutions to these problems will be applicable to a considerably wider audience future instruments such as the Square Kilometer Array will be faced with even larger data transfer, storage, and processing challenges.

The processing of the EVLA's data output will present another stimulating technical challenge, as datasets as large as ~50 TB per project will be used to generate the images required by astronomers. These images can be exceedingly large up to 32,000 x 32,000 pixels for each of hundreds to thousands of frequencies. Each image must be corrected for the temporal and spatial errors created by the atmosphere, the antennas, and the instrumental electronics. Included in the budget estimate is the creation of an imaging algorithm development group, to design, test, and implement the specialized algorithms needed to efficiently generate such large-scale images from very large datasets.

1.7.3 Education and Public Outreach

The establishment of nine new antenna sites within rural areas of New Mexico offers the NRAO a unique opportunity to establish an education and public outreach program to a community that is in general not well connected to advanced technology or cutting-edge science. The NRAO is preparing and will soon submit to the NSF a proposal to establish a program of education and public outreach which specifically targets the rural population of New Mexico. This program would:

- Provide outreach to communities through public information sessions and community member field trips, provide dynamic exhibits tailored to the communities located near the antenna sites, and provide an outreach van and trailer which will tour these communities for weekend workshops and lectures.

- Provide outreach to schools through a series of teacher workshops and student field trips to the central EVLA site to visit the array and its visitor center.
- Provide outreach to regional, state, and national audiences through creation of permanent exhibits which will be established at state visitor centers and taken to national conferences.

In addition to this locally-focused program, we will request funding under the EVLA operations budget for an EPO scientist, with the responsibility to collect, generate, and disseminate images generated by the EVLA and other NRAO facilities, and to oversee the science content of the NRAO web pages.

Finally, the presence of a cutting-edge facility, in combination with an adequately funded user support program, will invigorate university astronomy and physics departments, as this will encourage younger faculty and their students to use the telescope, and to develop better technologies and methodologies which will be applied both by the EVLA and its eventual successor, the Square Kilometer Array.

1.8 Why Complete the EVLA Now?

Phase II of the Expanded VLA Project will create unique capabilities that will provide exciting science rewards from a region of resolution and frequency parameter space that is largely unexplored by existing instruments, and which is appropriate for studies of the evolution of stars and galaxies. It is important to provide these capabilities now, because:

- The anticipated science is timely and exciting, and we have now in hand the technical means to achieve the needed capabilities.
- The resolution, sensitivity, and diffraction-limited wide-field imaging capabilities of the EVLA and ALMA are unique within astronomy. No other waveband can access the distant, evolving Universe with the $\sim$10 mas resolution and tens of Kelvin brightness temperature sensitivity which are critical for understanding the formation and evolution of structures in the Universe.
- The planned timescale for implementation and operation matches those of other major new facilities currently being designed or under construction in other wavebands, such as ALMA, JWST, and the GSMT, thus encouraging the multi-wavelength studies critical to understanding the physics of objects of interest.
- The technological development required for the project will enable and encourage further technical developments needed for planning and building the next-generation radio telescope – the Square Kilometer Array.
- Implementation of Phase II in concert with Phase I is the most efficient use of human and material resources, as much of the required electronic and software components required for the NMArray antennas are the same and can be built and installed simultaneously by the same individuals who will be implementing Phase I.

1.9 Endorsement of the EVLA by the AASC

Since the 1960s, the National Academies have commissioned a decadal review of astronomy and astrophysics, with the charge of assessing the field, and recommending new ground- and space-based programs for the coming decade. These reports, issued at the beginning of each decade, have proven to be highly influential in directing resources for new telescopes and programs.

The 2000 Astronomy and Astrophysics Survey Committee comprised 15 astronomers and astrophysicists, who established nine panels, comprised of over 100 prominent scientists, to deal with wavelength subdisciplines and other areas. The AASC report was issued in 2001, and included both an in-depth assessment of the key directions and questions for astronomy in this new millennium, and ranked recommendations for funding new telescopes and initiatives which the Committee believed would most effectively address these key science questions.

The 2000 AASC report identified five key problems which, they wrote, 'are particularly ripe for advances in the coming decade'. Amongst these were:

- Studying the dawn of the modern Universe, when the first stars and galaxies formed.
- Understanding the formation and evolution of black holes of all sizes.
- Studying the formation of stars and their planetary systems, and the birth and evolution of giant and terrestrial planets.

These three problems illustrate the Committee's judgement that a major focus for astronomy in the new millennium is in the area of cosmic evolution – of the Universe and its constituents. The capabilities of the completed EVLA would ensure that it will play a major role in providing answers to these key problems, for only the EVLA and ALMA will have the capability to detect ***and image*** these constitutents on astrophysically important milliarcsecond scales. The 2000 AASC recognized the EVLA as a critical instrument for astronomical research by giving the Expanded VLA Project the second highest priority amongst major ground-based facilities for construction in this decade. The importance of the EVLA was underlined by the Committee in its recommendation, when it wrote:

> The Expanded Very Large Array (EVLA) – the rebirth of the VLA, the world's foremost centimeter-wave telescope will take advantage of modern technology to attain unprecedented image quality with 10 times the sensitivity and 1000 times the spectroscopic capability of the existing VLA. The addition of eight new antennas will provide an order-of-magnitude increase in angular resolution. With resolution comparable to that of ALMA and [JWST], but operating at much longer wavelengths, the EVLA will be a powerful complement to these instruments for studying the formation of protoplanetary disks and the earliest stages of galaxy formation.

The EVLA will do this – and much more – for astronomy in the early decades of this new millennium.

Chapter 2

Project Description: Background, Linkages, and Goals

This document describes the capabilities brought to astronomy by Phase II of the EVLA Project. The primary goal for this final phase is to improve the resolution of the EVLA by an order of magnitude, thus enabling detailed imaging of objects much more distant, and younger, than those accessible to the VLA. Resolution improvements for any facility must be matched by sensitivity improvements, which for the EVLA are provided by Phase I of the project. Because of this synergy between the two phases of the EVLA, a description of the second phase's goals must include a review of the capabilities provided by the first phase. In this chapter, we thus describe the capabilities of, and benefits from, the complete Expanded Very Large Array, while emphasizing those aspects provided by Phase II.

We begin by discussing the key science directions for astronomy in this decade, as identified by the 2000 Astronomy and Astrophysics Survey Committee. We then discuss the instrumental requirements needed for addressing the key problems identified by this committee. There follows a description of 'astronomical discovery space', and the role of radio astronomy, and of the EVLA, within this space. Modern astronomy is increasingly a multi-wavelength discipline, and we discuss next the synergies between radio astronomy and other wavebands, and how the completed EVLA will play a key role, along with other new facilities, in advancing our knowledge of astronomy. New science from radio astronomy, and in particular from the EVLA, will have important impacts in many other disciplines, and we next discuss these on education and public outreach, on universities and graduate astronomy, and on technical development. Finally, we discuss why the EVLA should be considered a necessary prelude to the design, development and future construction of a 'next-generation' radio telescope – the Square Kilometer Array.

2.1 Key Problems for Astronomy to Address in This Decade

In their 2001 report entitled 'Astronomy and Astrophysics in the New Millennium', the Astronomy and Astrophysics Survey Committee (AASC) summarized the current state of astronomy and gave its recommendations for funding new initiatives in this first decade of the new millennium[1]. The key problems for astronomy in this first decade of the new millennium, as identified by this Committee, are given in the Executive Summary of their report. They are:

- Determining the large scale properties of the Universe: the amount and distribution of its matter and energy, its age, and the history of its expansion.
- Studying the dawn of the modern Universe, when the first stars and galaxies formed.
- Understanding the formation and evolution of black holes of all sizes.
- Studying the formation of stars and their planetary systems, and the birth and evolution of giant planets.

[1]The report can be accessed on line at: http://books.nap.edu/books/0309070317/html/index.html

- Understanding how the astronomical environment affects Earth.

It is clear from these identified priorities that the evolution of the Universe, and the formation and evolution of the material bodies within it, figure prominently amongst the key problems which, in the committee's words, 'are particularly ripe for advances in the coming decade'.

The context from which these key recommendations arose lies in the rapid advances of our knowledge of the Universe in the past decade – advances enabled by the rapidly improving technologies in all electromagnetic wavebands, from radio to gamma ray. In the Committee's words:

> The decade of the 1990s saw an enormous number of exciting discoveries. For example, for centuries humanity has speculated about the possible existence of planets around other stars. This speculation ended in the past decade with the discovery of extrasolar planets, and the number of planets known continues to grow. Astronomers peered far back in time, to only a few hundred thousand years after the Big Bang, and found the seeds out of which all galaxies, such as our own Milky Way were formed. At the end of the decade came evidence for a new form of energy that may pervade the Universe. Nearby galaxies were found to harbor extremely massive black holes in their centers. Distant galaxies were discovered near the edge of the visible Universe. In our own solar system, the discovery of Kuiper Belt Objects some of which lie beyond the orbit of Pluto – opens a new window on the history of the solar system.

Using these recent discoveries as background, the Committee wrote about the fundamental goal of astronomy, and of directions for this current decade:

> The fundamental goal of astronomy and astrophysics is to understand how the Universe and its constituent galaxies, stars, and planets formed, how they evolved, and what their destiny will be. To achieve this goal, we must survey the Universe and its constituents, including galaxies as they evolve through cosmic time, stars and planets as they form out of collapsing interstellar clouds in the Galaxy, interstellar and intergalactic gas as it accumulates the elements created in stars and supernovae, and the mysterious dark matter and perhaps dark energy that so strongly influence the large-scale structure and dynamics of the Universe.

The focus on studying the formation and evolution of the fundamental constituents of the Universe – stars, gas, dust, and the galaxies in which these are found is very clear.

Since the time these words were written, new discoveries of the large-scale structure of our Universe have served to emphasize the need to understand the formation and evolution of its constituents. The flat geometry of the Universe, the apparent acceleration of its expansion, and the need for 'dark energy' and 'dark matter' certain to be present, but so far unidentified – have made cosmic evolution of the Universe and of its constituents one of the key problems for astronomy in this decade, and probably beyond.

2.1.1 Required Telescope Parameters to Resolve Cosmic Evolution

How should we study objects so distant in time and space? What instrumentation will be needed to sharpen our view? The essential characteristics are quite straightforward to determine. There are four key parameters to consider: Resolution, Sensitivity, Frequency Coverage, and Imaging Field of View. We consider each in turn, using the identified key science problems as our guide:

- **Resolution:** Consider the study of star and planetary formation. A physical resolution of 1 AU is desirable, as this is the scale at which we expect to detect structures related to planetary orbits. The nearest large star-forming region is the Taurus complex at a distance of 140 pc. At this distance, 1 AU subtends 7 milliarcseconds. For more distant complexes such as Orion, the nearest region of active high-mass star formation at 450 pc distance, 7 milliarcsecond angular resolution will provide a linear resolution of ~3 AU, adequate to resolve details on the scale of Jupiter's orbit.

  Next consider the study of the formation and evolution of galaxies. Observations of nearby active star-forming galaxies show that most of the activity occurs within 100 pc of the center. A linear resolution of 50 pc will allow resolution of these regions. The apparent angular size of a 50 pc structure declines

from 100 milliarcseconds at $z = 0.02$ to 6 milliarcseconds at $z = 1.6$, then slowly increases as a function of redshift due to the geometric properties of our expanding Universe. Thus, a telescope with resolution of $\sim$ 5 milliarcseconds will enable imaging with 50 pc or better linear resolution *at any redshift*, as shown in Figure 2.1. The optimum frequency for observations of thermal emission processes by the EVLA is ~30 GHz, for which ~300 km baselines will be needed to obtain the desired resolution.

Studies of cosmic evolution are not limited to thermal emission processes. Non-thermal synchrotron emission from relativistic electrons, produced by the most violent processes in the Universe, is most usefully observed in the 1 – 4 GHz frequency range. A telescope with $\sim$ 350 km baselines will provide resolution of $\sim$ 100 milliarcseconds at these frequencies – providing linear resolution of better than 1 kpc anywhere in the Universe. Such a capability will allow resolution of galactic disks, halos, non-thermal relativistic jets and their hotspot terminations at any redshift.

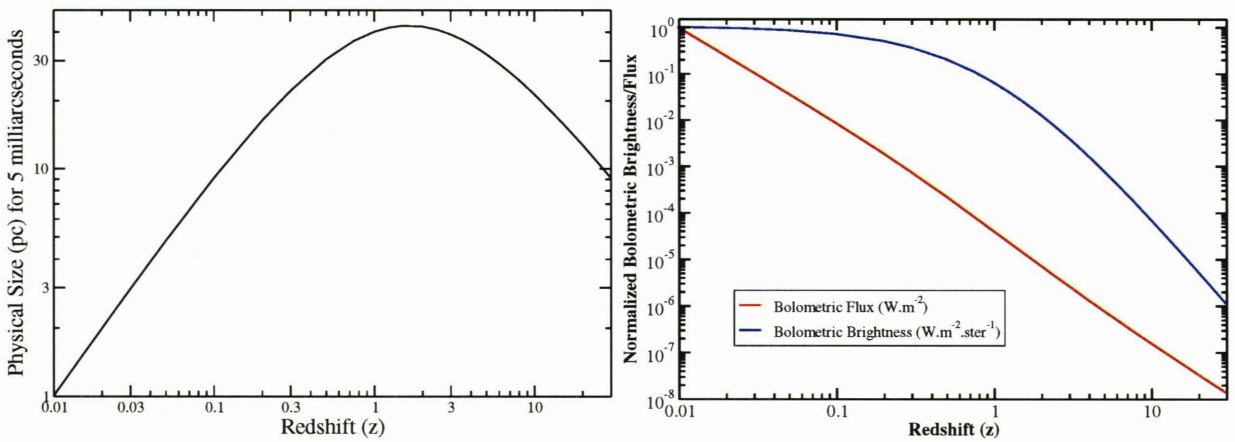

Figure 2.1: The familiar relationships for angular size, brightness and flux density in a static, Euclidean universe are not preserved in an expanding universe. The left panel shows the physical size of an object subtending an angle of five milliarcseconds, as a function of redshift. Beyond $z \sim 1.6$, the physical resolution improves for fixed angular resolution! The right panel shows the bolometric brightness (blue) and bolometric flux density (red) as a function of redshift, normalized to unity at $z = 0.01$. The rapid decline in brightness beyond $z \sim 1$ underscores the need for high sensitivity for studies of our early Universe. The relations shown are computed using $\Omega_m = 0.27$, $\Omega_\Lambda = 0.73$, and $H_0 = 71\,\mathrm{km\,s^{-1}Mpc^{-1}}$.

- **Sensitivity:** A high resolution telescope must be sufficiently sensitive to detect the emission within its resolution beam with good signal-to-noise ratio (SNR). The necessary sensitivity can be derived from the emission processes of interest. Ionized gas regions have typical physical temperatures of $T \sim 10^4$K. In order to study their interior properties in the continuum, we must observe them at a frequency where they are optically thin – at an opacity of $\tau \sim 0.1$ to 0.01.[2] The apparent brightness temperature will thus be $T_b \sim \tau T \sim 100 - 1000$ K. Obtaining good SNR will then require a brightness sensitivity of $\sim$ 10 K. The same argument can be applied to observations of dusty disks, whose physical temperatures are typically a few hundred Kelvin. For studies of the internal structures of such objects, it is necessary to observe them at low optical depth[3], leading again to a desirable surface brightness sensitivity of ~10 K. A third example is the study of extragalactic jets, whose brightness temperatures are 10^4 to 10^6K at 1 GHz[4]. Due to cosmic dimming, the apparent brightness of such objects will be reduced by one to four orders of magnitude, so their study will require good (10K) brightness sensitivity for a good SNR for distant objects.[5] The need for high sensitivity is especially important for studies of objects at high

[2]This will typically require observations at rest frequencies above ~5 GHz.

[3]This will typically require observations at a rest frequency below $\sim$ 100 GHz

[4]For synchrotron emission, there is a strong frequency dependence of the brightness temperature: $T_b \propto \nu^{-2.7}$

[5]Observations of synchrotron-emitting sources are especially susceptible to the decrease in surface brightness due to cosmic expansion. The surface brightness of a source with spectrum $S \propto \nu^{-\alpha}$, observed at constant frequency, declines as $(1+z)^{3+\alpha}$ – a factor of thirteen at $z = 1$, and a factor of $\sim$ 7000 at $z = 10$ for a synchrotron source with $\alpha = 0.7$. The effect is less pronounced (but still severe) for flat spectrum emission, such as optically-thin bremsstrahlung, but is relatively minor for optically thick thermal emission and dust emission, for which the emissivity rises sharply with frequency.

redshift, where cosmic diminution is important, as shown in Figure 2.1.

The required point-source sensitivity, σ_S, (which is directly connected to fundamental telescope parameters) can be derived from the following relation:

$$\sigma_S \sim \nu_G^2 \theta_{arc}^2 T_b \qquad \mu\text{Jy}$$

where σ_S is the point-source sensitivity in μJy[6], ν_G is the frequency in GHz, θ_{arc} is the resolution in arcseconds, and T_b is the desired brightness temperature sensitivity. For the sensitivity and resolution goals given above, and at a fiducial frequency of 30 GHz, the required sensitivity is

$$\sigma_S = 1\ \mu\text{Jy}.$$

- **Frequency Coverage:** Obtaining sub-microjansky continuum sensitivity with a telescope with the collecting area of the VLA requires both high antenna efficiency and very wide instantaneous bandwidths. For studies of both thermal and non-thermal processes, the latter requirement necessitates broad frequency coverage between 1 and 50 GHz[7]. Wide bandwidths and frequency coverage are however required for more than continuum sensitivity – spectral lines whose rest frequencies are in the millimeter bands, and which provide unique and valuable information on the conditions in the early Universe, are redshifted into the centimeter band. Observing these transitions from high redshift, early Universe objects will require complete frequency coverage over the range for which the VLA antennas have sufficient sensitivity. Thus, for comprehensive studies of the distant and evolving Universe, continuous frequency coverage from 1 to 50 GHz is needed.

- **Imaging Characteristics:** It is important to distinguish between *resolution* and *imaging*. Mere resolution can be obtained with a single-baseline interferometer, and might be sufficient to measure the angular diameter of an isolated bright object such as a star. Understanding the physics of complex, distant phenomena requires much more than simple resolution. What is needed is the ability to make images which correctly represent the full complexity of the object of interest, and which span a very wide range of angular structures. The required angular range can be estimated from images of local objects. The well-known VLA images of the nearby supernova remnant Casseopeia A, or of the nearby radio galaxy Cygnus A, are ~1000 pixels on a side, with angular structures which span the full range, and some emission still not resolved. There is no reason to believe that the more distant objects we wish to study will be any less complex, so future instruments must be capable of imaging a field of view $\sim 10^4$ times the diffraction-limited resolution. With a maximum baseline of 350 km, the telescope must therefore provide a well-sampled range of spacings down to 30 meters.

The essential instrumental requirements for successful imaging of cosmic evolution are then:

1. Baseline coverage spanning 30 meters to 350 kilometers
2. Point-source continuum sensitivity of 1 μJy.
3. Continuous frequency coverage from 1 to 50 GHz

These are very demanding requirements, requiring coherent, real-time interferometry over distances ten times greater, and sensitivities ten times better, than those of the present VLA. Until recently, there were no practical means to meet these requirements. But the advent of new technologies, particularly wide-band fiber-optic transmission and high speed digital processing, has dramatically expanded the boundaries of our capabilities. The approach of the NRAO to provide these needed instrumental capabilities is thus to build upon the existing VLA, which has already in place the site, infrastructure, and most of the required collecting

[6] $1\mu\text{Jy} = 10^{-32}\,\text{watt}\,\text{m}^{-2}\,\text{Hz}^{-1}$

[7] This frequency range is set by the VLA's antennas – their pointing and surface accuracy are not sufficient for work above 50 GHz, and the small subreflector prohibits operation below 1 GHz from the Cassegrain focus.

area. The sensitivity and frequency coverage requirements will be met within Phase I of the Expanded VLA Project. The resolution and baseline coverage requirements will be met by Phase II of the Expanded VLA Project. The result of implementing both phases of the project will be a facility unmatched by any other, current or planned, in this waveband.

These capabilities were known to the 2000 AASC, which recognized the unique and valuable role of the EVLA in addressing the key problems listed in its report. On this basis, the committee gave the EVLA its second highest recommendation for major ground-based facilities for construction in this decade. In the words of the committee:

> The Expanded Very Large Array (EVLA) – the rebirth of the VLA, the world's foremost centimeter-wave telescope – will take advantage of modern technology to attain unprecedented image quality with 10 times the sensitivity and 1000 times the spectroscopic capability of the existing VLA. The addition of eight new antennas will provide an order-of-magnitude increase in angular resolution. With resolution comparable to that of ALMA and [JWST], but operating at much lower frequencies, the EVLA will be a powerful complement to these instruments for studying the formation of protoplanetary disks and the earliest stages of galaxy formation.

2.2 Discovery Space in Astronomy

The previous section has explained why a high resolution highly sensitive radio telescope with wide frequency coverage is needed to permit original discoveries into the formation and evolution of the constituents of our Galaxy. This need for high resolution and sensitivity is not restricted to radio astronomy alone. A full understanding of the physical mechanisms at work in distant objects nearly always requires spectral information from many wavebands. For example, relativistic electrons spiraling in magnetic fields emit synchrotron radiation, most typically observed in the radio bands at frequencies lower than 10 GHz. The same electrons which produce these radio photons can Compton scatter them (the so-called Synchrotron-Self Compton mechanism) into the X-ray band, providing an extra window into the emitting process. Observations of the radio and X-ray emissions from regions where these processes are at work can be used to determine the magnetic field intensity in the source, and the physics of the emitting processes. Both wavebands are needed, as the magnetic fields cannot be uniquely derived from observations at radio or X-ray wavelengths alone.

In a similar vein, warm dust within a nearby star-forming region will emit the bulk of its energy in the infrared. This continuum emission is accompanied by spectral lines with rest frequencies typically above 20 GHz emitted by cold molecules and atoms. From these emissions we can learn the temperature, extent, and kinematics of these regions. But the far infrared emission from such regions in distant young galaxies will be redshifted by the cosmological expansion into the millimeter band, or even into the centimeter band, thus requiring an observing capability in these wavebands in order to understand the physical characteristics of such sources in the early Universe.

These simple examples illustrate an important requirement for modern astronomy: access to the entire electromagnetic spectrum with high sensitivity and high resolution. No single instrument can provide this capability, so it is necessary to design and build multiple instruments, each of which covers a range of the spectrum. It is also necessary to track and apply technical improvements, as astronomy remains fundamentally limited in sensitivity and resolution at all frequencies. The spectacular recent discoveries concerning the large-scale structure of the Universe are in fact based on such application of new technologies.

Two of the most important parameters which describe the capabilities of any telescope are its frequency coverage and angular resolution. These define the axes of what may be described as 'Astronomical Discovery Space'. A telescope's capability will fill a region of this space, delimited by the telescope's resolution, its field of view, and its range in frequency. Figure 2.2 shows the coverage of a number of current and planned astronomical telescopes. The upper boundary for each is given by the telescope resolution, the bottom boundary by its field of view. The spectral wavebands are identified by their common names along the top of this figure.

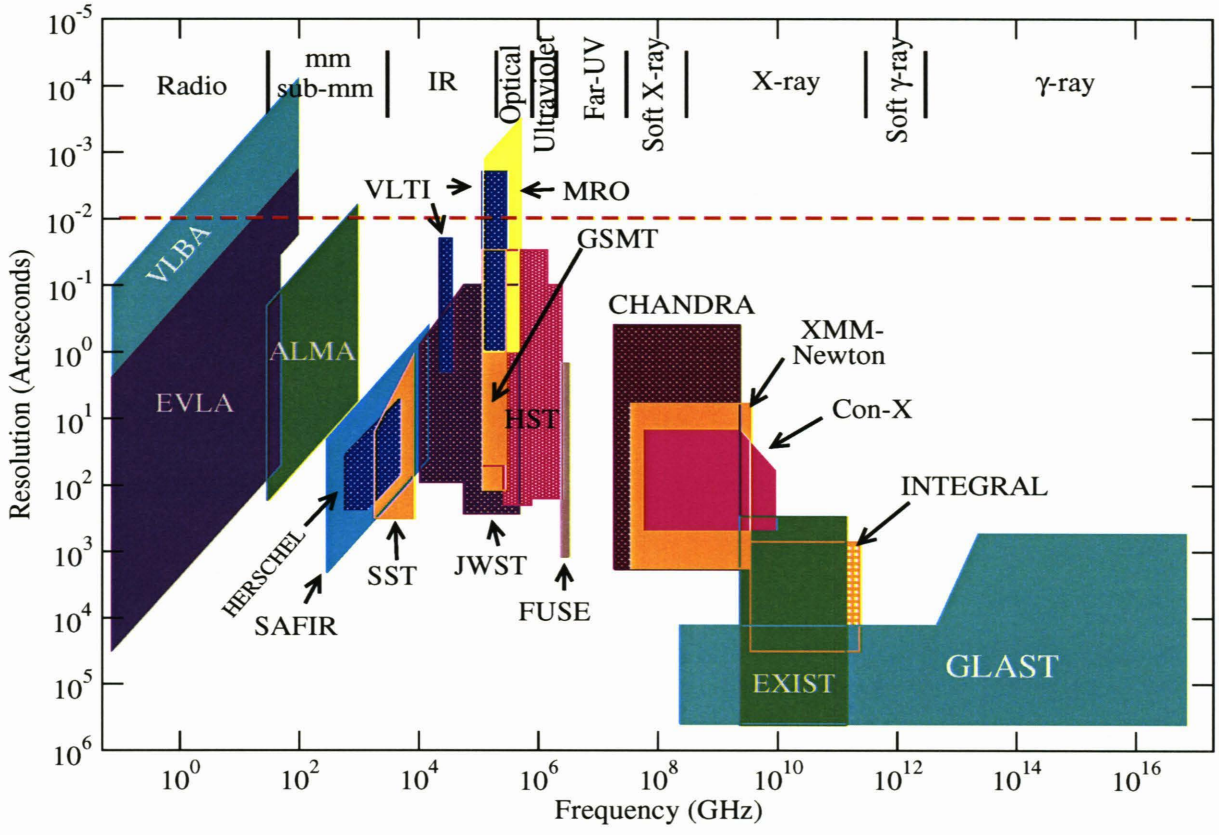

Figure 2.2: The resolution and field of view as a function of frequency for selected current and future astronomical imaging telescopes. The high resolution limit for each instrument is determined either by the diffraction limit or the detector pixel size. The low resolution limit is the field of view, set either by the element beamwidth, or the size of the pixel array. Nearly all instruments utilize mosaicing modes to enable coverage of much larger angles, which will generally extend each instrument's angular coverage by one to two orders of magnitude downwards. These extensions are not depicted here. The boundaries shown are approximate, and for many instruments, the coverage within each box is not continuous. The horizontal red dashed line marks a resolution of 10 milliarcseconds. See section 2.5 for brief description of the instruments shown here.

2.2.1 The Role of Radio Astronomy

Figure 2.2 shows that radio astronomy covers a significant fraction of astronomical 'Discovery Space'. Critical information from a wide range of astrophysical phenomena is found within this region, including, for example:

- Thermal continuum emission from dust, gas, and solid bodies throughout the Universe;
- Molecular line emission from gaseous bodies such as star forming regions;
- Atomic line emission from galaxies, especially from hydrogen and helium;
- Free-free emission from ionized gas near hot, rapidly evolving stars;
- Synchrotron emission from relativistic electrons accelerated by shock waves or directed energy beams from black holes;
- Unique information on cosmic magnetic fields, arising from synchrotron radiation, Zeeman splitting, and Faraday rotation;
- Absorption signatures from thermal gas and synchrotron self-absorption.

The information available within the radio frequency band is critical to our understanding of these and other processes; in many cases it cannot be obtained in any other waveband. The two most powerful and flexible radio telescopes currently under construction are ALMA[8] and the EVLA. ALMA will provide an entirely new and state-of-the-art imaging capacity covering the frequencies from 30 to 950 GHz[9]. When completed early in the next decade, it will revolutionize our understanding of the processes governing thermal emission from cool gas, dust, and solid bodies throughout the Universe. However, ALMA will not operate below $\sim$ 30 GHz (and possibly not below 86 GHz), where non-thermal synchrotron emission and absorption, free-free (bremsstrahlung) emission and absorption from ionized gas, and many highly redshifted emissions from early Universe objects are found. Observations of these processes will be made within the 1 50 GHz frequency range covered by the EVLA. In addition, understanding the physics of thermal objects which can be usefully imaged by both ALMA and the EVLA will be greatly advanced from using both telescopes, as the lower frequency emissions originate from deeper in the object. With ALMA and the EVLA together, a more complete three-dimensional picture of the emission processes will be possible.

2.2.2 Coverage of Discovery Space by the EVLA

The EVLA Project will produce a telescope to allow sensitive observations within the area of 'Discovery Space' shown in Fig. 2.2. The project, for the reasons given in Section 2.3 has been divided into two overlapping phases: Phase I, which addresses the sensitivity, frequency coverage, and spectral resolution requirements; and Phase II, which addresses the spatial resolution requirements.

The improvement in coverage of 'Discovery Space' by Phase I is shown in Figure 2.3 (note that the abscissa and ordinate are reversed from Figure 2.2) . Also shown in the figure is the current coverage by the VLBA, and the expected maximum coverage by ALMA. The existing frequency coverage by the VLA is shown with light green trapezoids, while dark green shows the result of implementing complete frequency coverage between 1 and 50 GHz. To avoid confusion, the 27-antenna VLA, following Phase I, will be called the EVLA27. The improvement in frequency-resolution coverage by implementation of Phase I is impressive, but there is no expansion in the coverage to lower resolution, or to higher resolution, where the large gap between the VLA and VLBA – two orders of magnitude remains. This gap is a major barrier to a full understanding of the processes at work in our Universe.

The importance of covering these regions for the purpose of studying evolution of the Universe is shown by the superposed 'evolution lines', shown in red. The lowest shows the angular size and frequency evolution of a 2 kpc-scale object, (for example, galactic sub-structure) emitting at a rest frequency of 1420 MHz (the rest frequency of H I emission), between a redshift of 0.01 and 1.0. Without an expansion in capability to higher resolution and lower frequency, such objects will remain unresolved beyond $z = 0.1$. Similarly, the upper lines show the evolution of the angular size of a 50 pc scale object (left trace) and a 50 kpc size object (right trace) over all redshifts. (No frequency shift is shown here as a continuum observation is assumed). A 50 pc-scale source, when observed at 35 GHz, will be unresolved beyond $z = 0.05$ to the EVLA27. Objects at higher redshift can be detected, but not resolved. The need for a capability to image large-scale structure in the nearby Universe is demonstrated by the upper right trace, showing the evolution of a 50 kpc structure. Such a scale size can be imaged by the EVLA27 in the D-configuration at redshifts beyond 0.5, but subtends too large an angle at closer distance.

It must be emphasized that *imaging* the emitting objects in our Universe is essential to understanding their origin and evolution. Detection is not sufficient. Providing this imaging capability requires greater coverage of the frequency-resolution plane than that provided by Phase I. The great expansion in coverage provided by Phase II is shown in solid yellow in Fig. 2.4. Also shown in purple is the extra benefit obtained by combining the VLBA with the eight new antennas. The three evolutionary lines shown in the preceding figure are reproduced, and show that the completed EVLA will permit resolution of a hydrogen-emitting 2 kpc object out to $z = 0.4$ at 1000 MHz, and will resolve a 50 pc object at 35 GHz anywhere in the Universe. This same angular resolution will also allow the resolution of 1 AU-sized sources at 140 pc – the distance of the nearest star-forming molecular cloud.

The extra resolution coverage provided by Phase II of the Expanded VLA Project is needed to enable the

[8] Atacama Large Millimeter Array

[9] ALMA's final frequency coverage will depend on funding arrangements, including international agreements. The initial phase receivers will cover four bands, from 86 to 720 GHz.

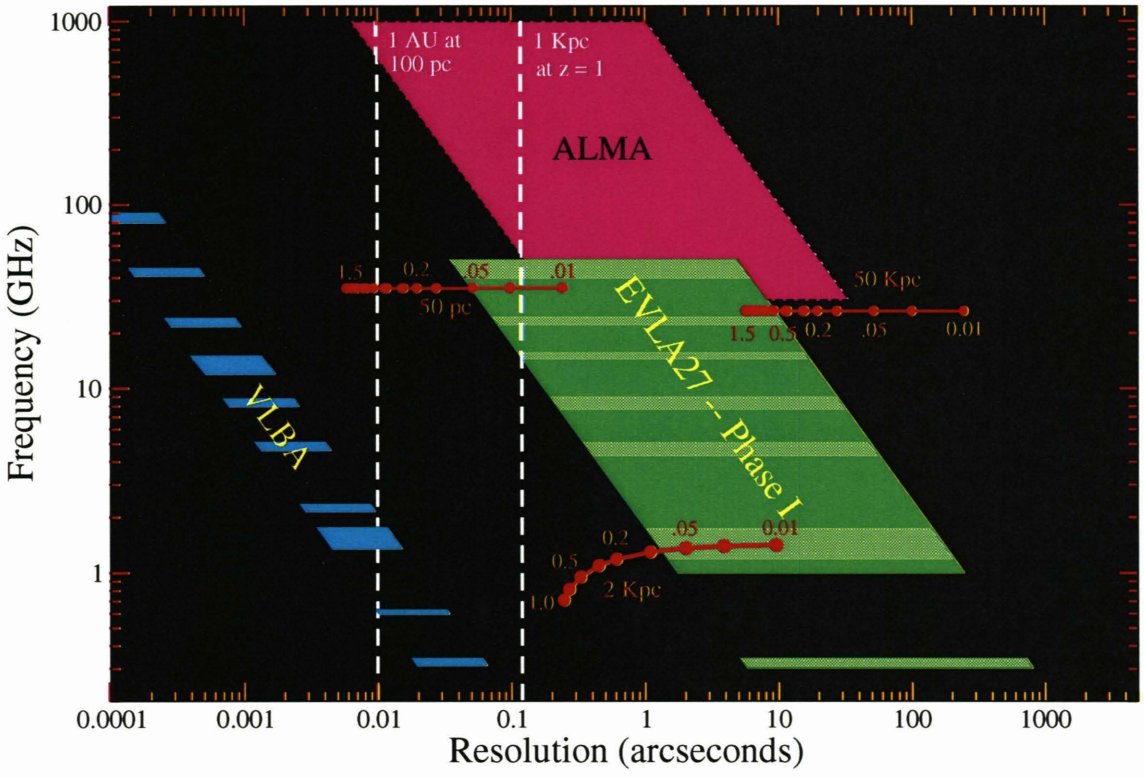

Figure 2.3: The frequency-resolution coverage after Phase I of the EVLA is shown in green, along with coverage by the VLBA and ALMA. The area covered by the EVLA will more than double that of the original VLA, shown within the narrow horizontal bands in light green. The vertical dashed lines show the angular size of an object of 1 AU in extent at the distance of 100 pc, and the angular size of a 1 kpc source at $z = 1$. The superposed red traces are 'evolution plots.' The lowest one shows the locus of observed frequency and angular size of H I emission from a 2 kpc object between $z = 0.01$ and $z = 1$. The present VLA cannot detect, or resolve, such an object in H I emission beyond $z = 0.1$. The upper traces show the evolution of the angular size of a 50 pc object (left) and a 50 kpc object (right) as a function of redshift between 0.01 and 30 (the minimum angular size occurs at $z = 1.6$). For these two examples, it is assumed the observations are made at a fixed frequency, so the frequency shift is not shown. A flat cosmology, with $\Omega_m = 0.27$ and $H_o = 71\,\mathrm{km\,s^{-1}\,Mpc^{-1}}$, is assumed.

EVLA to reach its primary goal: to be a powerful and flexible general-purpose radio telescope which can be used to resolve cosmic evolution, and to take full advantage of the unique information due to astrophysical emission processes operating at frequencies between 1 and 50 GHz.

2.2.3 Capabilities Provided by Phase II of the EVLA

Phase II of the Expanded VLA Project will add the following additional capabilities to those provided by Phase I:

- An improvement in resolution by an order of magnitude, providing tens of Kelvin brightness temperature sensitivity over the frequency range of 1 to 50 GHz. At the highest frequencies (18 to 50 GHz), a resolution better than 10 milliarcseconds will be obtained.
- Fast, high fidelity imaging of low-brightness ($\sim 10\mu$K) emission with tens of arcseconds angular resolution of objects whose extent exceeds the antenna primary beam.

Obtaining these capabilities will require the following:

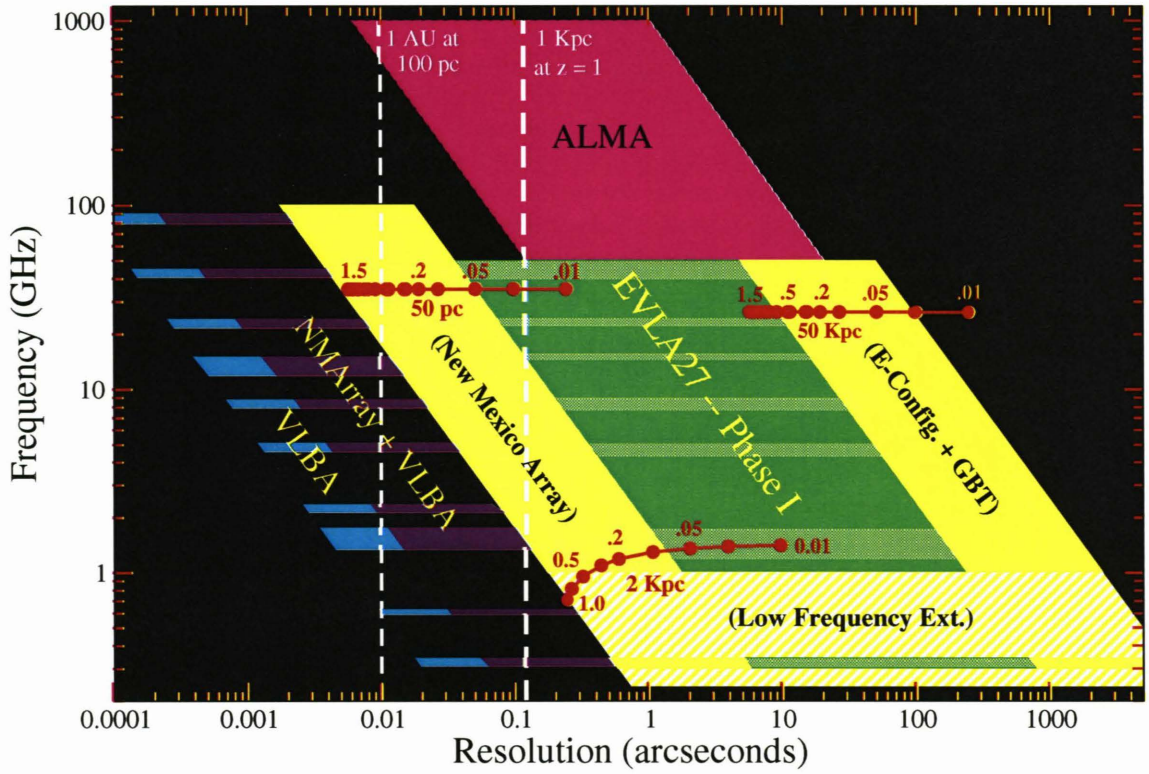

Figure 2.4: The frequency-resolution coverage after completion of the EVLA (Phase I in green, and Phase II in yellow) and ALMA projects, plus the incorporation of the VLBA into the EVLA. Phase II of the Expanded VLA Project will greatly increase the 'Discovery Space' area available to NRAO telescopes. The regions opened by each of the two components of Phase II are shown in yellow. The hashed yellow portion is the coverage available with a subsequent expansion of the low frequency capability. The 'evolution lines' from the last figure are reproduced, showing that combining the E-configuration and the GBT will allow imaging of 50 kpc structures as close as $z = .025$, and that 50 pc-scale emission will be resolved anywhere in the Universe with the addition of the New Mexico Array.

- Construction of eight new antennas, located at distances of up to $\sim$ 250 km from the EVLA center to provide baselines with lengths up to 350 km. These antennas will be outfitted with receivers which match those outfitted on the EVLA27 as part of Phase I, and with Mark 5 disk recording systems operating at 2 Gb/sec[10];
- Modification of the Pie Town and Los Alamos VLBA antennas to be fully compatible with those of the EVLA;
- Connection of the eight new, and the two upgraded VLBA antennas, to the EVLA correlator by fiber-optic lines, providing 16 GHz total IF bandwidth per antenna. These ten antennas will constitute a new subarray – the New Mexico Array (NMArray) – which will operate as a part of the EVLA in real time, or as a standalone array, or in combination with the VLBA;
- Construction of a new, compact E-configuration for the EVLA27 antennas, providing baselines ranging from 30 to 250 meters.
- An expansion of the WIDAR[11] correlator to 40 stations, to enable real-time correlation of the 10 New

[10]The disk recording requirement is based on a projection of VLBA capabilities in 2013. VLBA improvements would not provided by this project.

[11]Wideband Interferometric Digital ARchitecture – the formal name for the correlator designed and built by the Canadian Herzberg Institute for Astrophysics for Phase I of the project

Mexico Array antennas with the 27 EVLA27 antennas;

- Implementation of the WIDAR correlator's designed ability to allow correlation of disk-recorded data from the VLBA antennas simultaneously with real-time data from the EVLA. Data from the New Mexico Array antennas will be processed either in real time, or via disk recording.

Full details on these components are given in Chapters 4 and 5.

The result of these changes will create a single array comprising 45 antennas: 27 EVLA27, 10 New Mexico Array (comprising eight new and two upgraded VLBA antennas), and the eight remaining VLBA antennas. This array will be operated from a single site, using a single correlator. The EVLA and New Mexico Array antennas will have full-bandwidth, real-time correlation. The VLBA will remain a delayed-time system, utilizing the Mark 5 disk recording system at 2 Gb/sec[12].

This combined operations mode will permit a wide range of subarraying, including:

1. **The full 37-antenna EVLA:** When the EVLA27 is in its A-configuration[13], the EVLA27 and 10 New Mexico Array antennas will commonly be operated as a single, real-time subarray, providing maximum resolution, sensitivity, and spatial imaging characteristics. The eight remaining VLBA antennas will operate in a VLBI mode, using the Mark 5 disk recording system at 2 Gb/sec. Up to four other compatibly equipped antennas can be added to this VLBA subarray.

2. **The 27-antenna EVLA27 and the NMArray as separate arrays:** When the EVLA27 is not in its A-configuration, its 27 antennas will operate as an independent subarray, while the 10 New Mexico Array antennas could operate as a separate full-bandwidth, real-time subarray, offering excellent sensitivity and resolution. This will be ideal for astrometric and monitoring experiments which currently can only be done when the VLA is in its A-configuration. Any number of EVLA27 antennas could be added to the New Mexico Array, to improve spatial frequency coverage when needed. Concurrently, the eight remaining VLBA antennas, plus up to four other VLBI antennas, could operate as a separate subarray from disk recorded data at 2 Gb/sec.

3. **The EVLA27 and the VLBA+NMArray as separate arrays:** With the EVLA27 operating as a single 27-element real-time subarray, the ten New Mexico Array and eight remaining VLBA antennas, plus up to eight other VLBI antennas, could operate as a disk-based system at 2 Gb/s.

There are many more combinations available. A comprehensive description of the possible subarraying is in EVLA Memo #50.

When long distance broadband data transmission becomes economically feasible, the VLBA and the EVLA will be operated as a single, flexibly configured telescope, running in real time. This future capability will not be provided by this project.

2.3 The Two Phases of the Expanded Very Large Array Project

When completed in 1980, the VLA provided an order-of-magnitude improvement in resolution and sensitivity over all other radio telescopes. These improvements, combined with its imaging fidelity and speed, have made it the most heavily used and productive radio telescope in the world. But the VLA's fundamental capabilities have changed only slightly since 1980, as few resources were available to take advantage of rapidly improving technologies. The NRAO was only able to make incremental improvements to some subsystems, and to expand the array's frequency coverage through addition of three new frequency bands.

By the 1990s, it was clear that the gap between the capabilities of the existing VLA and those which would be enabled through application of new technologies was so great that the most effective approach would be a comprehensive redesign of the VLA's electronics, rather than a piecemeal application of new technologies in specific areas. A general goal of improving the VLA performance by an order of magnitude in all its capabilities was defined, and a comprehensive plan to achieve this was developed in the late 1990s.

[12]This provides 512 MHz of bandwidth when running at 2 bits/sample.

[13]The VLA has four configurations, known as 'A', 'B', 'C', and 'D', with maximum baselines of 35, 10, 3.5, and 1 km, respectively.

However, it became clear that some of the technical problems associated with certain components of the plan could not be solved in time to prepare a single proposal ready for submission by mid-2000, and it was decided to split the proposal into two, roughly equal halves. The first half included those components for which the technical solutions needed were already in hand – frequency coverage, receiver sensitivity and bandwidth, wideband fiber optic data transmission over moderate distances, and a wide-bandwidth correlator. The proposal for this first phase was ready for submission to the NSF by mid-2000, at the same time the initial 2000 AASC report was issued.

The key remaining component of the EVLA project, an expansion of the array by a factor of ten, and two potential minor components, an array configuration designed for low surface brightness imaging, and a low-frequency capability, needed further technical studies before a proposal could be written. These studies, and the preparation of the Phase II proposal, were deferred until after the Phase I proposal was completed and submitted, and the project had begun.

National Science Foundation funding for the Expanded VLA Project began with Phase I funding in 2001. This initial phase of the project is now well underway, and its completion by 2012 will improve the sensitivity, frequency range, and spectral resolution of the array by typically an order of magnitude.

Once the first phase had begun, attention turned to development of a Phase II proposal. Technical issues concerning its major component – an expansion in resolution by an order of magnitude – have been satisfactorily resolved, and we are ready to proceed. We have also decided that one of the minor components – the addition of a low-frequency capability – had to be dropped from the project, as the technical problems have proven to be very difficult, and the estimated cost ($20M) too high.

2.4 Science with The Expanded Very Large Array

Astronomy is an observational rather than an experimental science. Starting with Galileo's first telescope, the major advances in astronomy have not come from testing theories or models, but from new discoveries of unexpected phenomena made possible by new instruments with new capabilities to explore the parameter space of sensitivity, frequency, angular, spatial, and temporal resolution. This has been particularly true in radio astronomy. Beginning with the discovery by Karl Jansky of previously unsuspected non-thermal radio emission, radio astronomy has provided the means for discovery of solar radio bursts, radio galaxies, quasars, pulsars, gravitational lensing, the first extra-solar planetary system, cosmic masers, the enigmatic rotation curves of galaxies leading to the discovery of dark matter, and the cosmic microwave background. All of these were unanticipated and all were discovered by scientists exploiting new observational capabilities provided by radio telescopes.

Completion of the EVLA will open up a new regime of discovery space with the improvement in sensitivity and angular resolution by an order of magnitude or more combined with unprecedented image quality. Using past history as our guide, we can anticipate a wide range of new science as a result of this expansion. For example, the EVLA will have sufficient sensitivity to detect galaxies with active galactic nuclei (AGN) and star forming regions at the highest redshifts, unimpeded by the obscuration from the surrounding gas and dust which limits observations at optical, infrared and even millimeter wavelengths. The EVLA will have sufficient angular resolution to distinguish between star-forming regions and AGNs, and to image regions of star formation at any redshift. Within our Galaxy, the EVLA will be able to image both the thermal and non-thermal emission from thousands of stars as well as all the novae. Using the new EVLA frequency bands, observers will be able to image the intensity and polarization of the non-thermal radiation from both galactic stars and distant galaxies at constant angular resolution. This will give unique insight into the magnetic fields which pervade the cosmos.

The EVLA will operate at full sensitivity from 1 GHz to 50 GHz. Throughout this frequency range the EVLA will provide a resolution range extending over four orders of magnitude thus providing high quality selectable imaging capabilities better than those of any other telescope operating at any wavelength, on the ground or in space. The EVLA will provide for the next generation of astronomers what the VLA has for the last – a flexible, powerful telescope for research in astronomy, operating at meter-to-millimeter wavelengths.

2.4.1 Science with the EVLA Enabled by Phase II

The EVLA's unique imaging capabilities on the milliarcsecond scale combined with μJy point-source sensitivity result in an extraordinarily wide range of anticipated unique and original science. A comprehensive survey of expected scientific benefits provided by the completion of the Expanded VLA Project is given in Chapter 3 and in Appendix A. Among the prominent examples are:

- AU-scale imaging of local star forming regions and proto-planetary disks, to probe the intimate connections between accretion and outflow;
- resolution of the dusty cores of galaxies, to distinguish star formation from black hole accretion, and to provide an unbiased census of both processes over most of the age of the Universe;
- providing the highest resolution images at any waveband of the earliest galaxies – even as far back as $z \sim 30$, should such galaxies exist;
- imaging of galaxy clusters with 50 kpc or better linear resolution at arbitrary redshifts, to understand structure formation throughout the Universe;
- resolution of the centers of galaxies and quasars, to understand the environment and formation of relativistic jets at all cosmic epochs;
- imaging of thermal sources at milliarcsecond scales, including stellar photospheres, proto-planetary disks, and H II regions;
- mapping the three-dimensional distribution of both temperature and density in nova shells;
- resolving individual compact H II regions and supernova remnants in external galaxies as distant as M82;
- tying together the optical and radio reference frames with sub-milliarcsecond precision;
- measuring accurate parallax distances and proper motions for hundreds of pulsars as distant as the Galactic center;
- measuring the velocity and acceleration of the ionized gas within a few tenths of a parsec of the Galactic center, thus giving dynamical information on the gravitational effects of the nearest super-massive black hole;
- resolving extragalactic accretion disks on parsec scales, by observing optical depth effects over factors of ten or more in frequency;
- imaging central starbursts surrounding active galactic nuclei (AGNs), to separate the energy contribution from each,
- providing 50 pc or better resolution for galaxies at any redshift, helping to distinguish star formation from AGN activity, mapping the magnetic field strength and structure, imaging H I absorption lines, and probing the surrounding intergalactic medium;
- imaging flares in nearby giant and supergiant stars; and
- monitoring and imaging the full evolution of the radio emission associated with X-ray and other transients.

As was the case with the VLA, the vast new area of 'discovery space' which will be opened by the EVLA holds the promise of many unanticipated or serendipitous discoveries, and makes it likely that the most important discoveries to be made cannot be anticipated. The greatest impact of the EVLA will thus be measured not by the answers to today's questions, but by the answers to the questions raised by tomorrow's observations.

2.5 Synergies of the EVLA with Other Future Telescopes

Nearly all aspects of modern astrophysics require observations made throughout the electromagnetic spectrum. Each frequency band carries its own unique information and the instrumentation and techniques differ in each band. The EVLA will cover the frequency range from 1 to 50 GHz, or a factor of 50. It will combine the best sensitivity with the widest range of resolution of any telescope in radio astronomy. The EVLA will complement the current and next generations of instruments operating in other parts of the electromagnetic spectrum, including for example:

- at millimeter and submillimeter wavelengths: ALMA, SMA[14], CARMA[15], PDBI[16], and the LMT[17];
- in the infrared: SST[18], SOFIA[19], HERSCHEL, JWST[20] and SAFIR[21];
- in the X-rays: Constellation-X and EXIST[22];
- in the γ-rays: GLAST[23];
- in ground-based optical/IR: Numerous planned and operating large-aperture or interferometric facilities, including LSST[24], GSMT[25], TMT[26], LBT[27], the Keck interferometer, the VLTI[28], NPOI[29], CHARA[30] array, and the MRO[31] array.

For maximum impact, the EVLA should be completed in time to match the operational windows of the listed facilities.

Among the main problems which will be addressed by the infrared and millimeter-wave facilities are star formation in the Galaxy, and galaxy formation in the early Universe. For star formation, optical and near-infrared observations provide spectacular images and detailed spectroscopy of relatively dust free regions, while millimeter and submillimeter telescopes map out the molecular gas and thermal dust emission. The EVLA in turn will fill out the picture by imaging the most obscured regions in proto-stellar disks where planets might form, mapping out the acceleration regions of thermal and non-thermal jets, and providing the complete spectral information needed to disentangle synchrotron, thermal gas, and dust emissions from AGNs and supernovae in regions of active star formation.

Similarly, optical and infrared instruments are used to measure redshifts and emission lines in the most distant galaxies, and to trace the detailed morphology of these sources at the wavelengths most often studied locally. Observations with ALMA, SST, and SOFIA will be sensitive to the bulk of the luminosity of starburst galaxies shrouded in dust, and will allow astronomers to follow the evolution of the molecular gas from which stars are formed. The EVLA will give important complementary data on the cosmic evolution to $z = 0.4$ of the hydrogen content of galaxies, as well as the redshifted low-order transitions of such vital molecules as carbon monoxide. The EVLA will see through the dust to image ultraluminous infrared galaxies with unparalleled angular resolution, showing the relative contributions from active galactic nuclei and star formation regions, providing an independent dust-free estimate of the rate at which stars are formed, and simultaneously measuring the strength and orientation of the magnetic fields.

[14] Sub-Millimeter Array
[15] Combined Array for Research in Millimeter-wave Astronomy
[16] Plateau de Bure Interferometer
[17] Large Millimeter Telescope
[18] Spitzer Space Telescope, formerly known as SIRTF – Space InfraRed Telescope Facility
[19] Stratospheric Observatory For Infrared Astronomy
[20] James Webb Space Telescope, formerly known as the Next Generation Space Telescope
[21] Single Aperture Far InfraRed Observatory
[22] Energetic X-ray Imaging Survey Telescope
[23] Gamma-ray Large Area Space Telescope
[24] Large Synoptic Survey Telescope
[25] Giant Segmented Mirror Telescope
[26] Thirty Meter Telescopes, formerly known as CELT – California Extremely Large Telescope
[27] Large Binocular Telescope
[28] Very Large Telescope Interferometer
[29] Navy Prototype Optical Interferometer
[30] Center for High Angular Research in Astronomy
[31] Magdalena Ridge Observatory

While individual telescopes such as the HST[32] and the VLA have clearly had an enormous impact, multifrequency studies provide much better insight into astrophysical phenomena. The importance of radio data is illustrated by high resolution VLA observations used to locate distant galaxies detected at submillimeter wavelengths by low resolution confusion limited SCUBA[33] observations; by studies of high redshift quasars found optically by the Sloan Digital Sky Survey; and by deep VLA imaging of the Hubble and Chandra[34] Deep Fields and the SST First-Look Survey field.

The connection between radio and high-energy observations is perhaps more dramatic, since both trace highly energetic phenomena. Many target-of-opportunity proposals on ASCA[35] and RXTE[36] were triggered by VLA radio observations, and *vice versa*, with the VLA providing sensitive and comprehensive monitoring, as well as imaging, of the jets accelerated by black hole X-ray binaries. The X-ray/radio correlation for active stars is as tight as the far-infrared/radio correlation for star-forming galaxies, with correspondingly important implications for energy loss mechanisms. On larger scales, Chandra, and XMM-Newton[37] provide vital information on the amount and distribution of hot gas in galaxy clusters, while the VLA traces the equally pervasive magnetic fields and relativistic particles which provide the power sources for cooling cores of clusters. Similarly, the same active galactic nuclei which emit the gamma-rays which will be seen by INTEGRAL[38] and GLAST are generally strong radio sources. The VLA provides accurate light curves as well as sensitive probes of both continuum and line absorption in these objects, giving unique information on the accretion disks and any obscuring material, as well as on the active galactic nuclei themselves. At the same time, higher resolution imaging with the VLBA gives unique insight into the kinematics of these enigmatic objects and relates the flow of relativistic plasma to the high energy radiation.

Finally, while GLAST will find and localize gamma-ray bursts, and JWST and Keck track their optical light curves, find their host galaxies, and measure their redshifts, only the EVLA will be able to provide extinction-free statistics on gamma-ray burst afterglows, follow the emission from the initial relativistic fireball to the late sub-relativistic stage, and directly measure source sizes and expansion rates. Full realization of the potential of X-ray and gamma-ray satellites requires the complementary radio observations that only the EVLA will provide.

The EVLA with ALMA and SST

The EVLA will provide an excellent match to both ALMA and SST, as illustrated in Figure 2.5. This shows the anticipated continuum sensitivities of the EVLA, ALMA, and SST (formerly SIRTF), along with the spectrum of the ultra-luminous starburst galaxy, Arp 220, redshifted to z = 0.5, 2, 8, and 32. The EVLA will easily detect the redshifted thermal emission from such high-luminosity objects, and will be essential for observations of the non-thermal, and optically-thin thermal emission at all redshifts. Observations of the thermal emission at lower frequencies will typically see deeper into the source, and hence provide information on conditions closer to the center. Higher frequency emission comes from further out, as the opacity due to dust is higher at higher frequencies. An understanding of the physical processes at work in such objects requires complementary imaging capability over the entire frequency range of source emission.

An excellent example of the benefit of complementarity between telescopes operating in different frequency bands is given by the recent discovery of CO emission from J1148+5251, a galaxy discovered by the SDSS[39], at z = 6.418 by Walter, Carilli, and Lo (2003). The CO emission from the 3 2 transition was observed at 46.6 GHz with the VLA. Confirmation that this weak emission line is indeed from CO was provided by subsequent observations of the 6–5 and 7–6 transitions at 93.2 and 108.7 GHz respectively by the PDBI. Three telescopes in three different wavebands – optical, millimeter, and radio were combined to produce this result. This example also underscores the need for continuous frequency coverage. Figure 2.6 shows the observed frequencies and apparent angular sizes for 1 kpc-scale CO emission at various redshifts. The dark red circle marks the frequency of the observed 3–2 transition fortuitously lying within the existing 40 –

[32]Hubble Space Telescope
[33]Submillimetre Common-User Bolometer Array
[34]Chandra X-ray Observatory
[35]Advanced Satellite for Cosmology and Astrophysics
[36]Rossi X-ray Timing Explorer
[37]X-Ray Multi-Mirror Mission
[38]INTErnational Gamma-Ray Astrophysics Laboratory
[39]Sloan Digital Sky Survey

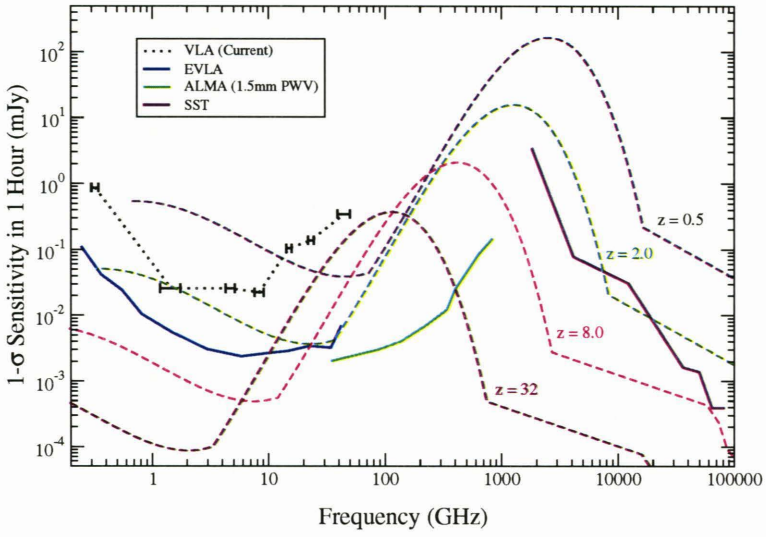

Figure 2.5: The spectra shown by the dashed lines are of the luminous star-forming galaxy Arp 220 as it would appear at the annotated redshifts. The large 'bump' is due to infrared emission from warm dust; the low frequency 'tail' is due to synchrotron and thermal gas emission. Separation of these components requires observations over a range of frequencies sufficient to span these spectral signatures. The EVLA, ALMA, and SST are all needed for studies of such objects over a wide range of redshift.

50 GHZ VLA band. The stronger 2–1 and 1–0 transitions both lie outside existing bands, and hence are not observable to the VLA. The full frequency coverage provided by the EVLA and ALMA in the radio and millimeter bands are required to provide the maximum information from such systems at any redshift.

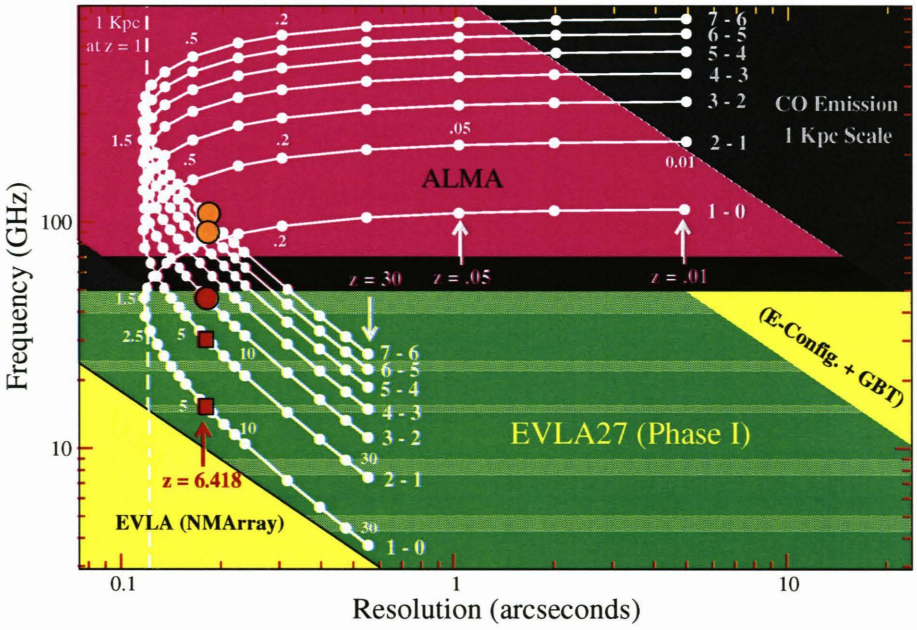

Figure 2.6: This figure shows the angular sizes and frequencies for CO emission from the noted transitions for a 1 kpc-scale object at various redshifts. The observed CO 4–3, 6–5 and 7–6 transitions from J1148+5251 are marked by the red and orange circles. Two other transitions, 1–0 and 2–1, which lie outside the VLA's current frequency coverage, are marked with red squares. The horizontal black band marks the 50 – 70 GHz band blocked by atmospheric oxygen. The full frequency coverage provided by both the EVLA and ALMA are needed for investigations of such emission from high redshift sources.

2.6 The Broad Impact of the Expanded Very Large Array

Astronomy is the science of the Universe, and of our place in the Universe. The spectacular images provided by the HST, the VLA, and other front-line telescopes are eagerly sought by the media and the public. The public's curiosity about the Universe is broad, and we should be pleased to continue to satisfy this curiosity, for it is the public which ultimate pays for new facilities and for research.

The ultimate reason for astronomical research, and this project, is to give mankind a better understanding of our place in the Universe. During the next decade, the EVLA, combined with ALMA, JWST, and many other major new observatories currently under development, will reveal more fully the story of cosmic evolution. What we learn from these facilities and the research they will enable will be communicated to the public through a variety of media, aided by our EPO programs. The discoveries which will be made will help clarify the currently incomplete and murky picture of our Universe, and will be the EVLA's greatest impact, and greatest legacy.

The EVLA will provide the NRAO with a valuable opportunity to expand its Public Education and Outreach program. We are preparing an accompanying EPO proposal whose goals and impact are summarized below.

2.6.1 Public Education and Outreach

The Very Large Array is one of the most scientifically productive telescopes on the world. More than 2,200 researchers from around the world have used the VLA for more than 10,000 different observing projects. Nearly 200 refereed journal articles per year are produced using VLA data. It has made a significant contribution to our knowledge in all branches of astronomy, from planetary astronomy to cosmology. It crosses specialty boundaries in astronomy, and its ripple effect also expands into physics, chemistry and technology.

The impact of the VLA in the public sector is at least as great as that for the astronomical research community. Millions of people have been introduced to the Very Large Array, and to the excitement of astronomy, through numerous documentaries and educational films. The array has played a significant role in feature films, commercials and print ads, making the VLA the most widely recognized telescope array in the world. Photographs of the array and of the celestial images it has produced are seen in magazine articles and textbooks[40]. These visual images serve to inspire the public, more than 50,000 of whom journey to visit the VLA site each year. The VLA Visitor Center exhibits and guided tours acquaint the public with radio astronomy. Seeing the magnificent antennas in person inspires the imagination and encourages further inquiries by the curious to learn more about 'what's out there', thus promoting a society that is scientifically and technically literate. For our visitors, the VLA serves as a stimulus to learn about astronomy, and about our place in the Universe.

The powerful new observational capabilities of the Expanded VLA will keep the instrument at the frontiers of science, and allow the scientific community to make fundamental new discoveries. Such discoveries, disseminated through the news media, schools, museums and other means, will excite and inspire the public and young people, further enhancing the nation's scientific literacy. Young people who are inspired by such discoveries to enter scientific or technical career fields will form the backbone of the high-tech workforce that will ensure the nation's continuing economic competitiveness.

The National Radio Astronomy Observatory has a unique opportunity to complement the intellectual merit of the Expanded VLA Project with an education and public outreach program which will target the communities near the antenna sites, the citizenry of New Mexico and the U.S., and, indeed, an international audience. The NRAO plans to implement teacher workshops, student field trips, dynamic exhibits, information sessions, and a traveling astronomy van as the tools used close to home. Broader impacts will be realized through the use of the World Wide Web, exhibits placed at observatory visitor centers and museums throughout the southwestern United States, and information disseminated at national teacher and science center workshops. As the Very Large Array expands, so will its audience and the opportunity to promote science literacy, astronomy, and radio astronomy through education and public outreach efforts. To reach these goals, a separate proposal is being prepared for submission to the NSF.

[40] A recent prominent example is Time magazine's placing the VLA on both covers of its recent special edition 'Great Inventions'.

A critical aspect of any outreach program is the collection, generation, and distribution of the spectacular images produced by the array. We plan to add to our staff a full-time EPO scientist with the responsibility to oversee these critical activities.

Impact on the Local Community

The local communities which are home to NRAO employees will enjoy a major benefit: the full-time presence of well-educated, technically-adept, community-active individuals and their families who will contribute far more to their communities than just their tax dollars and local expenses. NRAO employees have been in the past, and will continue to be in the future, heavily involved in local government, support of schools, community service organizations, and youth activities. The EVLA will increase the number and extent of these vital community support activities.

Impact on New Mexico

Even though the EVLA is located near the center of the state, it is too far away from most schools for a one-day field trip, and overnight trips are generally cost and time prohibitive. With the new NMArray antennas distributed throughout the state, we will be able to bring antenna technology closer, making tours and educational resources more accessible to more of the state's school-aged children. News releases of local lectures and special events will increase New Mexicans' awareness of this scientific instrument and stimulate their interest, encouraging attendance at the events and a trip, not only to the nearby antenna, but to the central array as well.

Classroom presentations, lesson plans, and teacher and student workshops focusing first and foremost on residents of New Mexico will help our schools address national science standards by using local resources and making science applications more real to the school and general population.

We expect to see increased vacation visits to the array by families and by teachers seeking a personal experience over the summer, thus bringing more tourism dollars to the state and to local communities.

Impact on the Nation

Education and public outreach programs pertaining to the EVLA will serve as models for other observatory and science museum outreach programs, especially those serving areas of similar geography and demographics. Workshops presented at national conferences, such at the Association of Science and Technology Centers and the National Science Teachers Association will disseminate the information about the programs and provide a platform for forming future education collaborations.

Beyond this, the nation will see a distinct rise in the number of and excitement in news releases associated with discoveries made by the EVLA an NSF-supported facility open to researchers from around the world.

Impact on the World

The increased media attention from the scientific discoveries by the national and international users of the EVLA, along with the NRAO's heightened education and public outreach programs will raise the public's awareness and appreciation for U.S. radio astronomy discoveries and bring them an understanding of our place in the Universe. It will generate increased interest in science and astronomy, providing resources, both written and on the Web, for further exploration by curious individuals. That these discoveries and capabilities are made by a U.S. built and operated facility, open to the world's astronomers, will enhance the world's appreciation of U.S. support of science and education.

Impact on Knowledge

As a telescope which will be a 'great observatory' in every sense of the phrase, and will be the leading radio telescope in the world for the scientifically rich 1 – 50 GHz frequency band, the EVLA can be expected to vastly increase our knowledge of the Universe, and of mankind's role within the Universe. Research conducted with the EVLA, in conjunction with knowledge obtained from other instruments in other wavebands, will expand not only our cosmic horizons, but will surely stimulate the minds of generations to come.

2.6.2 Impact on the University Astronomy Community

The NRAO's primary function is to provide world-class radio astronomy facilities to the astronomical community. The health of the field depends on continued support of these researchers and regular addition of new scientists into the discipline. Our user community is large, consisting of nearly one thousand astronomers from throughout the world, located at both well-known research institutions and at smaller, undergraduate-dominated teaching institutions. More than 200 individuals have received PhDs, about half of which are from U.S. universities, for work based wholly, or in large part, on data taken with the VLA.

Our goals are to serve this diverse community and to involve our users in making decisions about the future of the discipline. Furthermore, by providing exciting new capabilities, we can collaborate with the universities to ensure a continuing flow of new talent, both technical and scientific, into the field. The VLA has always been a key element in the NRAO's efforts to train the researchers of the future in radio astronomy, via week-long summer schools, summer student programs, and visits by numerous graduate students for terms ranging from a few days to a few years. The continuation of this process of training tomorrow's researchers requires an instrument with state-of-the-art technology to address the scientific challenges of today. The best students will want to work at the best facilities. To fulfill these functions, we must have a telescope capable of addressing the key scientific issues of the day.

The primary impact of the Expanded VLA Project on the university community will be to provide an instrument with much better sensitivity, spatial and spectral resolution, and frequency coverage, to enable better research. This enhanced capability will encourage more university faculty to utilize the instrument, and will encourage more students to take up astronomy as their choice of study.

The AASC recommended development of a program to support increased user participation in and utilization of research facilities such as the EVLA. The Committee recommended an annual funding level of 3% of the capital cost of the facility for this corresponding to \$5.5M/yr for the EVLA. The NRAO endorses this recommendation and will encourage the NSF to establish such a program.

2.6.3 Foreign Involvement

Phase I of the Expanded VLA Project is being jointly funded by three countries. The Mexican research foundation Consejo Nacional de Ciencia y Tecnología (CONACyT) has awarded a grant of \$2M to the project, and an agreement with the Canadian Herzberg Institute for Astrophysics (HIA) for an investment of \$14M is now complete. The Mexican commitment will be used for construction of electronics modules and other components. The Canadian commitment is to design and build the Phase I correlator, which is designed to enable straightforward expansion to encompass the EVLA Phase II requirements. These partnerships will provide improved performance at a lower cost to the U.S., as well as take advantage of technical expertise in these countries.

The Expanded VLA Project will keep the NRAO and the United States at the center of centimeter wave astronomy by ensuring that the VLA's sound infrastructure is the base on which we build in the future. The more advanced instruments of the future will require multi-national involvement, and the Expanded VLA Project will build the relationships that will lead to significant benefits to the U.S. from such worldwide efforts. In fact, the relationships built up over many years of VLA operations have been vital to the creation of the international consortium that is now constructing the ALMA telescope.

2.6.4 Technical Development

The EVLA will be a major developer and user of networked information systems. The 37 EVLA antennas will each be sending to the central correlator approximately 100 Gb/second via a partially owned and partially leased fiber optic network. The aggregate of 3.7 Tb/sec will be conveyed over fiber that is already in place.

The theoretical maximum correlator output will be about 30 GB/sec. Although the EVLA will rarely operate at such an output rate (the currently planned maximum rate is 1.6 GB/sec, and the initial rate will be a relatively modest 25 MB/sec), the archiving and processing requirements for the normal observing modes will be extremely challenging. Part of the requested budget is for development of the archiving and processing systems which will be needed to handle the anticipated data flow; these systems will provide the calibrated data and images provided as a resource through the National Virtual Observatory. The solutions

to these problems will be applicable to a considerably wider audience – future instruments such as LOFAR and the SKA will be faced with similar, or larger, data transfer, storage, and processing challenges.

The processing of the EVLA's data output will present another stimulating technical challenge, as databases as large as ~50 TB will be used to generate the images required by astronomers[41]. These images can be exceedingly large up to 32,000 × 32,000 pixels for each of hundreds to thousands of frequencies. Each image must be corrected for the temporal and spatial errors created by the atmosphere, the antennas, and the instrumental electronics. Included in this project would be funding to establish an imaging research group which will develop and implement the specialized algorithms needed to enable efficient large-scale imaging with very large databases.

The EVLA will also encourage development of, and be the test-bed for, the technologies needed for the next generation radio telescope the Square Kilometer Array – a facility which may have up to 50 times the sensitivity of the EVLA. The linkage between the EVLA and the SKA is discussed in Section 2.7.4.

2.6.5 A Wide-Bandwidth Real-Time Distributed Network

Phase II of the EVLA project will develop a wide-bandwidth, real-time fiber-optic network to ten remote sites within the state of New Mexico, using already available commercial fiber. The establishment of this network will be attractive to other projects which need real-time access to data taken over a wide geographical area, and will encourage such projects to locate within New Mexico. Examples include:

- A low-frequency radio astronomy telescope, the Low Frequency Array, being promoted by a consortium led by the University of New Mexico, and including the University of Colorado, the University of Texas, LANL, and NMIMT. This facility would cover the 10 – 90 MHz frequency range, and would comprise dozens of remote sites spanning southern New Mexico. The project would utilize and expand the network being set up by the EVLA.

- The Square Kilometer Array (SKA), a 'next-generation' radio telescope with goals of one square kilometer of collecting area and approximately 50 times the sensitivity of the EVLA, with perhaps hundreds of remote sites, with baselines extending to a few hundred kilometers. The US Southwest is a viable site for such an array, and development of the infrastructure by the EVLA will provide a powerful incentive for location of this major international project in New Mexico.

- EarthScope, a $200M interdisciplinary Earth Observatory designed to answer fundamental questions about earthquakes, volcanoes, continental evolution, hazards, and Earth structure, is the first NSF MRIFC project in the history of Earth Science. One of the two core EarthScope seismology components, the USArray, is a massive moving 10-year deployment at 2000 seismograph sites (400 sites at a time, with real-time data delivery), designed to scan the interior of the Earth. EarthScope is interested in locating some of their sites in proximity to ours, in order to utilize our real-time data transport systems.

The establishment of a real-time wide-bandwidth distributed fiber-optic network for the EVLA can be expected to attract other projects with similar data collection requirements, as the technology needed to access and utilize the extensive optical fiber already in place within the state will be implemented by the EVLA Project.

2.7 The EVLA and Other Present and Future Radio Telescopes

There are many radio telescopes, including the present VLA, operating in the 1 to 50 GHz frequency band. However, none has the *combination* of speed, flexibility, sensitivity, spectral and angular resolution and range, and image fidelity which the EVLA will provide. Other radio telescopes are optimized for performance in some key parameter such as collecting area or resolution at the cost of flexibility and capability in other areas. For example, the Arecibo radio telescope has much more collecting area than the VLA and is a powerful instrument for observing pulsars or H I in distant galaxies. But, it has limited sky coverage, inadequate

[41] The EVLA's fundamental database comprises measures of the spatial coherence function, rather than the spatial brightness images produced by direct imaging telescopes. The two are related through a Fourier transform.

resolution for imaging most radio sources, cannot operate above 10 GHz, and its sensitivity for continuum observations is limited by confusion[42]. The GBT[43] has full sky coverage, but has poorer resolution, and higher confusion, than Arecibo. However, either of these telescopes, when combined with EVLA E-configuration data, will provide unprecedented sensitivity, resolution, and image quality for studying low surface brightness radio sources.

2.7.1 MERLIN and e-MERLIN

The facility which most closely matches the resolution of the EVLA is the MERLIN[44] array in England. This facility comprises six antennas with a maximum baseline of ~210 km, and operates at five narrow bands between 151 MHz and 22.2 GHz. It is currently undergoing an upgrade ('e-MERLIN'), scheduled for completion in 2007, which will greatly increase its bandwidth and sensitivity at very modest cost. Like the EVLA, this is a leveraged project, utilizing already established infrastructure. Some of e-MERLIN's anticipated capabilities are similar to those of the EVLA: maximum point-source sensitivity of $\sim 1.4\mu$Jy, and full-field imaging.

However, e-MERLIN's bandwidth (2 GHz per polarization), tuning range (1.3 1.8 GHz, 4 – 8 GHz, and 22 – 24 GHz) and imaging capabilities will be short of those of the EVLA. Much of e-MERLIN's sensitivity is due to the 240-ft Lovell telescope, which can not operate above 8 GHz. e-MERLIN's sensitivity at 22 GHz will be more than a factor of 20 poorer than that of the EVLA, and the tuning range, above 8 GHz, will be limited to 22 to 24 GHz. e-MERLIN promises wide-field imaging through the use of bandwidth synthesis, but at low frequencies the field of view will be limited by the Lovell telescope to 10% of that of the EVLA, and imaging quality and sensitivity will be severely compromised by the need to downweight the five dominant baselines using the Lovell telescope. At high frequencies, the much smaller fractional bandwidth and smaller number of antennas (5 vs. the EVLA's 37) will severely limit full-field imaging capabilities. Only the EVLA will be able to offer full-field imaging capability over thousands of resolution elements, at any frequency between 1 GHz and 50 GHz.

2.7.2 The GMRT

The GMRT[45], located in India, is a large array consisting of thirty 45-meter-diameter fixed antennas specifically designed for use at frequencies below 1.6 GHz. Fourteen of these are located in a central one square kilometer area, the other 16 are sited along three arms, with a maximum baseline of 25 km. This facility is specifically designed for low-frequency operation, and at present supports observations in 5 discrete narrow frequency bands between 153 and 1420 MHz. Its factor-of-three advantage over the VLA in aperture area is approximately offset by a system temperature (at 1420 MHz) currently four times higher than the VLA's. As a fixed array, with a large central concentration of collecting area, the GMRT does not have the imaging flexibility of the configurable VLA. Its maximum resolution is a factor of 14 poorer than the EVLA's, and its correlator bandwidth of 32 MHz falls far short of the EVLA's new correlator (1 GHz at these low frequencies). This will especially limit projects requiring wide bandwidths – continuum experiments needing high sensitivity, and spectral line experiments requiring wide velocity range.

2.7.3 The ATA

The Allen Telescope Array (ATA) is a new array developed jointly by the SETI institute and the University of California, Berkeley. Employing novel off-axis 6.1 meter antennas, it will comprise up to 350 antennas, and will operate between 0.5 and 11 GHz in a phased-array mode for SETI and, with a correlator, as an astronomical imaging array. The antennas will be arrayed over a ~ 750 m extent, providing a resolution about three times that of the EVLA's E-configuration. In terms of low-surface brightness imaging capabilities, the capabilities of the ATA and the E-configuration of EVLA27 are within a factor of a few when the ATA is tapered to the resolution of the E-configuration. The ATA will have superior mosaicing speed, where ND

[42]This condition occurs when the mean separation of sources, at the sensitivity limit of the telescope, approaches ~7 times the telescope resolution

[43]Green Bank Telescope

[44]Multi-Element Radio Linked INterferometer

[45]Giant Metre-wave Radio Telescope

is the critical metric, and a superior point-spread function, which should permit faster deconvolution and higher fidelity. The E-configuration will have superior brightness temperature sensitivity, where ND^2/T_{sys} is the critical metric.

The critical advantage of the E-configuration, and the most important reason for its implementation, is that its identified key science will be obtained from the high frequency ($\nu > 18$ GHz) bands, which are not planned for the ATA.

2.7.4 Beyond the EVLA – the Square Kilometer Array

Over the past decade radio astronomers have been discussing the feasibility for a next generation radio telescope with a sensitivity more than an order of magnitude greater than that of the EVLA. Since the system noise temperature of existing radio telescopes is already approaching a minimum determined by the cosmic microwave background (CMB) and the atmosphere, the discussions have focused on how to obtain greatly increased collecting area at an affordable cost. A goal of constructing a radio telescope with an effective area of $10^6\,\mathrm{m}^2$ and system noise of 50K, thus providing a sensitivity of $\mathrm{A_e/T_{sys}} = 20,000\,\mathrm{m}^2/\mathrm{K}$ – about 50 times that of the EVLA has been adopted by an international steering committee. This proposed telescope is known as the Square Kilometer Array, or SKA.

It will be important that the SKA have sufficient angular resolution to avoid the effects of confusion at the high source density corresponding to the SKA continuum sensitivity as well as to adequately image, rather than just detect, distant galaxies. To achieve the resolution needed to keep confusion noise below the thermal noise for integration times longer than a few hundred hours, overall SKA dimensions of hundreds of kilometers at high radio frequencies to thousands of kilometers at low frequencies may be needed, although the precise requirements are unclear as the microjansky source density is unknown.

The cost of achieving the SKA sensitivity goal using conventional construction techniques is prohibitive. For example, the goal can be met by replacing each of the 45 elements of the VLA, the New Mexico Array, and the VLBA by large high efficiency low-noise radio telescopes such as the GBT. This will improve the sensitivity of the EVLA by about a factor of 25 and give good performance for frequencies between 50 MHz and 100 GHz. However, the cost of about 6 billion dollars is unrealistic, and there will be too few elements to achieve the dynamic range of 10^6 – 10^7 needed to fully exploit the sensitivity. For about the same price we could achieve comparable sensitivity by building 25 x 45 = 1125 EVLA type dishes. This could give improved image quality and better sidelobe suppression. However, the costs of broadband data transmission, correlation, and data processing will significantly increase this already unrealistic cost.

An SKA concept using smaller antennas in the range of 6 to 12 meters equipped with low cost MMIC[46] amplifiers and a novel broad band feed is under active study by the U.S. SKA Consortium. Other concepts are being studied elsewhere and include dipole arrays which allow instantaneous electronic steering of multiple beams, but which are limited to lower frequencies. The geographic requirements for the SKA of low radio-frequency interference (RFI) environment and low water vapor content combined with reasonable living conditions for the operations staff are similar to those of the EVLA. Thus, if located in the United States, the central configuration will be located in the desert southwest, probably at or near the current VLA site.

There are many challenges to successfully building the SKA, including cost effective broadband data transmission and correlation for thousands of spatially separated antenna elements, high dynamic range imaging and archiving, image pipelining, and achieving the desired collecting area over a range of 100 or more in frequency, all at reasonable cost. Current, optimistic cost projections are in the range of one to two billion dollars.

Most of the techniques and instrumentation being developed for the EVLA will be important in the planning for the SKA. This includes establishing criteria and evaluating remote station siting around New Mexico, advanced correlator designs, development of RFI excision techniques, the use of fiber optic broadband data transmission, configuration optimization, advanced imaging techniques including multiple-field calibration in the presence of non-isoplanatic screens, non-coplanar and high dynamic range imaging, pipelining and the creation and effective use of data archives. These are all critical problems which will limit the performance of the SKA, and which must be solved before an SKA can be designed and constructed.

Completion of the EVLA is an essential step towards defining the scientific program of the SKA, as well as addressing many of the technical issues. In particular we need to begin to explore the sub-microjansky sky

[46] Microwave Monolithic Integrated Circuit

with sub-arcsecond resolution in order to determine the source density at these very low flux density levels, as this will fix the array dimensions needed to avoid confusion. Also of concern is the effect of natural confusion due to finite source size this could limit the sensitivity no matter how large the array. Observations with the VLA and MERLIN have indicated that at the 10-100 μJy level, the median source size at 20 cm is about one arcsecond. However, as this is at the limit of the VLA's current sensitivity and resolution, it is important to extend these observations to lower flux density and better angular resolution, to see whether the SKA sensitivity will be limited by thermal noise or by natural confusion.

The EVLA is based on well established concepts using 25-m antenna elements and cooled low noise receivers. The main challenge for the SKA is to reduce the cost of building large collecting areas by an order of magnitude or more. If this can be accomplished, even if only over a limited frequency range, the new technology could be used to increase the collecting area of each of the ten sites of the New Mexico Array. We also plan to ultimately extend the real-time operation of the EVLA to each of the eight remaining VLBA antennas, so the sensitivity of the highest resolution observations may also be improved by locating additional collecting area at the VLBA sites, and by the wider bandwidths which are made possible by fiber access.

In this way it would be possible to approach the full capability of the SKA in a deliberate fashion, and at the same time maintain the viability of the radio astronomy user community during the long SKA design, development and construction period which may extend over several decades.

The VLA site may also serve as a support base for an array of 12-m class antennas being discussed by the JPL Deep Space Network. The JPL array is intended as a prototype for a much larger array to be used primarily for spacecraft tracking, but may also serve as one prototype for the SKA. NRAO is working with JPL in exploring the feasibility of placing this prototype array near the VLA and possibly participating in its operation. This would provide valuable experience in operating large arrays needed for detailed planning of the SKA. Later use of the same technology to increase the EVLA sensitivity or possibly to construct a larger SKA prototype would provide a smooth transition to the SKA itself.

2.8 Overview of This Document

The remaining chapters are specific to Phase II of the EVLA Project. We have argued in this chapter that only radio astronomy has the capability to image the formation and evolution of structure in our Universe on angular scales of tens of milliarcseconds – corresponding to physical scales of tens of parsecs or better anywhere in the Universe with brightness sensitivities of tens of Kelvin. The scientific potential of this unique capability is described in Chapter 3, which is focused on science opportunities involving evolution of structure in the Universe, and in Appendix A, which gives a comprehensive description of new science enabled by the EVLA from the full spectrum of astronomy.

We have described in this overview the basic technical capabilities in sensitivity and resolution needed to achieve this science. Chapter 4 expands on these, and gives the anticipated technical goals for Phase II of the project. The proposed means of achieving these requirements is given in Chapter 5. Also in this chapter will be found the specific technical capabilities of the completed EVLA sensitivity, resolution, brightness sensitivity, array configurations, etc.

We have argued that this project is a leveraged one – it builds upon the existing, major facility of the VLA that is already in place and operational. This approach results in significant savings in many areas – cost, schedule, and in long-term operations costs. Chapter 7 lays out the expected operational modes and costs for the completed array.

This document concludes with three appendices which provide supporting material for this Project Description. The first provides a comprehensive survey of anticipated science benefits which will be provided by the completed EVLA. These examples are selected from the full realm of astronomy, and illustrate the EVLA's broad relevence for modern astronomy. The second appendix provides a detailed description of the surface brightness sensitivity for both the EVLA and ALMA. This is a key – and widely misunderstood capability of imaging arrays. The final appendix provides details on the required re-location of the Los Alamos VLBA antenna.

Chapter 3

EVLA Key Science: Resolving Cosmic Evolution

Phase II of the EVLA Project is intended to provide important new scientific capabilities, which will lead to unique and fundamental contributions across the entire range of modern astrophysics. The primary goal of this phase of the Project is to exploit fully the superb sensitivity, flexibility, and imaging capabilities given by Phase I, by providing the highest possible spatial resolution, and the greatest possible surface brightness sensitivity. The scientific drivers are many and diverse, ranging from solar system radar imaging experiments, to the mapping of thermal emission from ionized gas in star forming regions, to imaging dark matter on galaxy scales through gravitational lensing. Virtually every experiment benefits from the highest resolution compatible with the available sensitivity, and many are simply impossible without adequate resolution to separate different physical regions. At the same time, many important observations lie at the limit of even the EVLA's sensitivity, and imaging large-scale, low surface brightness features requires concentrating all the movable antennas of the EVLA into the smallest possible physical area. These general considerations lead to the design described in the next several chapters.

This chapter concentrates on describing the scientific impact of the proposed second phase of the EVLA Project in one key area: cosmic evolution, from the formation of stars to the evolution of galaxies and galaxy clusters throughout the Universe. The first section deals with the contributions of the New Mexico Array in its most powerful mode, acting in conjunction with the VLA to create a 37-element array with ten times the resolution and ten times the sensitivity of the current instrument. Next we describe some key experiments involving the New Mexico Array in its other roles, providing short spacings for the VLBA, and working as a stand-alone instrument. The other major component of Phase II, the compact E-configuration, is dealt with in the third section. The final section summarizes the importance of the EVLA in creating a general purpose instrument, comparable and complementary to NASA's "Great Observatories" and front-line ground-based telescopes such as Keck and ALMA. A wider survey of possible experiments is given in Appendix A.

3.1 The Full EVLA: Imaging the Evolving Universe

Sensitivity and resolution are the two most important parameters of any telescope. The first phase of the EVLA provides a factor 10 or more improvement in continuum sensitivity, and an even larger gain in frequency coverage, compared with the current VLA. The missing element is ***spatial resolution***, to image what one detects. Much of the science is at the limits of the resolution currently available: the inner parts of accretion disks, the regions where jets are accelerated and collimated, shocks and interaction zones, the innermost dense cores in star forming regions, and the most distant galaxies. This is a strong driver for obtaining the highest possible resolution, together with high sensitivity and good image quality. Radio data are particularly important, because small, dense regions tend to be both complex and highly obscured. Radio observations provide a very different view of the Universe from those at millimeter or optical wavelengths, seeing through even the highest dust columns to image the innermost cores of these regions. Radio images are sensitive both to the thermal emission from dust and ionized gas, and to the synchrotron emission from relativistic particles. Disentangling these different processes requires imaging over a wide range of

radio wavelengths and similar resolutions. Similarly, understanding how these central cores relate to the total energy emission as seen in the submillimeter, and the outer envelopes traced by the starlight, requires comparable spatial resolution over the entire energy spectrum.

This is one of the key motivations for the New Mexico Array, the most ambitious part of Phase II of the Expanded VLA Project. Combining two VLBA antennas with eight new antennas spread over the state of New Mexico, the NMArray will provide baselines 10 times longer than the current VLA, giving a corresponding order-of-magnitude increase in resolution, and allowing astronomers to take full advantage of the corresponding sensitivity improvement given by Phase I. Furthermore, the resolution of the New Mexico Array, as high as ~ 2 mas, can be matched to that of ALMA, the VLTI, and the JWST, enabling true multi-wavelength studies at the same resolution. The resulting science is very diverse. Within the Milky Way, for instance, the full 37-antenna EVLA will map out the three-dimensional mass distribution of every new nova; measure accurate parallaxes for ~ 200 pulsars, to distances of $\gtrsim 8$ kpc; and provide accurate mass models for the inner few hundred parsecs of the galaxy, by measuring proper motions and ionized gas and circumstellar masers. In this section we illustrate two especially important areas of the resulting scientific opportunities, within the overall theme of cosmic evolution.

3.1.1 Massive Star Formation

Stars are fundamental to our study of the cosmos. On one level, the condensation of gas into stars, and its subsequent release in stellar winds and violent explosions, is one of the fundamental cycles in the Universe. On another level, the study of stars is the study of our own origins. The heavy elements out of which we are made – the calcium in our bones, the iron in our blood – were produced inside stars. The energy we depend on for life, the fuel which powers plant growth and thus produces the air we breathe and the food we eat, is the light of the nearest star. The very planet we live on was created out of the debris left over from the formation of the Sun. Some of our most basic questions what is the origin of life? is there life beyond the Earth? – are tied directly to the question of how stars and planets are created. Understanding the process of star formation is one of the great challenges facing astronomy in the 21st century.

The basic question of star formation is, how to concentrate enough gas into a small enough place for fusion to occur. The simple answer is clear: gravity! But the details are far from obvious. How is the angular momentum of the infalling gas removed? How is magnetic pressure overcome? Why is infall *universally* accompanied by outflow? Does the accretion process work the same way in high- and low-mass stars, despite the tremendous difference in radiant energy output? What determines the ultimate mass of the star?

The process of massive star formation in particular, and the related issue of what determines the likelihood of forming stars of a given mass (the initial mass function), has a profound impact on our understanding of the evolution of stars and galaxies throughout the Universe. Most of the luminosity emitted by an ensemble of stars is generated by the highest-mass objects, so observations of stars and star-forming regions at high redshift are in fact primarily measuring the massive star content of these distant systems. And yet, we do not understand the process of massive star formation in our own Galaxy.

The sensitivity and resolution provided by the full EVLA will play a key role in increasing our understanding of this important process. Most young, massive stars are located at large distances from the Sun, making sensitivity and resolution essential to detect these objects across the full extent of the Galaxy, and to eliminate the problem of confusion caused by multiple stars forming in clusters. Furthermore, the youngest regions remain deeply embedded in dense clouds of gas and dust, obscuring them at optical and infrared wavelengths. The dust emission can be optically thick even at millimeter wavelengths, and the tell-tale emission from gas ionized by a forming massive star may be obscured or confused by the dust emission at higher frequencies, such as those accessible to ALMA. By contrast, the ionized gas can be detected at EVLA frequencies, where the dust emission is optically thin, even in the most highly obscured parts of the Galaxy. Here we focus on two examples of possible science resulting from studies of massive star formation using the full EVLA: the use of the EVLA with the New Mexico Array to establish whether the jets, outflows, and disks commonly observed to accompany the formation of Solar-type stars also occur for massive star formation; and the connection between massive star formation in our Galaxy with that in external galaxies.

Accretion and Outflow in Massive Star Formation

A clear picture is emerging of how low-mass, Solar-type stars form from the gravitational collapse of a dense core in a molecular cloud (Lada 1999; Shu et al. 1999). Infalling material from the molecular cloud is funnelled onto the forming protostar via an accretion disk; these protostars are also observed to be accompanied by collimated jets and energetic winds (see Appendix A for more details), which are believed to be responsible for removing the angular momentum of accreting material, allowing the young star to grow in mass. However, a fundamental problem arises when the mass of the star exceeds $\sim 10 M_{\odot}$: the luminosity of the star itself becomes sufficiently high that radiation pressure can overcome the gravitational attraction of the forming star on the infalling material, thereby halting the accretion, and preventing the star from continuing to grow. And yet stars considerably more massive than $10 M_{\odot}$ exist in our Galaxy; how, then, do they form? Do low- and high-mass stars form via the same accretion processes, or do alternative, more exotic models, such as the coalescence of intermediate mass stars, need to be considered?

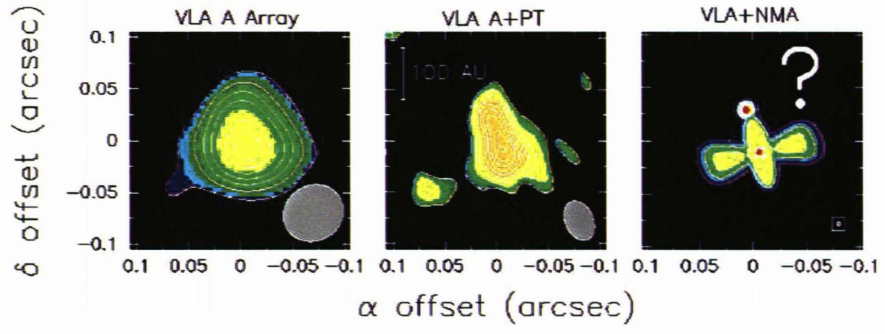

Figure 3.1: VLA 43 GHz images of the massive protostar G192.16−3.82. At a distance of ~ 2 kpc the source has a luminosity of $\sim 3 \times 10^3\, L_{\odot}$, which implies the presence of an early-B star with a mass of 8 to 10 $M_{\odot}$. The left panel shows an image using the A configuration alone; the middle panel shows the improvement from adding a single distant antenna from the VLBA (Pie Town). This emission is modeled as a central massive protostar surrounded by an 80 AU diameter disk (oriented roughly north-south), with a wide-opening-angle ionized outflow (roughly east-west); a companion protostar is also included, to account for the N/S asymmetry. The right panel shows what the New Mexico Array would see (accounting for thermal noise), if this model were correct. In all images, the synthesized beam is shown in the bottom right corner. Images courtesy D. Shepherd, based on Shepherd, Claussen, & Kurtz (2001).

There are various ideas of how radiation pressure can be overcome (e.g., Yorke 2002), but studies of massive star formation aiming to test these ideas face other problems. Few candidate massive protostars exist because the observed initial mass function implies many fewer massive stars compared with low-mass objects, and the lifetimes of these massive stars are very short. Furthermore, massive stars form not in isolation but in clusters, where the prodigious energy output of just one star of a few $\times 10 M_{\odot}$ can ionize and heat gas over several parsecs. The possible signatures of accretion and outflow, on the other hand, occur on small scales and can be lost in the confusion of these large-scale phenomena. These various factors combine to give only a very few examples of massive protostars to date, none of which is significantly more massive than $10 M_{\odot}$. One of the best examples is G192.16−3.82 shown in Figure 3.1, a massive protostar at $d \sim 2$ kpc with a high-velocity CO outflow on large scales. The best current VLA images (*center*) can barely distinguish the jet from the accretion disk. The full EVLA by contrast (*right*) would easily separate the two, and provide a detailed look at the disk brightness distribution, as well as the jet origin and collimation. The full EVLA will enable such studies to be extended to massive protostars all the way to the Galactic Center, thereby increasing the number of young, massive protostellar candidates, and testing whether massive stars form via accretion and outflow, or whether other mechanisms are at work.

Another example illustrates both the power of the full EVLA, and the gap in resolution that currently exists between the VLA and the VLBA. The Orion molecular cloud complex is the nearest region of massive star formation, located at a distance of ~ 450 pc. Embedded in the molecular cloud behind the well-known H II region, M42, is radio source "I," a massive protostar associated with SiO masers that trace the three-

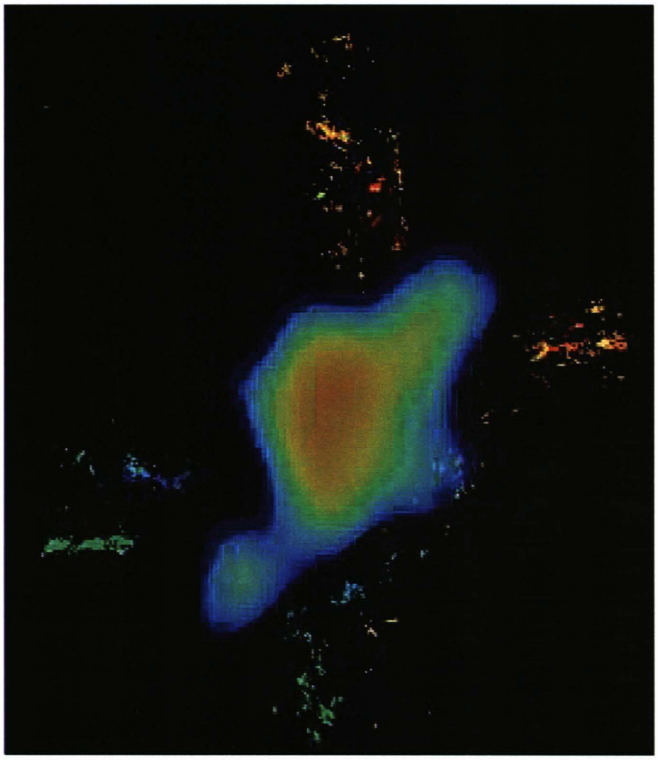

Figure 3.2: Source 'I' in Orion. The small dots are SiO masers, imaged using the VLBA with a resolution of 0.35 milliarcsec, equivalent to 0.16 AU at a distance of 450 pc. The colors of the dots represent the line-of-sight velocity of the SiO masers, and show a clear gradient from blueshifted masers in the south and east, to redshifted masers in the north and west. It is possible that this motion is the result of rotation in a disk about an axis oriented north-east to south-west. Superposed on the VLBA image is thermal radio continuum emission detected using the VLA at its highest current resolution (A configuration, including the Pie Town VLBA antenna, at a wavelength of 7 mm). The resolution of this VLA image is approximately 35 mas, or 16 AU. The full EVLA is needed to determine whether this emission arises from dust or ionized gas, to resolve the structure of the disk at multiple wavelengths, and to bridge the gap in resolution between the VLA and VLBA. Image courtesy K. Menten, M. Reid, L. Greenhill and C. Chandler.

dimensional velocity field on scales the size of the Solar System, as shown in the VLBA image in Figure 3.2. The masers seem to show material flowing outwards from the surface of a disk, but in order to verify this picture, the disk itself must be imaged. The best current images were obtained at 7 mm by using the VLA in its most extended configuration, and including the VLBA antenna at Pie Town as part of the array. Although a structure having the expected orientation of the disk is detected, it is barely resolved (two or three resolution elements), and these data give no spectral information to determine whether the emission arises from dust or from ionized gas. The full EVLA will be able to image the disk with ten times better resolution, allowing direct measurements of the disk structure, and establishing whether the accretion/outflow picture developed for low-mass star formation can be applied to Source I.

Overviews of Local Star Formation: Supernova Remnants and H II Regions in External Galaxies

While observations within the Milky Way provide our most detailed look at the star formation process, such studies must focus on individual examples and the chance placement of star forming regions near the Sun. A combination of uncertain distances, extreme and variable absorption, and line-of-sight confusion make it difficult to build up a global picture of star formation in the galaxy. This is important because conditions vary so much both within and between galaxies: pressures, temperatures, and metallicities are very different

in the Galactic Center than in an outer spiral arm, and different again in the bars of SB galaxies and the bulges of S0s and ellipticals. Current observations also suggest that much of the star formation in the Universe may take place very rapidly and under extreme conditions, in bursts of star formation triggered by strong dynamical interactions and mergers. It is thus crucially important to understand how environment affects the star formation process, and how that process itself alters the local environment.

Nearby galaxies play an important role here, by allowing detailed studies of entire populations of star formation regions, spread over a wide range of environments but at the same, and known, distances. Both the H II regions ionized by young massive stars, and the supernovae and supernova remnants those stars produce, emit strongly at radio frequencies; moreover, the resulting radio photons can penetrate even the densest dust, allowing a unique, unobscured view of the sites of massive star formation. The EVLA would allow major advances in imaging both supernova remnants and H II regions.

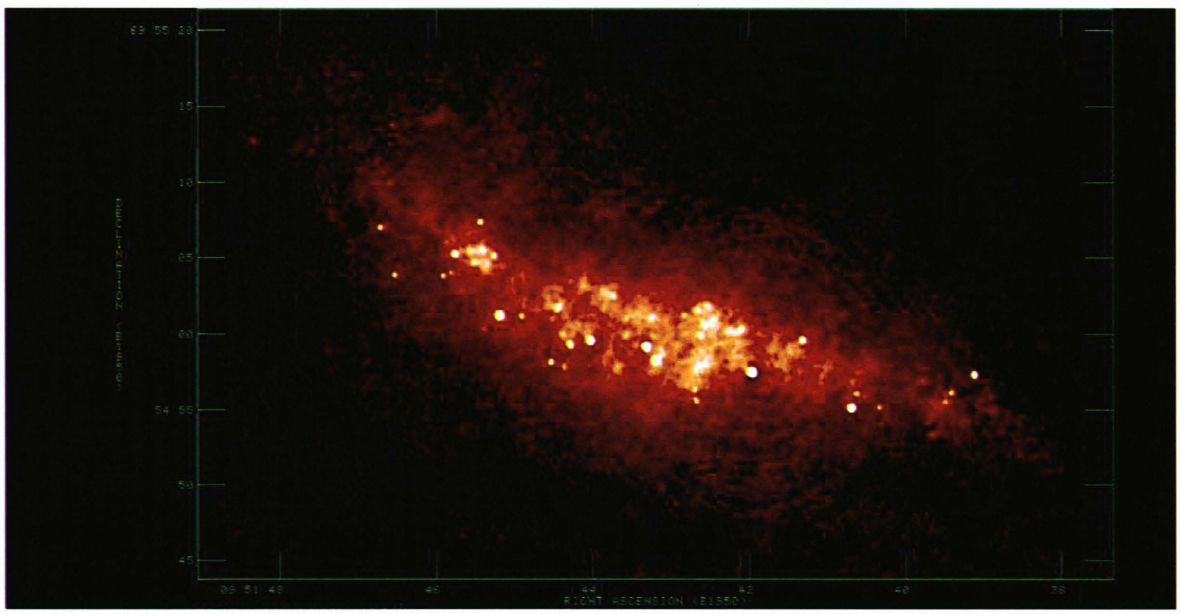

Figure 3.3: The nearby starburst galaxy M82, as seen in combined MERLIN and VLA observations at 5 GHz, with a resolution of 50 mas. The $\sim$ 50 compact sources are supernova remnants, many of which have been resolved into shells. The NMArray will give a factor 10 higher sensitivity, provide detailed spectral and polarization information, and (working at $\sim$ 50 GHz) give ten times higher resolution. From Muxlow et al. (1994).

Supernova remnants (SNRs) are among the most spectacular star formation indicators, as well as being important sources of turbulence, high energy particles, and metals in the interstellar medium — all of which are themselves tied to future star formation activity. Currently only a few extragalactic remnants can be studied (e.g., Fig. 3.3) with poor sensitivity and at most a few beams across each source. The New Mexico Array will provide more than 10 times higher resolution, with sensitivity sufficient to image both spectral indices and polarization, and to detect a complete sample of SNRs at a single known distance. This will allow the detailed study of SNR physics (such as shocks and magnetic field compression) in a wide variety of physical environments. Further, the enormous sensitivity of the EVLA will allow detailed studies of cosmic ray propagation, using the radio surface brightness and spectral shape as a tracer of the relativistic particle population, as a function of distance from each SNR. The same observations will reveal all the H II regions in the galaxy, giving a dust-free estimate of the total number of ionizing photons. For the nearest galaxies (Local Group), the NMArray will even resolve individual *ultracompact* H II regions, created by single O & B stars. The result will be an unprecedented, precise, accurate, and unbiased look at the effects of star formation within nearby galaxies, over a sufficient range in distance to include normal spirals, dwarfs, and even starburst galaxies.

The EVLA will also make important contributions to the study of the most extreme mode of star formation in the local Universe: the formation of super star clusters. Because of the large number of massive

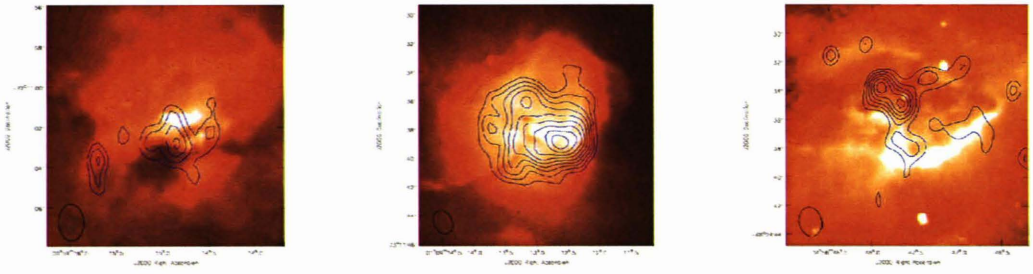

Figure 3.4: Three sample ultracompact H II regions in the Magellenic Clouds, as seen in Hα (from HST; color scale) and 8.4 GHz radio continuum emission (contours; from the Australia Telescope Compact Array). The linear resolution of the radio data is ~ 1 pc. Candidate regions were selected by their IRAS colors. The full EVLA will allow higher-resolution imaging of entire galaxies, out to the distance of NGC 253 (2.6 Mpc). From Indebetouw, Johnson, & Conti (submitted).

stars densely packed into these clusters, they can have a violently disruptive effect on their host galaxies — blowing bubbles, expelling gas, enriching the interstellar and intergalactic media, and triggering further star formation. The effects of massive star clusters were even more important in the earlier universe when galaxy mergers were common, and the formation of massive star clusters was ubiquitous. However, despite the important role of these clusters, the mechanism of their formation is not understood. Because these objects are invisible to optical and near-infrared light during their earliest stages, sensitive and high-resolution radio observations are required to probe their birth environments. High frequency ($\gtrsim 15$ GHz) observations are particularly useful for investigating the dense H II regions surrounding embedded super star clusters because they become optically thick at lower frequencies. The increase in sensitivity that will be achieved with EVLA Phase I will allow the detection of natal super star clusters at high frequencies out to the distance of the most luminous starbursts, including ultraluminous infrared galaxies such as Arp 220. The increase in spatial resolution in Phase II is required to resolve and image these objects out to this distance. The EVLA will thus provide important insights into the star formation process on scales ranging from individual star births in the Milky Way, to the creation of massive star clusters in starburst systems.

3.1.2 The Formation and Evolution of Galaxies

Cosmology over the past few decades has largely focused on the basic parameters of the Universe; its size, its age, and its evolving geometry. These studies, culminating in the Wilkinson Microwave Anisotropy Probe (WMAP), have shown that we live in a flat, accelerating Universe, whose basic parameters have been determined by a number of different methods, and are no longer hugely controversial. For instance, the WMAP results give an age for the Universe of 13.7 ± 0.2 Gyr, a baryon density of $\Omega_b h^2 = 0.0224 \pm 0.0009$, and a Hubble constant of $H_0 = 71 \pm 4$ km/sec/Mpc (e.g., Spergel et al. 2003), and these values are consistent with measurements based on supernova distances and globular cluster ages.

With this basic framework in place, the challenge now is to understand the development and evolution of physical structures within that framework: the gas and galaxies which populate the Universe. This requires observations both at high redshift, when the first objects (galaxies and black holes) condensed out of the primordial gas, and nearby, where similar processes can be studied in much more detail. As with local star formation, the basic driver — gravity — is clear; and as with local star formation, the details are much less obvious. In particular, once the gas has reached high enough densities to form the first stars and black holes, the heat from stellar fusion, combined with accretion-generated energy from material falling into black holes, begins to have an important impact on the dynamics. Galaxy formation thus represents the complex interactions amongst gravitationally-powered infall, gas dynamics, and energy input from the stars and black holes which are made in the process.

We are still far from understanding the details of this complex process. Two important insights come from recent work on the history of (luminous) energy generation in the Universe, and the ubiquity of massive black holes in galactic nuclei. Regarding energy generation, current observations suggest that both the star formation rate (Fig. 3.5) and the quasar luminosity function (Fig. 3.6) peak at intermediate redshifts

($z \sim 2-3$). Regarding nuclear black holes, there seems to be an amazingly tight correlation between the central star formation (as indicated by the total bulge mass) and the mass of the central black hole (Fig. 3.7). Thus the stars and the central black holes seem to be closely connected. This may be related to the observation that star formation in the most actively star-forming galaxies (UltraLuminous InfraRed Galaxies, or ULIRGs) takes place within the central tens or hundreds of parsecs of the galaxy. This same star-forming gas may funnel down to the central black hole, adding to its mass, and perhaps creating an active galactic nucleus (AGN).

To understand the nature of and the connection between these two phenomena, we need to answer questions such as:

- How much of the "action" in the early Universe is star formation, and how much is AGN?
- What is the joint history of star formation and black hole formation and growth?
- How can we distinguish between heating sources (star formation vs. AGN)?
- How does star formation differ in different environments, and at different times?
- What are the feedback mechanisms amongst gas infall, galaxy formation, winds, and AGNs?

These are very challenging questions. Observationally, the regions of most active star formation, as well as the central engines which power AGNs, are hidden in regions of very dense gas and dust, which absorbs most of the optical and even infrared light. Far infrared and sub-millimeter observations provide an excellent calorimeter of the total energy re-radiated by the heated dust (Fig. 2.5), but cannot probe the innermost parts of the system where that energy is generated. These regions are also intrinsically complex: one has to disentangle many complicated, overlapping processes, and compare high resolution and high signal-to-noise observations of the nearby Universe with comparatively crude measurements at higher redshifts. Further, redshift effects make it impossible to compare directly data taken in any one waveband. We need a *complete* picture, across wavelength, both at any given redshift, and to track individual features across redshift; and we need very high (and preferably matched) resolutions, both nearby and far away, at those different wavelengths.

Centimeter wavelengths, in particular, play an important and unique role. While optical, UV, and IR observations see only the outermost envelope of the activity at the heart of galaxies, and far IR and submillimeter data can assess the total luminosity being generated but not its source, radio observations can pierce even the densest dust layer, and lay bare both star formation and AGN activity. This requires both sensitivity to detect the emission, and spatial resolution to separate the two processes. The first phase of the VLA Expansion Project will provide the sensitivity; the main goal of the second phase is to provide the resolution. The interesting scales are those of the galaxy as a whole, and of the inner dust-enshrouded core. Galaxies are typically kiloparsecs in size, and the jets of low-luminosity AGNs have similar scales. The dust-enshrouded cores of ULIRGs are of order 100 pc across. Because an arcsecond corresponds to $\gtrsim 10$ kiloparsecs at any distant redshift[1], we need 0.1 arcsecond resolution at the low frequencies where Galactic disks and jets are most prominent, and ten times higher resolution at the high frequencies, where thermal emission and small-scale synchrotron radiation are strongest. These considerations set the scale of the New Mexico Array, whose ~ 350 km baselines will give resolutions of ~ 0.1 arcsec at 1.6 GHz, and ~ 4 mas at 45 GHz. The New Mexico Array will turn the EVLA into a true *imaging* instrument for galaxy formation and activity throughout the Universe. In the remainder of this section we focus on the role of the EVLA in distinguishing star formation from AGNs, and tracing their joint evolution from the earliest times to the present.

The Radio/FIR Correlation: Linking Star Formation to Magnetic Fields and Cosmic Rays: The use of radio data to probe global star formation rates rests in large part upon the radio/FIR correlation (Fig. 3.8), an extremely tight but still mysterious relation between the far infrared (FIR) and the low-frequency radio emission from star forming galaxies. It has proven very useful,[2] but its physical basis is far from understood.

[1] The WMAP (Wilkinson Microwave Anisotropy Probe) cosmology (e.g., Spergel et al. 2003) is assumed throughout, i.e., $H_0 = 71$km/s/Mpc, $\Omega_M = 0.27$, and $\Omega_\lambda = 0.73$.

[2] e.g., helping to distinguish starbursts from radio-bright active galactic nuclei (Condon & Broderick 1988), providing dust-free measurements of the cosmic star formation rate (Haarsma et al. 2000), yielding photometric redshifts for sub-millimeter sources that have no optical/IR counterparts (Yun & Carilli 2002), and permitting high-resolution radio imaging of star formation regions in sources found through submillimeter and far infrared surveys (Blain et al. 2002).

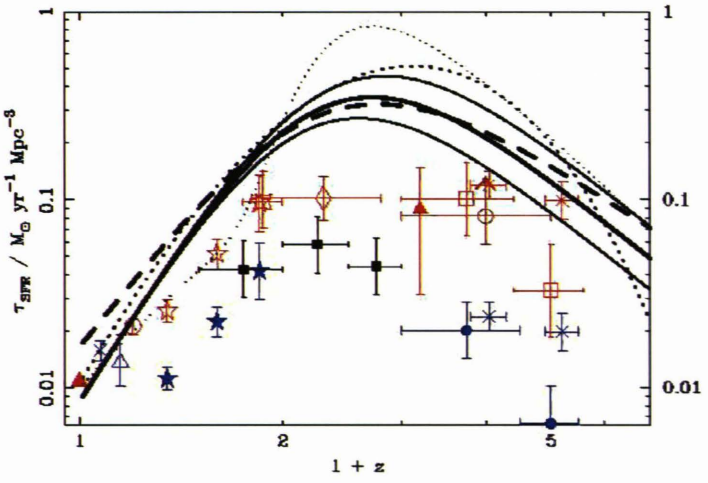

Figure 3.5: The star formation rate per unit comoving volume, as a function of redshift; often referred to as the 'Madau plot'. The absolute normalization depends on the initial mass function and the fraction of dust heating by active galactic nuclei. The points are taken from a number of optical and near-IR studies; the data in red are corrected for extinction, while those in blue are not. The lines show various model fits to the far infrared and submillimeter data. Note the importance of extinction in this logarithmic plot, in going from blue (uncorrected) to red (corrected) to solid line (FIR/submillimeter). From Blain et al. (2002).

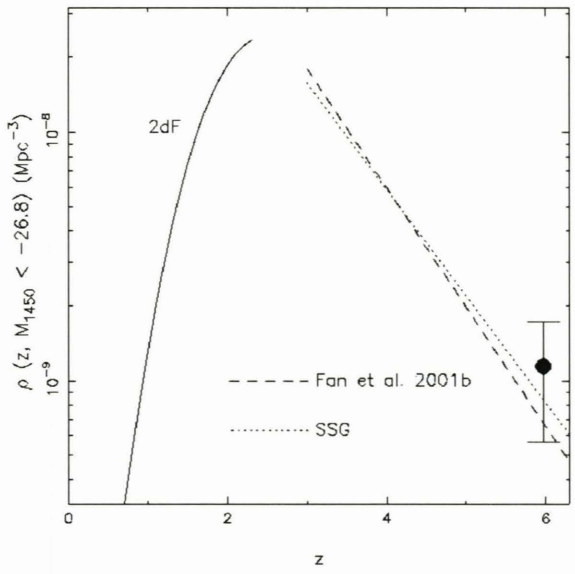

Figure 3.6: Evolution of quasar comoving volume density above a given luminosity. The dashed and dotted lines are two best-fit models; the solid line is the best-fit model for the 2dF survey (Boyle et al. 2000); and the large dot represents recent results from the Sloan Digital Sky Survey. From Fan et al. (2001).

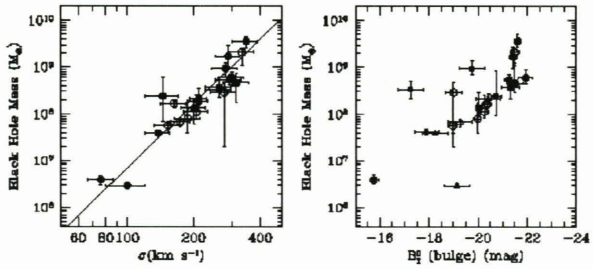

Figure 3.7: The mass of supermassive black holes in galactic nuclei, vs. central velocity dispersion (*left*) and bulge B-band luminosity (*right*). The tight correlation indicates a fundamental connection between the evolution of black holes and their host galaxies. From Ferrarese (2002).

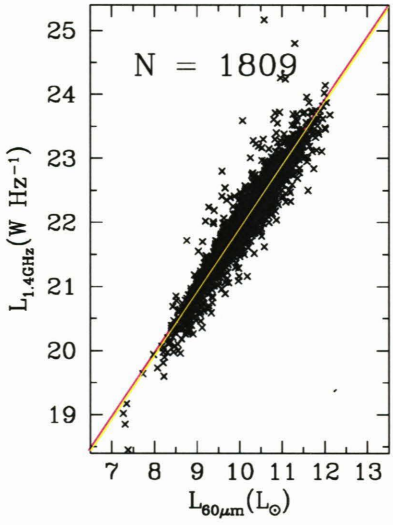

Figure 3.8: One example of the FIR/radio correlation for star-forming galaxies; this particular plot shows the *IRAS* 2 Jy sample of Yun et al. (2001). The solid line is a linear fit with a constant offset. After excluding $\sim$ 60 radio-excess objects (AGNs), the rms scatter is less than 0.26 dex.

The FIR emission comes from heated dust, and thus measures the current star formation rate. The radio emission is synchrotron, from particles accelerated in supernovae and SNRs. Thus it is also a consequence of recent star formation. But propagation is as important as SNRs to the cosmic ray distribution; and their synchrotron emission also depends crucially on the (local) magnetic field. Why then is the relationship between dust and cosmic ray emission so tight? Further, the radiation fields in the central regions of starburst galaxies are so strong that the relativistic electrons should suffer strong inverse Compton losses. So why does the *identical* relation hold for starburst and normal star-forming galaxies?

The radio/FIR correlation is clearly telling us something deep about the star formation process, but we do not yet understand it. To do so requires detailed studies at both FIR and radio wavelengths, at comparable resolution. ALMA will provide excellent high-resolution observations of the dust emission; the New Mexico Array is essential to provide similar data on the synchrotron radiation, particularly for compact starburst galaxies. With such data astronomers can address basic questions about the physical scales on which the relation operates[3], and the relative importance of different emission components[4].

Distinguishing Starbusts from Monsters: Before using the radio/FIR correlation to measure star formation rates, we have to be sure that the power source is indeed star formation, rather than accretion activity. Here

[3]How important is cosmic ray diffusion? How does this vary with magnetic field structure and strength?

[4]Does summing up supernova remnant emission give an even tighter correlation than comparing the total emission? What are the effects of correcting for dust temperature, or eliminating the cold dust emission?

too the EVLA will play a critical role. Imaging at high resolution is essential, because the most intense star formation often occurs near galactic nuclei. Radio imaging is particularly useful, first because radio photons can escape even the densest dust, and second because radio observations trace *both* AGN and star formation, as both produce synchrotron radiation. Indeed, radio jets represent one of the few unambiguous tracers of active galactic nuclei. For nearby galaxies, the New Mexico Array will show directly whether the emission is distributed (as in a starburst) or centered on a single central point (as in an AGN). Even in more distant systems there are unambiguous radio signatures, such as highly collimated radio emission misaligned with the optical galaxy (Fig. 3.9, 3.10). Only the NMArray can provide this important morphological information.

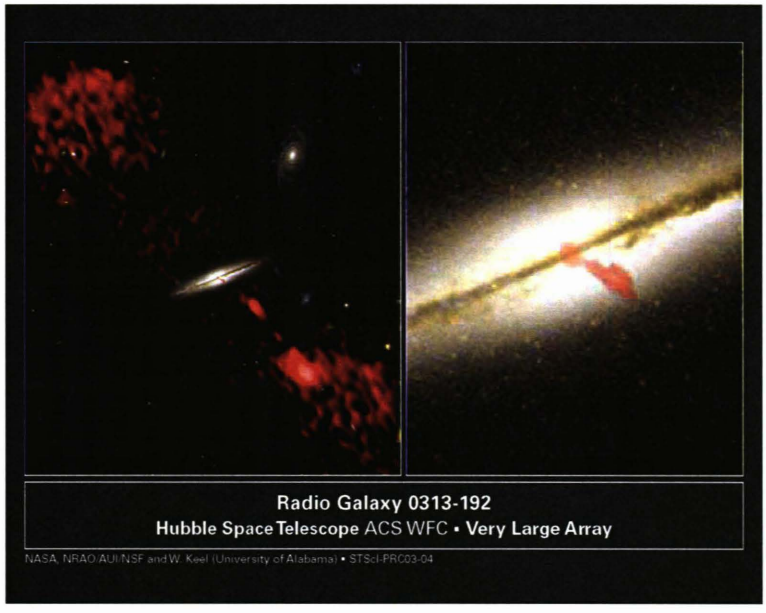

Figure 3.9: The edge-on spiral galaxy 0313−192, as seen at optical (black-and-white; HST) and radio (red; VLA) wavelengths. The optical morphology would suggest that the prime source of energy generation in this system is star formation, but the radio jets and lobes show a substantial AGN contribution. This particular example is both nearby and relatively bright and extended; the NMArray's combination of sensitivity and spatial resolution will be required to reveal the existence of AGN jets in more distant and typical systems. Image from Keel, Ledlow, & Owen (2003).

Star Formation and AGN at High Redshift

The EVLA will also be critical to understanding star formation in the early Universe, carrying out unique radio experiments which expand on and complement what ALMA and the JWST will be able to do at millimeter and optical wavelengths. A few of these experiments are outlined below.

An Unbiased Census of Star Formation and AGN Activity The deepest radio surveys (Fig. 3.11) show a substantial population of radio sources which are just barely resolved, at ~ 1 arcsec.

Similar surveys with the EVLA will both go much deeper and, with the New Mexico Array, provide a factor 10 higher resolution.[5] As discussed above, such imaging studies give crucial information on whether the detected sources are starbursts, AGNs, or something else altogether; a resolved jet for instance is a sure sign of AGN activity. Thus the full EVLA will provide *complete, unbiased surveys* of both star formation and AGN activity, out to redshifts of ~ 2 — covering roughly 3/4 of the age of the Universe. Such surveys will be complete, because radio observations are unaffected by dust obscuration; they will be unbiased, because radio data can detect both high-luminosity ULIRGs, and more typical low-redshift systems. This is illustrated in Fig. 3.12, which compares the sensitivities of various current and future telescopes. For the most actively

[5]Note that the radio source density is much higher than seen in even the deepest X-ray surveys; see for example Fig. 3.11.

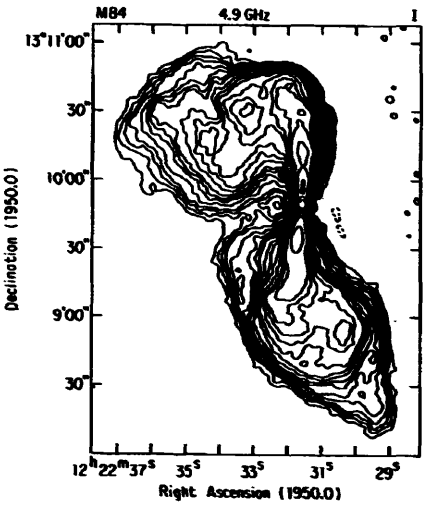

Figure 3.10: 4.9 GHz VLA image of the low-luminosity AGN, M84. While current high-redshift imaging is limited to the rare, high-luminosity objects, the NMArray will image the more typical low-luminosity systems, providing a much more sensitive (and unambiguous) probe of AGN activity in the early Universe. From Laing & Bridle (1987).

star-forming galaxies, most of the energy is re-radiated by dust in the far infrared; such galaxies actually appear brighter at higher redshifts, as the dust peak moves into the submillimeter. Submillimeter surveys are therefore ideal for detecting the most luminous star forming galaxies at essentially all redshifts; but they completely miss lower luminosity systems. The JWST will also be able to detect galaxies at virtually any redshift, but it will be very difficult to interpret the rest-frame optical/UV emission which JWST can see in these very dusty systems. Only the EVLA will be able to track the star formation in more pedestrian systems (like M82) out to the epoch of peak star formation in the Universe ($z \sim 2$; Fig. 3.5), and the EVLA's imaging capabilities will be critical in distinguishing AGNs from star-forming galaxies at all redshifts. One needs to combine observations at *all* wavelengths, to make an unbiased estimate of the total star formation rate, and to estimate the relative contributions of low and high luminosity systems.

Starbursts and ULIRGs in the Distant Universe Recent submillimeter observations suggest that ULIRGs, which are rare locally, may have been much more common in the past, and may even be the dominant source of star formation in the early Universe. The first phase of the EVLA Project will allow the detection of such sources, anywhere in the Universe; the New Mexico Array will provide the resolution required to image them. In particular, consider a source like Arp 220 (illustrated in Fig. 2.5), with a star-forming core with radius of ~ 100 pc, For such a source, the NMArray will

- at low frequencies, map out the synchrotron emission from supernova remnants and cosmic rays, to redshifts up to ~ 3;
- at middle frequencies, provide dust-free images of the ionized gas in H II regions to redshifts up to ~ 1, covering the bulk of the star formation in the Universe;
- at high frequencies, map out the thermal dust emission anywhere in the Universe (Arp 220 would be a 25σ detection in 12 hours at $z \sim 30$!).

Other instruments can detect these systems as well, and both the JWST and ALMA take imaging of ULIRGs as one of their fundamental science goals. But while the JWST can see only the unobscured outer parts of these galaxies, the EVLA can directly probe the actual star-forming core, despite the expected tens or even hundreds of magnitudes of visual extinction. Similarly while ALMA will provide superb images at the peak of the spectral energy distribution, only the EVLA can look through that re-processed emission to observe the actual power sources. In fact, thanks to the positive K-correction at high redshifts, the NMArray will provide the highest resolution of any telescope, even for the dust emission, for redshifts beyond $z \sim 2$.

Figure 3.11: A 10.6 × 7.7 arcmin^2 section of a deep ($\sim$ 120 hour) 1.4 GHz VLA image (rms noise $\sim 3\,\mu$Jy/beam); the resolution is $\sim$ 1.5 arcsec, and the image shown is roughly a tenth of the full field-of-view. Such images will become routine with the increased sensitivity provided by the first phase of the EVLA Project. The New Mexico Array however will be able to actually *image* all these sources, providing $\sim$ 10 beams across each source. This means that each of the pin-pricks in the current image will be resolved at roughly the level of the the extended, double-lobed source seen here in the southeast corner, aiding enormously in distinguishing AGN from starburst emission. Courtesy F. Owen (2003).

How important is this high-redshift imaging capability? A few years ago one could well have argued that there are unlikely to be any galaxies or AGNs beyond redshifts of a few; there simply hadn't been time to form any truly massive objects, and the first generations of stars might well be produced in a completely different fashion to the galaxy-based mechanisms known locally. This has dramatically changed: there are now a number of quasars known with redshifts above 6 (e.g., Fig. 3.13), and the recent results from WMAP require substantial ionization sources at redshifts $\sim$ 17. If these sources produce substantial luminosity in the rest-frame far-infrared — as all their known analogs do — the EVLA will be ideally suited to imaging them.

3.2 The New Mexico Array in Other Roles

So far we have concentrated on one aspect of the New Mexico Array, working with the EVLA27 to give a 37-element array with superb resolution and the maximum possible sensitivity and imaging quality. But this is only sensible when the EVLA27 is in its most extended (A) configuration. A great many experiments require a more compact distribution of antennas, for maximum sensitivity to structures on larger angular scales, and the EVLA27 will spend a significant amount of its time in the current B, C, and D configurations,

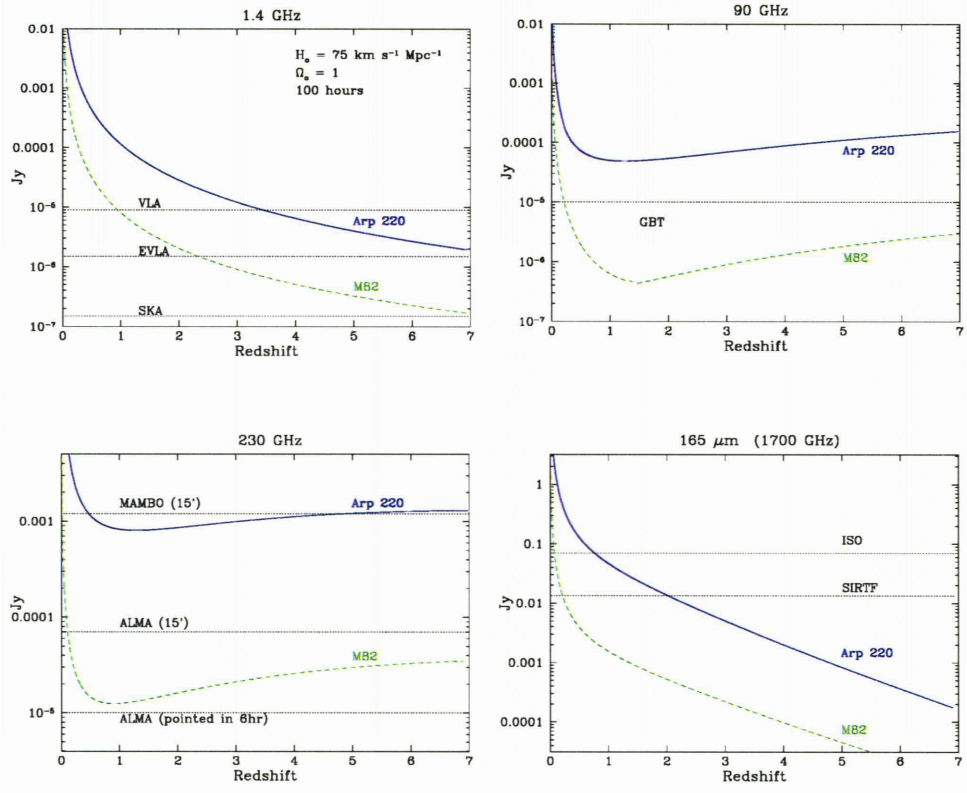

Figure 3.12: The flux densities of Arp 220 and M82 vs. redshift at various observing frequencies, overlaid on the sensitivities of existing and future telescopes. Far infrared and (sub-)millimeter surveys (here, 90 and 230 GHz) pick out the most luminous galaxies at basically arbitrary redshifts, but are much less sensitive to the fainter galaxies which may be much more typical. By contrast, the EVLA will provide an *unbiased* census of the whole range of star-forming galaxies, out to the redshift (~ 2) which is currently thought to represent the peak of both AGN and star formation activity in the Universe. The NMArray will provide simultaneous sub-arcsecond images, helping to distinguish the two energy production mechanisms. From Carilli (2001).

and in the new ultra-compact E-configuration (§3.3). During these periods the NMArray will fill two other important roles, providing short baselines for the Very Long Baseline Array (VLBA), and acting as a stand-alone instrument with continuum sensitivity at least as good as the current 27-element VLA, but with ten times the spatial resolution. Our goal is to provide a completely flexible instrument, covering two orders of magnitude in frequency and yielding sensitive and reliable images on scales from milliarcseconds to degrees. The astronomer will be able to select the antennas and configurations which match her science, rather than trying to find objects and experiments which can be made to fit the limited range of the VLA or the VLBA, which are currently operated as completely separate instruments.

3.2.1 Connecting the EVLA and the VLBA

Just as the New Mexico Array will provide long baselines (and hence high resolution) for the EVLA, it will also provide equally important *short* baselines for the Very Long Baseline Array (VLBA). Currently the VLBA is limited both by the small number of antennas, and by having only one baseline shorter than about 400 km. At 8.5 GHz this lack of short baselines renders all structures larger than about 20 milliarcseconds invisible to the current VLBA – it's as if we can see the tips of the waves, but not the underlying ocean. The VLBA can make exquisite images with milliarcsecond resolution, but may not 'see' 90% of the source flux; the VLA recovers the entire source, but with $\gtrsim 100$ times worse resolution, at a given frequency. The NMArray will fill this gap, providing reliable images with a spatial dynamic range of more than $10^4 : 1$ (by

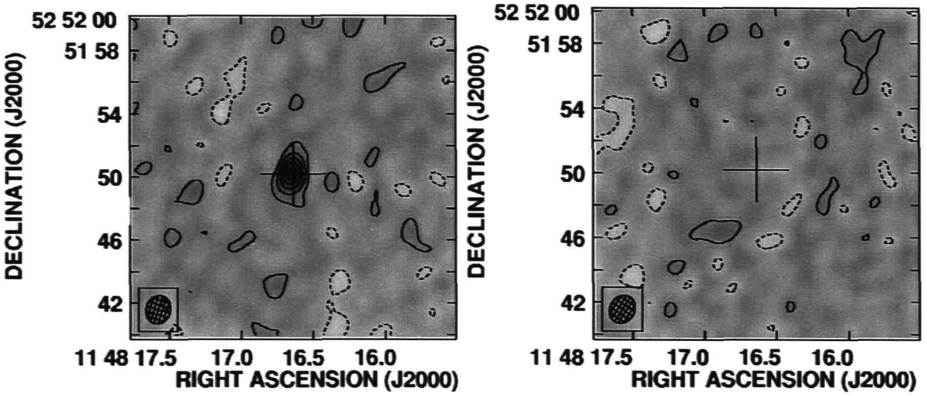

Figure 3.13: VLA observations of the highest redshift quasar, J1148+5251, at $z = 6.43$, showing the emission on (left) and off (right) a strong CO (3-2) signal. This quasar is one of those showing a strong Gunn-Peterson effect, providing direct evidence for substantial neutral gas prior to the end of the epoch of re-ionization; yet there has clearly been sufficient star formation to produce the metals required to form enormous amounts of molecular gas. If this source has a correspondingly high dust luminosity, the New Mexico Array will allow imaging it at a resolution of a few tens of parsecs. Note that this source was also detected (in other CO transitions) with the Plateau de Bure interferometer; combining these data yields an estimate of the temperature of the gas, ~ 100 K. The combination of the EVLA and ALMA will take such measurements to a new level of sensitivity and resolution. From Walter et al. (2003).

contrast, combining all four configurations of the current VLA gives a spatial dynamic range of only 500:1). This will also allow imaging with the same resolution over frequencies differing by more than a factor of 100, permitting the detailed study of important frequency-dependent effects like opacity, turbulent scattering, and Faraday rotation.

Perhaps the most obvious scientific impact will be on the study of jets in AGNs. There is growing evidence that jets from black holes play an important feedback role in galaxy evolution. For instance, nuclear star formation is associated with AGN in nearby galaxies (Fig. 3.14), and the radio jets are strongly interacting with the intracluster gas in the cores of galaxy clusters (Fig. 3.15; also §2.3.1 below). In addition, observations of high-redshift sources suggest the jet from the AGN is shock-heating the surrounding gas and possibly triggering star formation (Fig. 3.16).

There is thus ample evidence that jets are important to many aspects of galaxy evolution. But many aspects of the jets remain a mystery. High-quality, high-resolution images are needed to answer questions such as: how are the jets launched, and how are they collimated? What is the relation between accretion, central AGN luminosity, and jet production? How do the jets interact with the surrounding gas? The New Mexico Array will allow key advances in answering these questions, by tying the VLA and the VLBA together to create an instrument capable of imaging structure on scales from milliarcseconds to degrees, with similar resolution over a huge range in frequency.

On the smallest scales (few parsecs) this offers the prospect of detailed studies of the jet origins, by imaging accretion disks around AGNs through detailed mapping of the free-free opacity (Fig. 3.17). On somewhat larger scales (tens of parsecs) we will be able to measure "milli-halos" created by particles escaping the central engine (Fig. 3.18), and check for regions of nuclear star formation which would otherwise be swamped by the AGN (Fig. 3.14). On still larger scales (hundreds of parsecs to kiloparsecs) the NMArray will allow detailed studies of the *internal structures* of the large-scale jets. This will allow sensitive probes of gas entrainment and direct checks for variable flow speed within the jets, and resolve shocks and boundary structures in jet knots and hot spots. With excellent sensitivity and comparable resolution over a huge range in frequency, the EVLA+VLBA will also directly image particle acceleration regions, and measure rotation measures (RMs) and RM gradients both along and perpendicular to the jets. We know that collimated outflows also exist on galactic scales (microquasars, discussed more in the next section). The EVLA+VLBA will connect these to the accretion disks which power them, and reveal the details of their interactions with their surroundings.

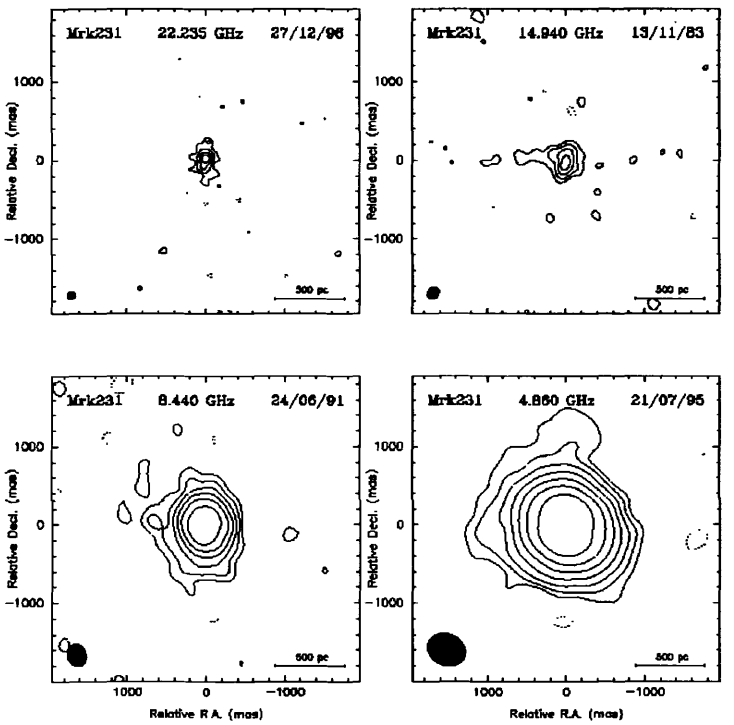

Figure 3.14: VLA images of the ultraluminous infrared galaxy Mrk 231, after subtraction of the AGN jet seen in VLBI imaging. The residual disk follows the radio/far-infrared correlation for star-forming galaxies, and this together with its morphology and the detection of four candidate radio supernova remnants suggests that the disk emission is dominated by star formation. From Taylor et al. 1999.

3.2.2 The New Mexico Array on its own

The New Mexico Array operating by itself will be a powerful imaging instrument, with continuum sensitivity comparable to the current VLA, while retaining that factor 10 improvement in resolution. The stand-alone NMArray would constitute the best instrument in the world for monitoring radio transients of all types, from galactic novae and microquasars to gravitational lens systems and gamma-ray bursts. The very flexibility of the VLA has made it a difficult instrument for these studies, since the array effectively changes character every few months when the configuration changes. This introduces systematic errors in long-term monitoring programs, especially since the smaller configurations are much more vulnerable to confusion. The NMArray will be available around the clock, every day of the year, and provide the resolution needed to image evolving sources and distinguish them from complex, extended backgrounds. Below we highlight the contributions of the stand-alone NMArray in a few key areas.

Mapping Dark Matter with Gravitational Lenses

Gravity is the fundamental force behind the formation of stars, galaxies, and indeed all the structure in the cosmos. Indeed, much of the mass in the Universe can be detected only by its gravitational effects. In a typical galaxy, for instance, the observed mass in stars, gas, and dust accounts for only $\sim$ 10% of the dynamical mass inferred from kinematic measurements. The distribution and extent of this missing "dark matter" are very difficult to determine; the most direct measures come from gravitational lensing, in which the appearance of some background object is distorted by a gravitational potential well along the line-of-sight. Observations of the positions and shapes of the resulting images can be inverted to map out the intervening lens. Those models are much more tightly constrained if the background source is variable, since the time delays between the different images reflect the differences in light travel time from the source. Radio observations are ideal for this sort of work, since the intervening galaxy (lens) is seldom

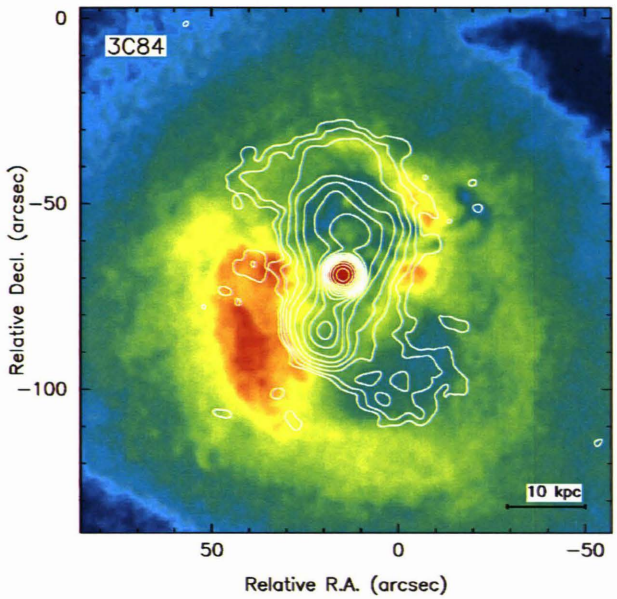

Figure 3.15: The cooling core source 3C 84 in the Perseus galaxy cluster: 1.4 GHz (VLA) contours over 0.5–1 keV (Chandra) color image, from Fabian et al. (2000). Note the anti-correlation between the radio lobes and the X-ray emission, and the bright X-ray rims around the radio lobes. These rims are cooler than the surrounding gas, and not the result of shocks; the bubbles themselves may contain hotter gas. The radio-emitting plasma has pushed the X-ray emitting gas aside.

a strong radio emitter, and one can be confident that none of the lensed images are obscured by dust. About 70 arcsecond-scale lenses are now known, and about half of those are radio emitters (Kochanek et al., `http://cfa-www.harvard.edu/castles/`); but only a few time delays have been measured. One major reason is the practical difficulties of making such measurements with current instruments. The VLA spends half its time in the compact C- and D-configurations, which prohibits sub-arcsecond imaging at frequencies below 22 GHz. Even in the appropriate configurations it is difficult to obtain consistent monitoring of any given source. Further, uncertainties in current radio light curves are dominated by systematic errors in the flux scale, errors which are due in large part to changes which inevitably occur in moving from one

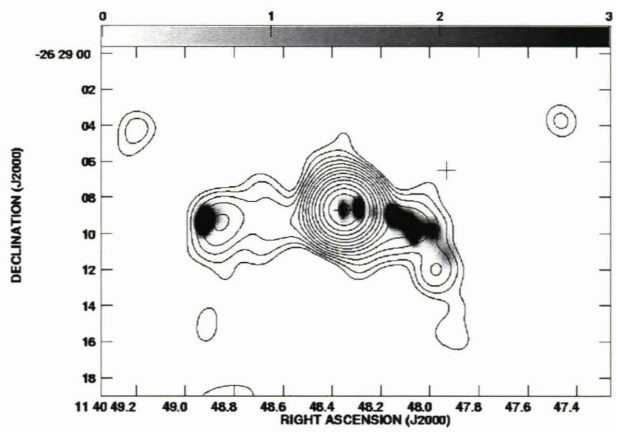

Figure 3.16: The $z = 2.2$ radio galaxy PKS 1138−262, showing the close correlation of the X-ray (contours, from Chandra) and radio (grayscale, VLA 5 GHz) emission. The X-rays are probably due to thermal emission from shocked gas, although there may be some contribution from inverse Compton emission. The resolution is 2 arcsec. From Carilli et al. (2002).

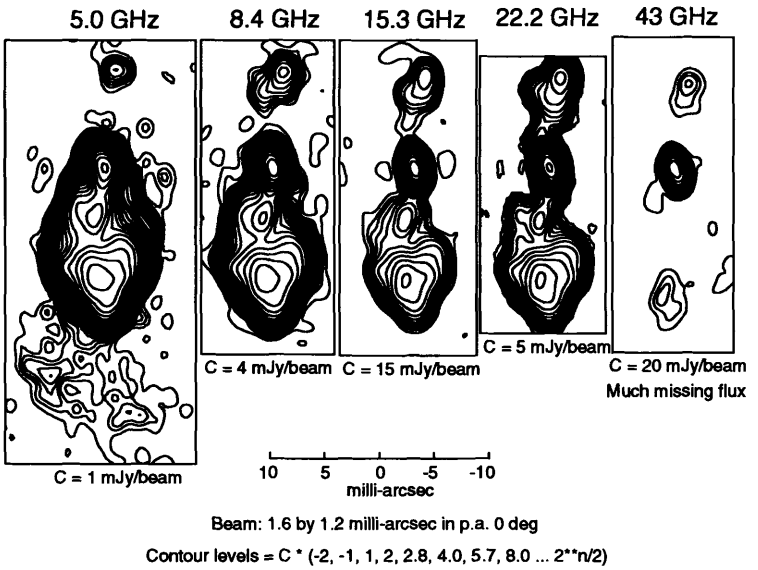

Figure 3.17: Matched-resolution VLBA images of 3C 84 (NGC 1275) from 5 to 43 GHz. Notice the complex spectral structure of the source — the southern extension is seen only at low frequencies, while the northern source gradual elongates towards the nucleus as the frequency increases. This is direct evidence for free-free absorption against the northern lobe; by mapping the spectral index across the source, Walker et al. (2000) were able to derive the parameters of the obscuring disk, including size, scale-height, and rough density distribution. This sort of imaging can be done now only for that handful of sources which happen to fit (at several frequencies) within the very limited spatial dynamic range of the VLBA, and which happen to have turnover frequencies in the correspondingly limited spectral range. This is equivalent to making spectral index maps with only one VLA configuration. Those few sources which *have* been explored in this way show a variety of structures and scale-heights. The NMArray will provide the intermediate VLA/VLBA spacings needed to extend these measurements to a much wider variety of sources.

configuration to the next. The NMArray will eliminate all of these difficulties, by providing a stable array with high sensitivity and excellent spatial resolution.

The Progenitors of Gamma-ray Bursts

One of the major difficulties in studying star formation at high redshifts is that most standard star formation tracers are simply too faint to be seen. In this regard, gamma-ray bursts (GRBs) may prove to be the perfect signposts. GRBs are extremely energetic explosions which drive relativistic shocks into their surroundings with bulk Lorentz factors ~ 300. The progenitor object(s) remain unknown, but there is mounting evidence that at least some GRBs are associated with the deaths of massive young stars. If it turns out that GRBs are normally tied to a young stellar population, they can be used as star formation indicators at arbitrary redshifts. One key observation in establishing this connection is to determine accurate astrometric offsets between (relatively) local GRBs and their host galaxies, to show for instance whether they lie preferentially in galactic disks (suggesting a young stellar population) or near the bulge. Radio observations are very useful in this regard, first in allowing very accurate absolute astrometry, and second in detecting the so-called "dark bursts," which are optically faint, presumably because of high visual extinction. The high resolution and good sensitivity of the stand-alone NMArray will permit good astrometric observations throughout the year, and much faster and more consistent follow-up than has been possible with the VLA. Once the GRBs have faded, the full EVLA can be used to image the host galaxy, giving an accurate position offset between GRB and host. In addition, the resulting well-sampled, multi-frequency radio light curves will determine GRB source sizes through scintillation (Fig. 3.19), provide better statistics on the range of GRB light curves, and, by avoiding source confusion throughout the year, follow the GRB's evolution from ultrarelativistic to non-relativistic shock.

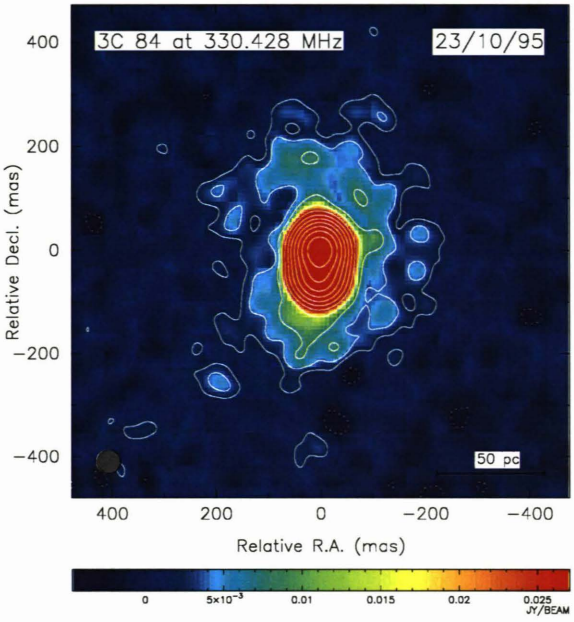

Figure 3.18: 330 MHz image of 3C 84 (NGC 1275), showing a very small (< 1 kpc) "milli-halo". This is probably produced by particles diffusing out from the nucleus. Ideally one would make spectral index maps to track the spectral aging, and use shorter-baseline information to figure out how far this halo actually extends. At the moment this is impossible: the source is just barely visible to the VLBA with a single VLA antenna added, and only at the lowest frequency was it seen at all. The NMArray would make this sort of imaging much easier, and extend it both to a wider range of frequencies, and to larger halos. From Silver, Taylor, & Vermeulen (1998).

Microquasars: Relativistic Jets from Stellar Corpses

Black holes and neutron stars are created in the explosions of massive stars, and represent the longest-lived relics of ancient star formation. In addition to tracing star formation in the distant past, these compact objects are the nearest analogues of the massive black holes which live in the galactic cores. As with active galactic nuclei, these galactic sources produce well-collimated, relativistic jets, known as microquasars. Unlike AGNs, however, microquasar jets evolve very rapidly, on timescales of days or weeks, offering astronomers the unique opportunity to follow them from creation through to eventual disappearance. Paradoxically, these relativistic outflows are closely associated with gas inflow, and one of the most important results from the study of these microquasars has been to associate jet ejection, as seen at radio wavelengths, with state changes in the accretion disk, as seen in the X-rays. Many questions remain. How are these jets launched and collimated? How similar are they to AGN jets? Why do some galactic sources produce very extended jets, while others are never spatially resolved? What makes persistent jet sources different from occasional transients? Why are the black holes in these X-ray binaries always $\sim 7\,M_\odot$, and how are so many black holes created? Does the black hole spin determine the nature and speed of the resulting jet, and if so, how? The answers have important implications not only for studies of accretion/outflow physics, but also for our understanding of stellar evolution, since these systems are among the few in which accurate masses can be measured for the end products of massive stellar evolution. The New Mexico Array will make two fundamental contributions to these studies:

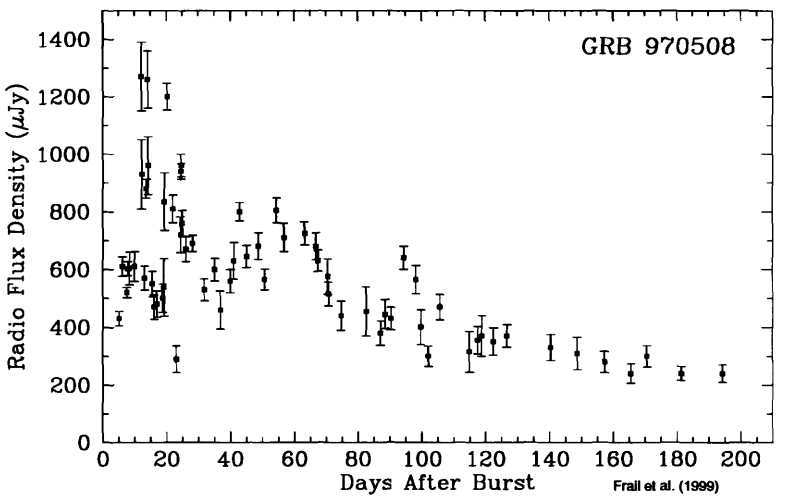

Figure 3.19: 8.5 GHz light curve of the radio afterglow from GRB 970508 (Frail et al. 1999). The flux density fluctuations at early times are the result of refractive interstellar scintillation, an interference effect produced by the intervening ionized gas along the line of sight. This scintillation provides a direct measurement of the angular size of the expanding fireball, and the only *direct* observational evidence that these sources and their afterglows are relativistic shocks. At late times (> 100 days) the radio light curve undergoes the same power-law decay seen at X-ray and optical wavelengths. When the GRB itself has faded from view, the NMArray will provide images and accurate astrometry of the host galaxy, yielding precise position offsets even for those 'dark' GRBs whose optical emission is either intrinsically faint, or obscured by dust.

- *Imaging:*
  Relativistic jets in the Galaxy expand so rapidly that they are resolved out by the VLBA in a matter of days; the VLA on the other hand, even when it happens to be in A configuration, can give only a crude idea of the distribution of the flux, which in any case often decays away entirely before being resolved (cf. Figure 3.20). The NMArray, uniting high resolution with sensitivity to extended emission, will give an unprecedented view of the full structure and evolution of these jets.

- *Monitoring*
  The NMArray is even more important for monitoring programs. The NMArray (working alone) will provide continuous frequency coverage with sensitivities comparable to the current VLA, with no confusion problems. This will result in continuous, sensitive, multi-frequency (5 or more) radio light curves for months, for any transient as strong as those which have so far been detected. Even without imaging one can learn the time offset between the radio ejection and the X-ray flare, whether there was a single or multiple outbursts, and whether the jets (assuming they are jets) are expanding freely. Since the NMArray provides imaging as well, one can check these models directly, and see the evolution of a jet in more detail than has ever been possible before.

These observations are particularly important because of the tie with current and upcoming high-energy space missions, which take observations of compact sources as one of their main justifications. Relativistic jets are no longer seen as an esoteric by-product of a few odd sources, but as a fundamental and unavoidable aspect of the accretion process (e.g., Markoff et al. 2003). The radio emission is the *only* unambiguous tracer of these jets, and offers the only consistent way to image them.

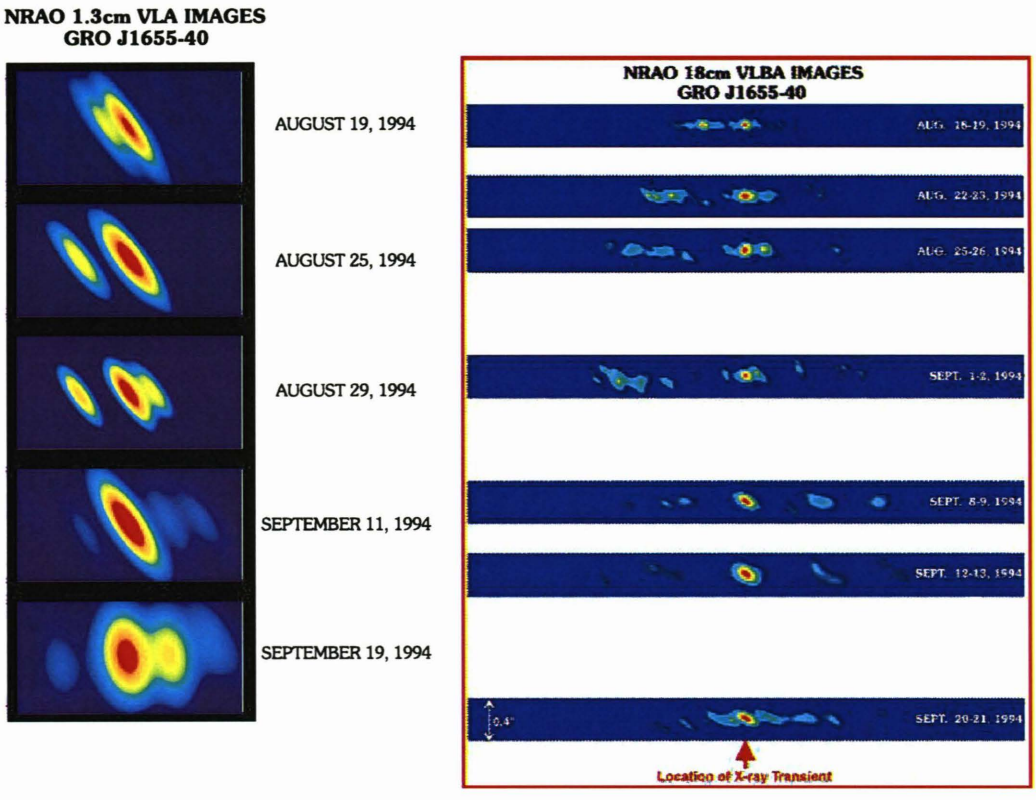

Figure 3.20: VLA 22 GHz (*left*) and VLBA 1.6 GHz (*right*) images of GRO J1655-40, a Galactic superluminal jet source (Hjellming & Rupen 1995). Note the timescale. By the second epoch the source was so extended that the VLBA missed more than half the flux density, picking out only the smallest and narrowest features. Resolutions are 20-40 mas for the VLBA, 200-400 mas for the VLA.

3.3 The E-configuration: Imaging Large, Faint Structure

Phase II of the EVLA Project also includes a smaller initiative in addition to the New Mexico Array: the creation of an ultracompact 'E' configuration to provide maximum surface brightness sensitivity, while retaining the excellent imaging fidelity which is the hallmark of the VLA. The E-configuration is designed to allow high-fidelity imaging of extended, low surface-brightness objects, at resolutions some three times higher than the Green Bank Telescope affords. By concentrating all the EVLA antennas into a compact space, the E configuration brings the full collecting area of the EVLA to bear on large-scale features which are too faint or too extended to be seen with the existing VLA configurations. The possible applications range from H I imaging of nearby galaxies and Galactic chimneys and shells (to column densities as low as $\sim 10^{17}\,\mathrm{cm}^{-2}$), to quantitative mapping of the interstellar magnetic field through Zeeman splitting of H I, molecular, and radio recombination lines. These and other experiments are detailed in Appendix A. Here we concentrate on one particular example drawn from our theme of the evolving Universe: imaging the Sunyaev-Zel'dovich effect in galaxy clusters.

In the hierarchical model of structure formation, primordial fluctuations are amplified by gravity, and collapse and merge to form larger and larger systems. Hence galaxies form before galaxy clusters, which are still in the process of merging today. The study of galaxy clusters thus offers the opportunity to follow on-going examples of the merging process which is thought to be responsible for making all of the structure in the Universe. By tracking galaxy clusters back in redshift, one can also see whether this merger process has changed in the recent past. One important clue comes from recent X-ray and millimeter observations, which suggest that the baryons in clusters must have been "pre-heated" before those clusters were formed,

either by star formation (though this would require a very efficient transfer of energy from supernovae), or by active galactic nuclei. This feedback between early galaxy formation and on-going collapse thus links the generation of observable structure to the history of energy generation in the Universe.

Detailed imaging is the key to understanding both the merger process and the constraints it places on non-gravitational heating. This is already clear locally from the magnificent Chandra images of galaxy clusters (see, *e.g.*, , Fig. 3.15), which show interactions between AGN jets and the intergalactic medium, and give strong evidence for on-going cluster-cluster mergers. But these X-ray observations are limited to nearby clusters, and are also highly sensitive to density clumping, with the X-ray emission scaling as the square of the electron density. Ideally one would like to trace the column density directly, and to be able to do so at arbitrary redshift.

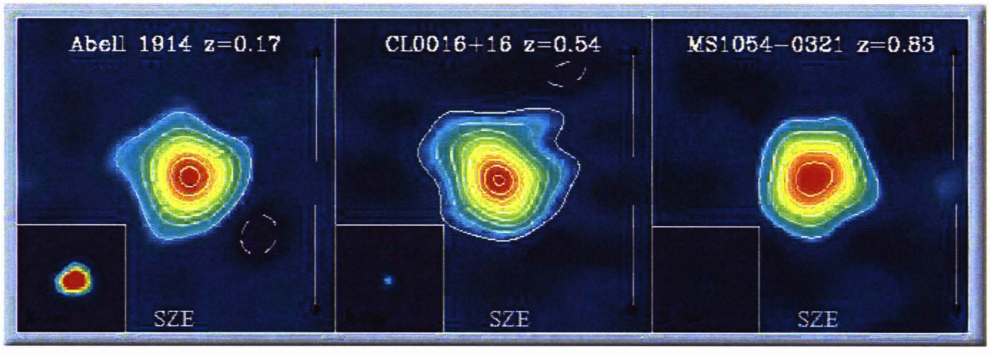

Figure 3.21: Sunyaev-Zel'dovich images of three galaxy clusters at redshifts 0.17, 0.54, and 0.83, compared with X-ray images of the same region; note that at $z = 0.83$ the Universe is about 1/3 its present age. The S-Z signature remains roughly constant, while the X-ray and other direct emission fades rapidly with z. These state-of-the-art observations were made with a resolution of ~ 60 arcsec at 30 GHz. From Carlstrom, Holder, & Reese (2002).

The Sunyaev-Zel'dovich (S-Z) effect is ideally suited for this work. The scattering of photons from the cosmic microwave background (CMB) off the hot gas in galaxy clusters introduces distortions in the CMB proportional to the gas column density, weighted by temperature. The ratio of the signal to the CMB is independent of redshift, so the S-Z effect can be used to map out the gas density of galaxy clusters at any distance. The optimal frequency for such studies, where the signal is largest and the confusion from other sources is lowest, is around 30 GHz. The best images available so far have resolutions ~ 60 arcsec (~ 500 kpc at $z \sim 0.8$), barely resolving the clusters (Fig. 3.21). One of the key uses of the EVLA's E-configuration will be to make similar images – but at a factor 10 higher resolution. This level of detail is essential to mapping out the density profile of the intracluster medium, particularly at high redshifts, where clusters are expected to be much more complex (due to on-going mergers). Surveys are currently underway to find hundreds of such clusters, out to redshifts of 2 or more; the EVLA will allow them to be imaged, at high enough resolution to look for the effects of pre-heating, and to study the details of the merging process (Fig. 3.22).

No other telescopes, current or planned, can make these images. The most compact configuration of ALMA would be competitive, but the low-frequency receivers needed are not part of the initial instrument plan. The GBT and CARMA will be ideal for providing the necessary short spacing (large angular scale) information, but will not achieve the necessary resolution.

3.4 Summary

This chapter has focused on the contributions of the second phase of the EVLA Project to the study of cosmic evolution. The New Mexico Array will make the EVLA the premier imaging instrument for seeing through the dust to the hearts of star-forming regions, and to distinguish the relative importance of accretion, outflow, and star formation, both in our galaxy and throughout the Universe. Working with the VLBA, the NMArray will give an unprecedented view of the surroundings of active galactic nuclei, and the detailed structure of jets from AGN. Operating as a stand-alone facility, the NMArray will be the premier radio monitoring instrument

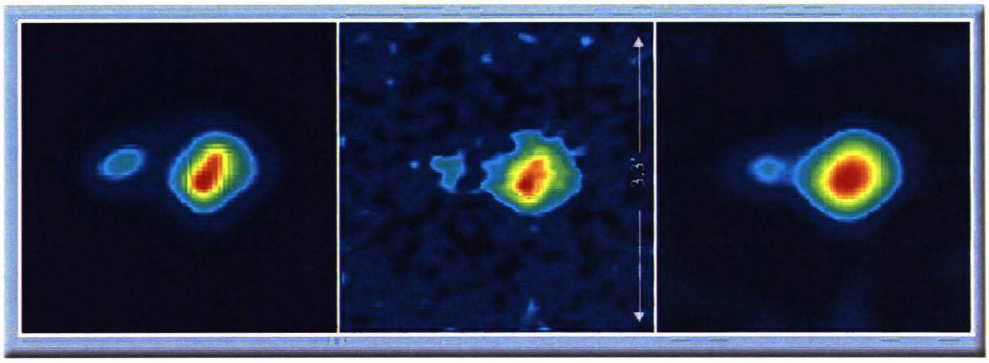

Figure 3.22: Simulated images of the Sunyaev-Zel'dovich effect due to a modest ($2.5 \times 10^{14}\,M_\odot$) cluster at $z = 1$. The image at left is from a hydrodynamical simulation. The central panel represents a ~ 6 hour exposure with the EVLA E-configuration at 30 GHz, giving a sensitivity of 15μK with a 9.7 arcsec beam. [The maximum resolution of the E-configuration would be ~ 6.4 arcsec at this frequency.] Finally, the right-most panel shows the same image convolved to a 22 arcsec beam, with a noise level of $1.7\,\mu$K. Note that Carlstrom's S-Z survey should discover some 500 clusters of this or higher mass, within the year. For reference, the Coma Cluster is about 10 times more massive than the one shown here. Figure courtesy John Carlstrom (2000).

in the world, tracking variability in gravitational lenses and gamma-ray bursts, responding quickly to high-energy outbursts, and providing high-resolution images of transient sources whenever they occur. Finally, a new, compact E-configuration will concentrate the power of the EVLA for the best possible surface brightness sensitivity and fidelity when imaging large structures. Combining these data with GBT observations will allow experiments ranging from mapping out the polarization and magnetic field structure of the local Milky Way, to imaging the formation of galaxy clusters by observing faint distortions in the cosmic microwave background.

These are important, and unique, contributions — but they are only a part of the EVLA's promise. Appendix A details a number of other possible projects, ranging from the determination of pulsar parallaxes, to the measurement of turbulence in the interplanetary medium, to the imaging of novae and planetary nebulae throughout the Milky Way, and the mapping of faint H I gas at the edges of nearby galaxies. The VLA has been an important instrument, not because it performed a single focused experiment, but because it provides an essential basic tool, for astronomers in every field. When the VLA was built, no star-forming cores had been discovered, and no star-forming galaxies were known beyond a redshift of one. Yet the VLA has made and continues to make fundamental observations in these areas, imaging stellar accretion disks and outflows, and providing accurate astrometry, photometric redshifts, and unique images of high-redshift systems. In the same way, the high resolution of the NMArray and the magnificent surface brightness sensitivity of the E-configuration will allow a whole range of observations whose importance we can hardly anticipate today. Like the Hubble Space Telescope, the Chandra X-ray Observatory, and the original VLA, the EVLA will truly be a 'Great Observatory.'

Chapter 4

Technical Specifications for Phase II

This chapter describes the technical capabilities that the Expanded Very Large Array must provide to meet the key scientific goals listed in Chapter 3, and the broader range of scientific goals given in Appendix A. The technical requirements listed are also based on a realistic assessment of the technologies expected to be available on the desired timescale for this project.

A note on nomenclature: In this and in the next chapter, a 'requirement' is a capability judged necessary for the EVLA to meet the scientific goals. A 'goal' is an extra capability which will provide significant extra scientific return. The term 'EVLA27' refers to the VLA antennas following the modifications from Phase I of the project.

The top-level technical requirements for Phase II of the Expanded VLA Project are:

- Maximum resolution approximately ten times that of the VLA, while maintaining the VLA's characteristic imaging fidelity.
- Continuum brightness temperature sensitivity (1-σ in 1 hour in Stokes I) at full resolution better than 60° Kelvin between 2 and 40 GHz, and better than 130° Kelvin in the 1 – 2 and 40 50 GHz bands.
- Full frequency coverage from 1 to 50 GHz on all antennas.
- A receiver capability at 327 MHz to match that present on the EVLA27 antennas.
- A flexible operational capability, to allow the antennas of the EVLA27, the New Mexico Array, and the VLBA to be combined into multiple simultaneous subarrays, according to the imaging goals of the observation or observations being conducted.
- A fast, accurate imaging capability with brightness temperature sensitivity of $\sim 60\mu$K (1 σ in 1 hour) on angular scales of $\sim 250/\nu_G$ arcseconds[1], for imaging objects larger than the antenna primary beam.

Each of these requirements is discussed in more detail in the following sections.

4.1 Obtaining Higher Resolution – The New Mexico Array

Increasing the array's resolution by a factor of ten requires increasing the maximum baseline length by the same factor. Thus it will be necessary to add new antennas at distances up to $\sim$ 250 km from the EVLA center. These new antennas, plus any VLBA antennas similarly outfitted and connected, will define a new array, the New Mexico Array, or NMArray, which can be combined with the EVLA27 antennas to define the full EVLA, operated as a standalone array, or combined with the VLBA. The number and locations of the new antennas are determined by the required sensitivity and imaging fidelity at full resolution.

Further requirements for the New Mexico Array are given in the following sections.

[1] ν_G is the observing frequency in GHz

4.1.1 Frequency Coverage and Bandwidth

The scientific goals require the same frequency coverage and electronics stability for the NMArray antennas as that for the EVLA27 antennas. As the data from the new antennas will be correlated with those from the EVLA27 antennas for many applications, the bands and bandwidths for the EVLA27, NMArray, and converted VLBA antennas must be the same. Because the NMArray antennas will commonly be used with the VLBA, they must be outfitted with 80–96 GHz band systems to match those on the present VLBA.

4.1.2 Sensitivity

The scientific goals for the EVLA and consideration of the expected capabilities of technology available in this decade result in the NMArray antenna mid-band sensitivity requirements given in Table 4.1, and shown in Figure 4.1. A degradation of these sensitivities by 10% at the edge of each band is acceptable. Note that the 80-96 GHz band requirement is based on matching the antenna sensitivity to the VLBA antenna sensitivity at this band.

Table 4.1: **Sensitivity Requirements for NMArray Antennas**

Band	Freq.	SEFD[a]	A_e/T_{sys}[b]
	GHz	Jy	m^2/K
0.30–0.34	0.32	1350	2.1
1 2[c]	1.6	265	10.8
2–4	3.0	255	10.8
4–8	6.0	290	9.5
8 12	10	340	8.1
12–18	15	405	6.8
18–26.5	23	600	4.6
26.5 40	34	650	4.2
40–50	43	1100	2.5
80–100	90	2820	1.0

[a]System Equivalent Flux Density: The source flux density which doubles the system temperature: $SEFD = 2 \times 10^{26} k T_{sys}/A_e$ Jy. For a 25-meter antenna, $SEFD = 5.62 T_{sys}/\eta_a$ Jy.

[b]$A_e/T_{sys} = 2760/\mathrm{SEFD}$, where A_e is the antenna effective collecting area in sq. meters

[c]The sensitivity requirement applies to 1.2–2 GHz.

4.1.3 EVLA Imaging Fidelity

The imaging fidelity[2] for the EVLA when observing in continuum mode at full resolution on a complex, extended source whose angular size exceeds 500 times the array resolution in both dimensions, must exceed 2000 for northern declinations, and 1000 for southern declinations. For spectral line, or narrow-band ($\Delta\nu \ll \nu$) observations, the fidelity on such a source must exceed 200 for northern declinations, and 100 for southern declinations. The imaging fidelity must be retained when the resolution is degraded by tapering by a factor of three. These requirements are based on the degree of image complexity seen on images made by the VLA.

The New Mexico Array, when used in a standalone mode, must provide fidelity exceeding 500 for objects up to 10 times the angular size of the synthesized beam, in order to allow astrometric and monitoring programs requiring semi-continuous observations.

4.1.4 Disk Recording Requirements

Because the antennas of the New Mexico Array will commonly be combined with those of the VLBA, the New Mexico Array antennas must be equipped with disk recording systems with a recording capability of 2 Gb/sec. Funding for this outfitting of the new NMArray antennas will be provided by the Expanded VLA

[2]The fidelity is defined as the true peak brightness of a source divided by the r.m.s. of the difference between the array's reconstructed brightness and the true brightness convolved to the array's resolution.

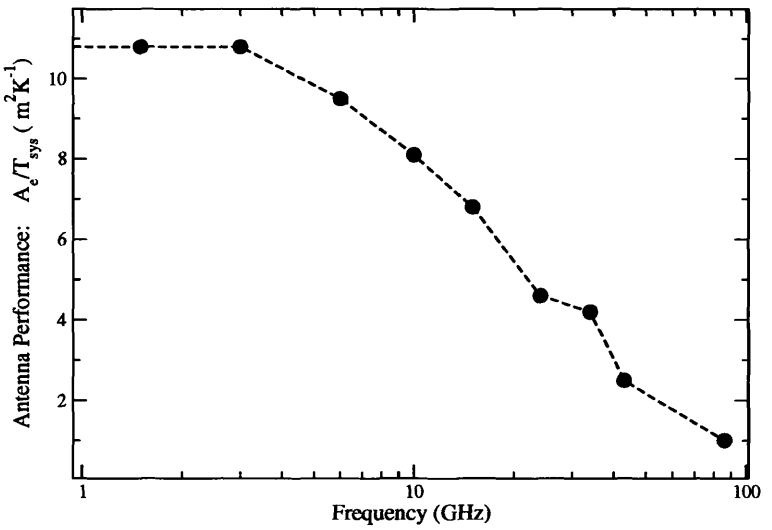

Figure 4.1: The required antenna sensitivity parameter, A_e/T_{sys}, for the NMArray antennas. The requirements refer to the band centers, marked by the filled circles. The dashed line is provided only for continuity. Degradation in performance up to 10% at the band edges is permitted. A greater degradation at the low end of the 1 – 2 GHz band is expected.

Project. Funding for conversion of the present VLBA tape recording systems to the new Mark 5 for the ten VLBA antennas will not be provided by the Expanded VLA Project.

4.1.5 Correlator Requirements

The signals from the New Mexico Array antennas must be conveyed to the 'WIDAR' correlator for real-time correlation with the EVLA27 antenna signals at the full 16 GHz bandwidth of the EVLA27 antennas. The correlator must be expanded to process these extra signals with the same capabilities that are being provided by Phase I.

The correlator must also be programmed to permit processing of the disk-recorded data from the VLBA and New Mexico Array antennas independently of, and simultaneously with, the real-time operation of the EVLA. The correlator must further be capable of independent correlation of multiple subarrays, which may be defined for both the real-time, and disk-recorded, data streams.

4.1.6 Operational Flexibility

The EVLA correlator being designed and built by the Canadian partner will have the capability to simultaneously correlate data in real time, or from disk recordings. The project thus plans to handle all correlations for the EVLA27, the New Mexico Array, and the VLBA in this single correlator. It is thus anticipated that the operations groups of these instruments will be combined. In general, the operating system must be capable of assigning these antennas to multiple (at least three) fully independent subarrays, one of which must correspond to the VLBA. The operating system must be able to assign an arbitrary number of antennas from the EVLA27 and New Mexico Array to any of these independent subarrays.

4.1.7 System Linearity to RFI

RFI will be present in all EVLA bands, and the receivers and signal chain must have sufficient linearity to permit astronomical observations at frequencies within any band in which RFI is present. The linearity requirements for the receivers on the NMArray antennas are the same as for Phase I, as listed in the EVLA Project Book[3].

[3]The EVLA Project Book is at http://www.aoc.nrao.edu/evla/pbook.shtml

4.2 Low Surface-Brightness Imaging of Very Extended Objects

The scientific goals require a fast, accurate imaging capability for low-surface-brightness objects whose angular extent exceeds that of the antenna primary beam. Such observations will require an efficient 'on-the-fly' mosaicing mode combined with a very compact configuration of antennas.

The brightness temperature sensitivity of any reasonably uniformly distributed array is inversely proportional to its filling factor – the fraction of the area of the array which is covered by its component antennas. The requirements of a low-resolution, high-surface brightness sensitivity capability suggest definition of a new, very compact configuration, to be denoted the E-configuration, with a maximum spacing of approximately 250 meters. This new E-configuration must provide, at modest cost, a substantially better imaging capability, as judged by fidelity and speed, than that provided by the existing D-configuration.

High pointing accuracy — $\delta\theta \leq \theta_{\rm FWHP}/10$ — will be required for such observations when taken at high frequency. The specific requirements are the same as for Phase I, as given in the EVLA Project Book.

4.2.1 Imaging Fidelity

The imaging fidelity in a one-hour observation of a complex source whose angular extent, in each angular dimension, is seven times the antenna's FWHP must exceed 300 for declinations between -10 and $+70$.

4.2.2 Inclusion of Total Power Data

Imaging objects larger than the primary beam necessarily means that an interferometer cannot measure the peak or shape of the central lobe of the visibility function. Such information can only be supplied from a 'single-dish' telescope, preferably from one of larger diameter which is specifically designed for such observations, or from an interferometer comprising much smaller antennas. The image processing software must specifically incorporate such data.

As it is much preferable to utilize 'total-power' data from an antenna considerably larger than the diameter of the antennas in an array for the purposes of mosaicing, and as the time the EVLA will be engaged in large-field, mosaicing activity is expected to be a small fraction of the total, it is anticipated that the GBT, or other similar large-diameter antenna, will provide the necessary data. Hence, there is no specific requirement placed on the EVLA antennas for utilization of total power data for imaging purposes.

4.3 Future Extension to the VLBA

The ultimate goal of the NRAO is to expand the VLBA's capabilities to enable real-time observing with the frequency coverage, sensitivity, and bandwidth of the EVLA. The means, timescale, and costs of achieving these capabilities are not clear at this time. This project thus does not include implementation of these capabilities. However, it is a goal of the Expanded VLA Project to prepare for this ultimate goal by combining the two current operational structures into a single group, unifying the array scheduling, and correlating all VLBA and EVLA data in a single correlator.

4.4 Future Extension to Low Frequencies

The frequencies below 1 GHz have rich scientific potential. Studies of H I emission to redshifts $\sim$1, and studies of steep-spectrum and high-redshift non-thermal emission are prime scientific goals enabled by observations made at frequencies below 1 GHz. Although implementation of this capability is not a part of this project, it is important that Phase II development not exclude the addition of this capability at a later time.

4.5 Computing Requirements

Support of the additional capabilities provided by Phase II necessitates special requirements in computing. For the most part, these special requirements are extensions of the requirements for Phase I, so that the

computing plan can be expected to be an extension of that for Phase I. The areas of greatest impact will be in the scheduling of the array and correlator, and in the subsequent offline data processing.

Computing support for the Expanded VLA Project is divided into three major groups: End-to-End (e2e), monitor and control (M&C), and offline processing. The requirements below are organized into these groups.

4.5.1 e2e Requirements

The e2e software encompasses a wide range of astronomer and telescope functions, including:

- Proposal preparation, submission, and handling;
- Observation preparation;
- Scheduling the telescope and correlator;
- Data archiving and distribution;
- Pipeline processing, including calibration and imaging.

The Expanded VLA Project will require for Phase II the same functionality in all these areas as for Phase I. Identified additional requirements are described in the following.

Proposal preparation, submission, and handling

This software must recognize the possible EVLA, NMArray, and VLBA subarray configurations and permit users to request these. The possible major subarray divisions are:

- The EVLA27, the NMArray, and the VLBA operating independently, with arbitrarily different parameters;
- The full EVLA operating as a real-time instrument (with the EVLA27 in any of its configurations), and the VLBA operating independently;
- The EVLA27 operating as a real-time instrument, and the NMArray+VLBA operating as a single array;
- Subdivisions in which the NMArray antennas can be divided between the EVLA27 and VLBA, or one or more EVLA27 antennas can be added to the VLBA or to the NMArray.

Observation preparation

This software must also be cognizant of the possible subarrays of the full EVLA, EVLA27, NMArray, and VLBA, and be able to generate the necessary files or scripts to control each of the elements of all of these sub-arrays. An added complication is that of integrating the Global VLBI experiments into this system. It is a goal that the proposal tool and the observation preparation tool accommodate the added complexity arising from Global VLBI observations.

Telescope and correlator scheduling

With the addition of the NMArray, which may be either correlated in real time or used with disk recording for correlation later with VLBA or other VLBI antennas, observation scheduling will become considerably more complex. The scheduling software is required to efficiently allocate telescope time to maximize scientific output. To do this the software must be cognizant of the different ways antennas can be used, and must ensure that high priority EVLA observations are not missed or deferred because one or two antennas are used for lower priority NMArray observations. Furthermore, active correlator scheduling will become necessary, because the WIDAR correlator will not have sufficient capability to handle all 37 EVLA antennas at full bandwidth in real time, and to simultaneously process recorded data from disk for a combined NMArray+VLBA observation. A scheduling program for the correlator must be written, to recognize when it has resources to spare and to efficiently use them for processing disk-based data.

Data archiving and distribution

The EVLA will adopt a model for data archiving and offline processing which is essentially the same as that which has been used for the VLA:

- All data products from the EVLA will be archived at the NRAO;
- The observatory will develop and support the necessary software to calibrate and image the data produced by projects scheduled on the telescope;
- The data from any project can be written to an exportable data set for observers who wish to reduce their data at home;
- The observatory will provide the data processing capability at the Array Operations Center and at the Charlottesville headquarters for reduction of data taken by its staff, and by those visiting observers who wish to reduce their data using NRAO facilities.

Data rate, storage, and transfer

The EVLA will support observations that require extremely high output data rates – up to 1.6 GB/sec. Such rates are, currently, prohibitively expensive to archive. A data output rate of 25 MB/sec was selected for the first phase of the EVLA because it can be implemented on standard hardware without major software development costs. Note that this is approximately 250 times the maximum data output rate from the current VLA. This rate will be sufficient for almost all standard EVLA observations (some exceptions being observations requiring special interference excision algorithms, rapid imaging of solar bursts, and high velocity resolution simultaneous observations of a large number (> 20) of spectral lines).

A 12 hour observation requiring the maximum data output rate of 1.6 GB/sec will result in a 10 TB archive. Because the normal evolution of computer capabilities will make archiving, access, and transfer of such data more affordable in the future, and the software and hardware capabilities to efficiently process such databases will grow (although at an uncertain rate) over time, we have made a plan for increasing the data output rate over time which matches these anticipated increases. This plan is given in Table 4.2 with a few examples of the sorts of observations that it will enable. This plan is very much driven by the expected industry development of capabilities, since we believe that any foreseeable increase in the ability to store and process correlator data would be useful for astronomy.

Planned Maximum Data Rates for Demanding EVLA Observations

Date	Data Rate MB/sec	Volume TB/yr	Example Imaging Capabilities
2008	25	75	-Full-field, full-polarization imaging in A-configuration -'On The Fly' imaging in C-config. at 10 times sidereal rate -Simultaneous observations of 16 spectral lines in 2 polarizations -RFI excision for L-band data in D-configuration
2012	250	750	-Solar flares with 60 msec time resolution and 0.1% bandwidth -Obs. of 27 recomb. lines in S-band with full poln. at 1km/sec -OTF imaging in A-config., full poln., any band -RFI excision by offline processing at L-band in D config.
2017	1600	4500	-Full-field full-polarization imaging for full EVLA -Solar flare imaging at 10 msec time resolution with EVLA27. -OTF imaging with full EVLA -RFI excision at L-band in B-configuration

Table 4.2: The planned expansion for the maximum data rate from the WIDAR correlator, and the types of experiments these increases will enable. The mean rate is expected to be much less – probably $\leq$ 10% of the listed values. The expected yearly archive volume, based on this mean rate, is also shown.

These rates are very large, and will generate data volumes, over 12 hours, of 1, 10, and 64 TB respectively for the three stages. The mean rate is much less clear, as this depends on the fraction of observing time that

such high data rate experiments will take up. A reasonable upper limit is 10% of the extreme rate, leading to predicted yearly data volumes of about 75, 750, and 4500 TB/year.

Supporting an initial data rate of 25 MB/sec is a requirement for Phase I. An increase of a factor of ten to a sustained rate of 250 MB/sec, and a total data volume of 750 TB/yr, is a requirement for Phase II.

Further expansion to the maximum planned rate of 1.6 GB/sec, and an anticipated total yearly volume of 4500 TB, is not a requirement for this project until well after 2012. This increase in rate and capacity, which will enable the most ambitious observing projects, must be accommodated within the operations and development plan, as given in Chapter 7. However, it appears that the rapid decrease in disk archiving costs may permit affordable archiving at much faster rates than the 2012 requirement. If so, and if the complexities of parallel channels for networking can be solved, the limiting factor in efficient throughput is likely to be the offline processing. This situation opens the possibility of archiving data from the ambitious experiments shown in the table well before the final target date of 2017. We make this a goal for the project.

As the observatory anticipates users wishing to reduce their data at their home institution, it is required that users must be able to efficiently transport databases of up to 10 TB to their home computers.

Pipeline processing

The overall goal of providing near real time calibration of data and production of default images remains the same for Phase II as Phase I. However, it is recognized that production of such default images for the most ambitious experiments that will be enabled by Phase II will necessarily be limited at the beginning of the project. This will be accounted for when setting the specific goals for pipeline processing as a function of time.

4.5.2 Monitor and Control Requirements

The overall requirements for Monitor and Control are the same for Phase II of the project as for Phase I. Here we summarize the expected additional specific requirements.

The major new components of Phase II of the EVLA project are, with their specific additional requirements for Monitor and Control:

- **The E-configuration** The requirements for this configuration are the same as for any other. No appreciable changes are anticipated.
- **The New Mexico Array.** The anticipated flexible use of this new array, and the necessary flexibility and constraints on the correlation of the data it produces, as described in Section 4.5.1, must be accommodated by the M&C system.
- **The WIDAR correlator.** The WIDAR correlator must be able to accept data from VLBA and standard VLBI antennas, and must provide at least the same correlation capabilities currently provided by the VLBA correlator.

4.5.3 Offline Processing Requirements

Offline processing encompasses the software which the observers use to edit, calibrate, image, and analyze their data.

The offline software must be capable of enabling the imaging to meet the overall scientific requirements. This means the software must allow an observer to make noise-limited images in all requested Stokes parameters, for all of the observational modes supported by the EVLA. The timescales, imaging modes, and data volumes are given in Table 4.2.

The impact of Phase II will be most notable in the size of the generated databases and in the large image sizes needed to support the computationally demanding experiments shown in Table 4.2. The methodologies in this imaging are not expected to differ from those required for Phase I. Existing software packages (notably, AIPS and AIPS++) are not currently capable of supporting the high-end scientific imaging requirements. To do so, a program of research and development of new algorithms for large-scale interferometric imaging is needed. This development is necessary not only for the EVLA, but also for all future interferometric instruments. The areas in which this research and development are needed include, but are not limited to:

- Correction for the polarization imposed by the antennas' primary beams. This is needed for high-precision polarimetric imaging in Stokes Q and U, and for all imaging in Stokes V.
- Development of algorithms to permit solution for a time and spatially variable phase screen over the array. This capability is critically needed for low frequency, full-beam observations, and for high frequency observations.
- Development of algorithms to permit characterization and removal of external interference (RFI) from the post-correlation data.
- Improvements in deconvolution algorithms, particularly for the case of bright, bounded emission which cannot be adequately described as a sum of regularly spaced delta functions. This requires that the imaging algorithms be able to represent emission by the sum of a set of images each with different image plane samplings, or as a sum of discrete components, including the different spectral indices of the various components.
- Correction for the spatially varying spectral index of the extended emission (vital especially as the fractional bandwidth expands). This is needed for all future observations utilizing "multi-frequency synthesis" imaging.
- Implementation of deconvolution algorithms that can accommodate the widely different primary beam sizes that arise from the use of very wide bandwidth systems.
- Development of on-the-fly imaging algorithms, to accommodate this new observing mode which is expected to be heavily utilized for the E-configuration.
- Development of new visualization methodologies to improve the human-computer interface.
- Parallel computing research, especially for coupled problems.
- Alternative calibration techniques.

It should be noted that many of these are in common with ALMA, and joint development will be pursued. Neither the EVLA nor ALMA – nor any future array – will reach its full potential without this development program.

Chapter 5

Technical Implementation Plan

5.1 Overview

Chapter 4 has listed the technical requirements needed to achieve the scientific goals given in Chapter 3 and in Appendix A. This chapter describes how these requirements will be met by the EVLA Project.

The plan presented here has been developed after surveying current and expected technologies which we expect are, or will become, available in the desired time frame for the project. This plan will be continually evaluated as new and potentially more cost-effective technologies are developed.

5.2 The New Mexico Array

The New Mexico Array (NMArray) is required to deliver the final major component of the EVLA: the improvement of resolution at all frequencies by a factor of ten, while preserving the sensitivity and imaging fidelity of the EVLA27. To achieve this goal we need enough antenna stations giving baselines up to ~ 350 km to provide both high sensitivity and good spatial frequency coverage at all declinations accessible to the array. These stations must have a sensitivity at least equal to that of the EVLA27 antennas. declinations accessible to the array. These stations must have a sensitivity at least equal to that of the EVLA27 antennas. As the NMArray will often be utilized as a stand-alone array for monitoring and astrometric observations, the design must provide good imaging characteristics for objects up to $\sim$ 20 synthesized beamwidths in extent. The NMArray will also be combined with the VLBA when the EVLA27 is in its more compact configurations, so the array design must also optimize the imaging characteristics of this combined array.

5.2.1 Station Selection Criteria

The critical metric in the design of the New Mexico Array is the cost/performance ratio. New antennas which are fully outfitted at all EVLA bands are expensive but minimizing their number to reduce costs will diminish both sensitivity and imaging performance. The compromise we seek is that which will achieve the most cost-effective science.

To find the best compromise, we have conducted extensive simulations on the imaging properties of various proposed configurations employing various numbers of new antennas. The results of these studies are summarized in the following sections[1]. Our conclusion is that ten antennas (eight new, and two converted VLBA antennas) added to the EVLA27 is the best compromise between the scientific goals and cost realities for the project. This is the minimum number of new antennas which can provide both the sensitivity and the imaging fidelity required to meet the science goals.

Another key issue to making the New Mexico Array affordable is to find a low cost means to transmit the full bandwidth (16 GHz 96 Gb/sec) signals back to the central site for correlation with those from the EVLA27 antennas. After reviewing existing technologies, the only practical choice is to use existing optical fiber. Building our own fiber network at \$35K or more per mile to remote sites around New Mexico is too

[1]The design of this extended configuration is the subject of EVLA Memos #7, 9, and 20, which may be found at http://www.aoc.nrao.edu/evla/memolist.shtml

expensive: ~$30M for burial costs alone, depending on the terrain. Thus our approach has been to design the array around the locations of existing fibers owned by local telephone companies, which we have found are willing to offer very good rates for leasing the necessary bandwidth. These companies often have excess fiber in the ground due to the minimum practical size of a fiber bundle available commercially. In rural areas, where their service is subsidized by the government, these companies have unused fiber strands which they are unlikely to ever use. They are therefore willing to lease these dark fibers for a 20-year period to us at much lower costs than companies without subsidies who own fibers in more commercially viable regions. In this arrangement, we will provide and maintain the electronics which send the signals through the fibers back to the central correlator at the central EVLA site. While the cost of the required electronics for the fiber transmission is still a significant part of the project, this approach has reduced the operating costs by a factor ~ 10 below other approaches we have considered and a factor of ~ 100 below the standard tariff levels per bit charged for ordinary applications. Operational costs, including fiber rental, are given in Chapter 7.

The decision to utilize commercial fiber for data transmission makes the location of existing fiber routes a major constraint on the location of the NMArray sites. Availability of three phase power is also a constraint, as we wish to avoid the need for running on-site generators, except for emergencies. Finally we need locations which have several available pieces of land within the acceptable radius of the nominal site location which we could use for the project, in order to permit the possible use of multiple small antennas, and for future expansion possibilities. We have avoided sites with any serious potential problems that we can identify (*e.g.*, environmental issues, high local population density, potential radio interference, nearby military activity, etc).

Within these constraints we have calculated the spatial frequency sampling ('*u,v* coverage') of trial arrays to look for acceptable candidate configurations. An initial judgement was made by examination of these simple plots. Once possible solutions were identified for the New Mexico Array, the candidate sites were investigated in detail, first on maps, then with site visits. Most of the sites, perhaps all, are on public land and we have discussed our plans for utilization of these sites with Bureau of Land Management and Forest Service representatives. When we believed we had a candidate configuration we have simulated imaging complex sources to provide a quantitative measure of the imaging fidelity. The details of the site selection process are described in EVLA Memo #51.

5.2.2 Array Design

Figure 5.1 shows the locations of the nine proposed new sites as blue dots. The central EVLA27 site is shown as the inverted red 'Y'. The N.M. state boundaries are in red, the interstate highways in blue, and U.S. highways in gold. All the sites are in relatively remote areas, but all have close access to existing commercial fiber.

We had initially planned to use eight new locations together with two existing VLBA antennas (Los Alamos and Pie Town) to make up the 10 NMArray sites. However, it has since become clear that Los Alamos National Laboratory will require the NRAO to move the Los Alamos VLBA antenna off their site due to its proximity to new, sensitive operations. Funding for this move is discussed in the Budget section of this document. The yellow dot with the red center in Fig. 5.1 shows the present location of the Los Alamos antenna. To meet both VLBA and EVLA requirements, we made two changes in the array design in response to the requirement to move the Los Alamos antenna. We plan to move this antenna to a site 50 km south of Vaughn NM, at which location it will serve the VLBA well. The loss of the long north-south baselines caused by vacating the Los Alamos site will be recovered by a new NMArray station in far southwest New Mexico. An additional benefit of this plan is that fiber access costs to the Vaughn site are far less than those to Los Alamos, which was proving to be more difficult and/or expensive than any of the other sites. This new location will allow us easy access to a fiber for which we have negotiated a low cost lease.

The spatial frequency coverage provided by this proposed configuration is shown in Figure 5.2. The left panel shows the single-frequency *u,v* coverage provided by the New Mexico Array alone, and the middle panel shows the single-frequency coverage for the full 37-antenna EVLA. Use of multi-frequency synthesis will radially stretch the *u,v* coverage by a factor of 1.5 to 2.0, thus producing outstanding coverage over all declinations, as shown in the right panel of the figure. This expected improvement is confirmed through use of multi-frequency synthesis in our trial simulations. Examples of the expected fidelity on a complex trial source with angular diameter $\sim 500\,\theta_{\rm FWHM}$ are shown in the left panel of Fig. 5.3, and for a smaller source

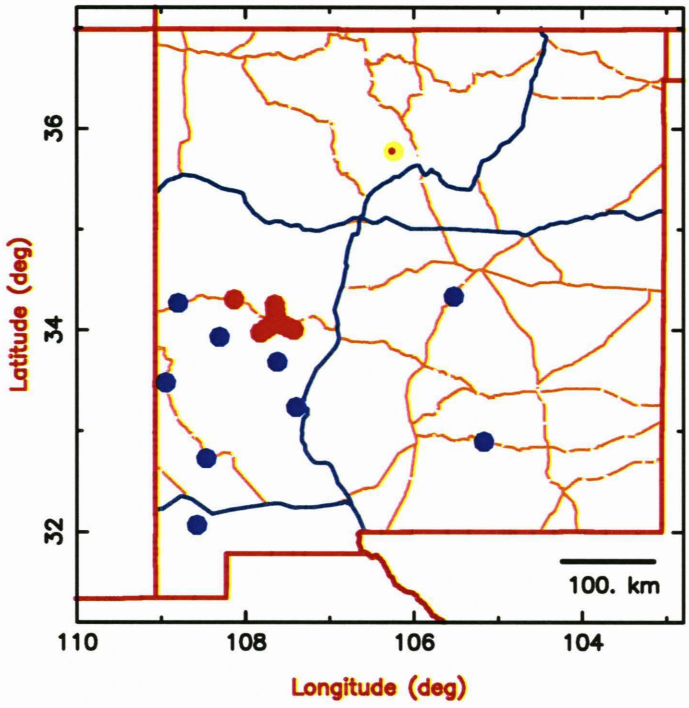

Figure 5.1: A map of New Mexico showing the proposed locations for the New Mexico Array antennas. The thick blue lines show the Interstate highways, the gold lines are U.S. highways. The nine proposed new stations are shown with large blue dots. The VLBA-PT site is marked with the red dot. The inverted red 'Y' marks the VLA. The yellow dot with the red center is the current location of the VLBA-LA antenna, which will be moved to the Vaughn site, shown by the most northeastern blue dot.

of extent $\sim 45\,\theta_{\rm FWHM}$ in the right panel.

The methodology utilized in these simulations is briefly described below:

- The visibilities corresponding to the trial array are calculated for a complex source model whose angular extent is approximately 1/3 of the fringe spacing of the shortest spacing in the trial array at the frequency selected. The AIPS program UVCON was used to generate these visibilities. The model used is an appropriately scaled image of Cassiopeia A, containing angular structure over a range exceeding 1000:1.[2]

- For 'monochromatic' simulations, these visibilities were computed for a single frequency. For 'multi-frequency synthesis' simulations, the visibilities were calculated at 8 equally spaced frequencies covering the range 1.2 to 2.0 GHz. A flat spectral index was assumed to simplify the imaging process.

- The AIPS programs IMAGR and VTESS were used to image and deconvolve the data. The resulting image was smoothed with a Gaussian beam whose FWHM is equal to that of the point-spread function. Because of the preponderance of short spacings resulting from the intra-VLA baselines, the outer spacings were given a high weighting in the deconvolution through use of the 'robustness' parameter in IMAGR.

- The original trial image was smoothed to the same resolution as the resulting deconvolution, and subtracted from the deconvolved image. The fidelity parameter plotted in Fig. 5.3 is the peak brightness of the convolved trial image divided by the r.m.s. of the difference image.

As it is anticipated that the EVLA will be used in a tapered mode to provide a resolution intermediate between that of the A-configuration and the full EVLA, the inner NMArray antenna locations were selected

[2]The choice of Cassiopeia A was made solely based on its recognizability and complexity. We believe the complexity of structure will be representative of sources that will be imaged with the EVLA.

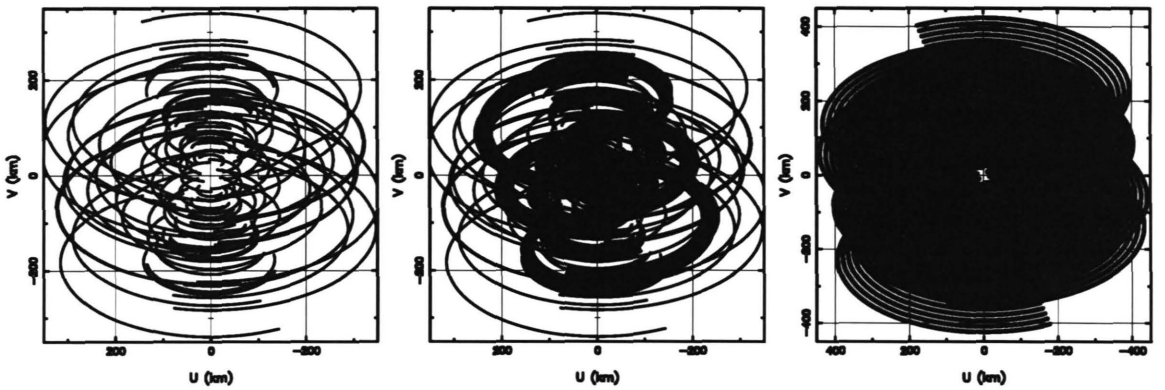

Figure 5.2: The left panel shows the spatial frequency sampling for a single-frequency observation at $\delta = 30°$ with the ten-antenna New Mexico Array. The center panel shows the coverage for the full 37-antenna EVLA. The dense sampling provided by the EVLA27 antennas dominates the sensitivity and imaging characteristics. The right panel shows the coverage for the New Mexico Array alone in a 'multi-frequency synthesis' mode, which will utilize the full bandwidth provided by the EVLA. The overall coverage is excellent. The coverage plot for the full EVLA when used in this mode appears the same at this resolution, except that the small center hole is eliminated.

to ensure good imaging for this application. The image fidelity with this degree of taper is shown in the left panel of Figure 5.4. The angular diameter of the trial source in this case is 40 times the (tapered) array FWHM. The right panel shows the imaging fidelity when the NMArray is used in a standalone mode for observing an object of more limited angular extent. We anticipate the NMArray will see extensive use as a separate subarray for monitoring expanding transient sources and for astrometric applications when the EVLA27 is in its compact configurations.

Although costs could be reduced by a reduction in the number of new antennas, such savings will come at a drastic reduction in EVLA performance. A reduction from eight to six new antennas will not only reduce the high-resolution sensitivity by 20% (which would require a 40% increase in observing time to make up the point-source sensitivity loss), but will cause a much larger loss in imaging performance. This is shown in Figure 5.5, which shows the impact on imaging of reducing the number of New Mexico Array antennas from ten to eight. The left panel shows the 37-antenna fidelity, the right panel the 35-antenna fidelity. In this simulation, one 'near' antenna (PT), and one 'far' antenna (Vaughn) were removed. The loss in fidelity is dramatic a factor of two to three. We believe the results shown will be representative of any similar pair removed from the array.

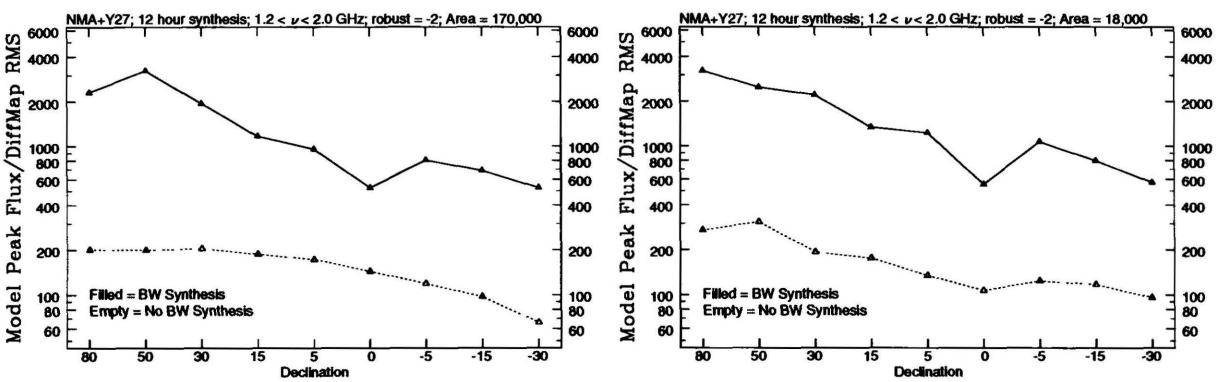

Figure 5.3: Anticipated imaging fidelity for large and complex sources with the full-resolution EVLA. The methodology of the simulations is described in the text. In the left panel, the trial source is 170,000 times the solid angle of the synthesized beam. In the right panel, it is 18,000 synthesized beams. For each simulation, the 'dip' at $\delta = 0°$ is due to the horizontal loci of the u,v tracks.

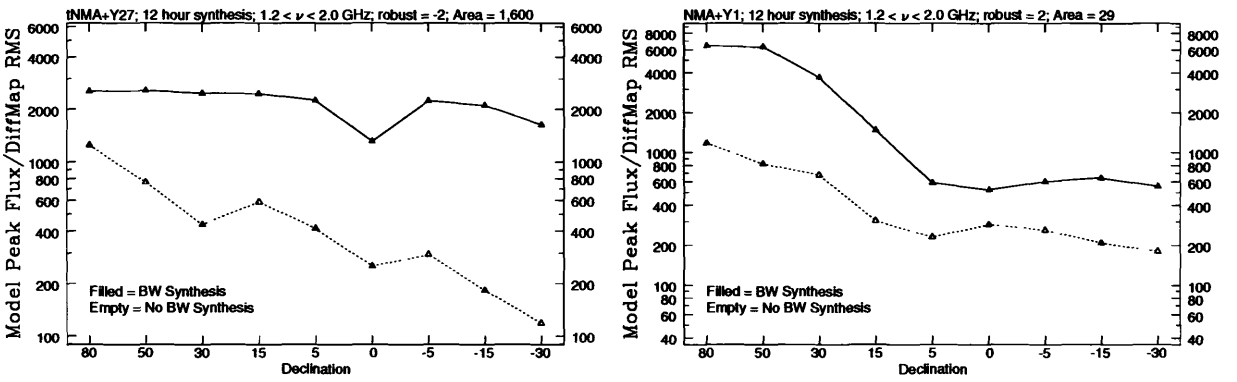

Figure 5.4: The left panel shows the fidelity when the EVLA data are tapered to a resolution one-third of the maximum. The source is the same angular size as the right hand panel simulation in Fig. 5.3, but because the array has been tapered, the number of resolution elements in the trial object is reduced to 1600. In the right panel is shown the fidelity of the New Mexico Array plus one VLA antenna to a trial source whose solid angle is 29 synthesized beams.

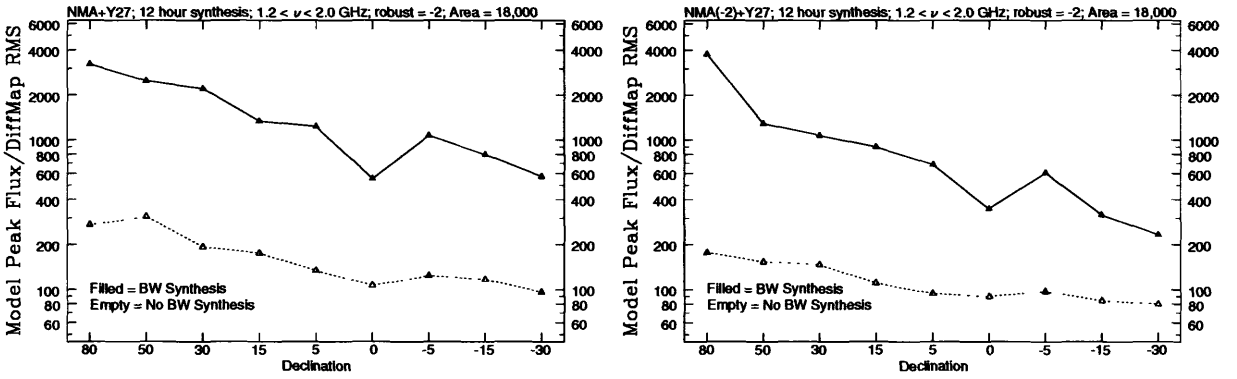

Figure 5.5: The effect on imaging fidelity of the EVLA by reducing the number of New Mexico Array antennas from ten to eight. The left panel shows the full EVLA, the right panel shows the EVLA minus two antennas. The antennas removed are at Pietown and Vaughn. The loss of fidelity is typically a factor of two to three, and worsens with decreasing declination.

5.2.3 Station Design

The station sensitivity requirements are given in Table 4.1. To provide this, each station must comprise at least $\sim$ 500 sq. meters of collecting area, plus state-of-the-art receivers. A station can be comprised of a single antenna, or a phased group of smaller antennas. We have carefully considered the costs and performance of each approach, and have concluded that the single antenna plan is the correct approach for this project. We have chosen to use 25-m antennas because:

- antennas of this size are close to the minimum in the total cost curve of antennas plus instrumentation for a given station sensitivity;
- the design is well understood;
- there is extensive experience in building antennas of this size among a number of manufacturers so we can expect a number of competitive bids; and
- there is much merit in having all the elements of an array be the same diameter, as this greatly simplifies the wide field imaging problem, and reduces the cost of post-processing.

Each of the ten elements of the New Mexico Array will thus be a 25 meter diameter advanced design precision antenna, equipped with state-of-the-art low noise receivers. These receivers and their intermediate-frequency and digitizer systems will be identical to the systems developed during the Phase I Project. Two of these elements will be existing VLBA antennas, upgraded with electronics to match the EVLA frequency bands. The other eight stations will have new antennas built to the same specifications as the two modified VLBA antennas.

Each site will need a small building ($\sim$ 300 sq. ft.) to house fiber connections, a temperature controlled enclosure for the hydrogen maser, a small work area and a bathroom. A backup generator is also needed. A gravel road is needed to connect the site with the nearest existing road. A fence is needed around the entire compound for security.

Availability of 3-phase power was a major consideration for picking the sites. Nonetheless, some of the sites are located at significant distance from existing 3-phase power. We estimate a total of 110 kilometers of new 3-phase power lines would need to be added to attach all the sites to the commercial 3-phase power network. However, two of the sites without 3-phase power have single phase power lines which we can convert to 3-phase at modest expense. For one site the nearest 3-phase power is six miles away; all others are much closer to existing 3-phase power. In total, and excluding last mile costs which are included in the civil work, we estimate we will need 15 miles of new power lines.

Last mile fiber costs for each site are included in the budget. The remaining fiber connections will be supplied by the local telephone companies at a cost which will be absorbed into the lease expense we pay each year. Most of the capital expense for the fiber is due to the electronics necessary to send the signals from the antennas back to the central EVLA site.

An Environmental Impact Statement (EIS) will be needed regardless of whether we locate sites on public or private land. There will be costs to acquire sites whether public or private.

In addition to the costs for each site, we need to add capital equipment for the maintenance of the sites. This includes trucks, laboratory and hardware repair equipment, warehouse space, etc. Costs for these items are included in the budget.

5.2.4 Local Oscillator Reference

Each station must be provided with a stable reference for its local oscillator system so that coherence can be maintained across the array. It is not considered feasible to distribute the reference on the fiber optic network because cost restricts the network to a single fiber which provides a signal path only in the direction from the antenna to the VLA site. The baseline plan costed in this document provides a hydrogen maser frequency standard at each station, as is currently done at the VLBA sites. An alternate approach, currently under development at JPL, is to radiate the master reference signal from the central EVLA site to all stations using a geostationary satellite. This approach is likely to be less expensive than hydrogen masers both for capital and operating cost, and will be used for the NMArray if it can be shown to meet our stability requirements.

5.2.5 Phase Stability and Water Vapor Radiometers

The electronic phase stability requirements for the EVLA electronics are set to ensure that residual phase fluctuations from the electronics will always be less than those introduced by the atmosphere. The imaging performance of the array will thus be ultimately set by the ability to calibrate out these atmospheric fluctuations. For stronger sources (typically, more than a few tens of milliJanskys), well-established self-calibration techniques will suffice at all frequencies. For weaker sources, calibration on nearby sources is very effective at lower frequencies ($\nu < 10$ GHz), but less so at higher frequencies. Over the past few years, considerable progress has been made in improving the stability of water vapor radiometers (WVRs) to the point where, under good weather conditions, WVR monitor data can be used to reduce the atmospheric phase residuals in the 40 50 GHz band to considerably less than one radian[3]. We have thus budgeted for one K-band WVR system for each NMArray antenna, using the budget estimates in EVLA Memo #74.

[3]See EVLA Memo #73 for a recent report.

5.2.6 Correlator Expansion

The Phase I version of the EVLA correlator can process 32 stations at the full bandwidth of 16 GHz. This is not enough for all 37 antennas of the EVLA. As the correlator capacity comes naturally in units of eight stations, we will expand it to 40 stations. This is sufficient to handle the requirements from the 37 EVLA and eight unconverted VLBA antennas because the VLBA will not be correlated at the full 16 GHz bandwidth, and the correlator design can accommodate two or four antennas per station input, provided their bandwidths are limited to 4 and 1 GHz respectively.

5.2.7 Predicted Performance

In this section, we give a brief description of the EVLA's point-source and brightness temperature sensitivities in various operating modes.

The Full EVLA

The continuum and spectral line point-source sensitivities, and the brightness temperature sensitivities at full resolution, for the 37-antenna EVLA are given in tabular form for each of the eight frequency bands in Table 5.1. The entries in the table are 1-σ, for an integration of one hour.

Table 5.1: **Expected Sensitivity (1-σ in 1 hour, Stokes I) of the Full EVLA**

Freq. GHz	Freq.Range GHz	Resn. mas	$\Delta\nu$ [a] GHz	T_{sys} K	Effic.	SEFD [b] Jy	CPSS [c] μJy	CBTS [d] K	LPSS [e] mJy	LBTS [f] 1000K
0.32	.30–.34	640	0.03	150	0.40	2100	130	3600	36	1100
1.6	1.0–2.0	130	0.50	26	0.50	293	4.5	124	2.5	68
3.0	2.0–4.0	68	1.5	29	0.62	265	2.2	57	1.2	31
6.0	4.0–8.0	34	3.0	31	0.60	290	1.7	42	0.9	23
10	8.0–12	20	3.0	34	0.56	340	2.1	53	1.1	29
15	12–18	14	5.0	39	0.54	405	1.8	46	1.0	25
23	18–26.5	8.9	7.0	54	0.51	600	2.3	60	1.3	33
34	26.5–40	6.0	7.0	45	0.39	650	2.5	64	1.4	35
44	40–50	4.6	5.0	66	0.34	1100	5.0	130	2.8	71

[a]The assumed usable single-polarization instantaneous bandwidth available for continuum observations. The value is based on RFI surveys.

[b]System Equivalent Flux Density: SEFD = $5.62T_{sys}/\eta_a$ Jy for a 25-meter antenna

[c]Continuum Point Source Sensitivity in μJy: $\sigma_\mu = 0.37\frac{SEFD}{\eta_s\sqrt{N(N-1)t_h\Delta\nu_G}}$ where $SEFD$ is in Jy, η_s is the correlator and image gridding efficiency, N is the number of identical 25-meter antennas, t_h is the integration time in hours, and $\Delta\nu_G$ is the single-polarization bandwidth in GHz. Multiply by $\sqrt{2}$ for single correlator observations.

[d]Continuum Brightness Temperature Sensitivity for full resolution of the full EVLA. Defined as the brightness temperature providing the CPSS within the solid angle of the synthesized beam: $\sigma_T = 1.30\frac{\sigma_\mu}{\nu_G^2\theta^2_{\rm arcsec}}$ where σ_T is the brightness in degrees K, σ_μ is the point-source sensitivity in μJy, ν_G is the frequency in GHz, and θ_{arcsec} is the resolution in arcseconds. This can also be expressed in milliKelvin as: $\sigma_{T,mK} \sim 0.34\sigma_\mu B^2_{km}$, where B_{km} is the maximum baseline in kilometers

[e]Spectral Line Point-Source Sensitivity for 1 km/sec velocity width. The sensitivity in mJy for a bandwidth corresponding to a particular velocity width is $\sigma_m = 0.21\frac{SEFD}{\eta_c\sqrt{N(N-1)t_h\Delta v_1\nu_G}}$ where Δv_1 is the velocity width in km/sec, and ν_G is the frequency in GHz. Multiply by $\sqrt{2}$ for single correlator observations.

[f]Spectral Line Brightness Temperature Sensitivity for the EVLA at highest resolution, with a 1 km/sec velocity width. The definition is the same as for CPSS.

The greatest strength of the EVLA will be its imaging capability over a very wide range in frequency and resolution. This is difficult to convey in a table or chart of point-source sensitivity, as the relevant metric for imaging is brightness sensitivity. A detailed description of the surface brightness sensitivity for both the EVLA and ALMA is given in Appendix B.

Performance of the New Mexico Array Alone

The resolution and sensitivity of the New Mexico Array used as a standalone array is shown in Table 5.2. The performance is very impressive – as a separate array, the NMArray will have better sensitivity than the current VLA. Although the maximum source size which can be reliably imaged will be limited to objects less than $\sim$ 10 times the FWHM, the NMArray will be ideal for imaging the expansion of transient objects, and for astrometry.

Table 5.2: **Expected Sensitivity (1-σ in 1 hour for Stokes I) of the New Mexico Array**

BandName	Freq.Range GHz	Freq. GHz	$\Delta\nu$ GHz	T_{sys} K	Effic.	SEFD Jy	Resn. mas	CPSS μJy	CBTS [a] K
P	.30–.34	0.32	0.03	150	0.40	1350	525	240	18000
L	1.0–2.0	1.6	0.50	26	0.50	293	105	14	920
S	2.0–4.0	3.0	1.5	29	0.62	265	57	7.8	500
C	4.0–8.0	6.0	3.0	31	0.60	290	28	5.8	390
X	8.0–12	10	3.0	34	0.56	340	17	6.8	450
U	12–18	15	5.0	39	0.54	405	11	6.2	420
K	18–26.5	23	7.0	54	0.51	600	7.4	7.8	515
A	26.5 40	34	7.0	45	0.39	650	5.0	8.5	565
Q	40–50	44	5.0	66	0.34	1100	3.9	17	1130
W	80–96	86	8.0	100	0.20	2820	2.0	35	2500

[a]At maximum resolution. Modest tapering will improve brightness sensitivity by a factor of two to three, at the cost of degraded imaging performance.

Variation of Sensitivity with Resolution

The design of the NMArray permits tapering to give higher brightness sensitivity of the EVLA at the cost of resolution. The relation between taper and both point-source and brightness temperature sensitivity is given in Figure 5.6, for the 34 GHz band (left pair of panels), and for the 86 GHz capability on the NMArray alone (right pair). For the full EVLA at 34 GHz, the range of taper can be very broad – over an order of magnitude. The plot shows the results over a factor of five in resolution. Over this range, there is little loss in point-source sensitivity, and a very large increase in brightness sensitivity.

5.3 The E-configuration

The design of the E-configuration is driven by the need to achieve better imaging of low surface brightness objects whose extent is comparable to or larger than the primary beam of the VLA. Although the GBT will easily detect the objects of interest with the required surface-brightness sensitivity, it will not provide sufficient resolution for many investigations. What the E-configuration will add is three times higher resolution than the GBT (operating at the same frequency) with good fidelity, while retaining the required surface-brightness sensitivity. As this configuration is designed for mosaicing observations of objects larger than the antenna primary beam, short-spacing information on baselines shorter than the antenna diameter will be required. It is assumed that such short spacing information will be provided by the GBT or another telescope of similar aperture, or by an array of much smaller antennas. The E-configuration extends the u,v coverage of these facilities so that higher resolution, high fidelity mosaiced images can be made using the EVLA27's large collecting area and powerful WIDAR correlator.

5.3.1 Configuration Studies

The essential goal in designing this configuration is to locate all 27 EVLA27 antennas within a $\sim$ 250 meter diameter circle. We considered two approaches to achieve this – a new, standalone array, and a design incorporating as many existing D-configuration antenna pads as possible. As expected, the former approach

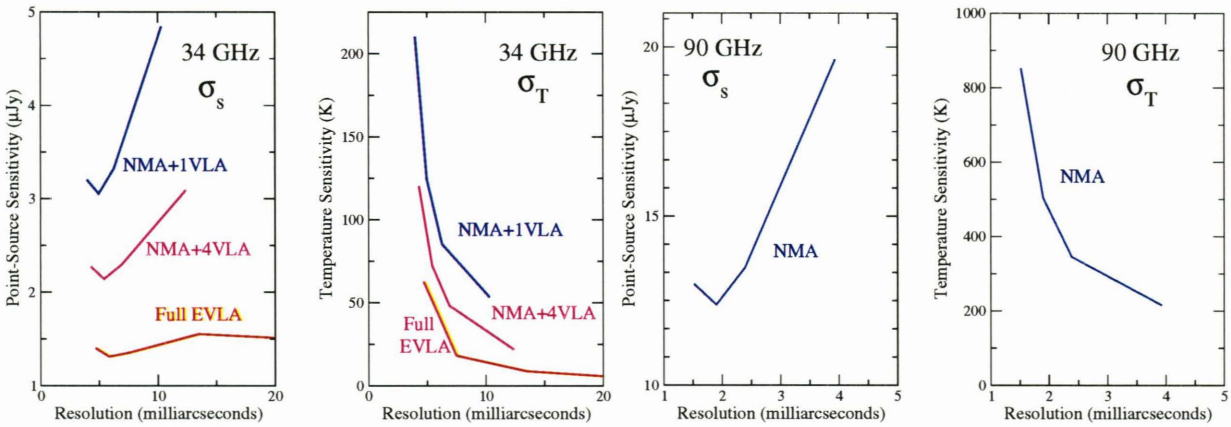

Figure 5.6: The anticipated point-source and brightness temperature sensitivities at 34 GHz (left pair) and 86 GHz (right pair), as a function of array resolution. These were calculated using simulated noise data, using imaging parameters appropriate for the expected imaging application, and an 8-hour integration for Stokes I. The red lines show the performance of the full 37-antenna EVLA. The magenta lines show the performance of the NMArray plus 4 EVLA27 antennas, and the blue lines show the NMArray plus 1 EVLA27 antenna. Performance in other bands can be derived by scaling the vertical axes by the point-source sensitivity values listed in Table 5.2, and the horizontal axes by the wavelength.

will provide the best imaging performance. But, we have found a design layout which incorporates 16 new pads, and provides almost as good imaging capability at about half the price of the stand-alone design.

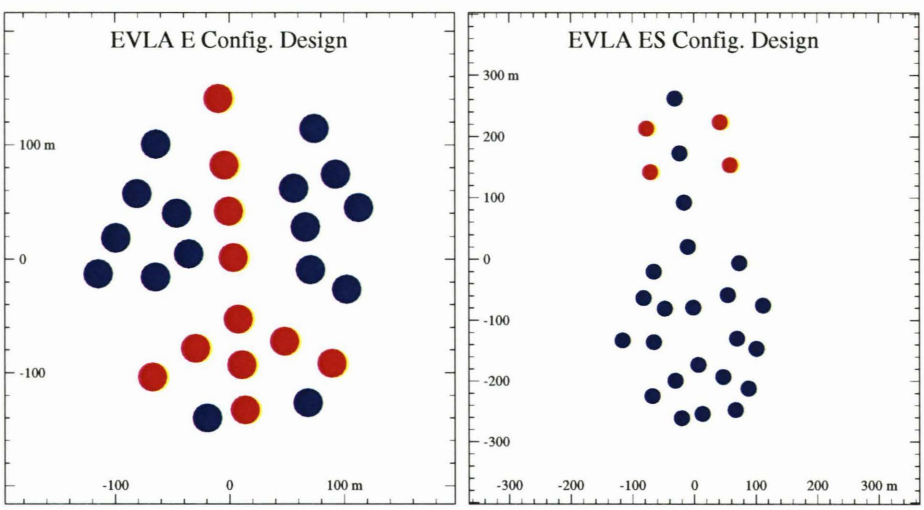

Figure 5.7: The left panel shows the proposed locations of the antenna stations for the E-configuration. The red dots indicate D-configuration stations that will be utilized, the blue dots indicate the new antenna pads. The dot sizes indicate the actual 25-meter diameter of the antennas. All stations are within 125 meters of the center. The right panel shows a modified E-configuration with an extended north arm which would allow better imaging at declinations south of -20 degrees. In this panel, the four red dots indicate the additional stations, and the blue dots show both the existing D-configuration stations and the new stations for the standard E-configuration.

A number of array layouts were studied using a process similar to that employed for the New Mexico Array: u,v coverage plots were first examined to give direction on which concepts were more likely to succeed, followed by detailed simulations to demonstrate how well the configuration worked in practice. The imaging process is also the same as that for the New Mexico Array, with an appropriate change in image size. Included in these studies were comparisons of the performance of the D-configuration with the E-configuration. As the objects used for the trials had an angular extent at least seven times that of the VLA antenna primary

beam, all reconstructions utilized GBT data.

Fig 5.7 shows the proposed locations of the E-configuration antenna pads. The left panel shows the standard E-configuration, designed for observations at declinations $\delta \geq -10$. In this panel, the blue dots denote the new antenna pads. The right panel shows a proposed extended ES-configuration, denoted 'ES', which moves four antennas to new pads, denoted by the red dots, to minimize shadowing and hence permit more effective observing of southern sources. The loss of sensitivity due to shadowing for both configurations is shown in Fig 5.8. The most immediate effect of shadowing is to reduce the sensitivity, but an equally severe problem is the increased ellipticity of the synthesized beam. The ES-configuration minimizes both problems.

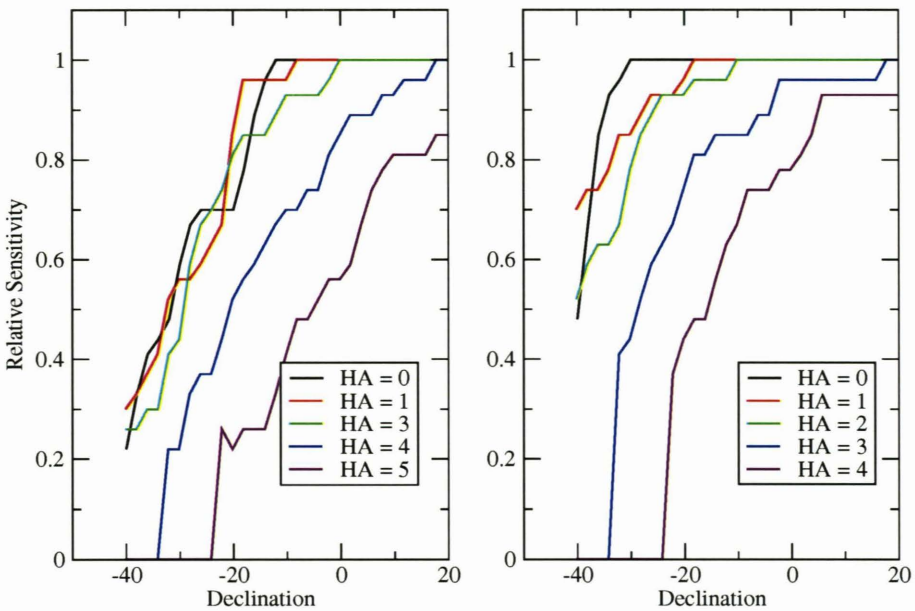

Figure 5.8: The loss of point-source sensitivity due to shadowing is shown for the E-configuration (left panel), and the north-arm extended ES-configuration (right panel), as a function of declination and hour angle. The extended configuration gives significantly better sensitivity, and a more circular synthesized beam south of $\delta \sim -10$. An antenna is considered fully shadowed if any part of it is blocked.

5.3.2 Performance Comparison with D-configuration

Although the D-configuration can in principle provide these observations, its performance will be much inferior to the E-configuration for reasons of time and image fidelity[4]. The scientific goals require fast, accurate imaging of very large objects with baselines up to approximately 250 meters. With the D-configuration, more than half of the spacings lie outside the range – and are hence not useful for reaching the required performance. For optimum speed and fidelity, these antennas must be placed into a circle of diameter of ~250 meters. The superior performance of the E-configuration is well illustrated in Figure 5.9, showing a comparison between the spatial frequency plane sampling with the present D-configuration and the proposed E-configuration.

The imaging performance of the E- and ES-configuration, compared to the existing D-configuration when tapered to the same resolution, is shown in Fig 5.10. This shows the results of a single 7 x 7 mosaic of a large and spatially complex object, done with both the D-configuration and the proposed E-configuration. For both simulations, GBT data have been added. The observing duration was one hour. Also shown is the fidelity on a far southern source, taken with the extended ES-configuration. The major gain of the ES-configuration is in maintenance of the sensitivity (due to reduced blockage), and the generation of a more circular synthesized beam.

Table 5.3 shows the expected point-source and brightness sensitivities for the E-configuration.

[4]See EVLA Memos #6 and #56 for discussion on compact array design and performance.

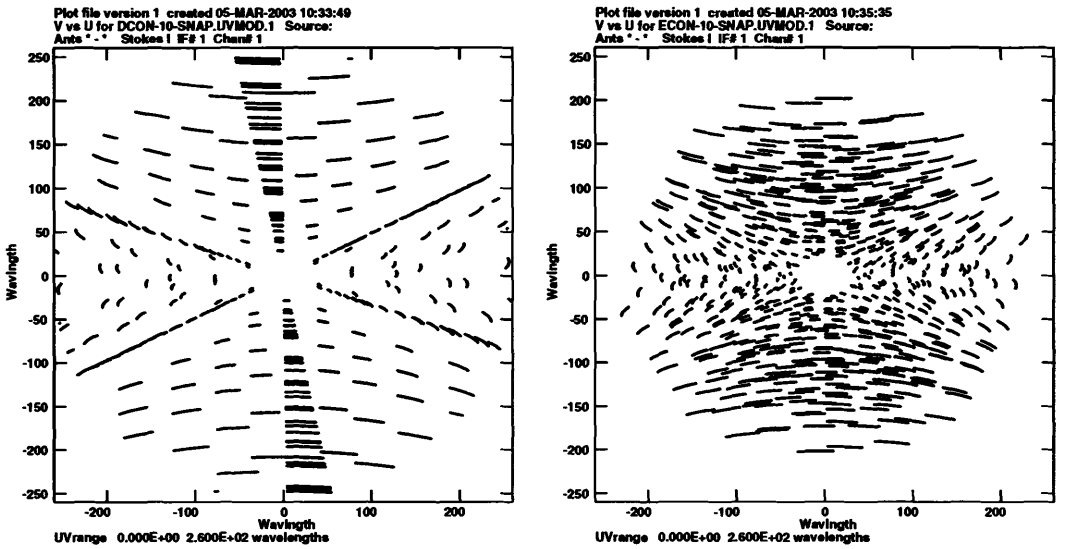

Figure 5.9: The left panel shows the spatial frequency sampling by the D-configuration for a one-hour observation at $\delta = -10°$, within a circle of radius 250 meters. An equal number of sample points lie outside this radius. The axes are in meters. The sparse, semi-regular sampling and the 'rays' result in poor imaging fidelity. The right panel shows the sampling by the E-configuration for the same integration and declination. The sampling is very much denser, more uniform, and more random. There are more than twice as many sampled points within the 250-meter radius. This antenna configuration will give much better fidelity and brightness sensitivity. Sampling within the central 'hole' is critical for mosaiced observations, and will be provided by single-dish observations.

5.3.3 Technical Implementation

Figure 5.7 shows the final concepts for the E-configuration, and the southern-extended E-configurationS. The detailed cost estimates are given in the budget section. The costs are dominated by the concrete needed for the new pads and the additional rail track which would be needed.

The configuration design ensures that the railroad tracks and antenna pads do not conflict with the location of the fiber optic cables, as the fiber routing for Phase I of the project was designed to enable future construction of the E-configuration layout shown in Fig. 5.7.

Table 5.3: **E-configuration Point-Source and Brightness Sensitivity in 1 Hour (1-σ, Stokes I)**

Band	Freq.	Resolution	CPSS	RMS Conf.[a]	CBTS[b].	LPSS	LBTS
GHz	GHz	arcsec	μJy	μJy/beam	μK	mJy	mK
1.2–2	1.6	120	6.2	610	135	1.8	37
2–4	3.0	60	3.0	93	64	1.1	23
4 8	6.0	30	2.3	14	50	.85	18
8–12	10	19	2.8	4.0	60	.78	16
12 18	15	13	2.5	1.4	57	.71	15
18–28	23	9.0	3.2	.50	67	.85	18
28–40	34	6.0	3.5	.17	74	.78	16
40–50	44	4.5	6.9	.082	140	1.1	24

[a]Calculated from $\sigma \sim 0.056\theta^2_{\rm arcsec}\nu_{\rm G}^{-0.7}$ microJy/beam. (Condon, priv.comm.)

[b]Conveniently expressed as: $\sigma_{\rm T} = \frac{T_{sys}}{f\eta\sqrt{Bt}}$, where T_{sys} = system temperature, B=bandwidth(Hz), t=integration time(sec), η = overall system efficiency, and f = filling factor (the fraction of the array area covered by its constituent antennas)

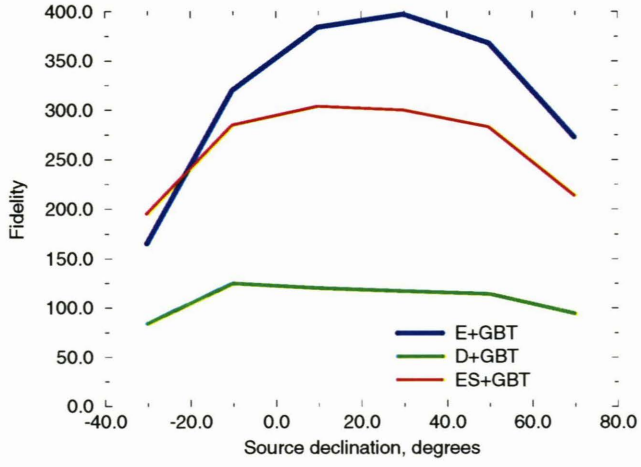

Figure 5.10: The fidelity of the proposed E-configuration compared to the existing D-configuration, with the southern-extended ES-configuration added. For all simulations, GBT data have been added. The simulation is of an object whose size is six times the antenna primary beamwidth, taken in a single 7 X 7 raster. The fidelity is defined as the ratio between the peak brightness in the model image to the rms of the difference between the model and reconstructed image.

5.4 Computing Plan

5.4.1 Overview

As noted in Chapter 4, the computing requirements for Phase II are very similar to those for Phase I. The greatest impacts of the increased requirements associated with Phase II are expected to be in the areas of telescope and correlator scheduling, and in the archiving, distribution, and reduction of the correlator data. In this section, we examine the additional computing costs associated with Phase II, including both the scale of computing and the software development costs. Some of the estimates for computing scale are based upon modeling described in EVLA Memo #24. The personnel estimates were derived based on the detailed planning for M&C, e2e, and offline processing done for the ongoing EVLA Phase I project. Incremental requirements for Phase II were estimated as a fraction of the total effort required for Phase I, and the Phase I numbers were than scaled by the appropriate amount. In some areas, such as M&C, the Phase I design work is well under way, and we have high confidence that the estimates are quite close to the mark. In some of the e2e areas, the EVLA Phase I work is less advanced at present. In these instances, we have compared our software requirements and personnel allocations against those for related activities in ALMA, and adjusted them slightly where appropriate.

5.4.2 e2e

The NRAO e2e system will be used to handle proposal preparation, submission, and handling, observation preparation, telescope scheduling, pipeline processing, and archiving. Some of these capabilities are common with Phase I and will require minimal changes. But others, such as the observation preparation, telescope scheduling and pipeline processing will require substantial development. All of these areas must be augmented to support observations with the expanded capabilities. For example, the scheduling software must take into account a wider range of observing scenarios. Similarly, the pipeline heuristics must be expanded to accommodate the particular problems of processing NMArray observations. Each of the sections of the e2e system will now be discussed separately.

Proposal preparation, submission, and handling

Proposal preparation tools suitable for the EVLA after Phase I will require an upgrade for Phase II. Feedback on constraints on available array configurations and correlator settings will have to be modified and expanded. We expect however that the logic and structure of the tool itself will require little change, the software will only have to support a slightly wider range of observational parameters. We have budgeted 0.5 FTE-years for this effort.

Observation preparation

The observation preparation tool will need a number of enhancements for Phase II. It will have to support a substantially increased use of subarrays. The extent of the reprogramming effort will depend on the actual definition of subarrays, such as whether an antenna will be able to be part of more than one subarray at a time. The E-configuration will require adding improved shadowing checks and alerts. We have budgeted 2.5 FTE-years for this effort.

Telescope and correlator scheduling

A major goal of Phase I of the EVLA is to have the array fully dynamically scheduled, *i.e.*, , what is being observed at any given time is determined at that time (or shortly before in any case) by examination of scientific priority, current conditions, and required conditions for the different projects. This philosophy is also adopted for Phase II, including all of the various subdivisions of the antennas. We expect this to have a major impact on telescope scheduling because of this increased subarray usage, and the wider variation in weather conditions over the various NMArray sites, requiring a slightly different scheduling approach than that necessary for Phase I. Correlator scheduling will become more complex due to the increased use of subarrays, and because of the incorporation of the VLBA. We have budgeted 1.0 FTE-year for telescope scheduling and 3.5 FTE-years for correlator scheduling for this effort.

Data archiving and distribution

We do not expect that Phase II will affect the data archiving software in a major way. It is estimated that 0.5 FTE-year will suffice for software changes to support the archive, plus 1.5 FTE-years for networking upgrades, both hardware and software. The volume of data that has to be handled will increase dramatically, requiring substantial upgrades of the archive, the networking, and the data reduction hardware both for the pipeline and for postprocessing. Assuming Moore's law continues to hold, we find that the Phase II requirements in 2012 can be met at a cost very similar to that of Phase I in 2008. This means another $250K for archive hardware, and $250K for networking upgrades.

Pipeline processing

The major impact on pipeline processing caused by Phase II will be in the tenfold to 100-fold increase in data rate. The addition of much longer baselines will have a significant effect on imaging. While the development of this software will take place in the AIPS++ group, its implementation and testing in a pipeline environment is part of the e2e system. In particular, the pipeline heuristics must be expanded to accommodate the particular problems in processing NMArray observations. We have budgeted 1.5 FTE-years of software personnel and 2.0 FTE-years of scientific staff personnel for this effort. Using the same arguments as in the data archiving case, we expect pipeline hardware suitable for Phase II in 2012 to cost the same as Pipeline hardware for Phase I in 2008 – $250K, plus an additional $50K in additional hardware.

5.4.3 Monitor and Control

The plan for meeting the Phase II requirements is outlined below, with estimates of the required additional personnel.

E-configuration

It is not anticipated that the E-configuration will require more than minor changes in the array M&C software, as the antennas and observing modes will be the same as for the D-configuration. A budget of 0.5 FTE-year has been allocated for minor changes throughout the M&C system.

New Mexico Array

Some adjustments to and extension of the M&C system will be required. Having the Pie Town and Los Alamos VLBA antennas and the NMArray antennas equipped with EVLA electronics will be of considerable help in keeping the needed modifications to a minimum. However, the command and monitor transit times to/from these antenna pads will be significantly different from those on the EVLA27 pads, and the local oscillator and time reference signals will be provided to these antennas in a different manner. These differences will require changes in the observing layer of the M&C system, and some modification of the code that runs in the antenna processors. It is also clear that the degree of operational flexibility required to simultaneously support operation of the EVLA27, VLBA, and NMArray subarrays will present new challenges, with new requirements placed upon M&C and operations support software.

The Phase II budget request includes the following items:

- The EVLA M&C design must be re-evaluated in light of new requirements related to the NMArray. For example, the latency requirements are more stringent for the NMArray. This will require 1.0 FTE-year for the re-evaluation, and 5.0 FTE-years for any necessary changes.
- The Observing Layer in the M&C will require some changes to incorporate the NMArray (2.0 FTE-years).
- The two VLBA antennas used in the NMArray must be accommodated within the core M&C software below the Observing Layer. This includes changes to the Antenna Control subsystem (2.0 FTE-years) and programming of the MIBs to be retrofitted to the two antennas (1.0 FTE-year).
- Array geometry calculations using the CALC package for 40 antennas will be extensive, and will require a high-end computing engine ($50K).

Correlator backend

The EVLA correlator will be increased from 32 to 40 inputs for Phase II, resulting in additional software costs. The increase in the number of inputs will require a change to the size of the CBE. The increase in the number of baseline boards and cluster nodes to support the correlator will require both additional hardware and software effort. We have budgeted $500K for the incremental cost of upgrading the CBE hardware. The corresponding software costs should be relatively modest, and we have budgeted 1.0 FTE-year for reworking and testing.

The initial Phase I maximum output rate of 25 MB/sec chosen for the correlator is based on current archiving capabilities and costs. To upgrade the system by 2012 to 250 MB/sec will require a reinvestment to the archiving system, as described above. The CBE will be capable of handling this data rate, and no upgrade will be needed. The interface and network connections between the CBE and the archive will need to be expanded, however. We have budgeted $100K for this hardware expansion.

A further expansion to the maximum planned rate of 1.6 GB/sec (or higher, if that is later judged to be necessary) is not a requirement for this project until after 2012, and would be developed under the operations plan as summarized in Chapter 7.

Use of the WIDAR Correlator for the VLBA

We will use the WIDAR correlator as the correlator for the VLBA. This has a number of scientific and operational advantages laid out elsewhere. The use of the WIDAR correlator for the VLBA will generate a number of requirements unique to Phase II in the areas of array operations and M&C. The monitor and control interface to the correlator must be expanded to accommodate VLBI input devices. The software that allows for configuration of correlator inputs, and the allocation of correlator resources will become more

complex. The VLBA correlation support software (job control, script generation, etc.) must be converted for use on the WIDAR correlator. Operational support tools with capabilities beyond those currently available will also be required to support combined EVLA and VLBA activities. This aspect of Phase II will require the following substantial investments in software design and engineering resources:

- The M&C interface to the WIDAR correlator (the Virtual Correlator Interface) must be expanded to accommodate the Mk 5 disk recording system (1.0 FTE-year).
- The current VLBA correlation support software (job control, script construction, etc.) must be converted for the WIDAR correlator (4.0 FTE-years).
- In order to reduce the number of operators, operational tools beyond those currently available must be provided to realize the potential improvements in efficiency (4.0 FTE-years).

5.4.4 Offline processing

The offline computing requirements for processing the high-end projects shown in Table 4.2 will be very large – a result of the high maximum data rate (1.6 GB/sec, leading to 50 TB data sets), and the very extensive image processing needed (typically 4000 image planes, each 1000 x 1000 pixels, for each polarization, with each sub-image requiring multiple passes through the entire data set). At this time, it does not appear we can afford to enable such a capability by 2012, so we have fashioned a staged approach based on Moore's law, which will enable the full capability of the array to be available at reasonable cost by 2017.

In the most simple terms, we expect to pay the same amount (in dollars of date) for computing at the end of Phase II construction in 2013 as we pay for Phase I in 2007 in anticipation of the correlator's arrival in 2008. This approach to computer upgrades will unleash the full capabilities of the WIDAR correlator incrementally by investing regularly. The initial maximum sustained rate for the correlator when it is delivered in 2008 will be 25 MB/sec. By reinvesting in 2012 the same amount of capital invested for Phase I in 2008 ($1M), we will increase the maximum sustained data rate by an order of magnitude to 250 MB/sec. This is still short of the full rate out of the correlator, which by this logic should be achievable by reinvesting again in 2017. Although this plan may seem conservative (we will quite possibly be able to afford to archive data at a considerably higher rate than 250 MB/sec by 2012), the problem of providing full-reduction capability for those very daunting observations is a complex one, and we must be careful in what we promise will be enabled by 2012.

This approach of utilizing Moore's law is of course not novel many other instruments, including ALMA, which will generate databases of multi-TB size are implementing the same approach of a staged increase in their data production, archiving and reduction capabilities.

Accommodation of the very large data rates, data volumes, and scale of offline processing which the EVLA will generate will require:

- Continual investment in expanding the archiving capabilities to meet the increasing data flow;
- A program of continuous upgrading of the offline processing capabilities at the observatory;
- An offline processing software package capable of handling the data volumes and scientific imaging requirements of the array;
- A vigorous and well-funded research and development program for large-scale interferometric imaging.

The planned improvements to accommodate the increased data flow are described in the preceding section.

To accommodate the increased scale of offline processing required by the NRAO staff and visitors, a budget of $300K has been allocated in this document. After this initial investment, postprocessing computing support for both staff and visiting scientists is considered as an operations issue, and is addressed in Chapter 7.

The NRAO currently has two software code bases, `AIPS` and `AIPS++`, which can perform many of the algorithms and image processing required for single field observations without additional modification. This provides a guaranteed level of functionality and performance that will accommodate many of the EVLA observing modes.

Phase II has additional challenges which bring new demands on the software and hardware for offline processing. The larger data volumes will require a high level of scalability in the computing rates from the underlying software, while new algorithms will need to be developed for analyzing the large-scale imaging experiments anticipated.

The scalability demands can be met through parallel processing along with efficient storage and access to data. A decoupling of the logical form of the data (the data model) from the physical storage representation is important to enable scalable storage mechanisms. Data parallelism can be exploited to allow nearly linear scaling of performance with the number of processors in a cluster. Parallel algorithms can be used to speed up the most computationally intensive algorithms such as FFTs and deconvolutions. Improving the overall performance of the data storage (*e.g.*, to minimize the I/O per flop since this doesn't scale advantageously with Moore's Law) and the efficiency of data access (tuned to the range of access patterns) will also generally improve the handling of very large data volumes.

The AIPS++ table system was designed to accommodate the higher data rates of future instruments, and has features to support this; however, additional work will be needed to enable efficient parallel access to shared data structures (a modification of the existing MeasurementSet), to explore and expand the variety of compression algorithms available, and to develop heuristics for data access tuned to common use cases. Efforts in these areas will occur in support of Phase I and ALMA prior to Phase II; however, we anticipate that additional resources will be required to realize these changes for Phase II. We have budgeted 8.0 FTE-years of computing personnel working in these areas to meet these demands in Phase II.

A program of research and development of new algorithms for large-scale interferometric imaging will be undertaken by the NRAO. A partial list of the areas needing development is given in Chapter 4. For this, we plan to develop an application development team led by a scientist, and fund it for the duration of the project. We have allocated 16.0 FTE-years for this in the budget. This team will work specifically on the issues related to the imaging requirements for the EVLA – most particularly in the area of high dynamic range, wide-field, high-bandwidth ratio imaging. The algorithms development team will need its own dedicated computational resources, and $30K for a modest sized Beowulf cluster is budgeted to support the work of this imaging development team.

The AIPS++ formalism supports flexible calibration and imaging techniques which can be employed over a range of instruments and experiments. The research and development for the large-scale imaging algorithms required for EVLA Phase II can be developed upon this foundation, but additional resources will need to be dedicated to this effort. A further area of focus will be development of parallel algorithms to reap the full benefits of the cluster computing hardware planned for Phase II. A collaboration with the NCSA and NRAO has provided an exploration of parallelized imaging algorithms within the AIPS++ package. The effort in this respect is contained within the 16.0 FTE-years budgeted for the application development team.

The key hardware requirements appear well met by the improvements implicit in Moore's law. Table 5.4 summarizes the situation.

Table 5.4: **EVLA Post-Processing Requirements**

Date	Data Rate MB/s	Avg. Compute Rate TFlop	2000 Equiv. Gflop
2009	25	0.5	8
2012	250	5.0	19
2017	1600	32	8

In this table, the data rate is that quoted in Table 4.2 for the staged deployment of the correlator's output capability. The "Avg. Compute Rate" is based on the metric of 100 to 10000 floating point operation (flops) per floating point value required to image radio astronomy data with an additional multiplicative factor of 100 to represent the magnification of processing demands to enable acceptable turnaround times (the ratio of observing time to processing time needs to be high enough to facilitate experimentation and iteration). This represents the peak compute rate – the average is assumed to be 10% of this value. The "2000 Equiv." column normalizes future years to the same year – 2000. It does this by dividing out the increases in computing power expected to occur based on extrapolation of Moore's law. Estimates of costs from EVLA Memo #24 are well in line with the current scaling of cost per rate of computing ($/Gflop).

The data processing requirements cover the range of data rates from Phase II. In particular, NRAO will provide a data processing capability for the reduction of any Phase II data performance by staff and visitors. To cover the peak data rates and more computationally expensive programs, a high performance computational cluster will be needed. This facility will be the means by which many observers reduce their data, and it will be required for the highest data rates and data volumes as desktop computers will not have the required computing capabilites. For non-peak data rates, the ability to export and distribute data to observer home facilities is also needed. Increased capacity in data storage media as a function of time (factor of 100 every 10 years) scales very favorably compared to the increase in data rates, and should enable shipping of disk-based storage bricks ($\sim$ 10 TB or larger) for modest cost – \$100 – \$200. The raw data from smaller programs with database sizes less than $\sim$ 1 TB will be practical to download via the Internet.

The hardware budget for off-line processing is shown in Table 5.5.

Table 5.5: **Budget for Post-Processing**

Item	Cost \$K
Modest Beowulf cluster for technology development	30
High performance cluster for 2012	190
Grid brick data storage (100 TB)	50
Data distribution media	10
Observer workstations	20

5.4.5 Computing infrastructure

The employees required to do the work outlined above (a total of 57.5 FTE-years) will require computing infrastructure support, both in system administration and hardware needs during the construction phase. We have budgeted 3.0 FTE-years for a system administrator to help with these needs during the construction phase. We have also budgeted \$100K for computing hardware infrastructure, including desktop workstations, power, cooling, and other items.

Chapter 6

Project Organization, Schedule and Budget

6.1 Implementation Schedule

The major milestones for the proposed baseline schedule are shown in Table 6.1. A Gantt Chart for this schedule is shown in Figure 6.1. For reference purposes, key Phase I activities are also shown. The basic assumptions that have been used to lay out this schedule include the following:

- First planning and development funding for the project will be available in FY 2006. The project is ready to begin at this time. However, should initial funding not be available until a later time than this, the schedule and budget contained in this document can still be used by slipping the schedule and budget profile by the appropriate amount of time. The completion date for the project would be delayed by this same amount of time and the total project cost will be increased by the amount of the cost of inflation for the period of the delay.
- The project will be completed at approximately the same time as the Phase 1 Project. This is the most efficient way to implement the project because the majority of the electronics is identical to Phase I electronics and can be built on the Phase I production lines.
- Those few design tasks that are new for Phase II do not start until after Phase I is in its routine implementation phase so that the Phase I design engineers are available for the new work.
- The time durations required for the various components of the project are consistent with the experience gained during the original VLA Construction Project, the VLBA Construction Project and the EVLA Phase I Project.

6.2 Budget

The budget presented here is for construction of Phase II. Operations costs of the EVLA are not part of this budget request, and are separately estimated in Chapter 7. All budget numbers in this document are in FY 2003 dollars. The cost for the project has been estimated by preparing a Work Breakdown Structure for the project detailed down to WBS Level 4. The Level 1 task, identified as task 6 in NRAO's overall WBS, is the complete EVLA Project. The eleven Level 2 tasks are shown in Table 6.2.

For every task in the Project a cost data sheet has been generated detailing the personnel, materials/services and travel cost expenses for the project by year. These costs are then rolled up to provide the total cost, The total cost for the project determined in this way, including the risk-based adjustments to project costs, expressed as the contingency, is shown in Table 6.3 for each of the eleven WBS Level 2 tasks. Table 6.4 shows the breakdown of the total cost amongst the two major components of the project (New Mexico Array, and E-configuration). The annual funding levels required to support this plan are shown in Figure 6.2.

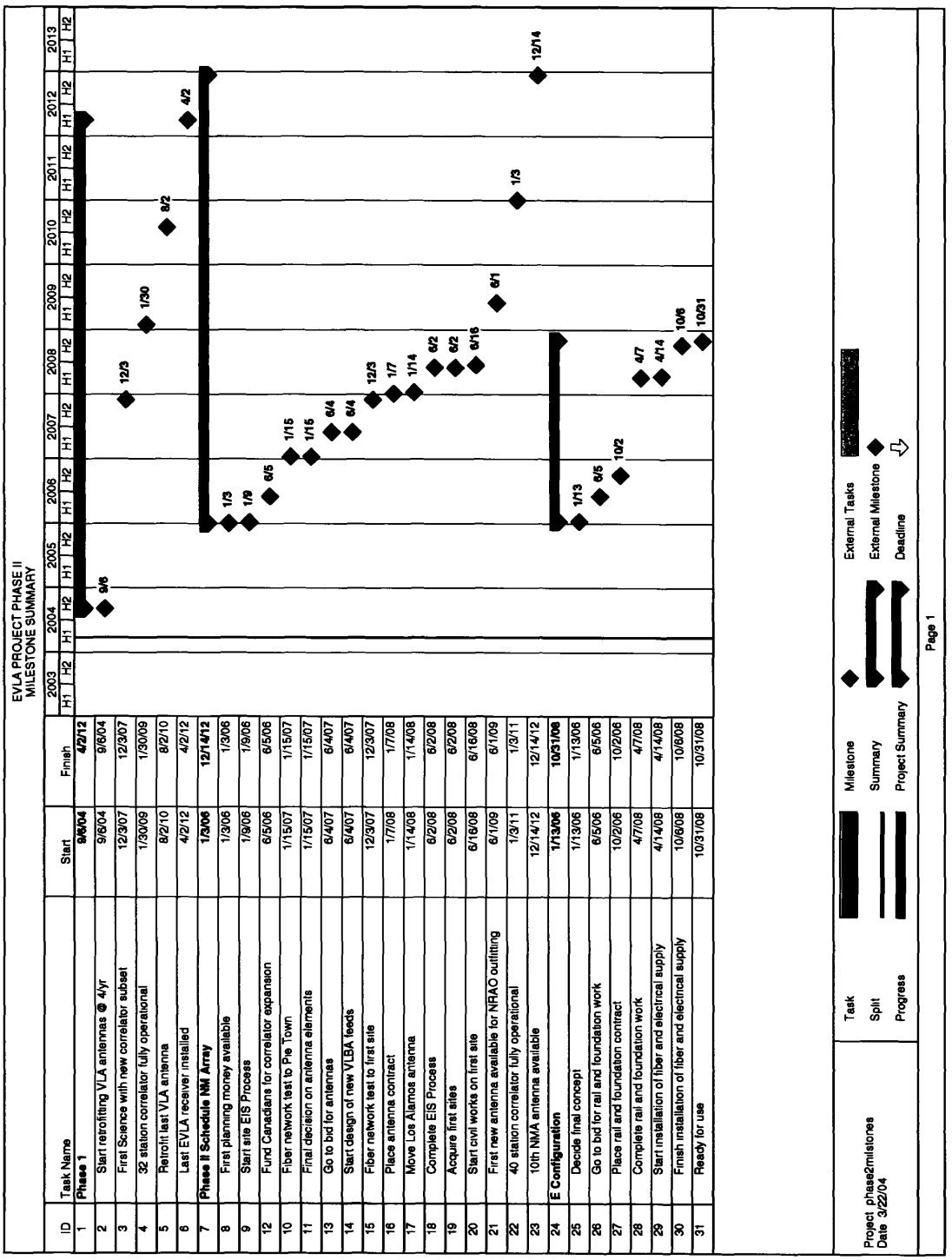

Figure 6.1: **Top-Level Schedule for the Major Components of Phase II. For reference, some Phase I milestones are included at the top of the chart.**

Table 6.1: **Implementation Schedule for Phase II of the EVLA Project**

Milestone	Date	Milestone	Date
Relevant Phase I Milestones		**New Mexico Array**	
Start retrofitting VLA ant. @ 4/yr	Sep 2004	First planning money available	Jan 2006
First science with correlator subset	Dec 2007	Start site EIS process	Jan 2006
32-station correlator operational	Jan 2009	Funding for correlator expansion	Jun 2006
Retrofit last VLA antenna	Aug 2010	Fiber network test to Pie Town	Jan 2007
Last EVLA receiver installed	Apr 2012	Final decision on antenna elements	Jan 2007
		Go to bid on antennas	Jan 2007
E-Configuration		Start design of new VLBA feeds	Jun 2007
Decide final concept	Jan 2006	Fiber network test to first site	Dec 2007
Go to bid for rail and foundation	Jun 2006	Place antenna contract	Jan 2008
Place rail and foundation contract	Oct 2006	Move Los Alamos antenna	Jan 2008
Complete rail and foundation work	Apr 2008	Complete EIS process	Jun 2008
Start installation of fiber and electrical	Apr 2008	Acquire first sites	Jun 2008
Finish installation of fiber and electrical	Oct 2008	Start civil works on first site	Jun 2008
Completed	Oct 2008	First new ant. available for outfitting	Jun 2009
		40 station correlator fully operational	Jan 2011
		Last antenna outfitted	Dec 2012

The cost estimate includes only costs which are incremental to Phase I. For example, the cost of a Project Manager is included only for those years which are not covered by Phase I, because Phase II will be managed by the same Project Manager as the Phase I Project (see Section 6.4). Included in the Project Management budget is the AUI management fee at a rate of 2.5% and the Project's share of NRAOs indirect management costs based on the predicted Project personnel levels.

Personnel costs have been estimated using the salary-plus-benefits costs shown in Table 6.5 which were obtained by averaging over the whole of NRAO for each of the personnel categories. These personnel costs are the full costs required to perform the Phase II work and do not assume any contributions from other funding sources.

The budget does not include the costs of moving the Los Alamos VLBA antenna from its current site near Los Alamos to the proposed new site near Vaughn NM. This antenna move is not a requirement of the EVLA Project, but is a requirement levied by Los Alamos National Laboratory. A discussion of the reasons for and the anticipated costs of moving this antenna are in Appendix C.

Table 6.2: **WBS Level 2 Tasks for the EVLA**

WBS No.	Task Name
6.01	Project Management
6.02	System Integration and Testing
6.03	Civil Construction
6.04	Antennas
6.05	Front End Systems
6.06	Local Oscillator System
6.07	Fiber Optic System
6.08	Intermediate Frequency System
6.09	Correlator
6.10	Monitor and Control System
6.11	Data Management and Computing

Table 6.3: **Cost Estimates for Phase II, in FY 2003 k$**

WBS	Task Name	2006	2007	2008	2009	2010	2011	2012	2013	Total
6.01	Project Management	321	861	1249	1539	1510	1469	801	583	**8334**
6.02	System Integration	87	143	136	540	375	286	1	1	**1570**
6.03	Civil Construction	722	5215	1813	1942	1883	120	0	0	**11695**
6.04	Antennas	11	25	9669	8902	8518	9058	92	52	**36326**
6.05	Front End Systems	11	200	905	1125	1186	1375	1105	953	**6860**
6.06	LO System	0	727	717	1165	448	448	0	0	**3504**
6.07	Fiber Optics	535	637	797	1016	951	555	26	26	**4541**
6.08	IF System	0	0	0	281	281	281	0	0	**844**
6.09	Correlator	0	5520	0	0	314	249	353	0	**6436**
6.10	Monitor & Control	13	9	18	190	197	178	504	0	**1109**
6.11	DM & Computing	5	10	34	24	24	49	19	1009	**1176**
	M&S	**1705**	**13346**	**15338**	**16723**	**15688**	**14069**	**2902**	**2624**	**82394**
	Wages & Benefits	758	1332	2036	2796	2906	3022	2209	1576	**16634**
	Sub-Total	**2463**	**14678**	**17374**	**19520**	**18594**	**17090**	**5110**	**4200**	**99028**
	Contingency	365	2168	3706	3993	3899	2591	784	704	**18210**
	Project Total	**2827**	**16846**	**21080**	**23513**	**22493**	**19682**	**5894**	**4904**	**117238**

Table 6.4: **Component Budget Summary in FY2003$k**

WBS	Description	NMArray	E-Config	Total
6.01	Project Management	8167	167	**8334**
6.02	System Integration	1570	0	**1570**
6.03	Civil Construction	6441	5254	**11695**
6.04	Antennas	36326	0	**36326**
6.05	Front End Systems	6860	0	**6860**
6.06	LO System	3504	0	**3504**
6.07	Fiber Optics	4521	20	**4541**
6.08	IF System	844	0	**844**
6.09	Correlator	6436	0	**6436**
6.10	Monitor & Control	1109	0	**1109**
6.11	DM &Computing	1176	0	**1176**
	M&S	**76953**	**5441**	**82394**
	Wages&Benefits	16481	153	**16634**
	Sub-Total	**93434**	**5594**	**99028**
	Contingency	17650	559	**18210**
	Project Total	**111085**	**6153**	**117238**

Table 6.5: **Salary-plus-Benefits Costs for Various Personnel Categories**

Salary Level	Category	Salary plus Benefits Cost ($K/year)
1	Top level manager	170
2	Senior engineer	119
3	Mid-level engineer	85
4	Technician	55
5	Tradesman	37

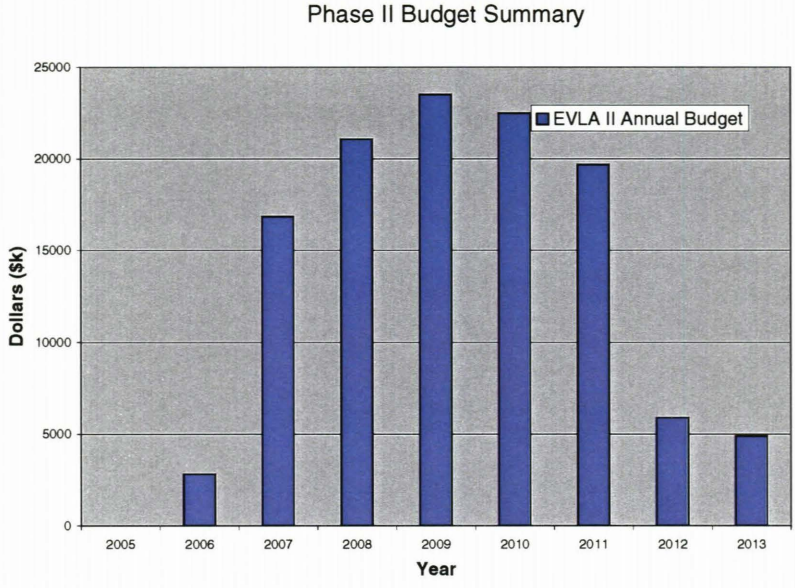

Figure 6.2: Annual Funding Levels required for Phase II.

6.3 Risk Analysis

The cost estimate, including contingency, is considered to be adequate based on NRAO's considerable past experience with the construction of the VLA, VLBA and EVLA Phase I Projects. The contingency allowance for the project has been estimated using a standard Risk Factor/Percentage method[1] applied to every element of the WBS. Below we summarize the key risk considerations for the project.

6.3.1 Management

As noted in Section 6.1, Phase II planning is based on the assumption that the project will be executed with substantial overlap in time with Phase I. This will allow the NRAO-supplied electronics systems to be built using the same production lines as are used for Phase I. There is a risk that the start of Phase II will be sufficiently delayed, for example until 2009, so that this overlap does not usefully occur. In this case the cost of the electronics systems will be higher than budgeted here, so sufficient contingency has been allocated for these systems to cover the added cost.

6.3.2 Systems Integration and Testing

This is not a high risk activity because the majority of tasks are similar to tasks already completed for the VLBA or already underway for the Phase I Project.

6.3.3 Civil Construction

The civil construction required for the new NMArray antenna sites is the same as the site construction already completed for the VLBA. The Phase II cost estimates are based on the VLBA actual costs and there are many contracting companies capable of performing the work. The civil construction required for the E-configuration is identical to the foundation and railway track work already completed for the VLA. The cost estimates come from companies that have recently done similar work at the VLA site and there are many such companies capable of doing this work.

[1] Sanders, G., Project Science Workshop, Planning for Performance Measurement, Cost Estimate-Risk Analysis. http://131.215.125.172/workshop2/talks/sanders02.pdf

6.3.4 Antennas

The eight new 25 m diameter antennas for the NMArray are the single most expensive item in the project. It is assumed that they will be identical to the VLBA antennas except for minor modifications based on VLBA maintenance experience. The cost estimate is provided by the company that originally built the VLBA antennas. This company is now the largest antenna manufacturing company in the world and the estimate is consistent with the actual cost of the VLBA antennas, corrected for inflation. NRAO owns the VLBA antenna design and a competitive procurement is planned to obtain the lowest possible price.

6.3.5 Front Ends

All receivers are identical to either Phase I receivers or, in the case of the 80 – 96 GHz band receivers, an existing VLBA receiver. NRAO has extensive experience in building these kinds of receivers and the cost estimates are based on actual Phase I or VLBA costs.

6.3.6 Local Oscillator System

The local oscillator systems are identical to Phase I systems except for the addition of a hydrogen maser frequency standard at each NMArray station. The hydrogen masers are a catalog item from a commercial company and NRAO has recently purchased several of them.

6.3.7 Fiber Optic System

The fiber optic network for the NMArray is based on leasing dark fibers from a number of different telephone companies that currently have installed fibers in excess of their needs, and installing NRAO-provided equipment on these fibers. The fiber lease cost estimate is based on estimates provided by the telephone companies, one of which has provided the dark fibers for the Pie Town Link for several years. Since the actual lease cost will not be finally known until contracts are negotiated several years from now, and since these costs will depend on fiber demand at that time, a relatively high (20%) contingency has been allocated for this lease cost. Additionally, 148 km of the required fiber network is not yet in place. Although the companies plan to have this fiber installed by the time it is required for the NMArray, there is a risk that the companies will not do this. Thus a contingency allocation of \$35K/km, the industry standard for new fiber installation, has been included so that NRAO can have this fiber installed if necessary. The equipment to be installed on the fibers is almost identical to Phase I equipment which has already been prototyped and tested.

6.3.8 Intermediate Frequency System

The intermediate frequency systems are identical to the systems already being prototyped and tested for Phase I.

6.3.9 Correlator

The expansion of the Phase I correlator from 32 to 40 stations, as required for Phase II, simply requires that more circuit boards and racks, identical to the Phase I units, be produced. The cost estimate for this has been provided by the EVLA Phase I Canadian partners based on their Phase I experience. The estimate includes all costs for the Canadian partners to do this work. The estimate is based on the assumption that the Phase II work can be done in parallel with the Phase I work, which will require a commitment to the expansion in 2006. There is a risk that the project will not be approved by this time so a contingency of 20% has been allocated to cover the increased cost.

6.3.10 Monitor and Control

Since the Phase I EVLA Monitor and Control system has been designed from the beginning with Phase II requirements in mind, there are no large changes required to the hardware and software systems which will

control the NMArray antennas. Significant changes are required to the software which controls the correlator with respect to installing the Mark 5 VLBI playback systems so that the EVLA correlator can function as a VLBI correlator. The cost estimates for this work have been provided by the software engineers who provided similar software for the VLBA correlator, and a 21% contingency has been allocated for it.

6.3.11 Data Management and Computing

In both the end-to-end software and offline software areas all major software packages required for Phase II data are also required for Phase I, with only incremental changes being needed to provide the additional functionality required for Phase II. There is a risk that the Phase I effort will not produce all of the currently planned software so a contingency allowance of 21% is provided to respond to this if necessary.

6.3.12 Descope Options

In the unlikely event that the amount of contingency is not adequate to complete the project, a number of straightforward, but scientifically costly, descope options are available.

6.4 Project Management

Figure 6.3 shows the organization chart for the Phase I Project. It is proposed that the Phase II Project will be completely merged with the Phase I Project to form a single combined Project. Figure 6.3 will then represent the organizational structure for the combined project. The numbers in Figure 6.3 indicate where responsibility for the 11 WBS Level 2 tasks defined in Table 6.2 lies within the organization. Resources will be added to the existing NRAO New Mexico Divisions to execute Level 2 tasks 3,4,5,6,7,8,10, and 11. Task 9 will be executed as a contract to the Herzberg Institute for Astrophysics.

The Project Management tools currently used for Phase I are Microsoft Project 2000 for schedule control and Excel for budget control. It is anticipated that these tools will not be adequate for the larger combined Phase I and Phase II Projects and so a transition will be made to a more substantial project management information tool. The Project will use the same tool which will soon be selected for NRAO-wide project management. This is likely to be Microsoft Project 2003, but a decision has not yet been made.

Since the Phase II project will be merged with the Phase I Project, other Project Management activities for Phase II will be identical to those already in place and functioning successfully for Phase I. Project oversight will be provided by the AUI Executive and Trustees, the EVLA External Advisory Committee, the NRAO Visiting Committee, the NRAO Users Committee and regular reports to the NSF. Project Change Control will be provided by a Change Control Board. Membership of this Board from within the Project will include the Project Manager, Project Scientist, Hardware and Software Systems Engineers and the Correlator Manager. Membership of the Board from outside the project will be appointed, as appropriate, by the NRAO Director. Details of these and other Project Management issues can be found in the EVLA Project Management Plan.

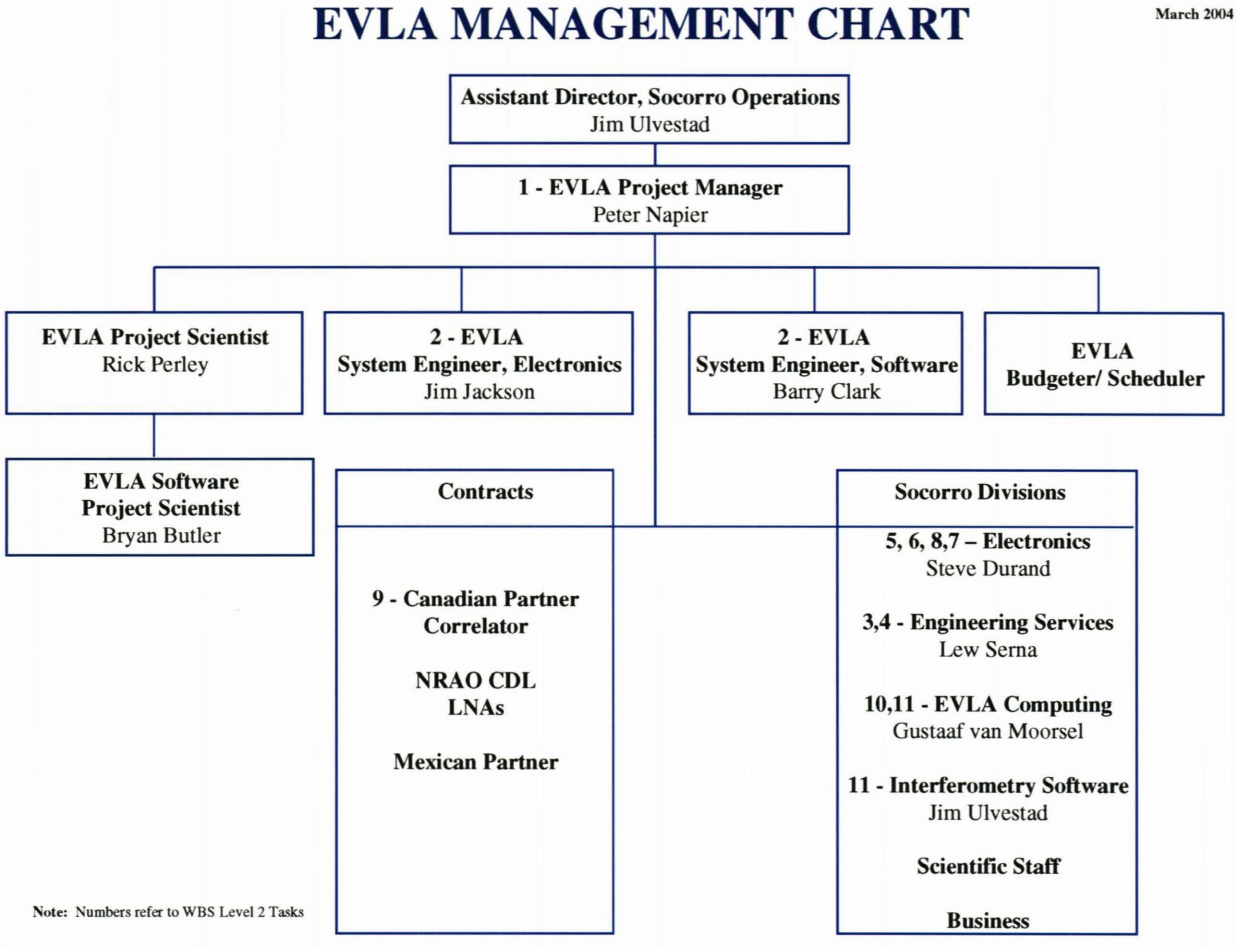

Figure 6.3: Organization Chart for both the Phase I and Phase II portions of the Expanded Very Large Array

Chapter 7

Operations Plan for the Expanded Very Large Array

7.1 Introduction

The EVLA and the VLBA will comprise a total of 46 antennas: 28 on the Plains of San Agustin, eight new New Mexico Array antennas at fixed locations in New Mexico, and 10 VLBA antennas[1]. These antennas will be assigned to various subarrays, with all correlations, whether in real-time or from disk recordings, done by the WIDAR correlator. The operations and maintenance of the entire array will be centralized and run out of the Array Operations Center in Socorro, NM.

This chapter describes the operations plan for these combined arrays, and provides an estimate of the expected increase in operations costs for the EVLA and VLBA over current levels. We emphasize that the incremental operational budget presented here is not part of the funding request for construction of Phase II of the EVLA.

A contingency of 15% has been added to the operations costs, analogous to standard practices for estimating construction costs.

7.2 EVLA Phase I Operations

Phase I of the Expanded VLA Project leaves unchanged from current operations the number of antennas, sites, and overall operational requirements. although the quantity of electronics will be increased, this will be counterbalanced by the removal of old and obsolete modules whose replacement or maintenance costs are high. It is thus anticipated that Phase I of the project will not add any significant increase in operations costs over those now expended for the current VLA.

7.3 EVLA Phase II Operations

The New Mexico Array portion of Phase II will increase the number of remote sites by eight, as well as add a significant amount of new electronics, including the necessary fiber optics and disk recording systems. The added maintenance responsibilities will not be counterbalanced by modernization of electronics, and hence we must anticipate a significant rise in operational costs.

Operational expenses for the NMArray fall into the following six categories:

1. Routine and Special Antenna Maintenance;
2. Technical Support for NMArray Equipment;
3. Site Facilities and Upkeep;

[1] Only 27 of the 28 EVLA27 antennas are used at any one time, as one antenna is undergoing routine overhaul

4. Array and Antenna Monitor and Control;

5. NMArray Scheduling;

6. Education and Public Outreach.

The operations plan summarized below is based on the detailed description given in EVLA Memo #52, found at http://www.aoc.nrao.edu/evla.

7.3.1 Routine and Special Antenna Maintenance

All ten antennas comprising the New Mexico Array will be located in New Mexico, and all will be operated from the Array Operations Center in Socorro. These sites will not need to be staffed on a daily basis, as they will be run remotely, with all data products conducted to the EVLA central site by optical fiber. Routine maintenance needs will be met by a weekly or bi-weekly visit to each site by one of three field groups, each consisting of two technicians, with each group handling three to four geographically grouped antennas. Two of these, the Eastern and Western Field Groups, will operate out of Socorro and the VLA site respectively, and handle those sites within about 100 miles of each center. These two groups will replace the VLBA Pie Town and Los Alamos site technicians, resulting in no net personnel increase. The new sites located in the southern part of the state will be maintained by a Southern Field Group, working out of Silver City or a nearby location.

The maintenance schedule for the NMArray antennas may result in at least one of those antennas being down for maintenance during some daytime scientific observations. If we do routine maintenance of the NMArray antennas on the same days as regular VLA maintenance days, the amount of additional downtime will depend on whether the maintenance of individual NMArray antennas is done weekly or bi-weekly. The alternative would be to have a dedicated set of two site technicians for each of ten antennas, requiring 20 FTEs instead of the six planned in the current operations concept. We have selected this "lean" operations plan in order to minimize the ongoing operations cost. Once the NMArray reaches its full operational state, we expect to incorporate the routine maintenance requirements into the dynamic scheduling software in order to minimize the impact on scientific observations.

Non-routine, or emergency maintenance will be met with a rotating system of trained technicians, who will be on-call 24 hours a day. Major long-term maintenance will be necessary approximately once per three years, and will be done by an augmented 'Tiger Team' which currently performs similar maintenance on the VLBA antennas.

7.3.2 Technical Support for NMArray Equipment

The addition of eight new antennas will require an increase in the number of spares by 20%. A total of 16 new FTEs will be needed to support the additional maintenance requirements (troubleshooting, module repairs, etc.) of the New Mexico Array. Supervision of the NMArray field group technicians can be designated to the existing VLBA field group supervisor. No new FTEs to support the software specific to NMArray operations will be necessary, as the NMArray will use existing EVLA tools for that work.

The main work area for the additional personnel will be primarily at the VLA site and the AOC. This will require an additional 2000 sq. ft of lab/assembly space along with appropriate test equipment. Warehouse space of approximately 5000 sq. ft. will need to be constructed to house the extra spares and repair parts.

7.3.3 Site Facilities and Upkeep

Regular maintenence of each NMArray antenna will require the following basic facilities and services at each site - an access road, security fencing around the perimeter, weed and pest abatement, ramp for unloading equipment, tank for water storage, commercial power and phone service. Each site will require a small building to house electronics (including the maser, UPS, and backup generators), work space for trouble shooting, storage for supplies, equipment, spares, toilet and sink, HVAC equipment for the building as well for the room housing the maser, PCs, and fiber connections. Each site will need a weather station. Each field technician will need a cellular phone and a laptop computer. In addition, the field groups will require a

specially outfitted vehicle to transport all required test equipment and spares. The major maintenance visits will require further special equipment. To support these visits, annual road maintenance will be required.

7.3.4 Array and Antenna Monitor and Control

When the project is completed, Array Operations will operate three NRAO arrays from New Mexico: the EVLA27, NMArray, and the VLBA. These are not fixed subarrays – NMArray antennas can be added to either the EVLA27 or the VLBA, and EVLA27 antennas can be assigned to the VLBA or the NMArray. In the long run, when real-time wide-band data from the entire VLBA are available, the entire 45-antenna array will be considered as a single operations entity, which will normally be flexibly configured into multiple subarrays, with the antenna assignments based on the science goals. Array operations plans are being made with this long-term goal in mind.

Currently, the VLA and VLBA are operated entirely separately. These array operations will be combined when the EVLA project is completed. This combination, despite the inclusion of eight new antennas, will not increase the required number of array operators – and will actually allow for a reduction as a more efficient operations model will be adopted.

It is anticipated that the central EVLA site will require two operations personnel during weekday daylight hours, to handle both correlator operations setup (including loading and unloading the Mark 5 disk packs for recording and playback, changing output disks or tape for recording data from the WIDAR correlator) and monitoring the traffic on the EVLA central site from personnel working on the antennas, as well as monitor and control of the antennas. On weekends, only a single operator will be required during daylight hours at the site. Telescope operators working evening, night, and holiday shifts would perform their duties from the AOC in space currently utilized as the VLBA control room. The Mark 5 disk systems will have sufficient capacity to enable at least 16 hours of playback with no operator present to swap disks.

If all operators are cross-trained in both VLBA and EVLA operating tasks, and if the operating software for the EVLA and VLBA can be unified, it should be possible to reduce the number of full-time equivalents (FTEs) in Array Operations by seven, from 26 to 19 FTEs.

7.3.5 Scheduling

Scientific observations with the EVLA will be scheduled primarily through dynamic scheduling software, as described in the e2e EVLA software requirements. This software will take into account scientific priorities, atmospheric conditions at both the central EVLA site and the NMArray sites, and equipment limitations. On the basis of these, the software will schedule array usage to make the most effective use of the instruments. The dynamic scheduling software designed for the EVLA will be built so that it is easily expanded to include the additional NMArray input. It will accommodate the WIDAR correlator's management of the VLBA Mark 5 observations simultaneously, and resolve any conflicts that may occur during simultaneous correlation of these recorded data with real-time EVLA data. A new FTE would not be required to extend the dynamic scheduling software to include the NMArray, since the task can be assigned at a high priority to existing personnel.

7.3.6 Configuration Cycles

The VLA normally cycles through its four standard configurations and the three associated hybrid configurations over a period of 16 months. For the EVLA, we anticipate maintaining this cycle period, as a compromise among the desire to offer each configuration fairly regularly, the effort taken to reconfigure, and the necessity to keep the configuration cycle out of phase with the Sun (so that the same part of the sky is not always up in the daytime for the same configuration). Following completion of the EVLA, the array will have five configurations rather than four, and we anticipate increased demand for the A-configuration due to the increased scientific capability when it can be combined with the New Mexico Array. Therefore, it is possible that we will have an extended period of time for the A-configuration, say five or six months rather than three, and commensurately shorter periods in the B-, C-, D-, and E-configurations. In any event, we will adjust the configuration cycle in response to proposal pressure, in order to maintain rough equality among the oversubscription rates in the different configurations, while retaining the basic 16-month cycle.

7.3.7 Education and Public Outreach

A program for education and public outreach has been developed for Phase I of the EVLA. An expansion of this program has been developed, and funding for this will be requested within a separate proposal to be submitted shortly. The central goals for this expanded plan are to outreach to communities through public information sessions and community field trips, dynamic exhibits tailored to each community near the antenna sites, a public outreach van and trailer for community and schools, and development of teacher workshops and student field trips to the central EVLA site.

We have also budgeted for an EPO scientist to collect, organize, prepare, describe, and disseminate to the public the images generated by the EVLA.

7.3.8 Annual Budget Increment for The New Mexico Array

The total additional annual operating cost for operating the New Mexico Array is summarized in Table 7.1. This operations increment is approximately 10% of the current annual operating costs of the VLA and VLBA. As the operations impact of Phase I of the project is expected to be negligible, we conclude that the total increment for operating the completed EVLA will also be 10% of current levels – showing the advantage of leveraging this project on the existing VLA infrastructure.

Table 7.1: **Incremental EVLA Annual Operations Cost Summary**

Group	**Cost**	**Subtotal**
	k$/yr	k$/yr
Field Group		
1. Vehicle Costs	43	
2. Southern Field Group Facilities	12	
3. Electricity, Phones	104	
4. Water, Roads	6	
5. Fiber Rental (assumes 20 year lease)	567	
Sub-Total		**732**
Maintenance Costs		
1. Per diem, mileage, fuel, accommodations	11	
2. Routine Upkeep	145	
Sub-Total		**156**
Personnel Costs		
1. Southern Field Group	138	
2. Overtime	14	
3. Electronics Division	563	
4. Engineering Services Division	430	
5. Education & Public Outreach	119	
6. Programming Support	0	
Sub-Total		**1264**
Other Costs		
1. Mark 5 Disks, Computer Equipment	16	
Operational Savings		
1. Operator Shuttle	(20)	
2. Array Operations	(336)	
Sub-Total		**(356)**
Net Incremental Costs for Routine Operations		1812
Contingency (15%)		272
Total Increment for Routine Operations Costs		**2084**
Continued Instrumental Development		5500
Total Requested Increment		**5500**

In addition to the ongoing routine operations, we show at the bottom of Table 7.1 the estimated annual

instrumental development cost. See Section 7.5.2 for explanation.

7.4 Operations Transition Plan

A major cost item for long-term operations will be the fiber rental cost for the New Mexico Array. We have assumed 20-yr leases at rates quoted by local New Mexico telephone companies. The beginning of the lease for fiber is staged over four years, according to the current plan for construction and connection of the 10 antenna sites. Each lease will be carried for one year in the EVLA Phase II construction budget, then transferred to the operations budget the following year as each new station is declared operational. The annual cost of fiber leases is estimated to be $567k once all the NMArray stations are operational.

Many of the improved capabilities provided by Phase II will be available before the project's completion in 2013. Antennas which are outfitted and available for science will be considered 'operational', and the budget for maintenance and use of such antennas will come from Operations. The period over which this transition occurs is expected to begin in 2010, and be completed at the end of 2013. We show in Table 7.2 an estimation of the increase in operating budget required during these transition years. The data are taken from EVLA Memo #55, with minor modifications.

In addition to the ongoing operations, we have added a staged implementation of the instrumental development budget discussed in Section 7.5.2. We suggest that this cost should be ramped up by 1/3 of the total amount (*i.e.*, by $1.8M) each year after the EVLA is fully operational at the end of 2013.

Table 7.2: **Anticipated Yearly Increments in Operations**

Year	Incremental Ops. Cost[a]	Instrumental Devel. Cost	Total
	k$/yr	k$/yr	k$/yr
2009	174	0	174
2010	992	0	992
2011	1835	0	1835
2012	2032	0	2032
2013	2084	0	2084
2014	2084	1800	3884
2015	2084	3600	5684
2016	2084	5500	7584

[a]Includes 15% contingency

7.5 User Support and Instrumental Development

A proper operational budget for any research instrument must include more than that necessary for essential operations. Modern telescopes depend upon the application of modern technologies for their power and flexibility. As technologies improve, so can the capabilities of the instruments, providing that the means of implementing these technologies is made available. A proper instrumental development program for the Expanded Very Large Array is essential if the telescope is to remain at the cutting edge over its projected lifetime.

A similar argument must be applied to user support. It is not sufficient to simply announce to the user community that a facility is ready for observing. Few users can bear the costs of travel, post-processing computing hardware, research time, or the training needed for themselves, and their students. A robust operational support budget is necessary for optimal use of the Expanded Very Large Array.

We discuss each of these programs below.

7.5.1 User Support

The National Science Foundation now provides funding for ground-based astronomical research by U.S.-based investigators, through an individual grants program. We estimate that an additional $5.5M must be allocated in this grants program, specifically for investigators using the EVLA. The mechanism for providing this funding would be up to the NSF. They might choose to administer this grants program in a manner similar to their current process. Alternatively, they might ask NRAO to administer the program by allocating funding to successful proposers in a fashion similar to that done now by NASA for its Great Observatories. (For example, the Chandra X-ray Center administers the funding for successful U.S. proposers to use the Chandra satellite.)

Without a robust funding program to support a heterogeneous group of U.S. investigators to use the EVLA for their research, this facility will fail to reach its complete potential as a forefront astronomical instrument. In this context, we note that a funding "metric" for U.S. investigators using Chandra and HST is that they receive an average of ~$1000 of funding per kilosecond (about 17 minutes) of observing time. The present VLA observes for nearly 24,000 kiloseconds in a year, and roughly 75% of this observing time is allocated to programs including one or more U.S. investigators. Therefore, an additional funding rate of $5.5M per year would amount to about $300 per kilosecond for programs involving U.S. investigators. This rate is considerably less than for the NASA Great Observatories, but would still enable many more U.S. scientists to use the EVLA successfully and produce their research results in an expeditious manner.

7.5.2 Instrumental Development

There are many areas where continued instrumental development can be expected to further increase the scientific capabilities of the EVLA after construction is completed in 2013. Since the completion of the EVLA is many years in the future, it is premature to develop a comprehensive plan for enhancements that would be pursued with the identified funding for research instrumentation. Such a plan must await the up-to-date scientific requirements and technical developments that cannot be identified specifically at this time. However, we can identify some of the likely candidates for instrumentation and algorithmic enhancements, and these are listed below:

- Enhance data-pipeline, archive, computing hardware, and software to permit a higher data throughput, specifically to increase the sustainable output data rate from the 250 MB/sec planned at the end of the construction period, to the 1.6 GB/sec rate, or higher, needed for the most data rate intensive scientific projects currently conceived;
- Continued development of enhanced computing algorithms for wide-field, low-frequency imaging and post-processing removal of radio frequency interference;
- Implement a low-frequency capability extending from approximately 240 MHz to 1 GHz;
- Install advanced water vapor radiometers at all 37 EVLA antennas, for improved tropospheric calibration and phase coherence;
- Install dual-frequency systems for improved ionospheric calibration, improving both imaging and astrometric applications;
- Extend the EVLA fiber connections to include the remaining VLBA antennas;
- Replace the IF systems of the remaining VLBA antennas to enable the full 16 GHz EVLA bandwidth;
- Expand the EVLA correlator to 48 stations, to enable full 16-GHz bandwidth, real time correlation with the full 45-antenna combined EVLA and VLBA.

Some of these improvements will cost less than a few million dollars, while the low-frequency enhancement might cost as much as $20 million, spread over several years. In aggregate, the instrumental developments listed above could cost over $30 million. Our requested annual budget for ongoing instrumental and algorithmic development of $5.5M/year, phased in over the first three years following construction, and maintained at that level, would permit the NRAO to enable the listed improvements – or other more timely ones – over a 6 – 8 year time period.

7.5.3 AASC Recommendations

The 2000 Astronomy and Astrophysics Survey Committee has highlighted the need for both user support and instrumental development, and recommended ongoing support for both at a level of 3% of the capital cost for major new facilities. This recommendation is in line with our requested operational budget.

Appendix A

Science Opportunities Opened by Phase II

Phase II of the VLA Expansion Project will provide enormously improved observational capabilities, which will have ramifications across the breadth of modern astronomy. Chapter 3 concentrated on one key area, cosmic evolution, with particular emphasis on the formation of stars and galaxies. This appendix takes a broader view, pointing out some of the advances to be expected in a wide variety of areas, ranging from pulsar astrometry, to Galactic polarization studies, to the imaging of H I absorption in damped Lyman alpha systems. This can only be a survey of some of the possibilities. Like the VLA itself, the EVLA is intended to provide an important range of general capabilities, rather than focusing on a single experiment or even a narrow astronomical field.

A.1 The Solar System

The second phase of the VLA Expansion Project will open up a number of exciting possibilities in solar system science. A few of these are described below.

A.1.1 Solar System Radar

The current Goldstone/VLA combined radar instrument is one of the most powerful in the world (*e.g.*, , Muhleman et al. 1995). Operating at 4 cm, it provides a resolution of about 0.3 arcsec when the VLA is in the A-configuration. This corresponds to $\sim$ 100 km at 0.5 AU, appropriate for geological size scales on Mercury, Venus, and Mars (Figure A.1). The technique is complementary to the powerful monostatic radars at Goldstone and Arecibo, in that the resolution is best in equatorial regions and poorest at the poles. It would be very interesting to obtain similar resolution with a combined Arecibo/VLA radar, working at 13 cm. This requires baselines about four times longer than the current A-configuration — *i.e.*, , the New Mexico Array. Longer-wavelength observations probe a different size scale of surface "texture," since size scales from about one-third to three times the wavelength are sampled well. Longer wavelengths also allow a deeper look into the subsurface: the maximum depth is roughly 10 wavelengths for normal soil surfaces, and much deeper for ices or underdense materials. This is especially important for the icy regions of Mars and Mercury and the "Stealth" region of Mars.

In addition to radar imaging of planets, imaging of small bodies could also be performed with the New Mexico Array alone at 4 cm, with the Goldstone/EVLA radar system, or by combining the NMArray and inner VLBA stations as a receiver for the Arecibo radar. Such experiments have been attempted on the VLBA, but have not been successful to date, due to limitations in the current VLBA correlator. Radar images of Near Earth Asteroids could be made with tens of beams across the body, allowing for real surface properties to be derived, along with their variation. In addition, the nucleus of a comet might be imaged, a very exciting possibility.

Requires: New Mexico Array

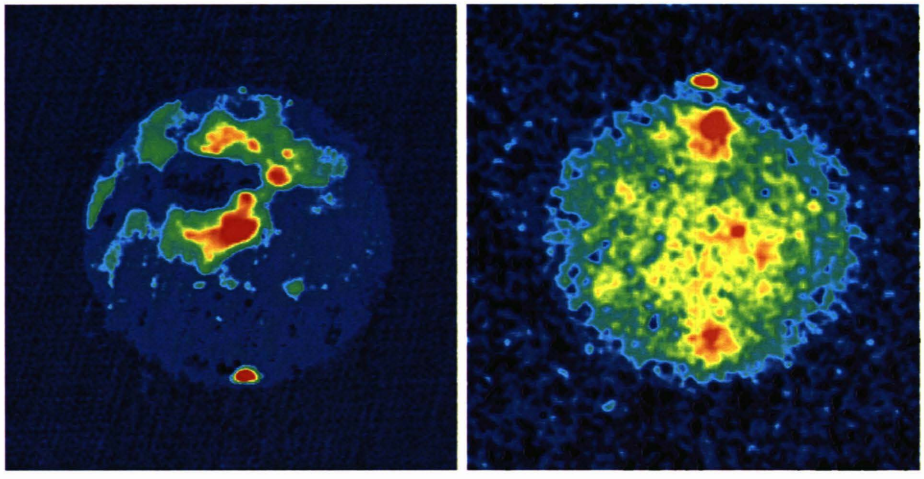

Figure A.1: Radar reflectivity images of Mars (*left*) and Mercury (*right*) made with the combined Goldstone/VLA radar at 4 cm (B.J. Butler, D.O. Muhleman, & M.A. Slade 1999). The EVLA will extend this imaging to much smaller bodies (*e.g.*, , near earth asteroids and cometary nuclei) and to 13 cm. The latter will probe much deeper into the subsurface than the current 4 cm imaging.

A.1.2 Imaging Synchrotron Emission from the Giant Planets

The imaging of the jovian synchrotron emission at radio wavelengths is a mature field (*e.g.*, , Berge & Gulkis 1976; de Pater 1990). Recent advances in tomographic reconstructions of the electron density in the magnetosphere are especially exciting (Sault et al. 1997; de Pater & Sault 1998; Santos-Costa et al. 2001; Figure A.2). The added resolution of the New Mexico Array would allow more precise determination of this 3-D structure, providing valuable information on the magnetic field of Jupiter, and on the surrounding electron field. So far, there has been no synchrotron emission detected from Saturn; this is probably due to disruption of the electrons in the magnetosphere by the dense ring system. Small pockets of such emission might still be present, but masked by beam dilution. The increased resolution and sensitivity of the New Mexico Array might detect and localize this emission. The situation for Uranus and Neptune is much less clear, with claims of detections and non-detections. If there is synchrotron emission, the higher resolution of the NMArray shouldhelp in its detection, since the beam dilution will be much less than for the A-configuration.

Requires: New Mexico Array

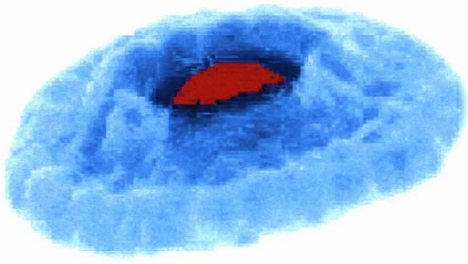

Figure A.2: A three-dimensional reconstruction of Jupiter's synchrotron radiation at 1.4 GHz, based on data taken with the VLA and the ATCA. The red circle represents the planetary surface. From Sault et al. 1997; de Pater & Sault 1998; and Santos-Costa et al. 2001; see `http://www.atnf.csiro.au/research/solarsys/jupiter/movies/` for the full movie.

A.1.3 Imaging Cometary Comae

Cometary comae are extremely large — approaching degree size scales. The emission is fairly smooth and so is resolved out with the VLA, even in D-configuration and at 20 cm (*e.g.*, , de Pater, Palmer, & Snyder 1986). All molecular line imaging of comets would benefit from the use of the compact E-configuration, including OH, H_2O, NH_3, and more complex organics (*e.g.*, , H_2CO and CH_3OH; see Snyder, Palmer, & de Pater 1989). For some comets, some luck would be required, since the EVLA would have to be in the E-configuration at the right time (*e.g.*, , Hyakutake); but others (*e.g.*, , Hale-Bopp) will remain in a reasonable geometry throughout the configuration cycle.

Requires: E-configuration

A.1.4 Turbulence in the Interplanetary Medium

The solar wind inflates a cavity around the Sun, extending to perhaps $\sim$ 100 AU, called the heliosphere; this is filled with a tenuous, magnetized plasma, known as the interplanetary medium (IPM). Radio interferometers like the VLA are ideally suited for measuring the angular broadening and intensity scintillations of background sources viewed through the IPM. These data can be used to deduce the solar wind speed and acceleration profile, to measure properties of the turbulence, and to map large-scale structures in the solar wind (Figure A.3). These studies exploit observations of sidereal background sources which, in the absence of the IPM, are either unresolved by the array or have known source structure. Phenomena such as angular broadening, scintillation and Faraday fluctuations are due solely to the intervening turbulent medium. Currently such studies are limited by sensitivity to occasional determinations of solar wind properties using a handful of bright sources at various elongations and position angles.

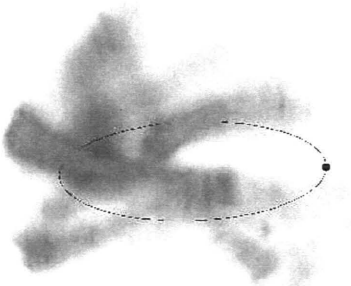

Figure A.3: An example of a tomographic reconstruction of the inner heliosphere, to a distance of 1.5 AU, which was derived from a combination of velocity data and interplanetary scintillation data obtained over one solar rotation period (23 June 1994 to 20 July 1994, Carrington Rotation 1884). Earth's orbit is as indicated. The technique is described in detail by Jackson *et al.* (1998).

Extension of the VLA to baselines of hundreds of kilometers will open up a number of exciting possibilities. The New Mexico Array will allow the sampling of baselines covering more than two orders of magnitude in spatial scale. This not only expands the range of solar elongations that can be probed in a given frequency band, but enables a critical portion of the spatial spectrum of the solar wind turbulence to be probed directly. The spatial spectrum of the solar wind is flatter than Kolmogorov on spatial scales less than some tens to hundreds of kilometers, yet may be Kolmogorov-like on the largest spatial scales. The transition is thought to occur on spatial scales that will be sampled directly by the NMArray. Coupled with the VLBA, the NMArray will provide comprehensive measurements of the spatial spectrum of the solar wind, as well as its temporal and spatial evolution, thereby providing powerful new constraints on the source, structure, and evolution of MHD turbulence.

Requires: New Mexico Array

A.2 Stars: Formation, Stellar Properties, and Evolution

A.2.1 Formation of Solar-Type Stars

The use of the full EVLA for understanding the formation of massive stars has already been described in some detail in Chapter 3. In general, by being able to image the emission from optically-thin ionized gas with unprecedented sensitivity and resolution, the full EVLA will be able to do for massive star formation what ALMA will do for understanding the formation of low-mass, solar-type stars. There are, however, some key examples where the addition of measurements of young, solar-type stars with the full EVLA will in fact provide information vital for the interpretation of the higher-frequency ALMA data. The optical depth of the emission from dust associated with star formation — dust in the molecular clouds from which the stars form, and dust in the circumstellar disks that may be the progenitors of planetary systems — increases with frequency as $\tau \propto \nu^{\sim 1-2}$. Thus the most deeply-embedded protostars, and the most massive circumstellar disks, are likely to be optically-thick in dust emission even at wavelengths of a millimeter. While ALMA will therefore be able to measure directly the temperature of the dust emission for these sources, it will only be able to probe down to the $\tau \sim 1$ surface. In these cases, the fact that the optical depth at frequencies accessible to the EVLA will be much lower than those available to ALMA, can be combined with ALMA results to provide information about both temperature and density distributions, and will even reveal the growth of dust grains into centimeter-sized particles for one or two of the brightest objects. The dominance of the dust emission in the ALMA frequency bands can also be problematic for studying emission from the ionized gas associated with thermal outflows from young solar-type stars. Again, the inclusion of full EVLA imaging at lower frequencies where the dust emission is optically thin will be extremely important for understanding fully these phenomena, at resolutions of a few to tens of milliarcseconds — a few AU at 140 pc, the distance of Taurus, the nearest star-forming complex. These two examples are described further below.

Thermal Outflows

Thermal outflows are very closely tied to the earliest stages of low-mass star formation (*e.g.*, , Königl & Pudritz 2000; Fig. A.4). They appear to be a universal feature of the youngest (Class 0) low-mass protostars; the fraction falls to 60% in Class I sources, 10% in Class IIs, and $\sim$ 0% in Class III objects (Gomez, Whitney, & Kenyon 1997), showing that the outflow is closely coupled to the accretion process. Indeed, the mass outflow rate (as determined, *e.g.*, , by P Cygni profiles, forbidden lines, thermal radio emission, and various molecular tracers) is directly proportional to the mass accretion rate (as determined by IR/millimeter excess, inverse P Cygni profiles, etc.; *e.g.*, , Cabrit et al. 1990, Cabrit & André 1991, Hartigan, Edwards, & Ghandour 1995). Further, the outflow momentum also correlates with the mass of the protostar. Thermal outflows are thus a fundamental part of the star formation process. Observationally, they carry away a significant fraction of the mass out of which stars are formed. In most theories they are also responsible for getting rid of the accretion disk's angular momentum, possibly through magnetic coupling with the disk. Indeed, these outflows may control the entire accretion process, and hence the initial mass function, by eventually halting the inward flow of the mass. Finally, these outflows are sufficiently energetic to affect the overall support of the molecular cloud as a whole; perhaps star formation is halted in a given cloud when the combined outflows from the stars it creates are sufficient to blow it apart.

Despite their importance, thermal outflows are at best poorly understood. A number of very basic questions remain unanswered:

- How are thermal jets and outflows formed, accelerated, and collimated?
- How much mass and angular momentum do they carry away?
- How does the accretion/outflow process work in binary star systems?

The full EVLA is designed to address these questions, combining high resolution ($\sim$ AU at Taurus) with sensitivity to the ionized gas which is the primary component of these outflows. One wants to work at

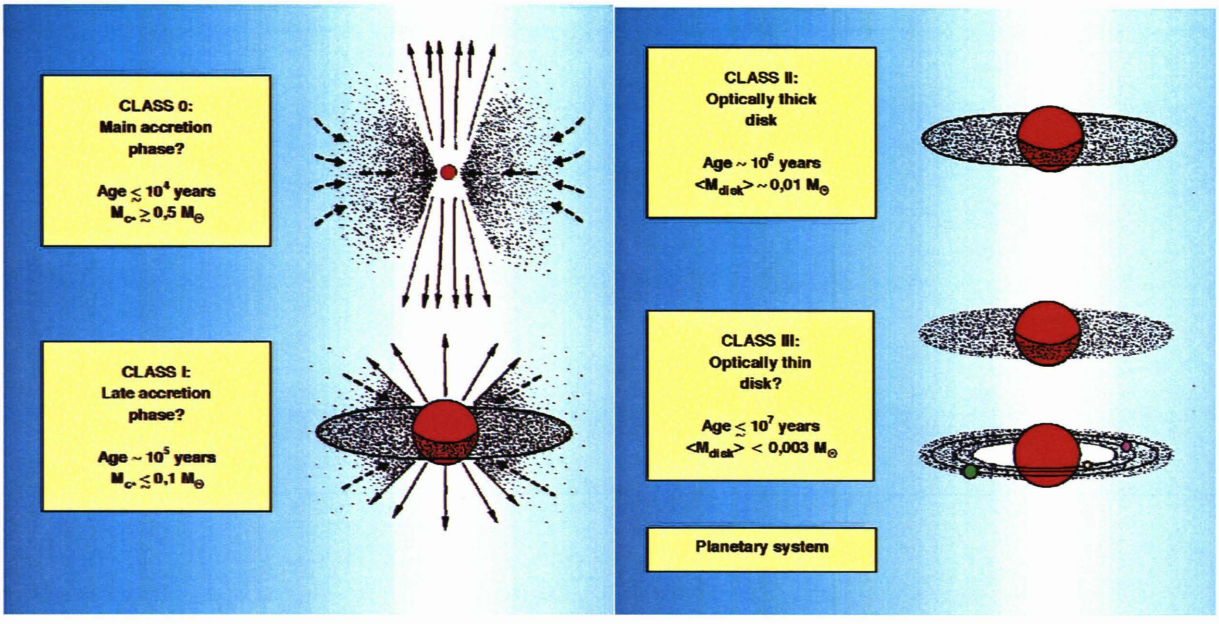

Figure A.4: In the current "standard model" of star formation, young stellar objects (YSOs) are divided into classes based on their spectral energy distributions. In the earliest stage of star formation, where most of the accretion takes place, the emission from Class 0 sources is completely dominated by far infrared emission from cold dust. In *all* cases the source also hosts a thermal jet, indicating the fundamental role of such outflows in the star formation process. In the next stage, Class I sources are less uniformly surrounded by dust; much of the accreting material is now in the form of a thin disk, and the observed emission is dominated by a combination of that from the star itself, and thermal emission from the disk and residual dust cloud. Class II sources are distinguished by the dominance of the stellar black body and the near disappearance of the dust cloud. Finally, Class III sources host a much less massive (and optically thin) disk, and may start to form planets.

high frequencies, since the free-free emission goes roughly as ν^0 to ν^2 (depending on the optical depth and geometry); at the same time one wants to avoid being completely dominated by the thermal dust emission, which goes as ν^{2-4}. The usual optical/infrared tracers are completely obscured by dust (Fig. A.5);

at the smallest scales (tens of milliarcseconds), the dust emission is likely opaque even at millimeter wavelengths. This requires observations in the centimeter band, at resolutions as close as possible to the size of the acceleration and collimation regions. Indeed, the best current limits on jet collimation come from the current VLA working at 8.5 GHz, where observations of L1551 IRS5 (Fig. A.6) show that the jets are already well collimated within 10 AU ($\sim$ 70 mas) of the protostars (whose positions are based on VLA 43 GHz measurements).

The NMArray will also allow astronomers to follow the detailed evolution of thermal outflows, through precise astrometric measurements of proper motions. One would like to measure not only velocities (and decelerations?) of individual 'blobs', but also the rate of ejection, and overall jet motions such as precession, both as fundamental inputs to jet models, and to tie back to the accretion disk, possible binary orbits, etc. (*e.g.*, , Fig. A.6). The state-of-the-art is shown in Figure A.7, which displays difference maps resulting from seven years of monitoring HH 80-81, two Herbig-Haro objects associated with a high-mass protostar. Based on these images Martí et al. (1998) show that the outflow velocity on these scales (some 800 AU) is about 500 km/s, and that such pairs are ejected every 10 years or so. With the combination of a factor 10 smaller beam and a factor 10 greater sensitivity, the NMArray could fully resolve even much slower outflows in a matter of weeks, and detect motions via similar difference images in a few days. This will finally permit studies of the details of protostellar outflows, on scales comparable to the Earth's orbit around the Sun, in a substantial sample of typical sources. Such observations are critical to understanding optical, near infrared, and (sub-)millimeter observations of jets on larger scales. Combining data from the NMArray, the JWST, and ALMA will connect the acceleration region to the swept up molecular material, and eventually to the

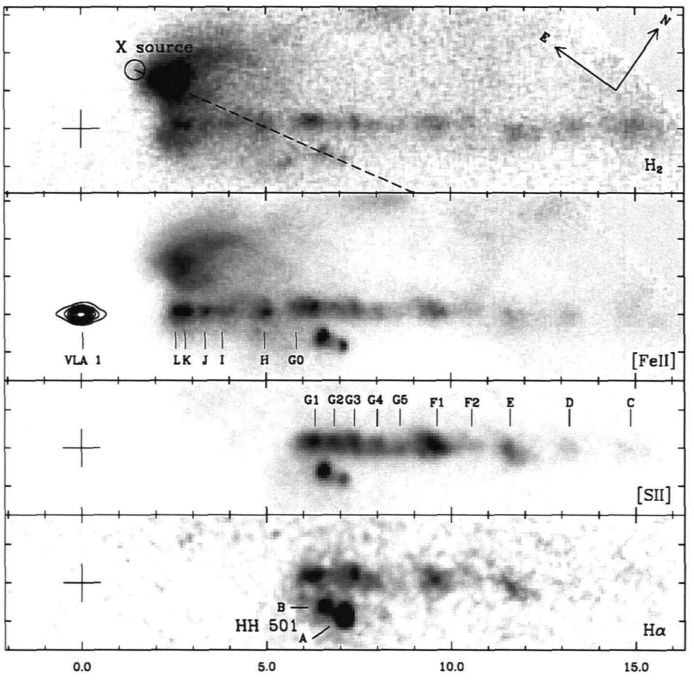

Figure A.5: The thermal jet in HH 1–2, combining VLA 8.4 GHz (*contours*) with HST optical and near-IR (*grayscale*) data. The [Fe II] panel in particular shows the radio emission from the thermal jet (VLA 1) extending about an arcsecond, while the [Fe II] picks up several arcseconds out and extends to $\sim$ 10 arcseconds. The NMArray will give at least a factor 10 higher resolution as well as filling in the missing emission, allowing us to follow the jet continuously from the origin to the working surface (the Herbig-Haro objects). Courtesy L. Rodríguez, based on Reipurth et al. (2000).

termination shocks in the molecular clouds (seen as Herbig-Haro objects).

Protostellar Cores

The earliest stages of star formation occur in dense cores within molecular clouds, shrouded by dust which may be opaque even at submillimeter wavelengths. For low-mass stars (*e.g.*, , Mundy, Looney, & Welch 2000) the best current models suggest opacities looking towards the central few AU of order a few at 350 GHz;[1] this is highly uncertain, since the distribution of this material on these scales in not yet known, but it is probably highly centrally concentrated. The minimum mass solar nebula for instance has an optical depth greater than 30 at 350 GHz at 1 AU, and the only current high-resolution images (of the brightest millimeter sources in Taurus) also show very high submillimeter opacities (*e.g.*, , Osorio et al. 2003; Fig. A.8). The implication is that ALMA may be limited to measuring down to the $\tau \sim 1$ surface of the innermost regions for some of the most interesting, young, and deeply-embedded protostars. By contrast, high-resolution imaging using the full EVLA at relatively long ($\sim$ cm) wavelengths where the dust emission is optically thin will enable the full structure of protostellar cores to be measured.

At its highest frequencies, ALMA will provide similar resolutions to the full EVLA. Comparing data from the two instruments will allow the measurement of grain sizes and opacities as a function of radius in circumstellar disks and envelopes, offering direct insight into the early stages of the coagulation process by which planets are formed. Similarly, while ALMA will provide the best images of the cool dust in the outskirts of the accretion disk, the full EVLA will fill in the crucial central part, where the submillimeter opacities may be high enough that ALMA will see only the outer "skin" of the accreting matter. By combining these

[1] A 0.5 $M_\odot$ envelope with an r^{-2} density profile gives opacities at 350 GHz of order a few at an impact parameter of $\sim$ 5 to 10 AU; a 0.1 $M_\odot$ disk of radius 50 AU gives similar *average* opacities. The opacity will be much lower at lower frequencies.

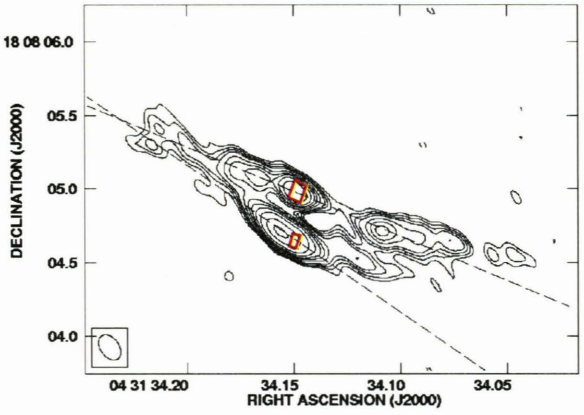

Figure A.6: VLA+Pie Town image of L1551 IRS5 at 8.5 GHz. The half-power beam (180×120 mas) is shown in the lower left. The small red rectangles mark the positions and deconvolved dimensions of the compact protoplanetary disks imaged with the VLA at 43 GHz; the dashed lines show the position angles of the jet cores. These data show the jets are already well collimated within 10 AU of the protostars, the most significant constraint yet on jet collimation in young stellar objects. Note too the bends in the jets, which may reflect orbital motions in the binary. From Rodríguez et al. (2003).

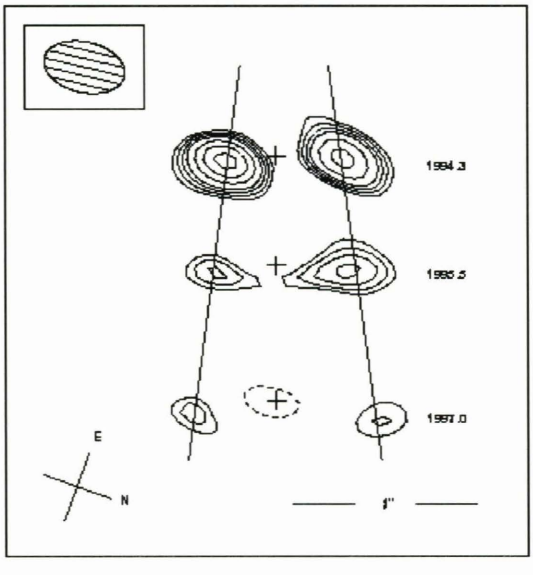

Figure A.7: Difference maps of the thermal radio jet in the HH 80–81 complex for the epochs 1994.3–1990.2, 1995.5–1990.2, and 1997.0–1990.2. Crosses indicate the position of the central source. The corresponding outflow velocity is $\sim$ 500 km/sec, with ejection occurring about every 10 years. From Martí et al. (1998).

two instruments we will therefore be able to measure fundamental quantities over the *entire* disk, such as the distribution of mass and temperature with radius, and the size distribution of the grains.

A.2.2 Stellar Imaging: Photospheres, Outflows, and Shocks

The combination of the upgrade in sensitivity and the increased angular resolution provided by the New Mexico Array opens an extremely exciting area of investigation – milliarcsecond resolution imaging of thermal radio emission. This capability is placed in context in the angular size versus brightness temperature plot

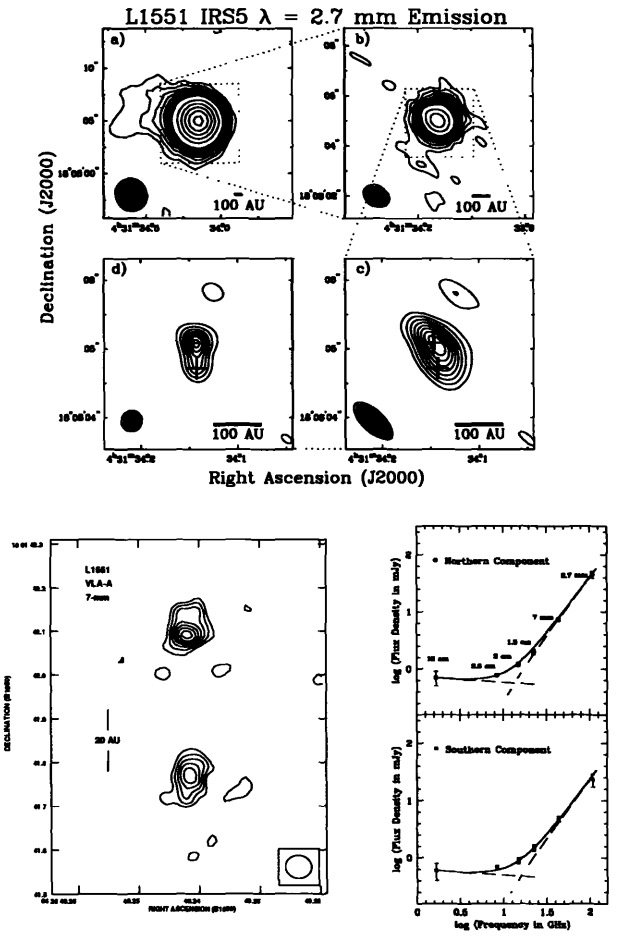

Figure A.8: Dust emission from L1551 IRS5. (*upper*) BIMA (Berkeley-Illinois-Maryland Array) images at 110 GHz with increasing angular resolution (Looney et al. 1997), showing that L1551 is composed of two circumstellar disks located within a flattened circumbinary structure embedded in an approximately spherical large-scale envelope. (*lower*) VLA images at 43 GHz with 50 milliarcsecond (7 AU) resolution (Rodríguez et al. 1998) clearly resolve the individual dust disks surrounding the members of the proto-binary system. The spectral decomposition shows that the dust dominates the emission – and is optically thick – down to $\sim$ 22 GHz, below which optically-thin free-free emission takes over.

in Figure A.9. The two diagonal dashed lines in the figure show the brightness temperatures required to produce flux densities of 100 mJy and 1 mJy within a given angular radius. Curves for the most powerful interferometric arrays characterize their maximum resolution (horizontal portion) and maximum sensitivity (diagonal portion). For a source with a given angular radius and brightness temperature to be *resolved* by an array (and therefore imaged), it must lie above the curve. We know that, at a brightness temperature of a few $\times 10^4$ K, radio sources can be broadly divided into non-thermal and thermal. Photo-ionized, nebular sources of thermal radio emission generally have equilibrium, kinetic temperatures of a few $\times 10^4$ K. Hence, compact nebular radio sources have brightness temperatures at this value or lower. Photospheric emission from stars, which is optically thick at kinetic temperatures of $10^3 - 10^5$ K, straddles this 10^4 K boundary. Figure A.9 shows the location of the stellar main sequence and giant branches for stars at a distance of 1 kpc.

It is clear from the diagram that, with current arrays, imaging at milliarcsecond resolution is restricted to high brightness temperature, non-thermal radio sources. For brightness temperatures just over 10^4 K, the MERLIN array provides images a resolution of tens of milliarcseconds. However, as the brightness

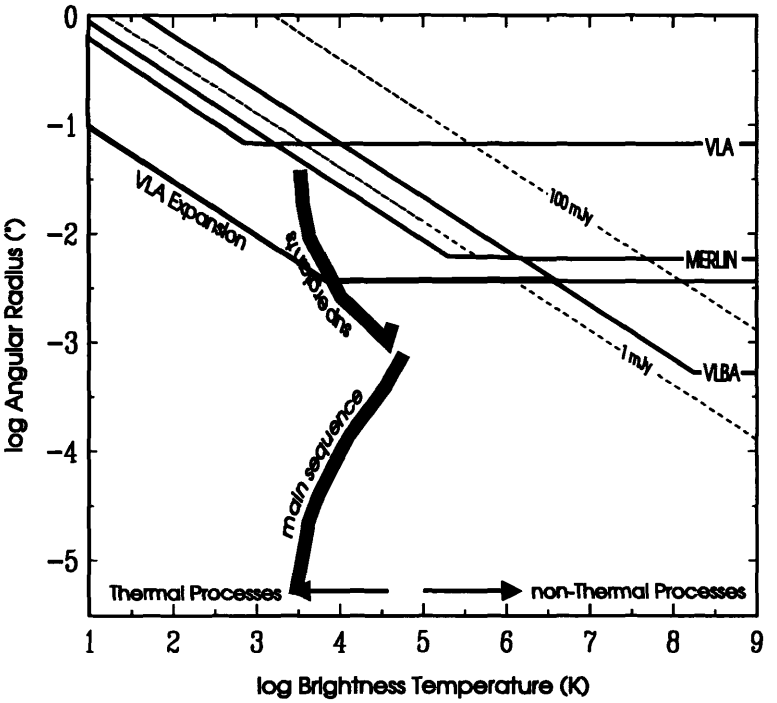

Figure A.9: Brightness temperature and angular size regimes accessible to imaging by interferometer arrays. The previously inaccessible region that will be opened up by an expanded VLA with the upgrade in sensitivity is shown by the shaded area.

temperature drops below this value, the minimum angular dimension over which detectable flux can be obtained increases rapidly. Consequently, imaging at milliarcsecond resolution of the entire class of thermal-emitting radio sources is an area of astrophysical investigation that has yet to be exploited. To access this area requires order-of-magnitude improvements in both sensitivity *and* resolving power. The New Mexico Array, in combination with the EVLA's enormous improvements in sensitivity, will provide that facility. The new region of observational parameter space that would be accessible to imaging by the completed EVLA is illustrated graphically by the shaded region in Figure A.9. This region encompasses a wealth of phenomena in stellar astrophysics that have hitherto been revealed only as "point sources" of radio emission.

For example, the imaging of the surface of Betelgeuse at 43 GHz (Figure A.10) was a technical *tour de force* for the current VLA, but it is the only star in the northern sky large enough for this to be possible. Radio images like this are crucial for understanding the bloated atmospheres of these supergiant stars, since they showed that existing models of the atmosphere based on visibility data were wrong. The combination of the NMArray resolution with the EVLA sensitivity will allow many more giant stars to be studied at multiple frequencies, improving atmospheric models for these stars and permitting us to study inhomogeneities in the atmospheres for a range of stellar types. and the disk size temperature on radius in atmospheric models to be tested with the vastly improved sensitivity of similar observations of stars 10 times smaller or away.

Angular resolution of a few milliarcseconds corresponds to a linear dimension of a few AU at a distance of one kpc. This distance is typical of the binary separation of semi-detached interacting binaries containing giant stars, such as symbiotic stars and recurrent novae. Other examples of thermal radio sources generated or affected by phenomena on AU scales are the winds and circumstellar environments of early-type stars and the very early stages of novae outbursts. At current resolving power, imaging investigations of these types of objects have been largely constrained to examination of ejected material that has propagated to large distances from the point of origin before becoming resolved. The NMArray will finally allow imaging of thermal radio emission on the scale of the interaction that gives rise to ejecta. Figure A.11 shows the maximum distance to which these and other types of objects would be resolved by both the A-configuration and the NMArray. For the current VLA, typical distances range from a few tens to a few hundreds of parsec.

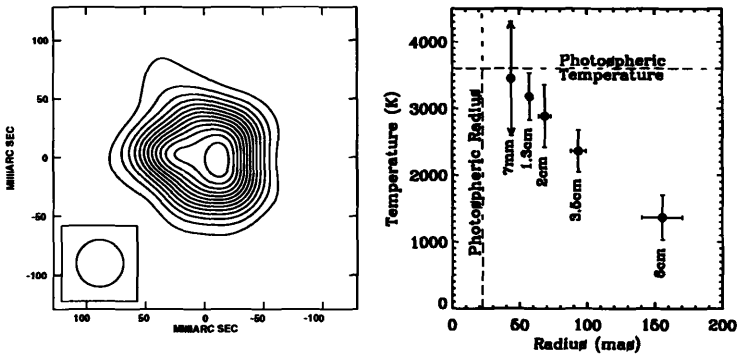

Figure A.10: (*left*) VLA 43 GHz image of Betelgeuse. The resolution is 40 milliarcseconds and the contour interval is 250 K (brightness temperature). (*right*) The variation of temperature in the atmosphere with radius, determined from the VLA observations of Betelgeuse at different frequencies which resolve the source size (Lim *et al.* 1998). The NMArray will give a factor ~ 10 higher resolution at 30 times higher sensitivity.

Unfortunately, the space density of these objects is sufficiently low that there are essentially no examples within this resolvable distance. For the NMArray, the resolvable distances increase to a large fraction of a kpc to several kpc. Red supergiant photospheres can be resolvable to beyond a kpc, the binary separation of 'D' type symbiotic stars and the very early stages of nova ejections can be resolved out to several kpc, and the circumstellar disks of Be stars out to several hundred pc. At these distances, significant populations of all of these types of sources can be probed on AU and smaller scales for the first time.

Dimensions of order 1 AU have crossing time of order 1 yr for velocities of tens of km/sec. Hence, milliarcsecond resolving power will allow direct measurement of the angular expansion rate of slowly expanding objects such as compact planetary nebulae and wind interaction shells in the interstellar medium. Combined with spectroscopic data, such measurements can provide accurate estimates of distance for a significant population of objects.

Requires: New Mexico Array

In the remainder of this subsection we discuss some specific imaging examples in more detail.

Thermal Winds in Early-type Stars

Stellar winds are of great importance both for stellar evolution, and for the interstellar medium (ISM). By removing mass from the star, they change the fundamental balance between gravity and radiation pressure which determines stellar structure (*e.g.*, , Chiosi & Maeder 1986); by expelling substantial amounts of matter they both stir up the ISM and pollute it with heavy elements (*e.g.*, , Abbott 1982; Leitherer et al. 1992). Exactly how all this works is far from clear: even the basic mass loss mechanisms are still subject to debate. This makes direct, detailed tracers of stellar winds as valuable as they are rare.

A case in point is the very strong winds from early-type stars. These can be observed through ultraviolet lines, hydrogen emission lines, and the infrared and radio continuum. In particular, measurements of the thermal radio flux density due to free-free emission give direct estimates of the stellar mass loss rate, and are often used to calibrate rates obtained by other methods. Recent observations show that the stellar winds are far clumpier than originally thought (*e.g.*, , Figure A.12). Since the free-free emission is proportional to the square of the density, such clumpiness implies a much lower outflow rate than derived assuming a smooth flow. A further complication is the presence of non-thermal (synchrotron) emission (*e.g.*, , Bieging, Abbott, & Churchwell 1989), which both increases the apparent flux density at a given frequency, and changes the observed spectral index (which is often used as a diagnostic of the wind geometry). Any change in the mass loss rates in turn changes estimates of initial stellar masses, with important consequences for models of the evolution of massive stars and galaxies.

The key to resolving these difficulties is to actually image the winds. This requires

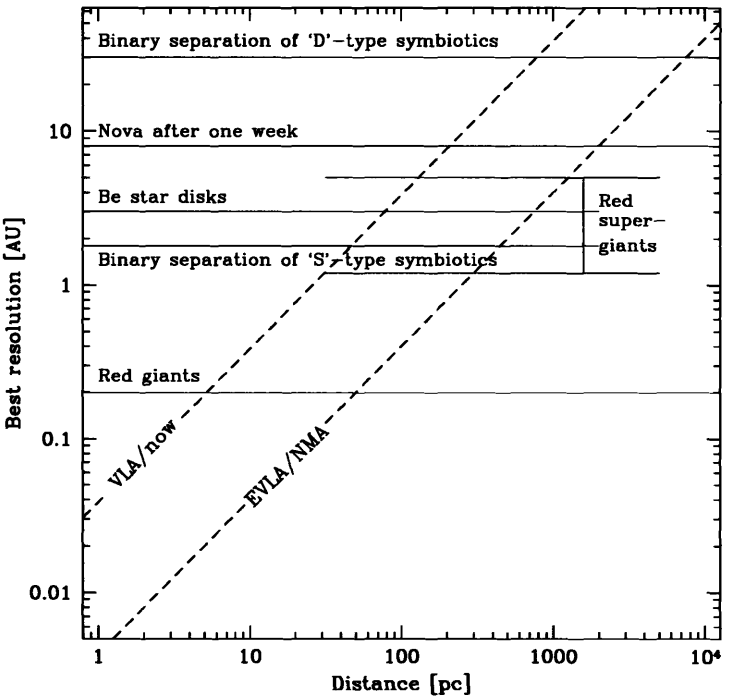

Figure A.11: The resolving power of the current and the expanded VLA (NMArray), compared to the linear dimensions of several known, thermal, radio-emitting astrophysical phenomena.

- excellent resolution with superb sensitivity, to see both the clumps and the underlying smooth emission;
- wide frequency coverage, (1) to check the relative contributions of thermal and non-thermal emission, and (2) to image the optical depth of the thermal gas, and hence map out both the density and the excitation temperature throughout the wind;
- the ability to image complex structures over a wide range of angular scales (cf. Figure A.12).

Only the EVLA, with the New Mexico Array's added baselines, can meet all of these requirements.

Requires: New Mexico Array

Masers on the Asymptotic Giant Branch

Early-type stars produce strong ionized winds, observable through free-free radiation; on the other end of the spectrum, late-type giants and supergiants produce substantial molecular outflows, which can be traced with exquisite detail through molecular masers. These asymptotic giant branch (AGB) stars are significant contributors of material to the interstellar medium, and also form an important part of the proto-planetary nebula evolutionary sequence. The masers are produced in the circumstellar envelope formed by mass loss from the dying star, and appear in a somewhat hierarchical distribution, with hydroxyl masers far out in the shell, and silicon monoxide masers quite close in to the photosphere (1.5-2.5 R_*); water masers are usually found somewhere in between. These masers are excellent tracers and diagnostics of the stellar outflows, since they are very bright, often significantly polarized, and are formed only under well-defined ranges of density and temperature. Maser observations therefore directly probe the kinematics and dynamics of the circumstellar region, including magnetic field magnitudes and alignments, and provide many constraints on mass-loss models, stellar pulsation models, and studies of stellar magnetic fields (*e.g.*, , Figure A.13).

The New Mexico Array will make a major contribution to these maser studies by filling in the gap in u,v-coverage between A-configuration and the VLBA. For example, VLBA observations of SiO masers at

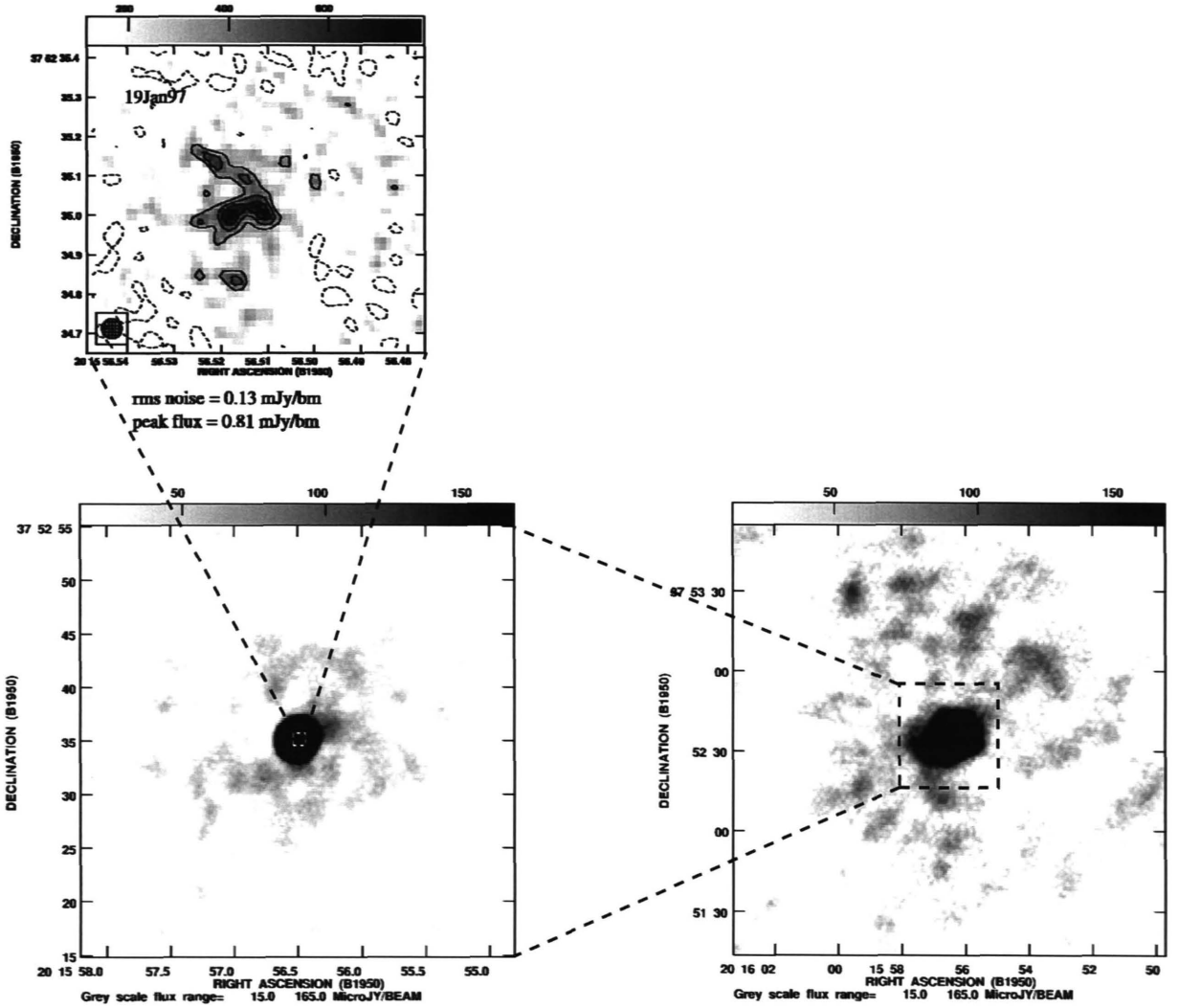

Figure A.12: The thermal wind of the luminous blue variable P Cygni. MERLIN 5 GHz images (top; Exter et al. 2002) show profound variability on timescales as short as a few days, but are severely limited in sensitivity (the peak contour here is 5σ) and resolve out much of the flux density. The VLA images at the same frequency (bottom; made by stacking *seven years* of monthly VLA monitoring, Skinner et al. 1998) also show very complex structure, on scales ranging from the (sub-arcsecond) resolution, to a few arcminutes. This extended emission is confirmed by comparison with optical images and VLA data taken at 15 GHz, which both show much of the same structure. The New Mexico Array by itself will allow imaging at the MERLIN resolution, with ten times higher sensitivity; the full EVLA will add another factor 10 in sensitivity, and provide incomparably more reliable imaging, of structures covering a much wider range of angular scales. The improved sensitivity will also allow imaging at much higher frequencies, allowing a factor 10 higher spatial resolution. These higher frequencies will also require adding in the short-baseline E-configuration, to allow mosaicing the large-scale structure: the primary beam at 43 GHz is only $\sim$ 1 arcmin FWHM.

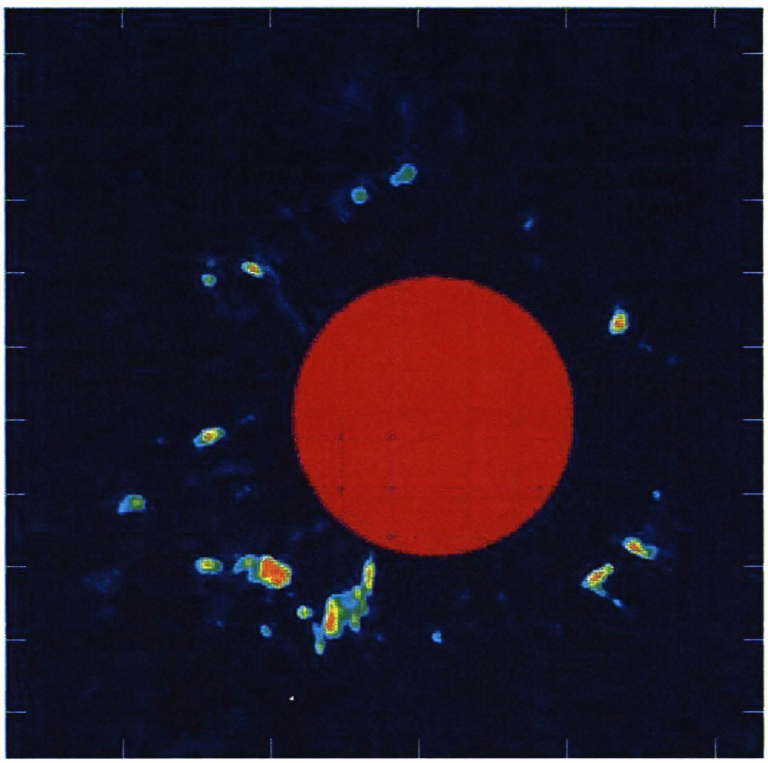

Figure A.13: VLBA image of the star TX Cam, showing the 43 GHz SiO masers forming a shell around the star (Kemball & Diamond 1997). The approximate size of the star is shown by the red circle. Multiple epochs provide direct determinations of the wind outflow speed; simultaneous polarization imaging allows mapping the changing structure of the magnetic field. These observations provide superb resolution but are missing of order half the flux. This missing emission must be more diffuse, and hence should (if imaged with the New Mexico Array) provide much more complete sampling of the atmospheric dynamics and magnetic fields.

43 GHz show clear "ring" structures (*e.g.*, , Figure A.13), but recover only $\sim 50\%$ of the flux density seen in single-dish measurements: fully half the flux density must be found on scales larger than those corresponding to the shortest projected VLBA baseline. This emission must be more widespread than the VLBI masers, and hence should probe the kinematics and magnetic field over a much larger fraction of the stellar wind. A recent lunar occultation experiment found the missing flux for one source — R Leo — on roughly the scale of the "ring" itself. Baselines between the EVLA27 A-configuration and the VLBA – *i.e.*, , those of the NMArray – are optimal for probing these structures. Another example of the use of the NMArray is the polarization observations of OH in the far reaches of the circumstellar shell. The 1 arcsec resolution of the VLA in the A-configuration just barely resolves the shell structures, but VLBI data resolve away most of the larger scale structure. Polarization observations throughout the circumstellar shell are important because they can give significant information about magnetic fields and/or the maser process itself. Finally, there are many weaker (thermal) lines (*e.g.*, , the $v = 0$ transition of SiO) which are too faint to see with the VLBA, but will be easily imaged with the New Mexico Array. The surface brightness sensitivity of the full EVLA will also extend current samples to many more stars, such as short-period Miras.

Requires: New Mexico Array

Resolving Active Stars

While the current VLA has detected stars across the Hertzsprung-Russell diagram both as thermal and non-thermal radio sources, there are very few objects that can be resolved spatially. The famous evolved star MWC 349 is an example of the surprises in store with real imaging. This star was the prototypical thermal

stellar wind radio source, whose $\nu^{+0.6}$ spectrum was for many years regarded as perfectly explained by spherical stellar wind models. However, when the VLA finally resolved the star, it was found to be anything but spherical (Figure A.14), showing at high resolution a curious edge-brightened polar outflow apparently associated with a dust disk. Another example is the Wolf-Rayet binary system WR 140 (HD 193793), whose flux was monitored monthly at the VLA for an entire 8-year cycle by White & Becker (1995). The modulation of the radio light curves results in a detailed model for the winds of the two stars and their interaction, predicting the presence of both thermal and non-thermal components in the system simultaneously. However, the binary orbit is only 26 mas across; the current VLA is unable to confirm the models with resolved images of the two components. The factor of 10 improvements in both sensitivity and spatial resolution offered by the EVLA will allow studies of the spatial structure of the outflows of many more systems, both single and binary, and to understand their properties in a systematic fashion impossible with the few examples that we presently have. Phenomena even more exotic than MWC 349 and WR 140 (stellar jets, disks, complex wind structures) probably lie just beyond the limits of observations with the current VLA.

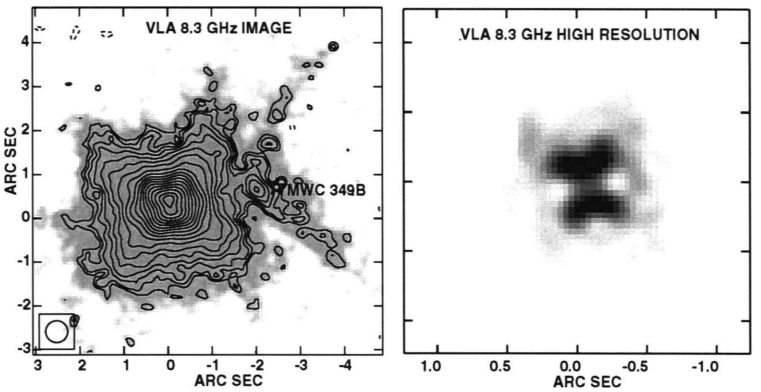

Figure A.14: VLA images of the thermal stellar-wind source MWC 349, a B[e] star. The left panel shows a naturally-weighted image intended to emphasize weaker features: in addition to the thermal emission from MWC 349 itself, a weak bow shock is seen at the location of the interaction with the wind of a B star companion, MWC 349B. The right panel shows a super-resolved MEM deconvolution, giving high spatial resolution in ares of strong flux (data from Rodríguez & Bastian 1994; courtesy S. White 1999).

Requires: New Mexico Array

Unraveling Galactic Novae

Galactic novae are the closest natural thermonuclear explosions to the Sun. Some tens of times each year a white dwarf in a binary star system in the Galaxy accumulates enough matter on its electron-degenerate surface to ignite a thermonuclear runaway explosion; the resulting blast produces substantial radio, infrared, optical, and ultraviolet radiation, which can be visible for weeks or months. The completed EVLA will provide excellent images of every nova found in the Galaxy, from a few days to years after the explosion, measuring shell masses and showing directly the varying physical conditions within the shell.

Radio emissions are uniquely valuable in providing a direct look at the entirety of the ejected mass; optical lines by contrast pick out regions of specific densities or temperatures. The potential of radio observations is best illustrated by the two novae which have been imaged in some detail at radio wavelengths, Nova QU Vul 1984 (Taylor *et al.* 1988) and V1974 Cyg 1992 (Pavelin *et al.* 1993; Hjellming 1996a,b). Both confirmed the tentative conclusion from radio light curve fitting: nova explosions eject five to ten times more mass ($4.8 \times 10^{-4}\,M_\odot$ for QU Vul, $3.1 \times 10^{-4}\,M_\odot$ for V1974 Cyg) than predicted by theoretical models of the explosion process. By contrast, optical mass estimates are typically a factor of ten lower but are derived mainly from spectral line observations that measure the mass only of the inner regions. The radio results imply either that white dwarfs are significantly more massive than usually supposed, or that the explosion

models themselves are wrong. This is a severe problem, because most known biases (*e.g.,* unmodeled opacities) work in the opposite sense, and because the physics is believed to be simple enough that there is little room for more fundamental disagreements.

Apart from simple mass estimates, sequences of radio images can show directly the *three-dimensional* distribution of both temperature and density within the source: the decreasing optical depth effectively 'peels the onion,' allowing one to see deeper and deeper into the source. The imaging sequence of V1974 Cyg (Figure A.15), for instance, revealed high temperatures (10^5 K) in the nova shell even 80–100 days after the outburst. The images also show clear morphological changes as the emission becomes optically thin, revealing the distribution of the gas as a clumpy ellipsoid with a 90-degree change in orientation between the outer and inner shell. Rather surprisingly, a detailed fit to these images also reproduces the shapes of the optical lines quite well (Hjellming 1996a,b).

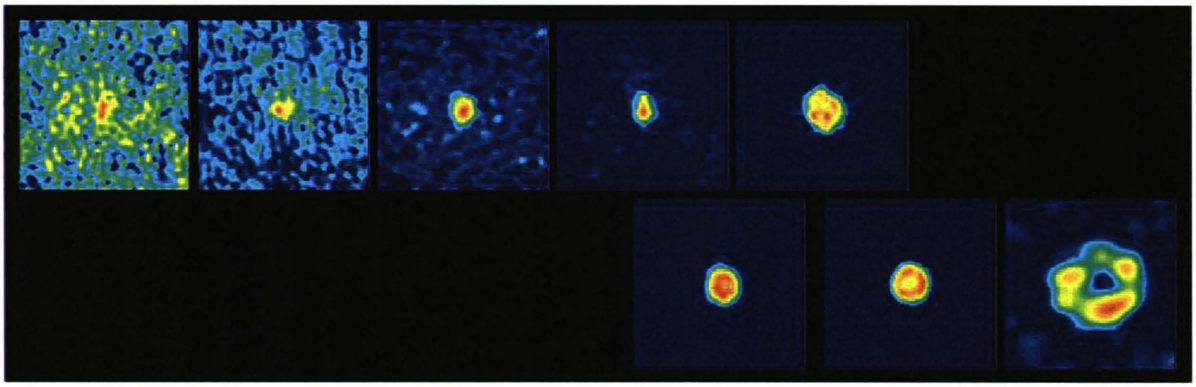

Figure A.15: MERLIN (*upper*) and VLA (*lower*) images of Nova V1974 Cyg 1992 (Pavelin *et al.* 1993; Hjellming 1996a,b). The 5 GHz MERLIN data were taken 81, 106, 155, 173, and 271 days after outburst; the 22.5 GHz VLA data were taken 255, 313, and 769 days after outburst. Note the evolution from a centered-filled source highly elongated north-south, to a shell slightly elongated east-west. This corresponds to the change from optically thick to optically thin emission, with the later images 'peeling away' the outer skin to reveal the three-dimensional structure. The New Mexico Array will have more than 30 times the sensitivity of MERLIN, and (by mapping at 45 GHz) about 10 times higher resolution. Novae like this one could be imaged within a few days of the explosion.

Radio imaging covering both the optically thick and optically thin stages thus provides an excellent observational probe of the *entire* gaseous content of ejected nova shells. The source elongation, shell thickness, and ejecta clumpiness derived from these images can then be combined with ultraviolet, infrared, and optical data to yield very detailed and accurate models. The EVLA will make these observations routine, as well as adding important new capabilities. For the first time, most nova shells can be imaged and resolved, determining brightness temperatures, temperatures during optically thick phases, and the evolution of both radial and clumping mass distributions. The inner and outer velocities of nova shells range from 500 to 5000 km/sec, with 1000–3000 being most common. The angular size is therefore

$$\theta = 0.57\,\mathrm{mas} \cdot \frac{v}{1000\ \mathrm{km/sec}} \cdot \frac{t_{\mathrm{day}}}{d_{\mathrm{kpc}}} \tag{A.1}$$

With superb sensitivity at 33 and 45 GHz, the completed EVLA will produce excellent images at $4-6$ mas resolution, resolving novae within a week of the outburst; within a month one could make the first detailed spectral index maps.

Requires: New Mexico Array

A.2.3 Astrometric Applications

The EVLA will provide a unique combination of sensitivity and angular resolution, making it the instrument of choice for astrometric observations of faint sources (see Table A.2.3). The improved sensitivity will also

allow the use of much fainter and closer calibrators; at 6 GHz for instance the mean separation between 13 mJy sources (detectable at 1000:1 signal-to-noise ratio in 1 minute) is only $\sim$ 30 arcmin.

Table A.2.3. Astrometry with the Expanded Very Large Array

		Full EVLA		New Mexico Array	
Frequency (GHz)	Resolution[a] (milliarcsec)	Rms Noise (μJy)	Rms Position[b] (μarcsec)	Rms Noise (μJy)	Rms Position[c] (μarcsec)
1.60	105	4.5	570	17	1,790
3.0	57	2.2	150	8.4	480
6.0	28	1.7	57	6.5	180
10.0	17	2.1	43	7.9	135
15	11	1.8	24	7.1	78
23	7.4	2.3	20	9.0	67
34	5.0	2.5	15	9.8	49
45	3.9	5.0	23	19	74
86	2.0	50	120	50	120

[a]The resolution listed is that of the New Mexico Array alone; the full EVLA's resolution will be 10–20% larger, depending on the weighting scheme used. The astrometric accuracies listed for the EVLA assume a 20% larger beam.

[b]Astrometric accuracy of the EVLA, defined as the resolution divided by the signal-to-noise ratio achieved for a 1 mJy point source in 1 hour (dual polarization)

[c]Defined as for the full EVLA

The result will be an astrometric revolution, with a wide variety of applications. Some of these are discussed below.

Requires: New Mexico Array

Tying Together the Radio and Optical Reference Frames

One of the chief problems with using stellar radio positions to tie the optical and radio coordinate frames is the extended and highly variable nature of bright non-thermal radio sources. The EVLA will provide sub-milliarcsecond positions for thermal sources (photospheres and single-star winds); these can then be combined with optical observations of bright stars from the *Hipparcos* and *SIM* missions to tie the optical (stellar-based) frame to the inertial (quasar-based) one. Unlike these short-lived missions, the lifetime of the EVLA is measured in decades, ensuring this frame-tie will remain accurate and reliable for a long time to come.

Requires: New Mexico Array

Tracking Stellar Flares

The astrometric capabilities provided by the NMArray will be a great boon for observers of both normal and active stars. For example, the EVLA will allow searches for positional changes during long-lasting (hours) flares, as might be seen in coronal mass ejections from active stellar coronae. The EVLA will be the first radio telescope able to detect the normal radio emission of ordinary stars like the Sun. Most of the (thousands of) stars within 25 pc will be detected as quiescent sources due to their photospheres alone, and any stellar activity will produce much larger fluxes whose time variability can be studied. The radio flares already known on nearby active stars are a puzzle because they are so much larger than the Sun's radio flares: they require either that brightness temperatures be much higher than on the Sun, implying very different physics in the acceleration mechanism, or else that the sizes of the radio sources be much larger than solar radio bursts. The EVLA will be the only telescope able to address this question; it combines the sensitivity needed to see the quiescent stellar emission, with the spatial resolution needed to measures offsets

between the flares and the quiescent sources. Such observations of both normal and active stars will provide direct constraints on the emitting regions, *e.g.*, , on the relative importance of surface emission and coronal loops. The results should help us understand the mysteriously tight correlation between radio and X-ray/Hα emission for most stars, and why that correlation fails for a few odd sources (like brown dwarfs). Similarly, observations of binaries, whether non-thermal (*e.g.*, , RS CVn and Algol systems) or thermal emitters (*e.g.*, , Be star binaries), will yield reliable, independent information on the nature of the binary components and the origin of their radio emission. Combining sub-milliarcsecond radio and optical astrometry (and imaging) for active stars will show directly the relation of active regions to the stellar photosphere and to optical star spots.

Requires: New Mexico Array

Brown Dwarfs

Brown dwarfs may be defined as objects which have masses too low for significant hydrogen burning, but too high to avoid fusion altogether: $13\,M_J < M_{bd} < 75\,M_J$, where M_J is the mass of Jupiter (*e.g.*, , Basri 2000). According to standard relations between stellar activity and spectral type, such late-type stars should not be active at all, and this is indeed true for Hα and X-ray emission. However, these sources *are* substantial radio emitters with quiescent levels of ~ 0.1 mJy, and frequent 20-minute flares of $1-2$ mJy (Figure A.16). These sources thus violate the radio/X-ray relations for earlier stars by some 3–4 orders of magnitude, indicating a dramatic shift in the nature of the dynamo. One clue is that the radio activity seems to be correlated with the rotation velocity, exactly opposite to what is observed in Hα, though it is not clear how this should be interpreted. The EVLA will have a significant impact on this field, by allowing detailed astrometric measurements of both the quiescent and the flaring emission. For nearby brown dwarfs (< 10 pc), the stellar disks are $60-120$ microarcsec across and the rotation periods are short ($2-12$ hours). It will thus be possible to observe a brown dwarf for several rotation periods, look for rotational modulation of quiescent emission, and group the emission into several bins corresponding to different rotation phases; one could look for positional changes at different rotation phases, and look for evidence of starspots/loops. Infrared variability has been interpreted as brown dwarf "weather" (photospheric condensates), and magnetic spots have been said to be ruled out, yet the radio flares cannot be explained. NMArray observations could test this hypothesis of magnetic spots/loops directly.

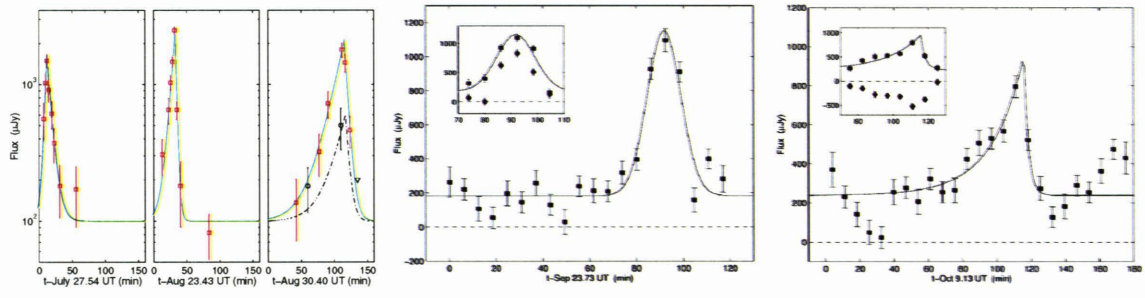

Figure A.16: Radio emission from three brown dwarfs, as observed with the VLA: (left) LP 944−20; (middle) TVLM 513−46546; (right) 2MASS J0096159+182110. The insets show the circularly polarized flux density ($\sim 60\%$). The sensitivity of the EVLA combined with the resolution of the New Mexico Array will allow sub-stellar astrometric measurements of both the quiescent and the flaring emission, providing direct measurements of changes with rotation and orbital phase, offsets between the flares and the normal emission, etc. From Berger et al. (2001) and Berger (2002).

Requires: New Mexico Array

Pulsars

Pulsar astrometry is important for many reasons.

- *Models of the Galactic electron density:* Model-independent distances from pulsar parallaxes provide essential calibration points for models of the Galactic electron density distribution (*e.g.*, , Taylor & Cordes 1993; Wood & Reynolds 1999; Roshi & Anantharamaiah 2000). Such parallaxes are particularly important for models of the local interstellar medium (ISM); these models in turn allow better distance estimates (based on dispersion measures) for nearby pulsars which are too weak for direct parallax measurements. Combining proper motions and parallaxes with observations of the interstellar scintillation (ISS) provides further constraints on the warm interstellar medium along the line-of-sight.

- *Neutron star population velocities:* The combination of parallaxes with proper motions gives accurate model-independent transverse velocities, while improved models for the warm ISM (see above) lead to better estimates of transverse velocities for *all* pulsars. Together these measurements constrain the shape of the pulsar velocity distribution, providing fossil information about the evolution of close binaries and core collapse supernovae. Such data can for instance characterize the role of diffusion of stellar orbits in the Galaxy's gravitational potential.

- *Pulsar birth sites & pulsar/supernova remnant associations:* The true ages of both pulsars and their associated supernova remnants (SNRs) can be estimated from the combination of the angular separation and the proper motion. Pulsar parallaxes can help clarify possible pulsar/SNR associations, while accurate astrometry allows some pulsars to be traced back to their birth sites in stellar clusters (*e.g.*, , Hoogerwerf, de Bruijne, & de Zeeuw 2001).

- *Nuclear astrophysics:* Pulsars provide one of the few direct probes of extremely dense matter. Accurate distances can be combined with observed thermal radiation from the neutron star surface to yield the size of the photosphere, providing a direct constraint on the neutron star equation of state.

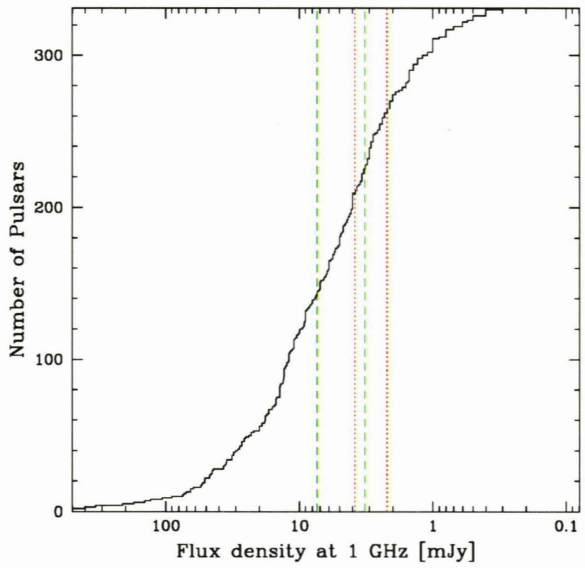

Figure A.17: Cumulative distribution of pulsar flux densities. The vertical lines indicate flux density limits for two different parallax estimates: the dashed green lines show pulsars whose distances could be measured if they were as far away as 8 kpc, while the dotted red lines show those which could be measured out to 3 kpc. The two lines in each case correspond to the range of measured spectral indices ($\nu^{-1.4} - \nu^{-2.4}$).

The New Mexico Array will be the best instrument in the world for pulsar astrometry. Most such measurements today are done at 1.4 to 1.8 GHz, because of the sharp decline in flux density with frequency ($\nu^{-2.4} - \nu^{-1.4}$). With the expanded VLA, most pulsar astrometry will probably be done in either the 2–4 GHz band or the 4–8 GHz band, since the increase in sensitivity more than compensates for the roughly

4 or 16-fold decrease in brightness. The higher frequency not only provides a smaller beam, but also reduces ionospheric effects by the square of the frequency ratio. Further, errors due to the differential troposphere (which currently dominate for parallax measurements of bright pulsars) will be much reduced, since the EVLA will be able to use much fainter and closer calibrators. Accurate parallaxes could easily be measured for $\sim$ 250 pulsars out to 3 kpc; $\sim$ 150 could be obtained, even if the pulsars were as far away as 8 kpc (Figure A.17). In addition to providing a large number of distances independent of electron density models, these data will yield very sensitive proper motion estimates, giving an unparalleled database of pulsar space motions.

Requires: New Mexico Array

A.3 The Milky Way

A.3.1 H II Regions

H II regions are the signposts of recent and on-going star formation, ranging in size from giant star-forming complexes like Orion, to ultracompact H II regions (UCHIIs), and the even denser hypercompact H II regions (HCHIIs) which are only a few hundred AU across. The UCHII and HCHII regions are of great interest because they represent the earliest (smallest) stages in the evolution of H II regions (*e.g.*, , Kurtz et al. 2001); the HCHII regions in fact may be pressure-confined by the residual hot molecular core out of which the massive star powering the region formed. Unfortunately, the HCHII regions in particular are very difficult to study, because no current instruments can resolve them. The vastly improved continuum sensitivity of the EVLA, together with the resolution afforded by the New Mexico Array, will allow the imaging of H II regions as small as 40 AU to distances of $\sim$ 10 kpc, well beyond the Galactic Center. Because of their extreme densities, HCHII regions remain optically thick up to at least $\sim$ 30 GHz, and radio recombination lines at 40-50 GHz will be the best and perhaps the only way to determine the kinematics of the ionized gas. The ionized gas motions may be crucial to understanding these objects, since current data suggest that remarkably broad line profiles (up to 250 km/s full-width at zero intensity) may be an intrinsic property of these regions.

As the HCHIIs evolve, they should be seen as ultra-compact and compact H II regions, on time scales of order 10^3 to 10^5 years. These are complex sources, often displaying cometary or jet-like extensions and hosting a variety of associated molecular masers. These structures may reflect density gradients in the molecular cloud, combined with the motion of the powering source. Current images do not resolve much of this structure. The New Mexico Array will be ideal for these studies, allowing not only detailed imaging, but measurement of accurate proper motions and expansion rates.

Requires: New Mexico Array

A.3.2 Supernova Remnants

Spectral Imaging of Supernova Remnants

The origin of cosmic rays (CRs) has been an outstanding problem in physics since their discovery (see also §A.5). There is a strong case to be made for CR production in supernova remnants (SNRs) because: (1) SNRs can easily provide the required energy; (2) the observed synchrotron radiation proves that SNRs can accelerate relativistic particles; and (3) both SNRs and CRs are rich in heavy elements. However, despite such qualitative evidence, the link between CR production and shock acceleration processes in SNRs remains poorly understood. One key observational diagnostic is spectral imaging.

High-resolution, multi-frequency observations are important because the radio spectrum constrains the energy spectrum and spatial distribution of the relativistic particles. The key is to relate measured spectral variations to the dynamical structure of the remnant, since models of particle acceleration in SNRs, either by shocks or by second-order Fermi (stochastic) acceleration in interior turbulence, predict structure in the particle distributions they produce. Measured variations must be related to acceleration processes or the energy spectrum of the seed particles; variations in older remnants can also be related to the compression of the cosmic ray gas and the interstellar magnetic field. Such studies are complicated by the presence of

free-free absorption, which modifies the observed spectrum at low frequencies. This makes the interpretation more complex, but also provides a valuable probe of both the shocked gas (Figure A.18) and internal ejecta and filaments.

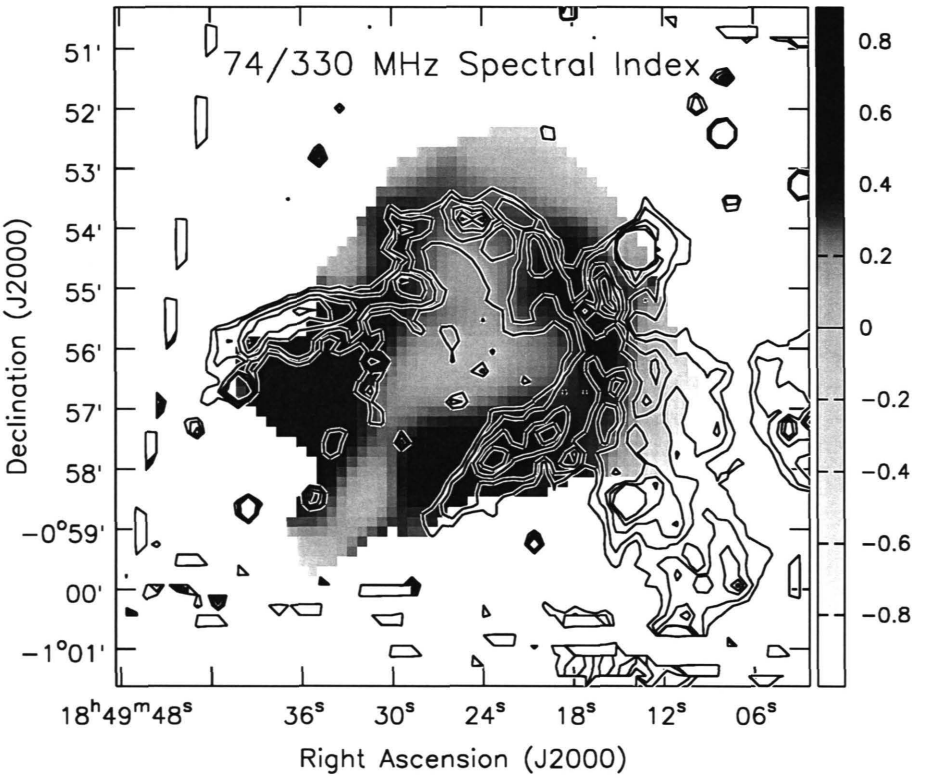

Figure A.18: The supernova remnant (SNR) 3C 391: 74/330 MHz spectral index (grayscale) with ISOCAM 12 − 18 μm contours. Note the impressive agreement between the regions with high spectral index and those with the strongest infrared emission. The spectral index indicates strong free-free absorption, while the bulk of the 12 − 18 μm emission arises from fine structure infrared lines formed in cooling post-shock gas. Both are therefore tracing the SNR/molecular cloud shock boundaries. Courtesy C. Brogan.

Only a handful of SNRs can be usefully studied with the current VLA, the key limitations being insufficient angular resolution at low frequencies, and insufficient surface brightness sensitivity at high frequencies. The EVLA will address both difficulties. First, the New Mexico Array will give resolutions of a few tenths of an arcsecond at 330 MHz. Second, the combination of the E-configuration and the Green Bank Telescope will allow accurate imaging of > 20 supernova remnants at 5–10 GHz, more than doubling the current sample. Astronomers can thus obtain accurate images at comparable spatial resolution over more than two orders of magnitude in frequency. Compared to the typical current factor of two or three, this represents a truly spectacular improvement.

Requires: New Mexico Array; E-configuration

Masers and Supernova Remnant Shocks

Supernovae are a powerful (and perhaps the dominant) source of energy and turbulence in the interstellar medium (ISM). That much is clear; but the details of their interaction with the surrounding gas are much less obvious. Most supernova remnants lie in the Galactic plane, and it is often difficult to tell with which gas along the line-of-sight the SNR is interacting, let alone make detailed estimates of important parameters like the shock velocity, density, and magnetic field strength. One important tracer is the 1720 MHz maser

line of OH, which is thought to originate in the post-shock molecular gas behind C-type shocks. These masers have been found in ~20 SNRs, or ~ 10% of those known in the Galaxy (Frail et al. 1996; Green et al. 1997). Apart from serving as signposts for SNR/ISM interactions, these lines themselves provide very useful diagnostics. Maser theory suggests they should only be pumped efficiently for densities of $\sim 1 \times 10^5\,\mathrm{cm}^{-3}$ and temperatures in the range $50\,\mathrm{K} \lesssim T \lesssim 125\,\mathrm{K}$ (*e.g.*, , Lockett et al. 1999), and this has been confirmed by molecular emission line data for these regions (see Frail & Mitchell 1998). Moreover, the maser line itself can be used to derive local magnetic field measurements via the Zeeman effect. Observations with the VLA have resulted in magnetic field detections between 100 and $4000\,\mu\mathrm{G}$ toward 10 different SNRs (Brogan et al. 2000 and references therein). These represent the first *direct* magnetic field estimates of the post-shock gas; they are also very significant, because field strengths of $\sim 1\,\mathrm{mG}$ exert a considerable influence on the properties of the shocked cloud.

The next step is to image these masers at higher resolution, to find out whether the derived magnetic fields are contaminated by blending. Since the typical spot sizes are > 100 mas, and these masers are intrinsically quite weak, this is next to impossible with the VLBA, even with phase referencing (*e.g.*, , Claussen et al. 1999). Furthermore, the limitations of the current correlator make it impossible to obtain sufficient spectral resolution for Zeeman work, while also measuring the linear polarization — a key parameter in theoretical modeling of masers, and the implied magnetic field strengths (*e.g.*, , Elitzur 1998). The New Mexico Array, combined with the VLBA, will provide the necessary brightness sensitivity to image even the weakest of these masers, while simultaneously resolving their complex core-halo structure. The new WIDAR correlator can then be used to provide simultaneously high spectral resolution and full Stokes polarization information. Such observations will both expand the current sample of masers, and remove key systematic difficulties in their interpretation.

Requires: New Mexico Array

A.3.3 The Galactic Center

Gas Motions and Stellar Masers

Recent infrared measurements have provided superb positions, proper motions, and radial velocities for stars within a few arcseconds of Sgr A* (Schodel et al. 2002; Ghez et al. 2003). Since their motions are completely dominated by gravitational forces, these stellar measurements very tightly constrain the mass distribution within the central few tenths of a parsec, and prove beyond a reasonable doubt that there must be a supermassive black hole at the Galactic Center. But this central region is also full of ionized and molecular gas, whose extreme properties (in terms of density, distribution, kinematics, and pressure) are unique in the Galaxy. This gas must play a role both in powering the central region, and in fueling the on-going star formation which somehow manages to take place in this extremely hot and turbulent region. In fact, the Galactic Center is surprisingly anemic, both in the luminosity its black hole manages to produce, and in the local star formation rate, compared with the more extravagant active galactic nuclei (AGN) and starbursts which are found both in the local neighborhood and at high redshift. What fuels Sgr A*, and why is it so under-luminous compared both to AGNs, and to the expected accretion luminosity? How does star formation proceed in these extreme environments? In order to answer these questions we must understand not only the stellar dynamics, but also the characteristics of the gas. In particular, we must understand the influence of such non-gravitational forces as the gas and radiation pressure, and the magnetic fields. The Galactic Center offers the perfect laboratory for measuring these hydrodynamic influences, particularly now that the mass distribution there is known so well. What is required is an instrument which can see the gas (even through the enormous absorption columns along the line-of-sight) with sufficient sensitivity and resolution to provide the required sub-milliarcsecond astrometry, on short enough timescales to follow the expected rapid proper motions. Ideally, these astrometric measurements should also be tied to the same reference frame as the stellar data, and should cover at least a few tens of parsecs.

The New Mexico Array will provide the perfect instrument for such astrometric studies, allowing several orders of magnitude improvement for both ionized gas and maser sources. A microarcsecond at the Galactic Center corresponds to about a million kilometers; measurements of this accuracy will become straightforward with the completed EVLA, especially since Sgr A* itself provides an excellent positional reference. These measurements will revolutionize our understanding of Galactic center dynamics. The current state-of-the-

art is illustrated by recent VLA observations of proper motions of the ionized gas, as seen in free-free emission (Zhao & Goss 1998; Yusef-Zadeh, Roberts, & Biretta 1998). Both groups observe motions up to 30 mas/year (1200 km/s). While the bulk motion of the gas is consistent with the gravitational influence of the black hole, the motions of individual features imply additional hydrodynamic accelerations, presumably from stellar winds, outflows, or explosive events. However, the limited sensitivity and angular resolution of these measurements confine them to measuring high velocity motions of rather bright sources. The best measurements to date give error bars between 35 and 180 km/s over an eight-year baseline, depending on signal-to-noise ratio. With a factor $\sim$ 30 increase in sensitivity, working at 45 rather than 22 GHz, and adding the long baselines of the NMArray, one could do a factor $\sim$ 70 better in a single year, making it possible to measure *accelerations* as well as simple velocities for many non-stellar sources in the Galactic center. This is particularly important for the low surface brightness features within a few tenths of a parsec of Sgr A*, which include long, narrow ($<$ 0.1 arcsec) filaments as well as H II regions. These astrometric data will complement radial velocity studies based on radio recombination lines, made possible by the first phase of the VLA Expansion Project. The result will be a three-dimensional map of hydrodynamic motions, which can be directly compared to the on-going stellar studies.

Gas motions are also of great interest on larger scales. In particular, one of the most important issues in the Galactic center is how molecular clouds tens of parsecs from Sgr A* are affected by the potential of the black hole (e.g, are the clouds orbiting, infalling, or outflowing from the Galactic center?). Proper motion studies of this more distant gas have been impossible before due to the relatively slow velocities of the gas outside $\sim$ 0.5 parsec of Sgr A* (distant gas clouds have velocities less than 50 km/s, compared to hundreds of km/s near Sgr A*). By observing the ionized gas in the photodissociation regions surrounding the molecular clouds, the NMArray will provide the first reliable, high-significance measurements of the proper motions of this slower-moving gas.

In addition to these ionized gas measurements, the NMArray will lead to great improvements in proper motion studies of stellar OH, H_2O, and SiO masers. While the ionized gas measurements probe hydrodynamical effects in local regions like the central parsec, and stellar data provide similar but purely gravitational measurements, these masers will show how the stellar dynamics are set by the Galactic mass distribution on scales out to hundreds of parsecs. The combination of broad frequency coverage, narrow frequency channels, superb resolution, and a huge primary beam ($\sim$ 30 arcmin for OH, or $\sim$ 75 pc) will make the EVLA by far the best instrument in the world for these studies.

Requires: New Mexico Array

A.3.4 The Interstellar Medium

Tracing the Ionized Gas and Galactic Magnetic Fields

Warm ($\sim 10^4$ K) diffuse ionized gas is a significant component of the interstellar medium (ISM). This gas constitutes roughly a quarter of the interstellar atomic hydrogen, and is probably the dominant phase of the ISM about a kiloparsec above the disk; the power required to keep it ionized roughly corresponds to the entire kinetic energy injected into the ISM by supernovae (*e.g.*, , Reynolds 1991). Understanding this warm ionized medium (WIM) is thus essential for any modeling of the ISM and its energetics. While recent work has focused on wide-field optical imaging (*e.g.*, , the Wisconsin H-Alpha Mapper [WHAM], Reynolds et al. 1998), radio observations also offer many useful probes, both of the ionized gas itself, and of the magnetic fields which influence its motions. The WIM itself was first identified through pulsar dispersion measures (Hewish et al. 1968), which continue to give essential information on column densities towards these sources. As discussed above (§A.2.3), the New Mexico Array will allow distance determinations for many more of these sources, providing essential input to models of the distribution of the ionized gas. In the same vein, the NMArray is essential to obtaining scattering measurements along some of the most interesting and highly scattered lines-of-sight. Typical scattering disks for OH masers near the Galactic center are 0.1 to 1 arcsecond, too small to be resolved by the VLA's A-configuration, too large to be imaged with the VLBA — but perfect for the NMArray.

The new E-configuration will also play an important part, providing sufficient surface brightness sensitivity to allow large-area studies of polarized synchrotron emission, combined with continuous spectral coverage to allow tracking changes in polarization angle as a function of frequency. Images of the polarized signal

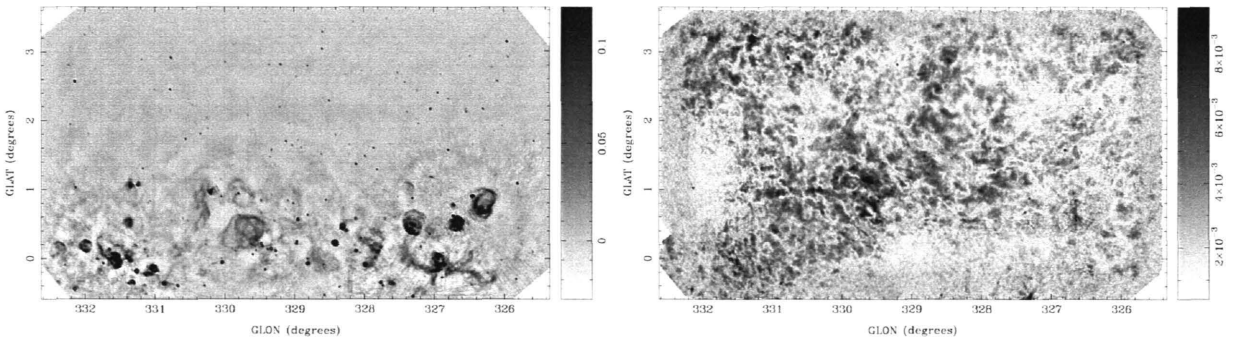

Figure A.19: Diffuse total intensity (left) and linearly polarized (right) Galactic emission (Gaensler et al. 2001). The total intensity illustrates the huge variety of sources in the Galactic plane. Note the almost total *lack* of correspondence between this and the polarized intensity; the foreground H II regions block the polarized signal, but the connection between the other sources and these structures is far from obvious.

(Figure A.19) show almost no correlation with the total intensity, apart from a few areas where foreground H II regions disrupt the magnetic field on small scales. The complex structure reflects both the initial polarized emission, and propagation effects. Linearly polarized signals are rotated as they propagate through the ISM; this Faraday rotation goes as ν^{-2}, and provides a direct probe of both the ionized gas density and the magnetic field along the line-of-sight. Imaging polarimetry thus traces the detailed structure of the ISM, and can be used for instance to check the relation between regions of turbulence and possible powering sources (*e.g.*, , supernova remnants). Following the time variability of the polarization could also provide measurements of size scales and velocities of the magneto-ionized gas.

Requires: New Mexico Array; E-configuration

The Interstellar Medium: Thermalized lines

Some of the most exciting scientific applications of the proposed E-configuration involve observations of spectral lines from atomic and molecular transitions with excitation temperatures of a few tens to a few hundreds of Kelvin. The 21 cm line of neutral hydrogen in our Galaxy has an absolute upper limit of about 130 K in brightness; non-maser molecular lines typically have much lower excitation temperatures. This means that these lines are extremely faint, even if they are fully optically thick. At the same time, existing surveys (*e.g.*, , Figure A.20) show that these lines exhibit complex structure on angular scales from arcminutes to degrees and beyond. Observations of objects with 10 K brightness temperatures are extremely difficult with the D-configuration; at 21 cm for instance an hour is required to obtain an rms of 1 K at 1 km/s resolution. Figure A.21 shows an example of what is currently possible with observations of ammonia in Orion, spending 30 minutes on each of 18 fields. Much of the flux is resolved away by D-configuration, and the relative paucity of short spacings makes it difficult or impossible for any deconvolution software to recover.

Another example is that of the high-altitude H I clouds recently discovered with the Green Bank Telescope (Figure A.22; Lockman 2002). These clouds are found to co-rotate with the disk, which is surprising for clouds more than a kiloparsec above the plane, but which allows good distance estimates based on tangent point velocities. This previously-unknown population may make up more than half the mass of the neutral gas halo of the Milky Way. A significant fraction of these clouds are surrounded by low surface brightness H I 'halos'. While preliminary VLA images do an excellent job of resolving the cloud cores, this more extended component is simply too weak and too extended to see with reasonable integrations in the D-configuration, while the GBT can just barely show that these halos are there. The E-configuration's combination of image fidelity and surface brightness sensitivity would be perfect for these sources, which are just a single example of the complexity of the interstellar medium: one needs sensitivity on *all* spatial scales to accurately represent these structures.

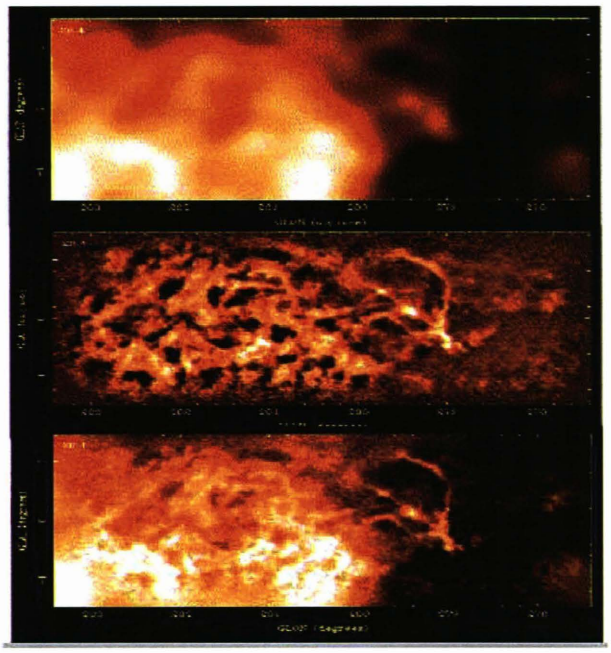

Figure A.20: HI images of the Galactic chimney GSH277+0+36 made with Parkes (top), the ATCA interferometer (middle), and the combined data (bottom) (McClure-Griffiths et al. 2002). Mapping large structures in the Milky Way requires both rapid (and accurate) interferometric mosaics, and supporting single dish data; the E-configuration will provide the one, while the Green Bank Telescope provides the other.

The E-configuration would allow the first truly large-scale VLA mosaics of Galactic H I emission. Current mosaics reveal a wealth of complicated filaments and structures at all spatial scales; but the image quality in D-configuration is severely limited by the effects of the incomplete Fourier plane coverage. The essentially complete Fourier coverage of E-configuration snapshots will allow much higher quality images, even in 30 second snapshots. A survey covering one quadrant and 10 degrees in Galactic latitude would take only 120 hours to complete, providing a magnificent database with 3 arcminute angular resolution and 0.5 km/sec velocity resolution. Such a fully-sampled survey would provide an important database for (1) modeling the gas dynamics in the Galaxy; (2) comparison with surveys of molecular gas and detailed modeling of the conversion between atomic and molecular gas in molecular clouds and photodissociation regions; (3) comparison with features in the radio continuum, giving distances to those continuum features which correlate with the H I; and (4) studies of the detailed interaction between violent events in the disk (SNR, H II regions, blow-out events) and the H I.

Requires: E-configuration

A.4 Galaxies and Clusters of Galaxies

A.4.1 Discrete Sources in Nearby Galaxies

The discrete radio source population in nearby galaxies is dominated by H II regions and supernova remnants (*e.g.*, , Fig. A.23). While these sources can be studied in more detail in our own galaxy, extragalactic surveys offer a number of advantages. First, one can sample a wide range of physical conditions, both within a single galaxy and between galaxies, and compare the effects of local conditions (pressure, temperature, density, and gravity) and star formation history, as well as the influence of more global factors such as active galactic nuclei, galaxy mergers, and galaxy type. Second, all sources in a given galaxy are at very nearly the same distance, avoiding many selection effects that plague Milky Way samples. And finally, any selection effects which *are* present tend to be easier to quantify and account for in subsequent analysis.

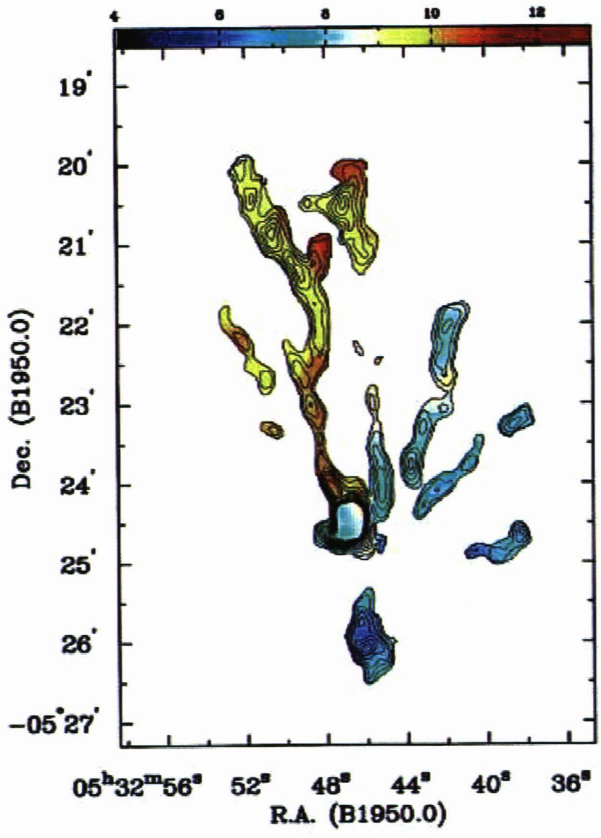

Figure A.21: The velocity field of the high-density ridges of the Orion nebula as mapped in ammonia by Wiseman & Ho (1998) using the VLA's D-configuration. This represents the "tip of the iceberg;" combining E-configuration and Green Bank Telescope observations would recover five to ten times more emission.

The two major problems are sensitivity and spatial resolution. Sensitivity is required simply to detect individual sources; spatial resolution is essential to separate them from each other and from more diffuse emission. High surface brightness sensitivity is also necessary to make actual images of individual sources.

The EVLA will provide factor of 10 or more improvements both in sensitivity and (with the New Mexico Array) in resolution, and these advantages will be multiplied by its broad, continuous frequency coverage, never before available on *any* radio interferometer. In the realm of H II regions for instance, the EVLA will

- resolve ultra-compact H II regions (0.1 pc, EM=10^7cm^{-6}pc) out to 1.4 Mpc. At M31/M33 (0.8 Mpc) these can be detected (5σ) in under 2 hours, from 3 to 33 GHz, and imaged (3 beams across) in 12 hours.
- image individual compact H II regions (0.5 pc, EM=10^7cm^{-6}pc) out to $\sim$ 4 Mpc. In the M81/M82 group, these could be *detected* (5σ) in half an hour; a 12 hour observation would give a 33 GHz map, again of every source within the 1.4 arcmin beam, at a resolution of 0.1 pc.
- resolve super star clusters (few pc, EM$\sim$ 10^{10}cm^{-6}pc) over 20 Mpc away. These super star clusters have properties analogous to ultracompact H II regions, but on vastly larger scales; they are invisible at optical and near infrared wavelengths. Their properties imply that they may be globular clusters in formation.

The result will be complete samples of a wide range of H II regions, at an identical distance, throughout the disk of another galaxy. Scientific interests include: dating H II regions by source sizes; checking for differences in size/morphology according to the local pressure; counting individual young stars, and comparing this with other star formation measures (note that the radio suffers from little or no extinction).

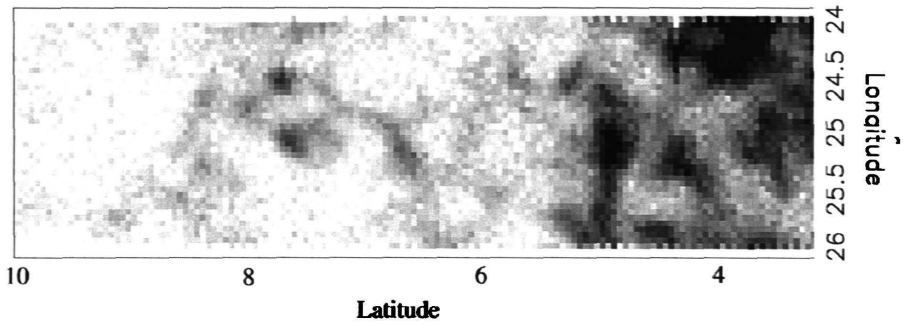

Figure A.22: The Galactic H I emission measured by the Green Bank Telescope in the region ($24° \leq l \leq 26°$, $2° \leq b \leq 10°$), averaged over LSR velocities 122–138 km/sec (Lockman 2002). Galactic rotation is expected to give a velocity of ~ 110 km/sec at these longitudes, so this emission must arise close to the tangent point: *i.e.*, , 7 kpc from the Sun. The two halo clouds at $b = 7.6°$ are thus more than 1 kpc above the Galactic plane.

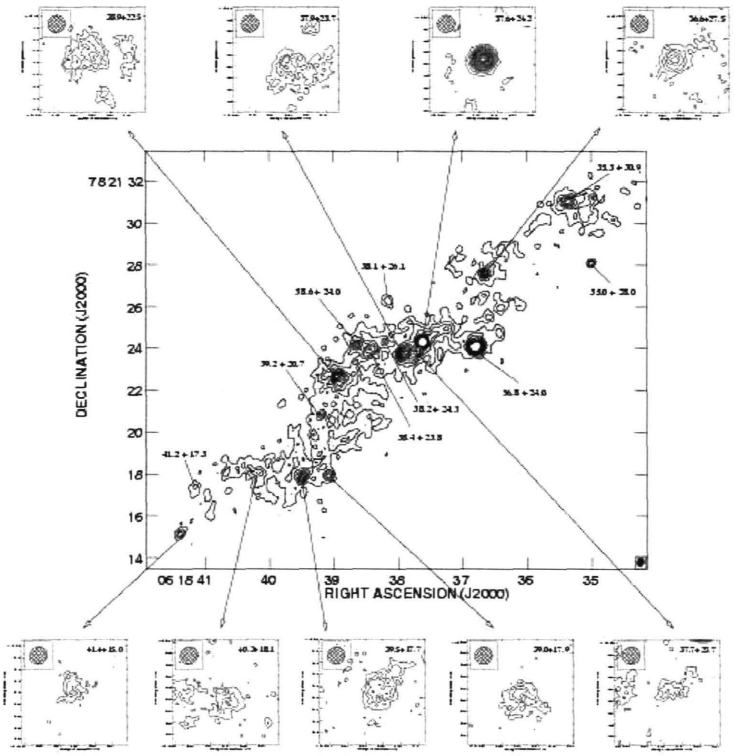

Figure A.23: The starburst galaxy NGC 2146 at 5 GHz, as imaged by combining MERLIN and the VLA's A-configuration (Tarchi et al. 2000). The peak contour in the central image is 640 μJy/beam. At a distance of 15 Mpc, only a small fraction of the compact sources are resolved with the 0.15 arcsec beam; some of the unresolved sources are supernova remnants, and some are probably ultra-dense H II regions associated with super star clusters. The sensitivity of the EVLA combined with the long baselines of the New Mexico Array will provide similar signal-to-noise with a 0.03 arcsec beam — just over 2 pc. The H II regions should be at least this strong at higher frequencies, and there the EVLA will allow *another* order-of-magnitude improvement in resolution.

These same observations will provide stunning images of complete samples of supernova remnants (SNRs); one could for instance easily image the extragalactic analogues of Tycho and Kepler in M82. *Resolving* SNRs yields much more information than simple detections. Such data are essential in distinguishing SNRs from background sources and spiral arms; in particular, imaging is required to discriminate between flat-spectrum

Crab-like and composite SNRs, and H II regions. More directly, images give important physical information about the SNRs themselves. For instance, the size gives an indication of the age of a remnant, and the relationship between size and surface brightness (the Σ-D relation) should also reflect the evolution of the source. The results of such studies in the Milky Way are muddled, at least in part, because of inhomogeneous samples and uncertainties in SNR distances. Studying SNRs in another galaxy provides better statistics (more SNRs, some indication of dependence on galactic environment, much better understanding of selection effects) *and* a common distance for all SNRs seen. Resolved images give SNR types (filled, shell, or mixed) as well, and consequently some indication of SNR histories and current power sources (pulsar *vs.* shock). The NMArray will provide a 2.4 GHz resolution of $\sim$ 0.3 pc at M33 (800 kpc), ideally suited to mapping these remnants.

Requires: New Mexico Array

A.4.2 Diffuse Emission in Nearby Galaxies

Untangling Thermal and Non-thermal Emission

The radio emission from normal galaxies is dominated by a combination of synchrotron emission from relativistic electrons, and thermal free-free emission from ionized gas. The two processes are distinguishable by their spectra: synchrotron emission is generally brighter at low frequencies ($\sim \nu^{-0.5}$ to ν^{-2}), while thermal emission is more slowly varying ($\nu^{-0.1}$) at high frequencies, and may become opaque (ν^{2}) at low frequencies. In general, synchrotron emission dominates up to about 20 GHz, while thermal emission is most important between $\sim$ 30 and $\sim$ 100 GHz. Untangling the two in any individual galaxy requires sensitive imaging at the same resolution over as wide a range of frequencies as possible. As the separation depends on the behavior of the *total* flux density with frequency, it is essential to retain sensitivity to large-scale structures at all frequencies. This makes wide-field spectral imaging a very demanding problem in terms of sensitivity and u,v-coverage. In particular, the thermal emission from normal galaxies is almost unexplored, because no imaging instrument has the simultaneous high sensitivity, high resolution, and wide field-of-view to make this work practical. The combination of the E-configuration and total power data from the GBT addresses all these difficulties. E-configuration collects all the area of the EVLA to provide the best possible surface brightness sensitivity at 30-40 GHz, with a resolution matched to the lower frequencies in A- or B-configuration (the beam at 32 GHz in E-configuration will be $\sim$ 6 arcsec, comparable to that of the B-configuration at 1.4 GHz). At the same time the E-configuration's superb Fourier plane coverage gives excellent snapshot imaging, allowing mosaics of many pointings (the field-of-view is only 1.4 arcmin at 32 GHz). Diffuse ionized gas with emission measures of a few cm^{-6}pc might be detectable with long integrations: a 6 arcsec beam filled with the warm ionized medium seen in the Milky Way would give a flux density of $\sim$ 0.2 μJy/beam at 32 GHz. (This would incidentally give the best possible limits on diffuse ionized gas in elliptical galaxies, since the deepest optical techniques rely on having fairly narrow and well-known velocities.) More reasonable integrations could trace faint star-forming complexes or regions of high electron density for the first time at radio wavelengths, giving a direct dust-free view of the star formation process. Knowledge of the true thermal emission is also critical to following the spectral aging of the synchrotron component, as well as to understanding the far infrared/radio correlation. Such studies are crucial to our understanding of galaxies in general, and the interstellar medium in particular.

Requires: E-configuration

A.4.3 Neutral Hydrogen in Normal Galaxies

Hydrogen is the fundamental building block of the Universe, its most abundant element and the raw material from which stars and galaxies are formed. Radio frequencies offer the unique capability of tracing this element in its ground state, via the spin-flip transition at λ21cm. This transition is quite faint, and emission studies (particularly with interferometers) have focused on pointed observations of the central regions of galaxies selected at optical or infrared wavelengths. This is however far from the whole picture. Recent observations have shown, for example, that the H I in both dwarf galaxies (Figure A.24) and ellipticals (Figure A.25) can be much more extended than, and morphologically distinct from, the optical emission. Similarly, in interacting galaxies (Figure A.26), the neutral gas offers a unique kinematic tracer of the history of the interaction. Even

the *absence* of H I can be revealing; the abrupt H I 'edge' seen at low column densities ($\sim 2 \times 10^{19}\,\mathrm{cm}^{-2}$) in a few galaxies has been used to constrain the ionizing flux of the cosmic ultraviolet background, as well as the surface mass density of galactic disks. Observational studies of Lyman α absorption systems and cosmological simulations of galaxy evolution both suggest that galaxies should be surrounded by substantial reservoirs of cold gas. The direct imaging of these absorption line systems, and their connection to particular galaxies, is thus of enormous interest.

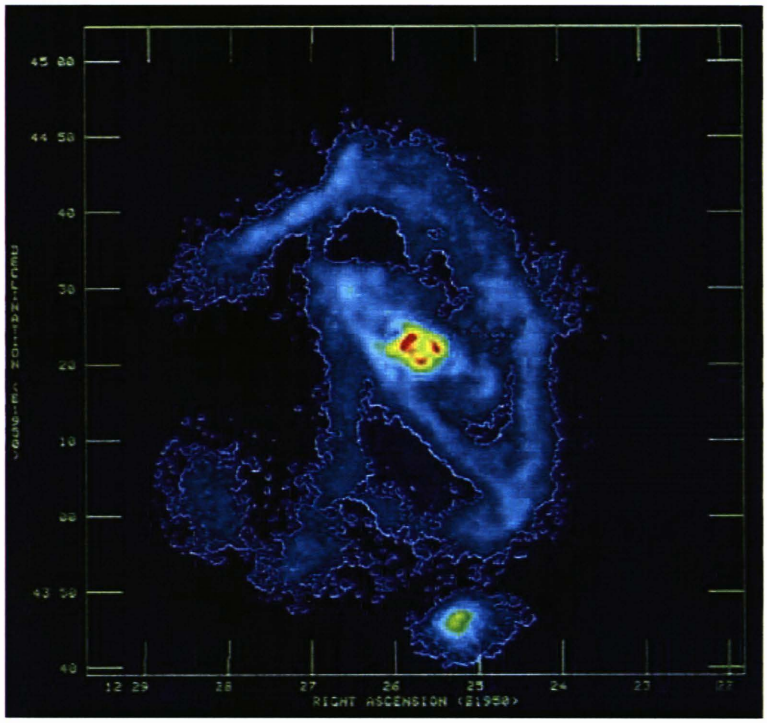

Figure A.24: Pseudo-color representation of the integrated H I distribution of the gas around the dwarf galaxy NGC 4449. This map was made from a mosaic of nine VLA D-configuration pointings plus the pointed map of DDO 125 (the bright object at the bottom edge), and covers more than a square degree. The optical galaxy fits well within the central bright spot in this figure; follow-up observations have found signs of star formation near the peaks of the H I column density, well outside the galaxy. From Hunter et al. (1998).

The absolute requirement for progress in this area is improved surface brightness sensitivity. Here the E-configuration will allow major advances, as illustrated by three overlapping experiments.

- *The edge of a galaxy:* A few hundred hours with the best current instruments achieve column density limits of a few times $10^{18}\,\mathrm{cm}^{-2}$, barely sufficient to suggest that galaxies have sharp edges at this limit. A similar observation in E-configuration could go a factor 10 deeper, allowing a definitive test, and showing whether this H I edge is uniform around the disk. This is critical information for models based on the flaring of the disk and its subsequent ionization by the intergalactic radiation field.

- *An All-Sky H I Survey:* In recent years all-sky continuum surveys covering almost the entire electromagnetic spectrum have become available, giving us a good indication of the distributions of stars, dust, hot gas, and relativistic electrons in the Universe. However, this information does not exist for neutral hydrogen, even in the local Group of galaxies. The high surface brightness sensitivity of the E-configuration, combined with the large instantaneous velocity coverage of the correlator, will finally make it feasible to survey H I over the whole sky, simultaneously covering a redshift range from 0 to

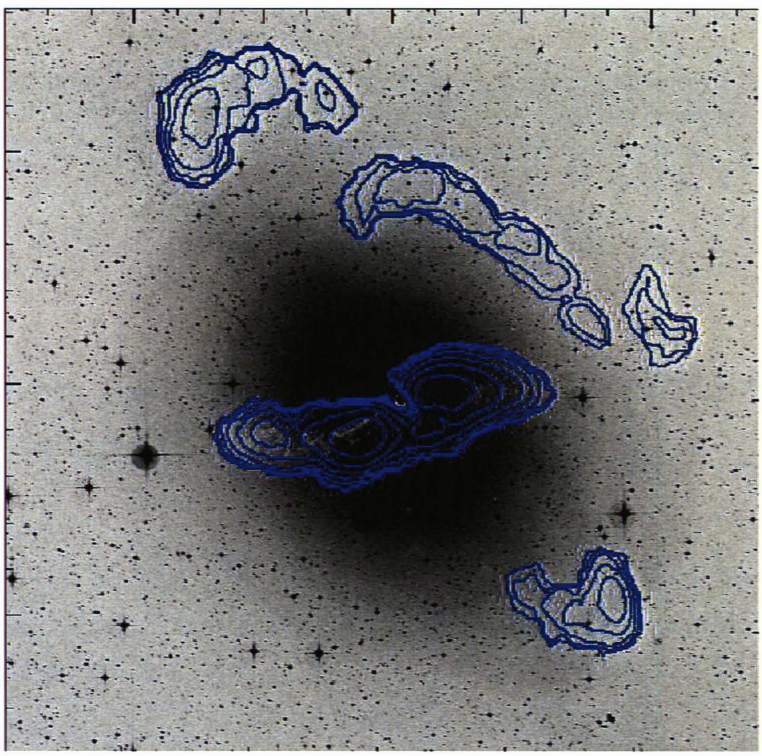

Figure A.25: Neutral hydrogen contours atop optical grayscale for the E/S0 galaxy NGC 5128 (Centaurus A). The H I distribution follows and is slightly displaced from the outermost diffuse shells. From Schiminovich et al. (1994).

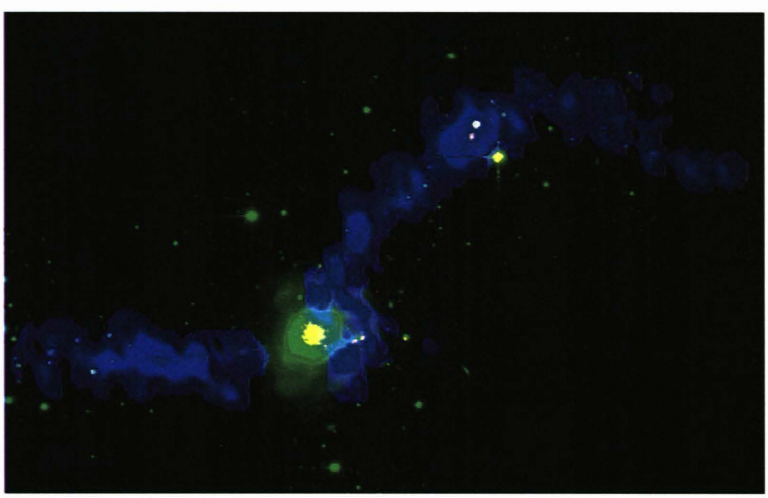

Figure A.26: A composite image of the optical light (green), star forming regions (yellow and pink), and cold atomic hydrogen gas (blue) in the well known merger remnant NGC 7252, the "Atoms for Peace" galaxy. The name derives from the pair of tidal tails and the loops surrounding the optical body. This system is the result of the merger of two spiral galaxies. The H I data show that the tidal tails are rich in gas, confirming the gas-rich nature of the progenitor disks. They also show that the inner regions are relatively free of cold atomic gas. These data support the idea that merging spirals can create gas-poor elliptical galaxies. From Hibbard et al. (1994).

0.1. This will give a complete inventory of H I mass, irrespective of a stellar association, to $10^5\,M_\odot$ within the local group, to $2.6 \times 10^7\,M_\odot$ at the distance of the Virgo Cluster, to $2.4 \times 10^8\,M_\odot$ in Coma, and to $3.5 \times 10^{10}\,M_\odot$ at the survey limit of $280h^{-1}\,\mathrm{Mpc}^2$. Note that even in the nearest cluster, Virgo, only a few per cent of the whole volume has been searched in H I. The total volume of this survey, $6.5 \times 10^7 h^{-3}\,\mathrm{Mpc}^3$, is such that about 10^6 galaxies should be detected with H I masses below $10^{10}\,M_\odot$. This assumes 3 minutes per pointing, giving a column density sensitivity of $3 \times 10^{18}\,\mathrm{cm}^{-2}$ over a 2.5 arcmin beam in a 12 km/s channel. The entire sky north of -30^o could then be observed to the 6σ mass limits above in a (mere) 2.7 years.

- *The local H I "web":* The Hubble Deep Fields have produced something of a revolution in extragalactic astronomy. A very deep (2700 hour) H I exposure in E-configuration would achieve a column density limit of a few times $10^{15}\,\mathrm{cm}^{-2}$ (in a 1 km/sec channel), and provide the deepest look yet at both the local and the most distant neutral hydrogen gas (since the EVLA's correlator will allow simultaneous observations from $z = 0$ to $z \sim 0.4$). Such a survey would begin to approach in *emission*, what quasar studies now provide in absorption.

  Requires: E-configuration

A.4.4 Radio Jets and Radio Galaxies

Most if not all galaxies with bulges harbor supermassive black holes; the more massive the bulge of the host galaxy, the more massive the black hole in its core. This suggests a direct relationship between the assembly of the galaxy and the central black hole. One possible explanation is direct feedback between the accretion-driven luminosity of the black hole and the accumulation of proto-galactic baryonic matter around it. Further, observations of high-redshift galaxies suggest a close connection between luminous AGN, molecular gas, and star formation. Closer to home, existing data have shown the importance of the large-scale interaction between the jet and its surroundings. Unfortunately, many important problems regarding jets remain unsolved. There is no accepted view of how these extragalactic jets are launched and collimated, nor even any consensus as to their content. We do not understand the impact of the jet on its environment, and vice versa. We do not even have a clear picture of the life cycle of a typical radio galaxy. To address these issues requires high-resolution images of the small-scale structure, such as the inner jet, and high-quality images of the large-scale structure.

High resolution: jet structure and origins

Jets are the pipeline by which the central black hole in an AGN connects to the outside world. The jet is the means by which the black hole produces the radio galaxy, and it is also the means by which it influences its surroundings (typically the plasma in a cluster of galaxies). These sources provided much of the impetus for the original design of the VLA, and a great deal has been learned from the resulting images. Some jets display extraordinary collimation, often over tens or even hundreds of kiloparsecs in length, which suggests a highly supersonic flow. Other jets expand gradually, reminiscent of subsonic, turbulent plumes known on Earth. Still other jets undergo a dramatic transition, from an initial strong collimation to a broader, but still ordered, tail flow; this is probably due to the onset and saturation of a fluid instability.

A few jets are close enough, and bright enough, to allow more detailed study. We know that jets are not always uniformly filled. In some sources they consist of twisted, magnetized helices, and may have "empty" (radio-faint) spines. M87 (Figure A.27) and Cygnus A (Figure A.28) are well-known examples. This echoes the parsec-scale structure of jets studied with the VLBA (although current VLBA images often leave much to be desired, being limited in sensitivity, fidelity, and spatial dynamic range). If these features are due to fluid or magnetohydrodynamic instabilities, fundamental quantities such as the density and speed of the jet can be derived — *if* the images are good enough to identify and measure the large-scale modes excited by the instability. Another example is relativistic motion of bright features in the jet. VLBI observations have show that this is common on parsec scales; the VLA has now detected such motion in two jets (M87, Cen A) on kiloparsec scales. The jet in M87 shows apparent speeds up to $2c$, as well as complex velocity structure between and within knots, and motions transverse to the jet axis.

[2] h is the Hubble constant in units of 100 $\mathrm{km\,sec}^{-1}\,\mathrm{Mpc}^{-1}$: $h = H_0/100$

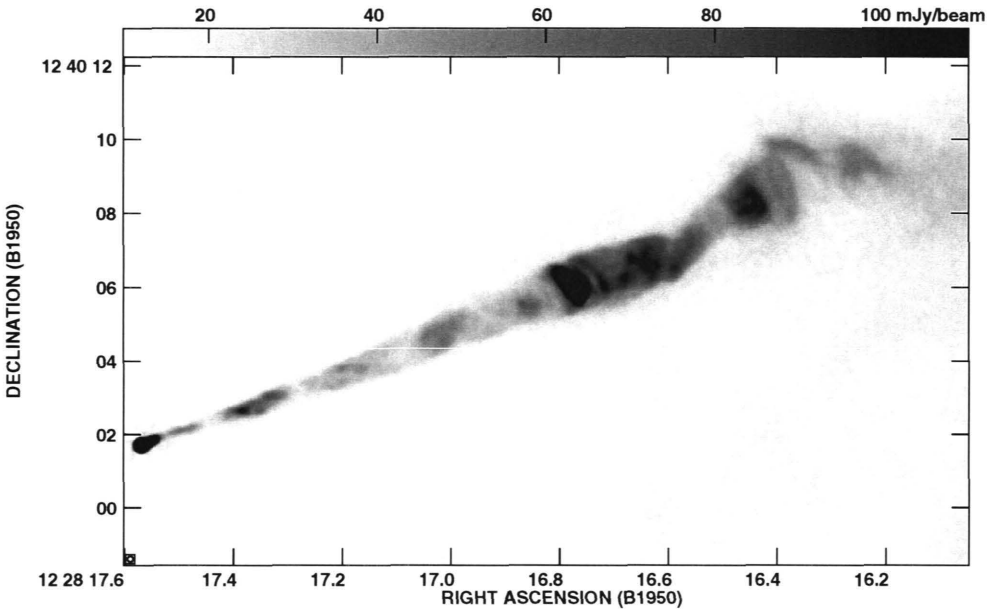

Figure A.27: VLA 15 GHz image of the M87 jet, the closest kiloparsec-scale jet in the northern hemisphere (Biretta, Zhou, & Owen 1995). Its closeness and brightness have permitted detailed study of the structure and proper motions in this jet. Helical structure can be seen in the inner jet, as well as bright outer knots which may be shocks in the flow. This image has $0.15'' = 12\,\mathrm{pc}$ resolution, which gives 8 beams across near the brightest part of the jet (Knot A); the NMArray will provide 10 to 30 times this resolution, with similar fidelity, giving more than *100* beams across the jet.

Despite this progress, fundamental questions remain unanswered, due to limitations of even the best current images. How does the transition from parsec to kiloparsec scales occur? Does the flow decelerate? Where and how does it collimate? Is there evidence for entrainment? On larger scales, is there evidence for relativistic motion, or currents, or for a high-speed spine in the flow? What is the structure of the magnetic field, and does it contribute to jet collimation? Is there Faraday rotation evidence of a confining field in the external plasma? Are there physical differences between jets which remain collimated and those which disrupt close to the black hole?

Furthermore, jets are not all identical. Understanding the variety of jet physics requires images of a large sample at a level comparable to the M87 data. The New Mexico Array is essential to provide these high-quality, high-resolution images, including polarimetry. The NMArray will provide 10 times better resolution than the current VLA. This will give few-parsec resolution on jets at $z = 0.5$ (for instance 10 or more beams across all of the Cyg A jet), thus enabling detailed study of a large number of jets at a resolution comparable to the current M87 image.

In addition to these larger samples, the few good nearby cases must be imaged at the best resolution possible. The jet in M87 is close and bright enough to allow detailed study of its kiloparsec-scale structure. The current M87 image has 8 beams across the brightest part of the jet (knot A); the NMArray will provide 10 to 30 times this resolution[3], giving sub-parsec resolution with more than *100 beams* across the jet. It is

[3]The New Mexico Array is a factor $\sim$ 10 larger than the A-configuration, giving a factor $\sim$ 10 higher resolution. The improved sensitivity of the EVLA will also allow it to observe at higher frequencies, improving the resolution by *another* factor of a few.

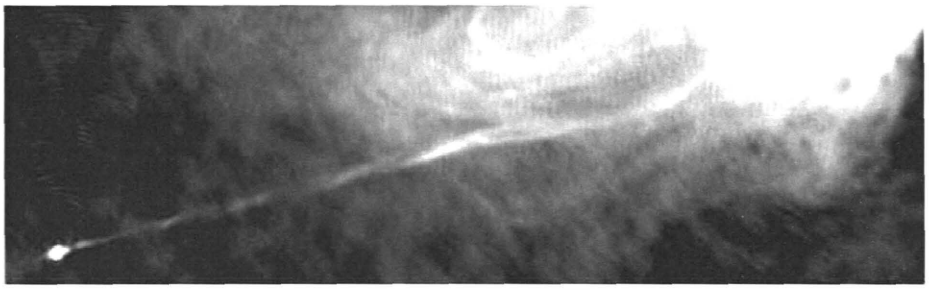

Figure A.28: VLA 4.5 GHz image of the Cygnus A jet, from Perley, Dreher, & Cowan 1984. The jet is only marginally resolved at 0.4″ resolution (~ 400pc at $z = .056$). Helical structure similar to that in M87 can just be seen in this image. Observing with the NMArray at high frequencies will give at least 10 beams across the jet, allowing it to be imaged at a level comparable to the current image of the M87 jet.

also close enough to learn more about the inner-jet region, and thus to explore the connection to the nuclear black hole. The inner jet displays rapid changes *in radio, optical, and X-ray*, on sub-arcsecond scales; we are seeing both synchrotron and inverse Compton scattering over these wavebands, but cannot easily sort out the physics of the emitting plasma. The higher resolution and good image quality of the EVLA will dramatically improve our understanding of this region. Current VLBI images suggest the jet collimates within a fraction of a milliarcsecond of the black hole, although this must be verified with higher quality images. Combining the VLBA and EVLA will produce images of very high resolution *and very high fidelity* to reveal the origins of this important jet.

Requires: New Mexico Array

A.4.5 Gravitational Lenses

Radio observations have historically played a key role in the study of gravitational lenses, starting with the detection and first resolved images of the first known lens, 0957+561. By now ~ 100 galaxy-mass lenses are known; a striking example is shown in Figure A.29. The VLA has made important contributions both in finding new lenses (*e.g.*, , the CLASS survey, Myers et al. 2003; Browne et al. 2003), and in measuring time delays for known systems (*e.g.*, , Fassnacht et al. 2002). Statistical studies provide important constraints on both the matter density and the equation of state of the Universe, which – because they depend differently on the fundamental parameters – are an important complement to constraints derived from the cosmic microwave background and type Ia supernovae. For individual lenses, measurement of the time delay can give both the geometric distance and the lens mass scale, and hence a direct estimate of the Hubble constant. Reliable time delays are now known for 9 systems (Kochanek 2002), of which 5 were determined by radio observations (four with the VLA, one with the Australia Telescope Compact Array). The next stage is to increase the number of time-delay systems known, and to increase the accuracy of the mass models. The ideal would be to find a "golden lens" system, in which the geometry would be simple enough (*e.g.*, , an isolated nearly spherical lensing galaxy) to introduce the minimum of model uncertainties.

Of course gravitational lenses can be used to derive mass profiles as well as (or instead of) distances. For instance, Treu & Koopmans (2002a,b) have been carrying out a program to combine the lensing observations with optical kinematics as determined through Keck observations for a sample of radio lenses (to avoid contamination by optical images). Indications from these studies are that two component models with dark matter profiles steeper than the canonical isothermal profile can explain the observations.

The two keys to further advances in this area are, first, finding more lenses; and second, determining accurate time delays for both the new lenses and those which are already known. The New Mexico Array will allow major advances in both areas, by providing the first extremely sensitive array, with long enough

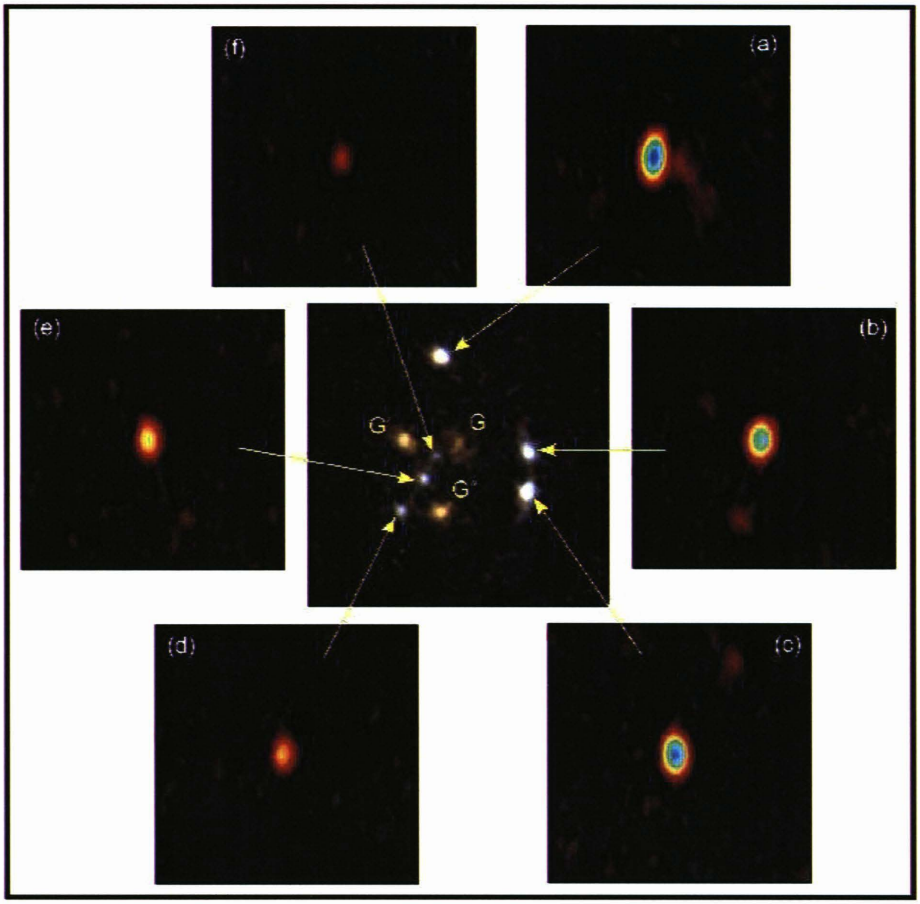

Figure A.29: The gravitational lens system B1359+154, found by the Cosmic Lens All-Sky Survey (CLASS). This composite shows the Hubble Space Telescope optical image, surrounded by six VLBA images of the lens background radio source (Rusin et al. 2001). This is the first arcsecond-scale system in which a source is lensed into more than four detectable images.

baselines to resolve lens components, which is available throughout the year for monitoring and surveying purposes.

Consider for example a large-scale search for new lenses, aimed at increasing the number of known lenses by a factor of ten. Observing with the stand-alone New Mexico Array at 5 GHz would give very clean statistics, resolving out most extended emission, and selecting for flat-spectrum objects where lensing geometries are easy to recognize. Based on the experience of CLASS, and the number density of flat spectrum, core-dominated sources in the FIRST catalog, such a survey would require observing some 8000 square degrees for $\sim$ 30 sec per pointing, resulting in a catalog of some $\sim 10^5$ sources, and taking about a year of observing time.[4] This assumes a blind survey, and a lensing rate similar to that found in CLASS. Of course these sources are much fainter, and the lensing rate may be lower; but on the other hand, the NMArray will give much higher resolution, and will be able to find any small-separation lenses that CLASS VLA observations did not resolve.

Given this new $\sim$ 1000-lens catalog, the stand-alone New Mexico Array will also be the perfect instrument for deriving their time delays. Such derivations rest on tracing variability between the different lensed images; so for instance image A might brighten first, then image B, and so on. The NMArray offers sufficient resolution to distinguish the lensed images; superb sensitivity, to trace very faint flux density variations; and year-round availability, essential for tracking flux density changes which are currently lost during the half of the year the VLA spends in its compact C- and D-configuration.

[4]Note that during this year both the EVLA27 antennas and the 8 remaining VLBA antennas could be conducting *completely independent* observations.

Requires: New Mexico Array

A.5 Particle Acceleration in the Universe

How relativistic particles are accelerated is an important question that connects many different areas of astrophysics. These particles definitely exist; they are observed both directly (the cosmic rays which reach earth) and indirectly (synchrotron emission from relativistic electrons seen throughout the Universe). Examples of the latter include supernova remnants, diffuse galactic synchrotron halos and the radio emission from spiral disks, radio jets, active galactic nuclei, and synchrotron halos in galaxy clusters. It is still not known, however, how or where these particles are accelerated. There are at least three attractive ideas: shock, turbulent, and electrodynamic acceleration. Distinguishing between these requires observations which can probe the plasma dynamics (where are the shocks? what is the magnetic field doing? where is the system turbulent?) as well as the energization (what particle energies are reached? with what efficiency?).

Radio astronomy is the fundamental tool for such studies. Radio images and resolved spectral energy distributions reveal the spatial and energy distribution of the relativistic particles (convolved with the local magnetic field). The physics however can be complicated, and diverse models exist which have not been easily testable with current systems. Sorting out these issues requires comparing theoretical models with high quality images, made at high spatial resolution, and well-sampled over a broad frequency range. The lack of spatial resolution, particularly in spectral index and spectral curvature determinations, has greatly hampered work up to now. The continuous frequency coverage of the EVLA will allow enormous advances, and permit observations which can test the models. The combination of the New Mexico Array, E-configuration, and continuous spectral coverage will allow "scaled-array" observations over a wide range of frequencies. The EVLA will provide the matched resolution essential for useful spectral studies, as well as the polarization information which reveals the geometry of the magnetic field. This combined with the EVLA's superb sensitivity will lead to well-sampled spectra at sub-arcsecond resolution over more than a decade in frequency. This broad range is important because the low ($\sim$GHz) frequencies reflect the initial particle acceleration ("injection"), while the higher frequencies probe particle aging and magnetic field decay.

One example is the detailed, high-resolution, broad-spectral-coverage study of known acceleration sites, such as the hot spots in radio jets (which require the high resolution of the NMArray and possibly the EVLA+VLBA combination), or supernova remnants (which will benefit from the addition of the GBT+E-configuration to reach the larger spatial scales). With such data, details of the acceleration physics can be studied: does a low-energy power-law range ever really exist? Can a low-energy injection limit be seen? Can one identify physical structures, such as shocks or magnetized filaments, which correlate with flat-spectrum regions? A galactic example of this is the Kepler supernova remnant (Figure A.30), which has small spectral index variations that are correlated with the radio structure, possibly suggesting that the primary acceleration site in this object is the *outer* shock. This remnant is one of the few that is bright enough to allow such work with the present system; the EVLA will allow several dozen galactic remnants to be imaged, at comparable quality to Figure A.30, but with better resolution and frequency coverage (§A.3.2). The same physics is at work in extragalactic hot spots, as seen in VLA images of the jets in M87 (Figure A.27) and Cygnus A (Figure A.28).

Requires: New Mexico Array; E-configuration

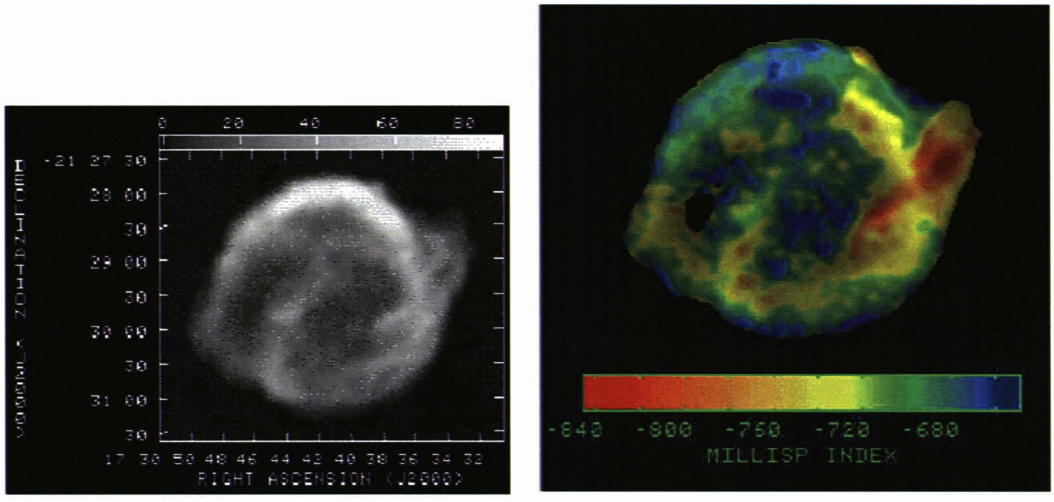

Figure A.30: Kepler's supernova remnant, as observed with the VLA at 1.4 and 5 GHz by Delaney et al. (2002). Left: Total intensity image, at 7″ resolution, showing both the simple circular shell expected in a remnant of this age, and the wisps and filaments which have developed within this structure. Right: a two-frequency spectral index map, showing that flatter and steeper spectral regions correlate with the filamentary structures. Such studies provide information on the nature of particle acceleration sites in the remnant; expanded frequency coverage will enable the study of details of the particle acceleration physics. The improved resolution and continuous frequency coverage of the EVLA will allow this type of study to be carried out on many such objects.

Appendix B

Surface Brightness Sensitivity of ALMA and the EVLA

The relevant sensitivity metric for an imaging array is that of surface brightness. Although the concept of surface brightness is well established from the emission process point of view, translating a synthesis array's capabilities into similar terms proves to be difficult, as both the array's resolution and fundamental point-source sensitivity are involved. It is perhaps not surprising that most descriptions of array performance provide these two quantities separately, and leave the user to figure out the conversion to brightness to judge whether the object of interest can be successfully imaged by a given array.

Below, we attempt to describe the EVLA and ALMA's imaging capabilities in terms of their surface brightness sensitivity. The reader should be aware that the chain of reasoning requires some attention, which is why this matter has been relegated to an Appendix. Still, for those willing to invest a little time, the discussion below illustrates the requirements for both resolution and sensitivity in order to properly study the physics of sources in a wide range of parameter space, and in particular, show the EVLA's advantage for studying optically thin emission.

Figure B.1 shows the continuum brightness temperature sensitivities of both the EVLA (shaded green) and ALMA (shaded yellow) with the apparent brightness temperature of blockbody emission (left panel) and optically thin bremsstrahlung (right panel) superposed.

Consider first the left panel. In light green is the range of surface brightness to which the EVLA is sensitive, for a one-hour integration, to $1-\sigma$, as a function of frequency. The resolution at which a particular brightness sensitivity is obtained is shown by the slanting red lines. The upper boundary of the green area is the limiting surface brightness of the full EVLA at full resolution. As the EVLA (and ALMA) are imaging arrays, their surface brightness sensitivity can be improved by tapering *i.e.*, reducing the resolution. Providing the point-source sensitivity is constant, the surface brightness sensitivity is inversely proportional to the square of the fractional reduction in resolution. For example, the point marked with the magenta dot shows that the surface brightness sensitivity of the EVLA at 6 GHz, in one hour, is 100K, and that the resolution of the array for this sensitivity is 30 milliarcseconds. The sensitivity can be improved (that is, the brightness limit is decreased), by tapering to a lower resolution, as indicated by the magenta dashed arrow. A factor of three degradation in resolution results in (roughly) an order of magnitude improvement in brightness sensitivity – indicated by the location of the blue dot at the end of the magenta line[1]. Another factor of three degradation in resolution provides another factor of ten improvement in brightness sensitivity, here marked by the orange dot at the end of the blue line. For this brightness sensitivity (1K), and frequency (6 GHz), the required baselines are provided by the A-configuration, as indicated by the approximately horizontal dashed dark green line.

Now consider a specific emitting body – a 10K black body. The black line in the left panel labelled '10KBB' shows the apparent brightness temperature of such an source. The black dot positioned on the curve within the green area indicates that at 1.5 GHz, the EVLA will provide a $1-\sigma$ detection at 10K sensitivity with 400 mas resolution. This point is a factor of $\sim$20 below the full-resolution sensitivity,

[1]This scaling assumes the point-source sensitivity is unchanged by the taper – which is of course not true. As the EVLA is heavily centrally condensed, the reduction in point-source sensitivity for moderate taper is in fact quite modest

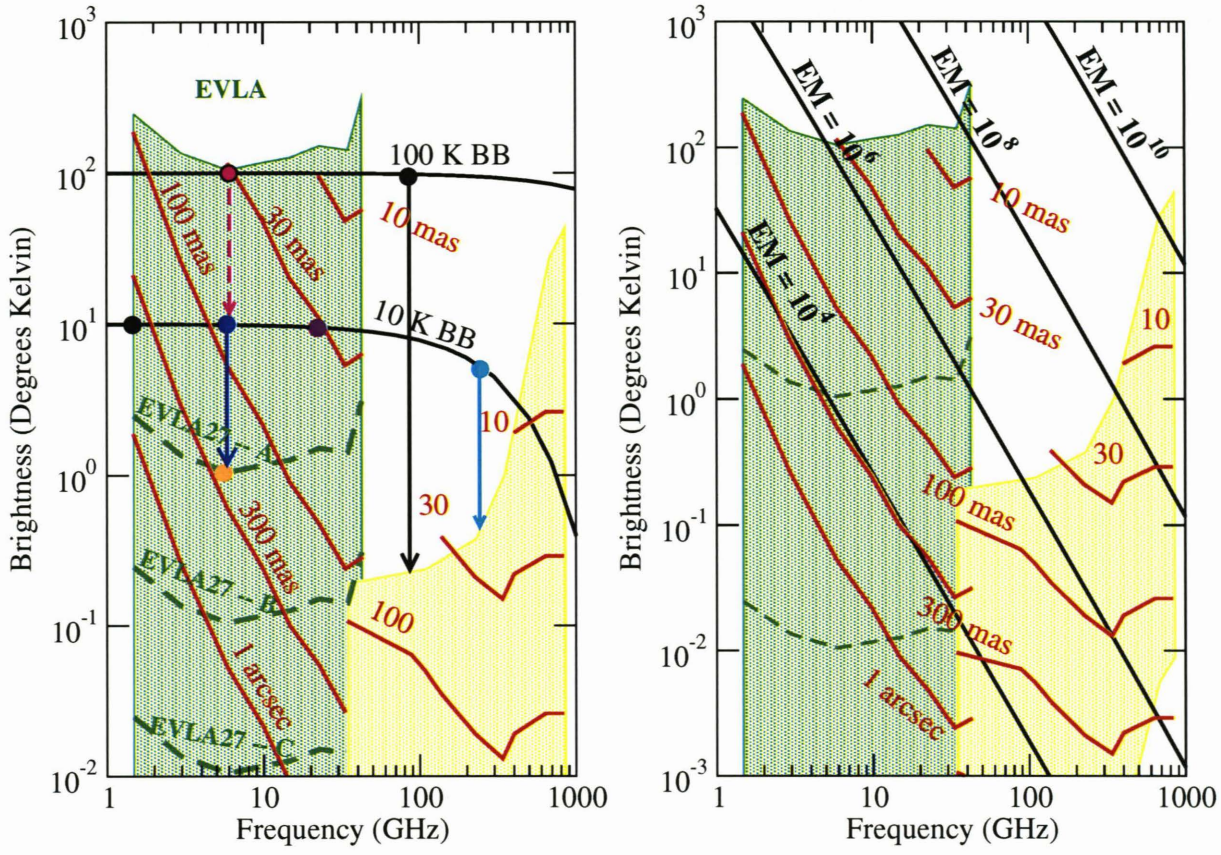

Figure B.1: The continuum brightness temperature sensitivity (1–σ in 1 hour) of the EVLA (shaded green) and ALMA (shaded yellow), as a function of frequency and resolution. The brightness temperatures of 10 and 100 K blackbody emission are overlaid in black in the left panel. In the right panel are overlaid the apparent brightness temperature of 10^4 K HII regions with emission measures (EM) from 10^4 to 10^{10} pc cm^{-6}. The array resolutions are shown in red. The upper boundary for each instrument is set by its brightness sensitivity at full resolution. A source can be *resolved* (at 1-σ in 1 hour) at the resolution given by the red lines if the source brightness (shown by the appropriate black line) lies within a shaded area. Refer to the text for a more comprehensive description.

indicating the array must be tapered by $\sim \sqrt{20} \sim 4$ to obtain this resolution/sensitivity combination. At 6 GHz, (blue dot), this same sensitivity is achieved with 80 mas resolution, and at 23 GHz (purple dot), this sensitivity is obtained with 30 milliarcseconds resolution. And so on.

The vertical distance between a particular brightness and a telescope coordinate within the covered (green) area is the SNR for a one hour observation. For example, a 300 mas resolution observation at 6 GHz (orange dot) is a factor of ten below the 10K BB curve. An observation of such an object with this resolution and frequency (which are produced by an untapered A-configuration observation) will be a $10-\sigma$ detection in one hour. Conversely, a 30 mas observation at this frequency (indigo dot) has an SNR of 0.1 – 100 hours will be needed for a $1-\sigma$ observation.

We can now consider the relative merits of the EVLA and ALMA for observing a blackbody of given temperature. A 100 K black body (top black curve) will be resolved by the EVLA at $1-\sigma$ in 1 hour with 80 mas resolution at 1.5 GHZ, 30 mas resolution at 6 GHz, and 5 mas resolution at 34 GHz. All of these are with the EVLA at full resolution – the horizontal black 100K line is more-or-less tangent with the top of the green EVLA sensitivity boundary. With ALMA, the situation is quite different. At 90 GHz, the 100K blackbody is a factor of $\sim$ 300 above ALMA's highest resolution (black dot and arrow) of 50 mas, so the SNR in one hour is $\sim$ 300. Similarly, for a 10K blackbody, ALMA will at 240 GHz obtain an SNR of $\sim$ 10 with 20 milliarcsecond resolution (cyan dot and arrow). The same object can be detected with the EVLA at 34 GHz with this resolution, but the SNR is only one. One hundred hours would be needed to match ALMA's

SNR at 240 GHz. This illustrates the power of ALMA for studies of sources with black-body spectra.

The EVLA will not have a primary role in studies of such sources. It will be most useful in a supporting role – separating thermal emission from non-thermal, and for observations of black-body-like objects where the opacity is a function of frequency: the lower frequency emission emanates from deeper within the source, so with sensitive observations over a wide frequency range – extending to the centimeter wavelengths a kind of three-dimension picture of the structure can be deduced.

The situation is quite different for optically thin emission, such as that from ionized H II regions. This is illustrated in the right hand panel. The green and yellow areas again describe the brightness temperature sensitivity range of the EVLA and ALMA. Superposed are the apparent brightness temperatures of bremsstrahlung emission, from regions with Emission Measures varying from 10^4 to a (very high) 10^{10} pc cm^{-6}. The slopes in these curves indicate that the emission in all cases is optically thin– thus allowing us to 'see through' such objects[2]. For this type of emission, there is a mild advantage for the EVLA for such studies – the EVLA provides higher resolution for a given SNR and EM. For example, for observing an H II region with $EM = 10^6$ with 30 mas resolution, the EVLA provides an SNR ~ 1 in one hour at all frequencies between 6 and 43 GHz. This resolution can be obtained on ALMA above 140 GHz, but with decreasing SNR this is due to atmospheric absorption and emission at the higher frequencies, decreasing ALMA's point-source sensitivity. The effect is seen in these brightness sensitivity curves by the sharp bend and rising red resolution lines above 240 GHz. For this same region, an observation at 650 GHz will have to be taken in a compact configuration, and smoothed to 300 mas resolution to obtain an SNR of one in one hour.

Although one may conclude that the EVLA has the edge for such studies, the situation is not so simple. Real sources are not uniform in either density or composition, nor isothermal, and a range of frequencies will be needed to separate these effect. Furthermore, the extreme end of such sources – those with $EM \geq 10^{10}$ pc cm^{-6} are optically thick below 40 GHz, making them opaque to the EVLA. Again, the correct conclusion is that both arrays are needed for precision studies of thermal emission whether optically thick or thin.

[2]The frequencies at which the emission becomes optically thick are $\sim$ 1, 6, and 40 GHz for EM = 10^6, 10^8, and 10^{10} pc cm^{-6}, respectively.

Appendix C

Relocation of the Los Alamos VLBA Antenna

As noted in Chapter 5, the layout of antennas for the New Mexico Array assumes that the VLBA antenna currently located at Los Alamos will be relocated to a new site. In this section we discuss the reasons for and the cost of this relocation.

In late 2002, the NRAO director received a letter from the Los Alamos National Laboratories (LANL) Deputy Laboratory Director for Science and Technology, requesting discussions 'with the ultimate goal of relocating NRAO's VLBA antenna from Los Alamos Technical Area 33 (TA-33) to another, as yet undetermined, location.' Our understanding is that the reason for this proposed move is a desire by the LANL and/or another customer to increase the use of TA-33 for highly classified work, and a corresponding desire to remove the antenna, and the NRAO personnel who must access the antenna, from the vicinity.

Based on this impending move, we have designed the configuration for the NMArray under the assumption that the Los Alamos VLBA antenna, which would be part of the NMArray, is moved to another location in New Mexico. Since the design of the NMArray configuration depends mutually on the location of all 10 NMArray antennas, this assumption is an integral part of the plan presented in this document.

In December 2001, the U.S. Department of Energy/National Nuclear Security Administration and the National Science Foundation signed a new 10-year agreement for use of TA-33 for the Los Alamos VLBA antenna. Part of this signed agreement is the termination clause (Provision No. 4), stating that 'This permit ... is revocable at any time by either party by giving thirty (30) days written notice to respective authorized representatives ...' Provision No. 24 of the agreement further states 'Upon termination, expiration, or relinquishment of this Permit, Grantee shall vacate the premises, remove its equipment, fixtures, appurtenances, and other improvements furnished and installed on the premises in connection with Grantee activities ...' In the context of this agreement, note that the 'Grantee' is defined specifically to be the National Science Foundation.

The obvious intent of the LANL is for the NSF to vacate TA-33 prior to December 2011. However, there currently is no funding allocated by the NSF to relocate the antenna. Therefore, in this document, we have identified the cost required to relocate the Los Alamos VLBA antenna as part of the NMArray. Our cost estimates are based on discussions with contractors who were involved in the original construction of the antenna and associated facilities.

Detailed costing is shown in Table C.1:

The budget presented in Table 6.3 does not include this item, since it is a requirement of the DOE/NSF agreement and is not an additional capability that is being requested by the NRAO. Although the time scale is still unclear, we have assumed a two-year duration for the move. The beginning year is assumed to be 2006, to which we allocate all site work, the environmental impact study, as well as 1/3 of the program management and engineering for the antenna move and 10% of the NRAO personnel costs. Therefore, the estimated cost in 2006 is \$1142K (including contingency). The remaining cost, for the actual antenna move, is assumed to take place in 2007, and amounts to \$3866 K (including the rermaining contingency) .

Table C.1: **Estimated Costs of Moving the Los Alamos VLBA Antenna**

Item	Cost($K)	Total($K)
A) Contractor Costs		
1) Antenna Move and Erection		
a) Program Management and Engineering	355	
b) Antenna Disassembly	785	
c) Antenna Installation	1630	
d) Shipping (within 100 miles)	80	
e) Addition for more distant shipping	50	
2) Site Work	725	
3) Environmental Impact Study	100	
Contractor Subtotal	3725	
Contingency (15%)	559	
Total Contractor Costs		**4284**
B) NRAO Costs		
1) Personnel (Labor, Engineering, Mngmt. etc.)	494	
2) Lodging	94	
3) Materials	45	
NRAO Subtotal	630	
Contingency (15%)	94	
Total NRAO Costs		**724**
Total Move Costs		**5008**

References

References

Abbott, D.C. 1982, ApJ 263, 723

Basri, G. 2000, ARA&A 38, 485

Berge, G.L. & Gulkis, S. 1976, in *Jupiter* (ed. T. Gehrels: Univ. of Arizona Press), 621-697

Berger, E. et al. 2001, Nature 410, 338

Berger, E. 2002, ApJ 572, 503

Bieging, J.H., Abbott, D.C., & Churchwell, E.B. 1989, ApJ 340, 518

Biretta, J.A., Zhou, F., & Owen, F.N. 1995, ApJ 447, 582

Blain, A.W., Smail, I., Ivison, R.J., Kneib, J.-P., & Frayer, D.T. 2002, Physics Report, 369, 111.

Boyle, B.J. et al. 2000, MNRAS, 317, 1014.

Brogan, C.L., Frail, D.A., Goss, W.M., & Troland, T.H. 2000, ApJ 537, 875

Browne, I.W.A. 2003, MNRAS 341, 13

Cabrit, S., Edwards, S., Strom, S.E., & Strom, K.E. 1990, ApJ, 354, 687-700

Cabrit, S. & André, P. 1991, ApJ, 379, L25-L28

Carilli, C.L., Holdaway, M.A., Ho, P.T.P., & De Pree, C.G. 1992, ApJL 399, L59

Carilli, C.L. 2001, in *Starburst Galaxies: Near and Far*, eds. L. Tacconi & D. Lutz (Heidelberg: Springer-Verlag), 309.

Carilli, C.L. et al. 2002, ApJ, 567, 781.

Carlstrom, J.E., Holder, G.P., & Reese, E.D. 2002, ARA&A, 40, 643.

Chiosi, C. & Maeder, A. 1986, ARA&A 24, 329

Claussen, M.J., Goss, W.M., Frail, D.A., & Desai, K. 1999, ApJ 522, 349

Condon, J.J. & Broderick, J.J. 1988, AJ, 96, 30.

Delaney, T., Koralesky, B., Rudnick, L., & Dickel, J.R. 2002, ApJ 580, 914

Elitzur, M. 1998, ApJ 504, 390

Exter, K.M., Watson, S.K., Barlow, M.J., & Davis, R.J. 2002, MNRAS 333, 715

Fabian, A.C. et al. 2000, MNRAS, 318, L65.

Fan, X. et al. 2001, AJ, 122, 2833.

Fassnacht, C.D., Xanthopoulos, E., Koopmans, L.V.E., & Rusin, D. 2002, ApJ 581, 823

Ferrarese, L. 2002, in *Current High-Energy Emission around Black Holes*, ed. C.-H. Lee (Singapore: World Scientific), 3.

Frail, D.A. et al. 1996, AJ 111, 1651

Frail, D.A. & Mitchell, G.F. 1998, ApJ 508, 690

Gaensler, B.M. et al. 2001, ApJ 549, 959

Ghez, A.M. et al. 2003, ApJL 586, L127

Gomez, M., Whitney, B.A., & Kenyon, S.J. 1997, AJ, 114, 1138-1153

Green, A.J., Frail, D.A., Goss, W.M., & Otrupcek, R. 1997, AJ 114, 2058

Green D.A. 2001, 'A Catalogue of Galactic Supernova Remnants (2001 December version)', Mullard Radio Astronomy Observatory, Cavendish Laboratory, Cambridge, United Kingdom (available on the World-Wide-Web at `http://www.mrao.cam.ac.uk/surveys/snrs/`)

Haarsma, D.B., Partridge, R.A., Windhorst, R.A., & Richards, E.A. 2000, ApJ, 544, 641.

Hartigan, P., Edwards, S., & Ghandour, L. 1995, ApJ, 452, 736-768

Hewish et al. 1968

Hjellming, R.M. & Rupen, M.P. 1995, Nature, 375, 464.

Hjellming, R. M. 1996a, in *Radio Emission from the Stars and the Sun*, eds. A. R. Taylor, & J. M. Paredes, (San Francisco: ASP), 174-181

Hjellming, R. M. 1996b, in *Cataclysmic Variables and Related Objects*, eds. A. Evans & J. H. Wood (Dordrecht: Kluwer), 317-320

Hoogerwerf, R., de Bruijne, J.H.J., & de Zeeuw, P.T. 2001, A&A 365, 49

Hunter, D.A. et al. 1998, ApJL 495, L47

Jackson, B.V., Hick, P.L., Kojima, M., & Yokobe, A. 1998, JGR 103, 121049

Kemball, A.J. & Diamond, P.J. 1997, ApJL 481, L111

Kochanek, C.S. 2003, ApJ 578, 25

Königl, A. & Pudritz, R.E. 2000, in *Protostars and Planets IV*, eds. V. Mannings, A.P. Boss, & S.S. Russell (Tucson: University of Arizona Press), 759-787

Kurtz, S. et al. 2001, RMxAC 10, 45

Lada, C.J. 1999, in *The Origin of Stars and Planetary Systems*, eds. C.J. Lada & N.D. Kylafis, 143.

Laing, R.A. & Bridle, A.H. 1987, MNRAS, 228, 557.

Leitherer, C., Robert, C., & Drissen, L. 1992, ApJ 401, 596

Li, Z. et al. 1991, ApJ 378, 93

Lim, J., Carilli, C.L., White, S.M., Beasley, A.J., & Marson, R.G. 1998, Nature 392, 575

Lockett, P., Gauthier, E., & Elitzur, M. 1999, ApJ 511, 235

Lockman, F.J. 2002, ApJL 580, L47

Looney, L. W., Mundy, L. G., & Welch, W. J. 1997, ApJ, 484, L157-L160

Markoff, S. et al. 2003, A&A, 397, 645.

Martí, J., Rodríguez, L.F., & Reipurth, B. 1998, ApJ, 502, 337-341

McClure-Griffiths, N.M. et al. 2001, PASA 18, 84

Muhleman, D.O., Grossman, A.W., & Butler, B.J. 1995, AREPS 23, 337

Mundy, L.G., Looney, L.W., & Welch, W.J. 2000, in *Protostars and Planets IV*, eds. V. Mannings, A.P. Boss, & S.S. Russell (Tucson: University of Arizona Press), 355-376

Muxlow, T. et al. 1994, MNRAS, 266, 455.

Myers, S.T. et al. 2003, MNRAS 341, 1

Osorio, M., D'Alessio, P., Muzerolle, J., Calvet, N., & Hartmann, L. 2003, ApJ, in press; astro-ph/0212074

Owen, F.N., Eilek, J.A., & Kassim, N.E. 2000, ApJ, 543, 611.

de Pater, I., Palmer, P., & Snyder, L.E. 1986, ApJ 304, L33

de Pater, I. 1990, ARA&A 28, 347

de Pater, I. & Sault, R.J. 1998, JGR 103, 19973

Pavelin, P.E., Davis, R.J., Morrison, L.V., Bode, M.F., & Ivison, R.J. 1993, Nature 363, 424

Perley, R.A., Dreher, J.W., & Cowan, J.J. 1984, ApJL 285, L35

Reipurth, B., Heathcote, S., Yu, K.C., Bally, J., & Rodríguez, L.F. 2000, ApJ, 534, 317-323

Reynolds, R.J. 1991, in The Interstellar Disk-Halo Connection in Galaxies (ed.: H. Bloemen), 67-76

Reynolds, R.J. et al. 1998, PASA 15, 14

Rodríguez, L.F. & Bastian, T.S. 1994, ApJ 428, 324

Rodríguez, L.F. et al. 1998, Nature, 395, 355-357

Rodríguez, L.F., Porras, A., Claussen, M.J., Curiel, S., Wilner, D.J., & Ho, P.T.P. 2003, ApJ, in press

Roshi, D.A. & Anantharamaiah, K.R. 2000, ApJ 523, 231

Rusin, D. et al. 2001, ApJ 557, 594

Sanders, G. Project Science Workshop, Planning for Performance Measurement, Cost Estimate-Risk Analysis. http://131.215.125.172/workshop2/talks/sanders02.pdf

Santos-Costa, D. et al. 2001, AdSpR 28, 915

Sault, R.J., Oosterloo, T., Dulk, G.A., & Leblanc, Y. 1997, A&A 324, 1190

Schiminovich, D., van Gorkom, J.H., van der Hulst, J.M., & Kasow, S. 1994, ApJL 423, L101

Schodel, R. et al. 2002, Nature 419, 694

Shepherd, D.S., Claussen, M.J., & Kurtz, S.E. 2001, Science, 292, 1513.

Shu, F.H., Allen, A., Shang, H., Ostriker, E.C., & Li, Z-Y. 1999, in *The Origin of Stars and Planetary Systems*, eds. C.J. Lada & N.D. Kylafis, 193.

Silver, C.S., Taylor, G.B., & Vermeulen, R.C. 1998, ApJ, 502, 229.

Sisterna, P. & Vucetich, H. 1990, Phys. Rev. D 41, 1034

Skinner, C.J. et al. 1998, MNRAS 296, 669

Snyder, L.E., Palmer, P., & de Pater, I. 1989, AJ 97, 246

Spergel, D.N. et al. 2003, ApJS, 148, 161.

Tarchi, A. et al. 2000, A&A 358, 95

Taylor, A.R., Hjellming, R.M., Seaquist, E.R., & Gehrz, R.D. 1988, Nature 335, 235

Taylor, G.B., Silver, C.S., Ulvestad, J.S., & Carilli, C.L. 1999, ApJ, 519, 185.

Taylor, J.H.& Cordes, J.M. 1993, ApJ 411, 674

Treu, T. & Koopmans, L. 2002a, ApJ 575, 87

Treu, T. & Koopmans, L. 2002b, MNRAS 337, L6

Walker, R.C. et al. 2000, ApJ, 530, 233.

Walter, F., Carilli, C., & Lo, F. 2003, Nature, 424, 406.

White, R.L. & Becker, R.H. 1995, ApJ 451, 352

Wiseman, J.J. & Ho, P.T.P. 1998, ApJ 502, 676

Wood, K. & Reynolds, R.J. 1999, ApJ 525, 799

Yorke, H.W. 2002, in *Hot Star Workshop III: The Earliest Stages of Massive Star Birth*, ed. P.A. Crowther (San Francisco: Astronomical Society of the Pacific), 165.

Yun, M.S. & Carilli, C.L. 2002, ApJ, 568, 87.

Yun, M.S., Reddy, N.A., & Condon, J.J. 2001, ApJ, 554, 803.

Yusef-Zadeh, F., Roberts, D.A., & Biretta, J. 1998, ApJL 499, L159